(12)

FG.

Revision

to

DNA EMP PREFERRED TEST PROCEDURES

(DNA 3286H) 787 482

September 1976

Instructions

The recipient is requested to remove the following pages from his/her copy of DNA 3286H and add the following pages:

Remove	Add
DD Form 1473 (Report date 29 August 1974)	DD Form 1473 (Report date September 1976)
i through iv	i through ii
1 through 4	1 through 10
	7-1 through 7-36
	8-1 through 8-40
	9-1 through 9-46
	10-1 through 10-42
	11-1 through 11-36
	12-1 through 12-46
	13-1 through 13-28
	14-1 through 14-40
	A-1 through A-10
I-1 through I-8	I-1 through I-12
D-1 through D-12	D-1 through D-10

UNCLASSIFIED

SECURITY CLASSIFICATION OF THIS PAGE *(When Data Entered)*

REPORT DOCUMENTATION PAGE

READ INSTRUCTIONS BEFORE COMPLETING FORM

1 REPORT NUMBER: DNA 3286H-Rev	2 GOVT ACCESSION NO.
3 RECIPIENT'S CATALOG NUMBER	
4 TITLE (and Subtitle): EMP PREFERRED TEST PROCEDURES (Selected Electronic Parts). Revision,	5 TYPE OF REPORT & PERIOD COVERED: Handbook
	6 PERFORMING ORG. REPORT NUMBER: IITRI Project E6230, E6261
7 AUTHOR(s): J.E.Bridges, W.C.Emberson, V.P.Nanda, W.C.Wells, L.C.Peach, L.B.Townsend, Dr. P.L.E.Uslenghi	8 CONTRACT OR GRANT NUMBER(s): DNA 001-72-C-0089, DNA 001-73-C-0149
9 PERFORMING ORGANIZATION NAME AND ADDRESS: IIT Research Institute, 10 West 35th Street, Chicago, Illinois 60616	10 PROGRAM ELEMENT, PROJECT, TASK AREA & WORK UNIT NUMBERS: NWED Subtask K99QAXEB097-07
11 CONTROLLING OFFICE NAME AND ADDRESS: Director, Defense Nuclear Agency, Washington, D.C. 20305	12 REPORT DATE: September 1976 13 NUMBER OF PAGES: 562
14 MONITORING AGENCY NAME & ADDRESS (if different from Controlling Office): IITRI-E6230-Rev, IITRI-E6261-Rev	15 SECURITY CLASS (of this report): UNCLASSIFIED 15a DECLASSIFICATION DOWNGRADING SCHEDULE

16 DISTRIBUTION STATEMENT *(of this Report)*

Approved for public release; distribution unlimited.

12 322p.

17 DISTRIBUTION STATEMENT *(of the abstract entered in Block 20, if different from Report)*

Review of this material does not imply Department of Defense indorsement of factual accuracy or opinion.

18 SUPPLEMENTARY NOTES

This work sponsored by the Defense Nuclear Agency under Subtask K99QAXEB097-07. Destroy this report when it is no longer needed. Do not return to sender.

19 KEY WORDS *(Continue on reverse side if necessary and identify by block number)*

EMP Hardening	EMP Surge Arresters
EMP Tests	EMP Filters
EMP Hardening Component	EMP Specifications

20 ABSTRACT *(Continue on reverse side if necessary and identify by block number)*

EMP preferred test procedures are provided to evaluate and characterize the performance of a number of electronic parts → next page

1) filters
2) surge arresters
3) gaskets
4) vents
5) coaxial cables and connectors
6) shielded enclosures
7) conduit systems
8) transformers and inductors
9) resistors

DD FORM 1 JAN 73 1473 EDITION OF 1 NOV 65 IS OBSOLETE

UNCLASSIFIED

SECURITY CLASSIFICATION OF THIS PAGE *(When Data Entered)*

175 350

19. KEY WORDS (Continued)

Surge Arrester Characterization
Filter Characterization
EM Gaskets
EM Vents
Coaxial Cable Shields
Shielded Coaxial Connectors
Shielded Enclosures
Shielded Rooms
Conduits
Resistor Damage
Capacitor Damage
Inductor Damage
Transformer Damage
Resistor Characterization
Inductor Characterization
Surge Arrester Damage
Filter Damage
Gasket Shielding Characterization
Vent Shielding Characterization
Surface Transfer Impedance
Surface Transfer Admittance
E-Field Shielding Effectiveness
H-Field Shielding Effectiveness
Conduit Couplers
Capacitor Characterization
Transformer Characterization

20 ABSTRACT (Continued)

10) capacitors.

Topics covered are experiment design, documentation, typical induced EMP transients, and the specific test procedures to evaluate the EMP behavior for each type of electronic component.

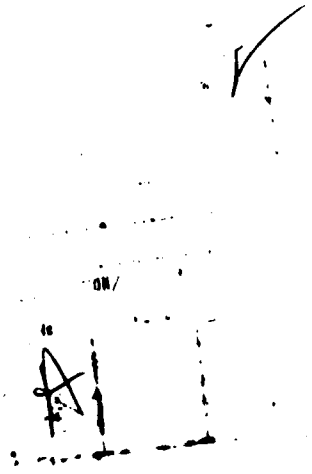

SUMMARY

IIT Research Institute, under contract to the Defense Nuclear Agency (DNA001-72-C-0084 and DNA001-73-C-0149), has developed EMP PREFERRED TEST PROCEDURES for selected electronic components. This is part of a continuing program to formulate and recommend procedures by which EMP test data may be obtained and reported.

In this connection, it is important to realize what these preferred procedures are and what they are not. They are a formal recognition of good practices and methods based on sound physical principles which can lead to useful EMP data. They provide a means of communicating useful information among workers in a large multidisciplined technology.

These preferred procedures are not necessarily cook-book simplifications and are not intended to be a "MIL-SPEC" or a panacea for designers of hardened systems. The EMP PREFERRED TEST PROCEDURES require some experience and intelligence on the part of the experimenter. These are somewhat different than "MIL-SPEC" testing which can usually be implemented by a responsible technician. The procedures emphasize the electrical test aspects. Some general guidance as to limits and other environmental aspects is provided; however, these are more properly considered in terms of the requirements for a specific system, such as design specifications. The procedures are designed to employ readily available or easily constructed laboratory equipment--generally operating below 100,000 volts and 100 MHz--and to be conducted in ordinary room-size laboratory space.

The material contained in this document is considered the best available and, where possible, it represents a concensus of recognized practices. Based on discussions with prominent members of the EMP community as well as other experts, preliminary outlines of the procedures were devised and actual tests conducted to validate the procedures. A draft of the procedures was then circulated among cognizant professionals in a number of

organizations, and revised as needed to harmonize various viewpoints. While the results in this document are based on the experience of a number of active recognized professionals, it must be noted that all possible situations could not be considered. Clearly, it is not the intent of this document to impose "National EMP Standards and Limits." Even if these were desirable, it would not be appropriate to do so today because of the rapid changes taking place in the state-of-the-art. In this regard, it is important that others take an active part in supplying additional information to effect improvements.

Much of the work presented in the first three sections in this edition of the EMP PREFERRED TEST PROCEDURES was summarized directly from DNA Document 2028H, entitled "TREE Preferred Procedures." IIT Research Institute, therefore, gratefully acknowledges the efforts of Mr. Richard H. Thatcher and Mr. Michael L. Green at the Battelle-Columbus Laboratories for their efforts on DNA 2028H.

Discussions were also held with staff members of a number of organizations in EMP hardening. All organizations cannot be acknowledged, but include U.S. Army Electronics Command, Picatinny Arsenal, Naval Surface Weapons Center, Harry Diamond Laboratories, Defense Civil Protection Agency, Construction Engineering Research Laboratory, Boeing Aircraft Corporation, Lockheed Corporation, International Rockwell, General Semiconductor Industries, Siemens Corporation, Signalite, Joslyn Electronic Systems, Electro-Data Technology, Sandia Laboratory, and Stanford Research Institute.

The principle contributors to this document are Mr. J. E. Bridges, Mr. W. C. Emberson, Mr. V. P. Nanda, Dr. L. C. Peach, Mr. L. B. Townsend, Dr. P. L. E. Uslenghi and Dr. W. C. Wells. Major W. Adams, Major W. Dean and Captain W. D. Wilson of DNA provided overall program review. The technical management was provided by Mr. I. N. Mindel and Dr. E. W. Weber. Much of the laboratory work was conducted by Mr. S. Smandra, Dr. J. Herro and Dr. Y. Shiau.

TABLE OF CONTENTS

TABLE OF CONTENTS (Continued)

TABLE OF CONTENTS (Continued)

TABLE OF CONTENTS (Continued)

2

TABLE OF CONTENTS (Continued)

TABLE OF CONTENTS (Continued)

TABLE OF CONTENTS (Continued)

TABLE OF CONTENTS (Continued)

TABLE OF CONTENTS (Continued)

7. TEST PROCEDURES FOR EM GASKETS

TABLE OF CONTENTS

3

7. TEST PROCEDURES FOR EM GASKETS

7.1 Introduction

EM gaskets play a major but often unrecognized role in the EMP susceptibility of a system. Critical defects in certain systems have arisen as a result of inattention to electromagnetic and environmental considerations in EM gasket design.

The purpose of this preferred test procedure is to measure the electrical performance of an EM gasket as a system component. Specifically, procedures are suggested which measure the electrical performance of small gaskets and, on a normalized basis, measure the performance of gasket materials which can be employed for either large or small gaskets. Other factors affecting gasket performance, such as temperature, corrosion and foreign material can be considered within the context of the electrical performance.

The procedures recommended for testing the performance of the gasket as a component, which are discussed in this chapter, are useful for the following purposes:

1. They provide the design engineer with a useful technique for evaluating the relative performance of various gasket materials.

2. The test procedures can be used by the designer for evaluating the electrical performance of gaskets under anticipated environmental conditions.

3. The test procedures provide the system interaction analyst with a fairly realistic measure of the intrinsic performance parameters of the gaskets. These parameters can be used rather simply to estimate the performance for symmetrical current flows through the gasket (radial, axial, or longitudinal), although complex analyses are required for non-symmetrical current flows across the gasket.

4. The test procedures supply, to some extent, combined mechanical and electrical design performance information, such as electrical performance as a function of gasket pressure.

5. Gasket manufacturers may employ the recommended tests in the design of new gaskets and present results in a data sheet format.

6. Those conducting manufacturing quality control or part acceptance tests can use the procedure as a guide for simple quick-look evaluations.

7. Those assessing EM degradation with age can use the procedures as a guide to measuring, on a relative basis, the aging characteristics of gaskets.

7.2 EM Gaskets

7.2.1 General Characteristics of EM Gaskets

An EM (Electromagnetic) gasket is a section of flexible conducting material used to preserve the continuity of an RF (Radio Frequency) or electromagnetic shield across seams, joints, hinges and connector fittings. EM gaskets are electrically imperfect for various reasons. They often have low conductivity and may exhibit imperfect contact between mating surfaces. They may exhibit anisotropic electromagnetic properties, such as greater conductivity in one direction than in another. Some EM gaskets also have small apertures or holes which can further degrade performance.

EM gaskets may be non-ideal in many ways other than electrical. They have a finite resilience, failing to return to their original shape if compressed beyond a certain limit. The degree of resilience is a function of the gasket's temperature, its age, the number of compression cycles it has been through and so forth. EM gaskets are also affected by environmental factors, such as extremes of temperature, dust, and corrosion. Treatment of mating surfaces and uniformity of pressure applied to the gasket, as well as the total closure pressure, are often important factors in performance.

By way of illustration, consider a gasket composed of a non-conducting elastomer material holding a matrix of conducting wires or particles. Depending on the type of elastomer employed, the ability of this particular gasket to conform to the mating surfaces can be a strong function of temperature. It is easy to visualize how such gaskets might perform well under normal room temperature conditions and be totally unsatisfactory when exposed to alternating extremes of tropical and arctic temperatures.

7.2.2 Characteristics of EMP Penetration at EM Gaskets

EMP penetration at a gasketed joint is determined by the nature of the EMP-induced current flow at the joint and by the electrical and mechanical characteristics of the gasket. These factors are discussed in this section.

7.2.2.1 Penetration for the Uniform Gasket Current Case

The most easily analyzed case of EMP penetration at a gasketed joint is that of uniform EMP-induced gasket current flow. A typical gasket application illustrating this case is depicted in Figure 7-1 which shows the use of an EM gasket to join two sections of circular conduit. A uniform gasket compressive force, F, is assumed to be applied at the circumference of the gasket mating surfaces. For this geometry, it is reasonable to assume that the current, I_s, induced on the outer surface of the conduit by an incident EMP, is uniform and parallel to the axis of the conduit. The impedance presented to the flow of I_s by the gasket discontinuity generates a potential difference, V_s, between the gasket mating surfaces. This potential drop, across the interior surface of the conduit wall, represents interference signal coupled to the conductor(s) in the conduit. Because I_s is assumed to be uniform about the circumference of the conduit, it follows V_s does not vary with position along the gasket. Therefore, V_s can be simply related to I_s using the transfer impedance concept (see Section 7.2.3.1).

7.2.2.2 Penetration for the Non-Uniform Gasket Current Case

The most general case of EMP penetration at a gasketed joint is that of non-uniform EMP-induced gasket current flow. A typical application illustrating this case is depicted in Figure 7-2 in which a gasket is used to

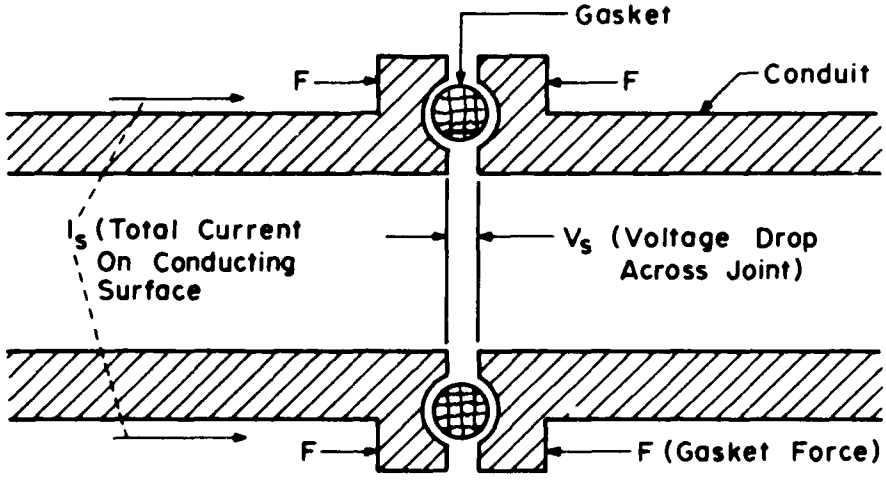

Figure 7-1. Cross-section of a circular conduit joined by a gasket.

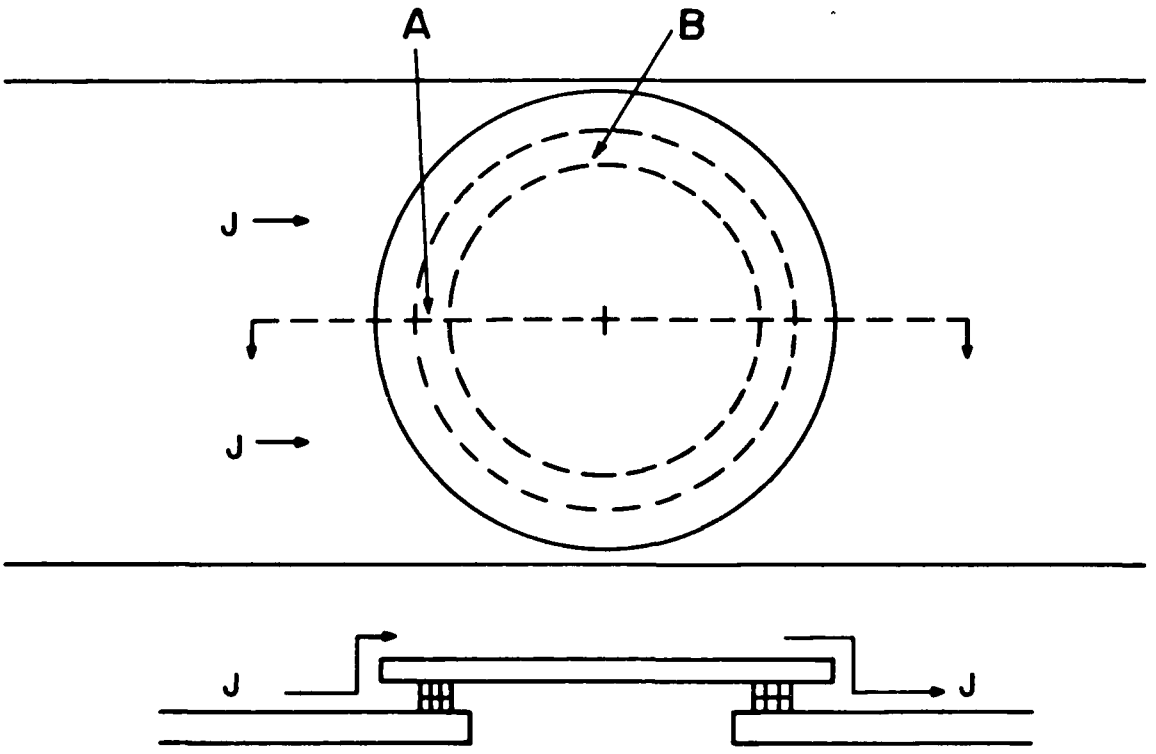

Figure 7-2. Non-symmetrical flow of current through a gasket.

electrically join a hatch to a conducting wall. Again, the gasket force, F, is assumed to be uniformly applied at the perimeter of the mating surfaces. Here, a uniform sheet current, J, is assumed to flow on the wall surface as a result of an incident EMP. However, it is to be noted that the current flow across the gasket is not uniform for this geometry. This current distribution has a maximum at Point A and a minimum at Point B. Therefore, the voltage potential induced between the mating surfaces is a function of position along the gasket. Here, interference coupled to the interior cannot be expressed as a single voltage, V_s. Instead, one must consider the total interior electromagnetic field structure resulting from the EMP excitation of the gasketed hatch. These fields are a function of the size and shape of the hatch and the interior space, as well as the gasket conductivity. Therefore, the use of a simple transfer impedance formulation to assess gasket shielding performance in such situations leaves much to be desired. Because of this complexity, there is no tractable alternative measure of shielding available other than a total measurement and mapping of the interior fields. However, if a transfer impedance measure is used, its inherent simplifications must be considered.

7.2.3 Gasket Shielding Performance Measures

From the viewpoint of avoiding system upset from EMP, the best gasket is the one having the greatest shielding effectiveness. The shielding effectiveness of a gasket can be judged by determining one of two quantities, the transfer impedance and/or the transfer figure of merit.

7.2.3.1 Transfer Impedance

For the case of a uniform, axial, EMP-induced gasket current, as illustrated in Figure 7-1, a complex gasket transfer impedance, $Z_T(\omega)$, can be defined in the same way

as the surface transfer impedance of a coaxial cable connector (Section 9.2.3) where $Z_T(\omega)$ is given by:

$$Z_T(\omega) = \frac{V_s(\omega)}{I_s(\omega)} \text{ ohms} = x + jy(\omega) \qquad (7.1)$$

In equation (7.1),

I_s = sheath current across the external part of the gasket.

V_s = coupled voltage across the inner surface of gasket.

x = $R_c + R_b$; where R_c is the contact resistance and R_b is the gasket bulk resistance.

$y(\omega)$ = a function of the size and shape of the apertures of both the gasket and the mating surfaces.

From the viewpoint of shielding effectiveness, the ideal gasket is the one where $Z_T(\omega) = 0$. The direct measurement of $Z_T(\omega)$ is the most exact characterization of gasket performance for the case of uniform gasket current.

A shielding performance measure of some use for the case of nonuniform gasket current is the normalized transfer impedance, Z_{TN}. Z_{TN} is defined as the product of the transfer impedance and the circumferential length, ℓ, of the gasket:

$$Z_{TN}(\omega) = Z_T(\omega) \cdot \ell \text{ ohm-meters} \qquad (7.2)$$

where $Z_T(\omega)$ has been determined for the case of uniform axial gasket current. Z_{TN} allows the estimate of the shielding performance of gaskets formed from gasket stock of constant dimensions, shaped to the desired form. Z_{TN} is also useful for comparing the performance of gaskets of different circumferences on a relative basis.

4

7.2.3.2 Transfer Figure of Merit

Measurement of $Z_T(\omega)$ over the EMP frequencies of interest is often a tedious and laborious process. Therefore, transient measurements are often desirable since only one measurement need be performed in most cases. Figure 7-3 illustrates the typical transient current test waveform and voltage responses of gaskets for the case of uniform axial gasket current.

Referring to Figure 7-3, a second gasket shielding performance measure called the transfer figure of merit, F_M, may be defined. This transfer figure of merit is the ratio of the peak output voltage, V_p, and the peak input driving current, I_p, given by:

$$F_M = \frac{V_p}{I_p} \text{ ohms} \tag{7.3}$$

The use of the transfer figure of merit is an expedient method for estimating gasket shielding performance in the time domain. However, it does not provide as thorough a characterization of performance as methods employing the transfer impedance. In the very special case (e.g., high performance gaskets) in which the waveshape of the observed output voltage is the same as that of the driving current waveform, the transfer figure of merit is identical to the magnitude of Z_T.

A useful time domain shielding performance measure for comparing gaskets of different circumstances is the normalized transfer figure of merit, F_N. F_N is defined as the product of the transfer figure of merit and the circumferential length, ℓ, of the gasket:

$$F_N = F_M \cdot \ell \text{ ohm-meters} \tag{7.4}$$

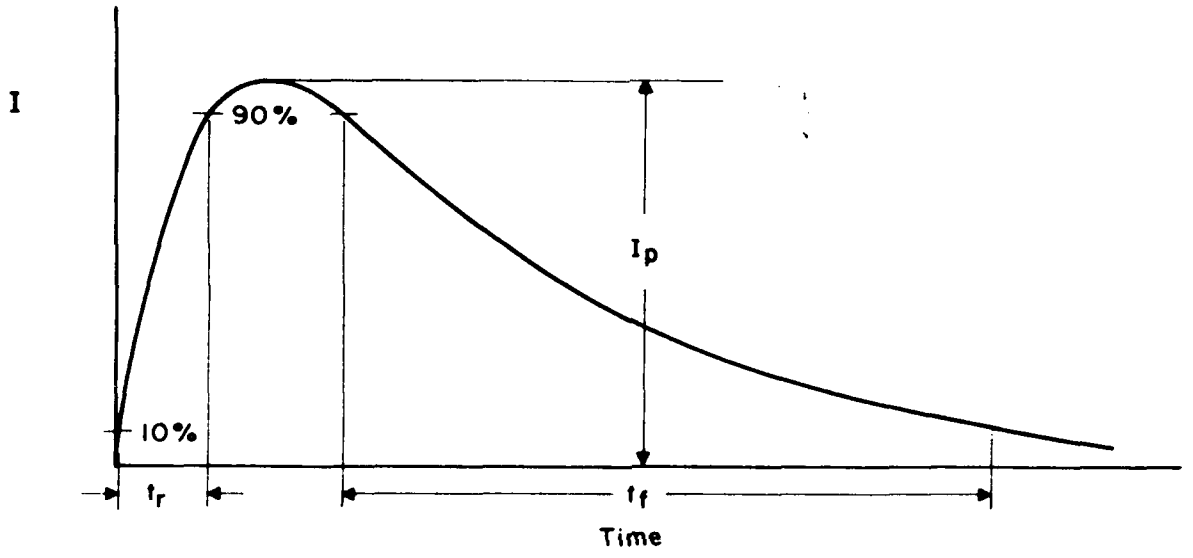

Figure 7-3a. Driving current waveform.

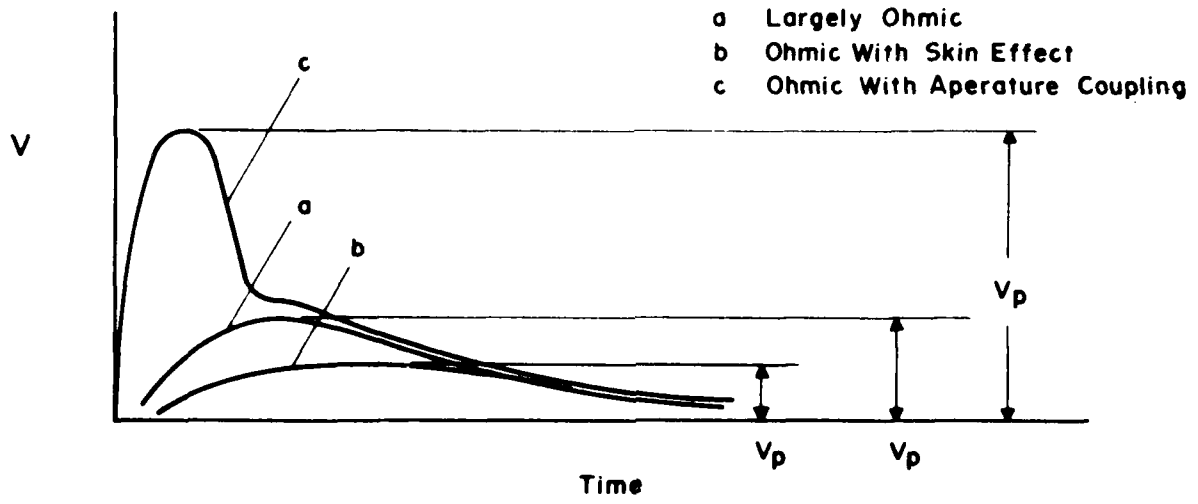

Figure 7-3b. Output voltage waveform.

7.2.4 Considerations in Testing Shielding Performance of Gaskets

7.2.4.1 Choice of Frequency or Time Domain Tests

Valid gasket shielding measurements can be performed in either the frequency or time domain. Test results in one domain can be related to test results in the other by the numerical Fourier transformation. The choice of domain depends upon the expected exposure conditions and the desired rigor of the test.

Time domain or pulse measurements can be very useful because they provide a rapid, qualitative check of gasket shielding. In this case, the measured quantities are the transient waveforms of the driving current and the output voltage. These tests are recommended for most situations where a broad band type of transient exposure is expected or where approximate results are acceptable.

Frequency domain or continuous wave measurements provide a quantitative test of gasket shielding at either discrete or swept frequencies. Here, the measured quantities are the amplitudes and phases of the driving current and the output voltage. These tests are advised where narrow band exposures (such as long duration, ringing type waveforms) are expected or where gasket performance requirements are critical.

7.2.4.2 Nonuniform or Nonsymmetric Gasket Current Flow

Gasket shielding for the case of uniform axial current flow, or for other types of symmetric current flow, can be accurately characterized by either $Z_T(\omega)$, (Equation 7.1) or by F_M (Equation 7.3). Procedures for this characterization are detailed later in this section. However, to investigate gasket shielding for the general case of nonsymmetric current flow, a test procedure must take into

account details of the interior portion of the shielded enclosure. At present, no procedure capable of directly evaluating this general case is available. Use of Z_{TN} (Equation 7.2) or F_N (Equation 7.4) must be made to approximate the gasket shielding for this case.

7.2.4.3 Gasket Characteristics

Anisotropy

A gasket with anisotropic electromagnetic properties cannot be characterized simply. For this case, no single scalar value of $Z_T(\omega)$ or F_M is adequate to describe gasket shielding for all likely directions of uniform flow.[1,2] Here, a complete description of gasket shielding based on measurements of the anisotropy may be required if a close estimate of gasket performance is needed.

Variation of $Z_T(\omega)$ With Compression Force

The gasket force is the ratio of the total compressive force applied by the mating surfaces to the mean circumference of the gasket (typically expressed in pounds per linear inch). In general, the gasket's transfer impedance decreases with increasing gasket force over the range of interest. To evaluate the shielding performance of the gasket as precisely as possible, the total compressive force, treatment of mating surfaces, and uniformity of compressive force experienced by the gasket in situ should be duplicated in the test procedures.

Lapped or Continuous Structure

A gasket is defined as continuous if it is manufactured in the form of an uninterrupted ring. Within certain limits, such gaskets can be tested directly in the test fixture to be detailed. A lapped gasket is manufactured as a long,

flexible section, and is then formed into a continuous ring. In this case, only the material and design of the gasket stock is tested, with the normalized transfer impedance used as the performance criterion. Therefore, the lapping junction should be made very carefully to guard against spurious leakage.

7.3 Transient Test Procedure

7.3.1 Scope

This test procedure is designed for the following purposes:

1. To evaluate the absolute electrical performance of small (less than 7 inch diameter) gaskets, provided that the other non-electrical critical parameters have been considered in the design and operation of the test fixture.

2. To evaluate the relative electrical performance of small (less than 7 inch diameter) gaskets.

3. To assess the relative electrical performance of gasket materials suitable for constructing large gaskets.

Procedures to measure the transient behavior of the gaskets are set forth using a simple transient test waveform. Other test waveforms may be more appropriate and should be considered for important critical gasket applications.

7.3.2 Test Fixture

Gaskets are manufactured in many shapes and sizes. It is, therefore, impossible to design a test fixture suitable for measuring all possible gaskets. This test fixture is suggested only as a guide for tests on specific gasket construction. The test fixture is most appropriate to measuring the relative performance of gaskets small enough to be tested within the test fixture, or portions of larger gaskets cut to shape to fit within the test fixture. Care must be taken that test conditions and surface treatments are comparable to the expected use environment.

Photographs of the suggested test fixture appear in Figure 7-4 and Figure 7-5. This fixture is designed to test ring-shaped gaskets up to approximately 7 inches in diameter by using a plate-gasket-slate sandwich structure.

7.3 Transient Test Procedure

7.3.1 Scope

This test procedure is designed for the following purposes:

1. To evaluate the absolute electrical performance of small (less than 7 inch diameter) gaskets, provided that the other non-electrical critical parameters have been considered in the design and operation of the test fixture.

2. To evaluate the relative electrical performance of small (less than 7 inch diameter) gaskets.

3. To assess the relative electrical performance of gasket materials suitable for constructing large gaskets.

Procedures to measure the transient behavior of the gaskets are set forth using a simple transient test waveform. Other test waveforms may be more appropriate and should be considered for important critical gasket applications.

7.3.2 Test Fixture

Gaskets are manufactured in many shapes and sizes. It is, therefore, impossible to design a test fixture suitable for measuring all possible gaskets. This test fixture is suggested only as a guide for tests on specific gasket construction. The test fixture is most appropriate to measuring the relative performance of gaskets small enough to be tested within the test fixture, or portions of larger gaskets cut to shape to fit within the test fixture. Care must be taken that test conditions and surface treatments are comparable to the expected use environment.

Photographs of the suggested test fixture appear in Figure 7-4 and Figure 7-5. This fixture is designed to test ring-shaped gaskets up to approximately 7 inches in diameter by using a plate-gasket-slate sandwich structure.

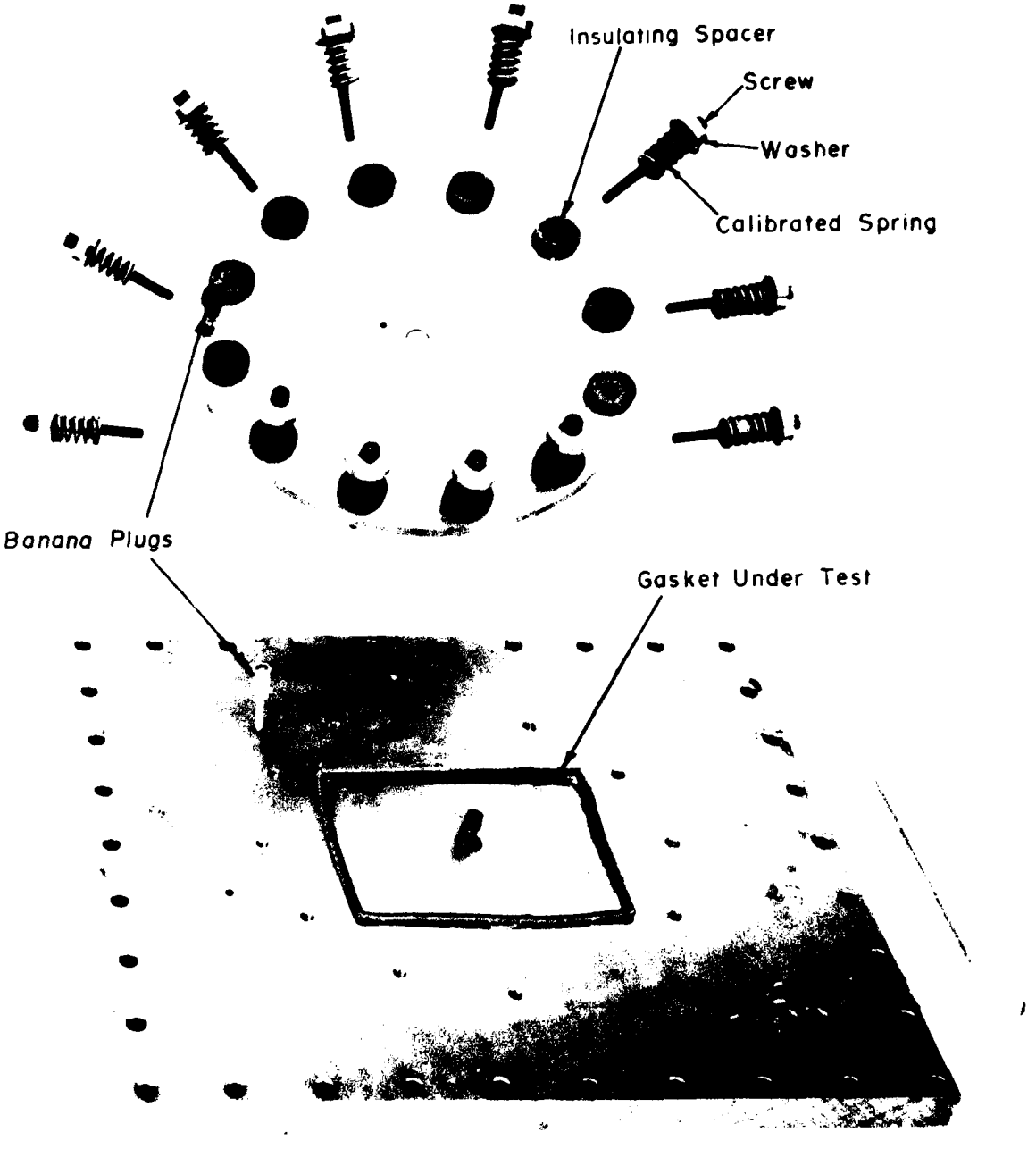

Figure 7-4. Exploded view of test fixture (front side).

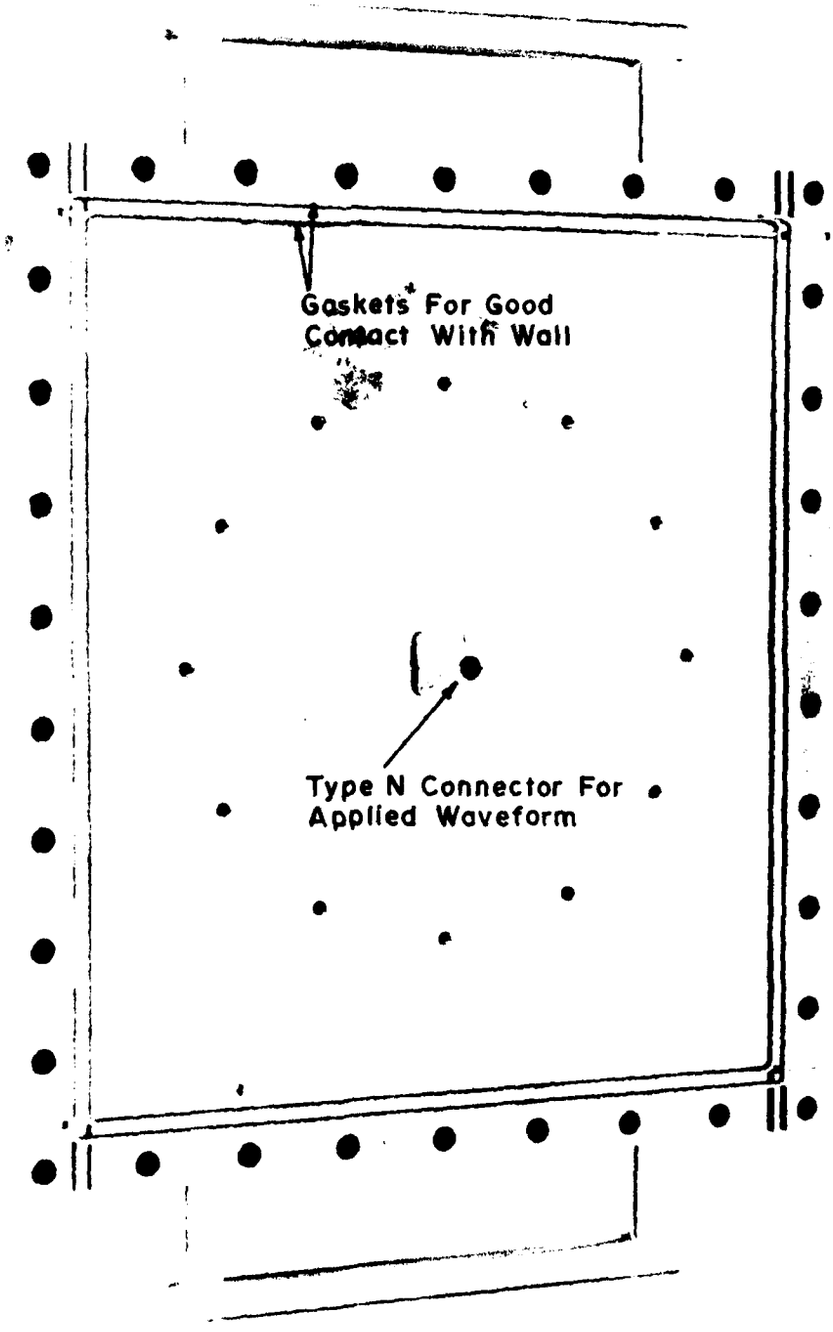

Figure 7-5. Back side of test fixture.

The plate surfaces contacting the gasket are machined or polished to be similar to surfaces expected in the gasket's application. Surface ground steel plates are used if the nature of the gasket's normal mating surfaces is unknown. A known, uniform gasket force is applied by using screws and calibrated springs to compress the test sample. Insulating spacers are used to isolate the springs and screws from the round plate.

The driving waveform is applied preferably to a type N connector although other connectors may also be used. The induced voltage is measured between two banana plugs--one on each gasket mating plate. This particular test fixture is mounted on the wall of a shielded enclosure or on a box containing the measuring equipment. This insures that the measurement instrumentation located within the shielded enclosure is isolated from the driving source and exciting currents. Additional EM gaskets (see Figure 7-5) are required to mount the test fixture properly to the wall of the enclosure or shielded box. However, since only a small current flows on the wall of the shielded enclosure, even when a large signal is applied through the driving cables, the test fixture does in fact measure the electrical performance of the test gasket and thus the electrical quality of the outer gasket is not critical. If necessary, welded or soldered seams can replace this gasket.

If a shielded room or box is not available, the tests can be made by means of a backshell shield such as shown in Figure 7-6. In this case, additional care is required to provide isolation between the driving pulse source and the measurement equipment. An arrangement such as shown in Figure 7-6 often produces reduced dynamic range.

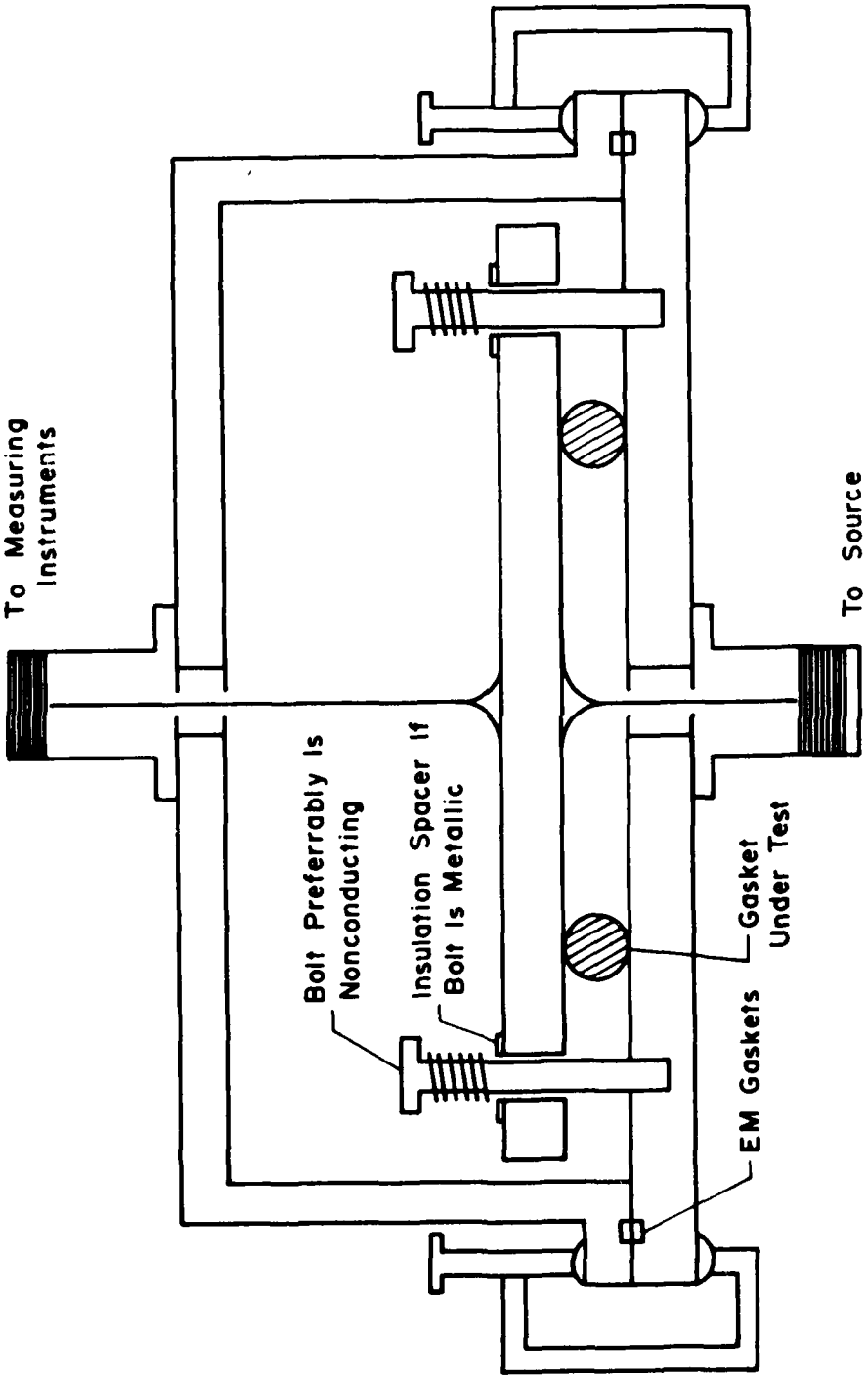

Figure 7-6. Schematic cross-section of test fixture using backshell shield.

7.3.3 Test Setup

The preferred arrangement of the measurement equipment is shown in Figure 7-7. The pulse source of Figure 7-7 may generate either a step function, damped sinusoid or a delta function. However, for EMP simulation the preferred pulse waveform is a double exponential, of the form $k(e^{-\alpha t}-e^{-\beta t})$, having approximately a 10 nanosecond rise time and a 1.0 microsecond fall time. This pulse is preferred because it is wideband and is also easy to generate. A current probe is used to measure the driving current waveform. Wideband oscilloscopes, each having a bandwidth on the order of 100 MHz or more, are used to record the output voltage and input current waveforms. The measured voltage and current waveforms should travel on 50 ohm coaxial cables terminated in 50 ohms at the oscilloscope.

The input port is nearly a short circuit; and in order to stabilize the pulse source feeding the test fixture, a 50 Ω resistor is inserted in series with the pulse generator and as close as possible (within several inches) to the input port of the test fixture.

7.3.4 Measurement Precautions

In Figure 7-7, the preferred arrangement locates the pulse source outside of the shielded enclosure with the measurement equipment located in the enclosure. Where this is not possible, the pulse source should be well-shielded and preferably isolated as much as possible both electrically and physically from the measurement equipment. Input and output probes should be calibrated to establish that their response is flat over the spectrum of interest.

In the case of very poor gaskets and/or surface materials, for which the ohmic resistance between the two contacting plates exceeds 3 Ω at very low frequencies, the

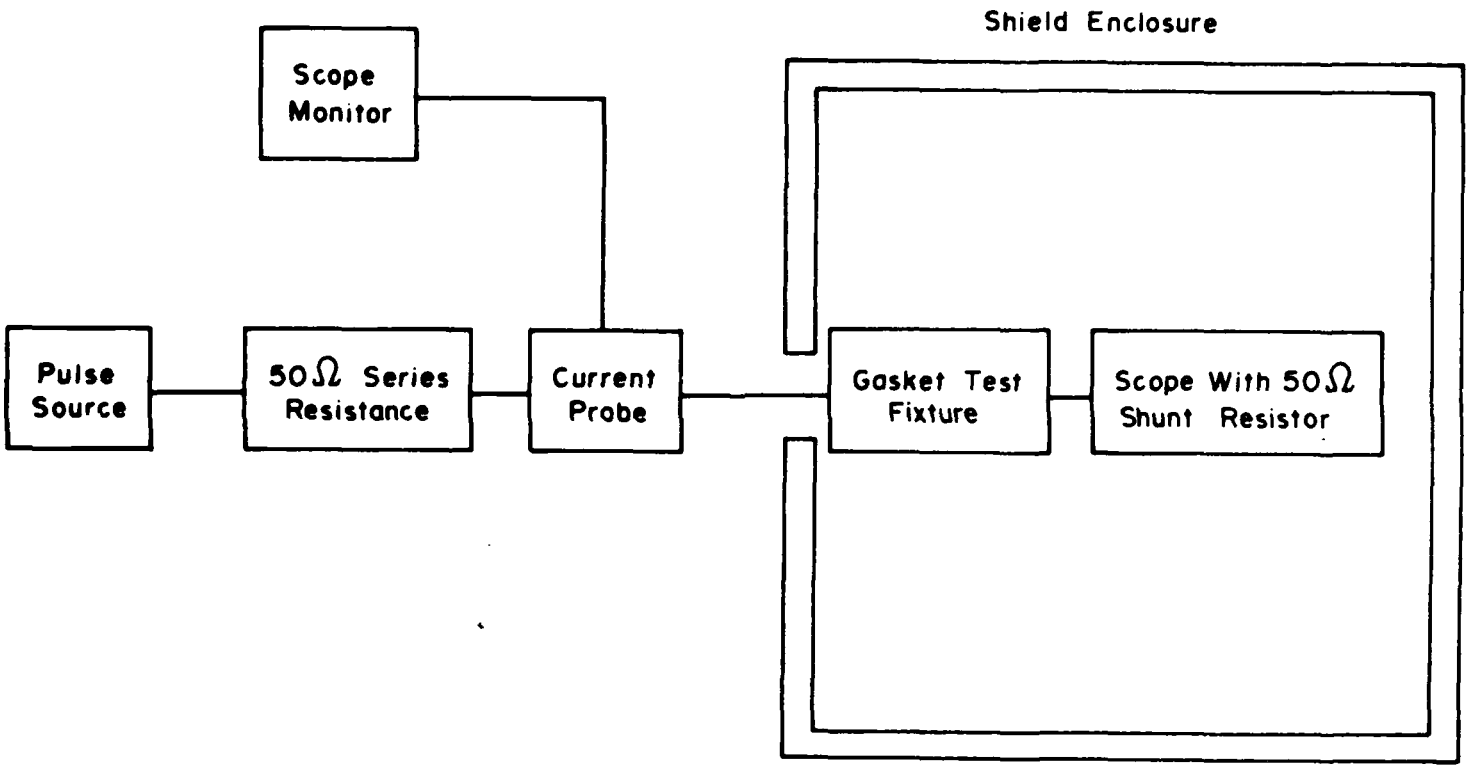

Figure 7-7. Preferred test setup for gaskets.

capacitance between the two plates should be taken into account in the calculation of the transfer impedance or the transfer figure of merit.

If the gasket is lapped, its performance may depend on the care with which the lapping junction is made (see Figure 7-8). Symmetrically mount the gasket under test in the fixture. Compress it uniformly by tightening alternate diagonal screws of the fixture.

The noise level of the system should be ascertained. This may be done in several ways. The most desirable way is to form an all-welded seal between the base plate and compression plate. This is not always practical, owing to the expense of fabricating the two plates, so several alternatives may be used. One alternative is to disconnect the cable from the type N connector and attach a short-circuited connector to this end of the cable while leaving it in the immediate vicinity of the gasket tester. On applying the waveforms, note any leakage which may penetrate into the measurement equipment via the case of the source. As an additional check on the noise level of the system, the entire space available for gaskets can be filled with gasket material perhaps by means of several rings of various sizes. The gasket force is then progressively increased and a corresponding reduction in the transfer impedance should be noted. If further reduction in transfer impedance does not occur with an increase in gasket force, then the measured value may be close to the noise or leakage limits.

7.3.5 Data Format

In reporting the results of the transient tests, the following information should be given: manufacturer and type of gasket, inner and outer diameter, thickness, and other factors pertinent to the overall gasket geometry. The applied force per linear inch, the age of the gasket, the number of compression cycles it has been through and the

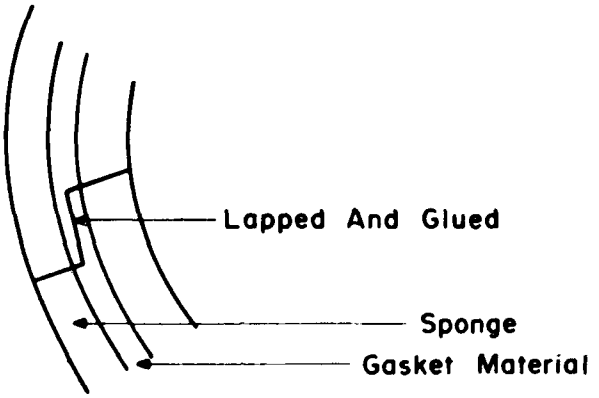

Gasket A

Figure 7-8a. Carefully lapped gasket--lapping junction barely visible.

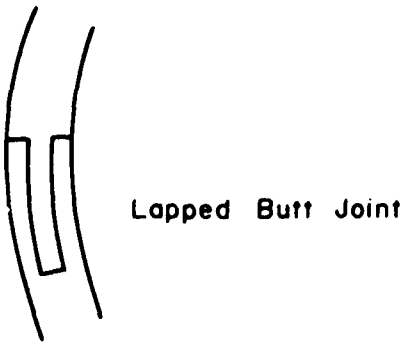

Gasket B

Figure 7-8b. Poorly lapped gasket--test jig with proper channel (groove) not available.

treatment of the contacting surfaces of the test fixture should also be noted. If the gasket is not continuous, the way in which the gasket is lapped should also be reported. The waveform of the input current and output voltages should be recorded. Typical data are shown in Tables 7-1 and 7-2. The transfer figure of merit for high performance gaskets is relatively insensitive to the waveshape of the driving waveform provided that the rise time is on the order of 10 nanoseconds or less. Where poorly performing gaskets are under test, or where the driving waveform does not meet these rise time requirements, the rise time of the test waveform should be specified along with the transfer figure of merit.

Table 7-1. Description of test gaskets.

Gasket	Manufacturer	Type	Material	Size (inches)			Lapped or Continuous
				Thick-ness	Width	Length	
A	Tecknit	Duostrip	Fluid Seal: Closed-Cell Neoprene Sponge Metal: 57% Steel, 50% Copper, 3% Tin (Technit SN/CU/FE)	1/8	5/16 Fluid Seal: 3/16	16	Lapped*
B	Tecknit	Consil-G	Conductive Silver/ Silicone Elastomer	1/4	1/4	15-3/4	Lapped*
C	Tecknit	Formed, Die #39	Silver Plated Brass	1/8	1/8	4-5/16	Continuous
D	Tecknit	Single Fin, Double Cover over Sponge #21-13816	Monel over Neoprene Sponge	1/2	1/2	13	Continuous
E	Tecknit	Standard EMI-RF	Fluid Seal: Neoprene Sponge Metal: Monel	1/4	3/8 Fluid Seal: 1/4	18	Continuous

*See Fig. 7-8

Table 7-2. Typical data and format.

Gasket	Deflection of Each of 12 Springs, in.	Applied Force lbs.(1)	Peak Input Current, A	Input Current Rise Time, ns	Peak Output Voltage (2), mV	Output Voltage Rise Time, ns	Circumference of Gasket, in.	Transfer Figure of Merit (3),	Normalized Transfer Figure of Merit, -in.
A	0.075	263	13	10	6.5	20	16.0	5.00×10^{-4}	8.00×10^{-3}
A	0.150	526	13	10	4.5	20	16.0	3.46×10^{-4}	5.54×10^{-3}
B	0.150	526	13	10	9800.0	10	15.8	0.754	11.9
C	0.150	526	13	10	3.0	30	4.3	2.31×10^{-4}	9.95×10^{-4}
D	0.150	526	13	10	38.0	40	13.0	2.92×10^{-3}	3.80×10^{-2}
E	0.150	526	13	10	7.0	40	18.0	5.38×10^{-4}	9.69×10^{-3}

NOTES:

(1) The Spring Constant of Each of the 12 Springs was 292 lbs. per inch.

(2) Minimum Detectable Signal = 1 mV.

(3) Minimum Measurable Transfer Figure of Merit = 8×10^{-5} ..

7.4 CW/Swept Frequency Test Procedure

7.4.1 Scope

Test procedures employing discrete CW waves are not recommended for general purpose gasket evaluation, except where EMP energies are concentrated in a narrow band or where the equipment to be protected has susceptibility in certain spectral regions. However, swept frequency methods using a network analyzer can be used as an alternative procedure to the transient test procedure for gaskets. The results of these two procedures can be related by a Fourier transformation. The swept frequency procedure has the following key features:

1) It is automated and fast.

2) It provides accurate and repeatable magnitude and phase data.

3) It can be used at frequencies above 100 kHz.

4) The dynamic range is about 100 dB.

5) It displays the gasket transfer impedance as a function of frequency in a single trace. The segments of the trace can be expanded for better resolution. This allows the gasket performance to be determined with good accuracy in the frequency range where the susceptibility is greatest.

7.4.2 Test Fixture

The test fixture, used in the preceding measurements, is also applicable for the swept frequency method. The details of this fixture appear in Section 7.3.2.

7.4.3 Test Setup

Figure 7-9 shows the preferred arrangement of measurement equipment for the swept frequency test procedure. The important elements are the network analyzer (Hewlett-Packard Model 8407A), the phase/magnitude display (H-P Model 8412A) and the RF sweep generator (H-P Model 8601A). The

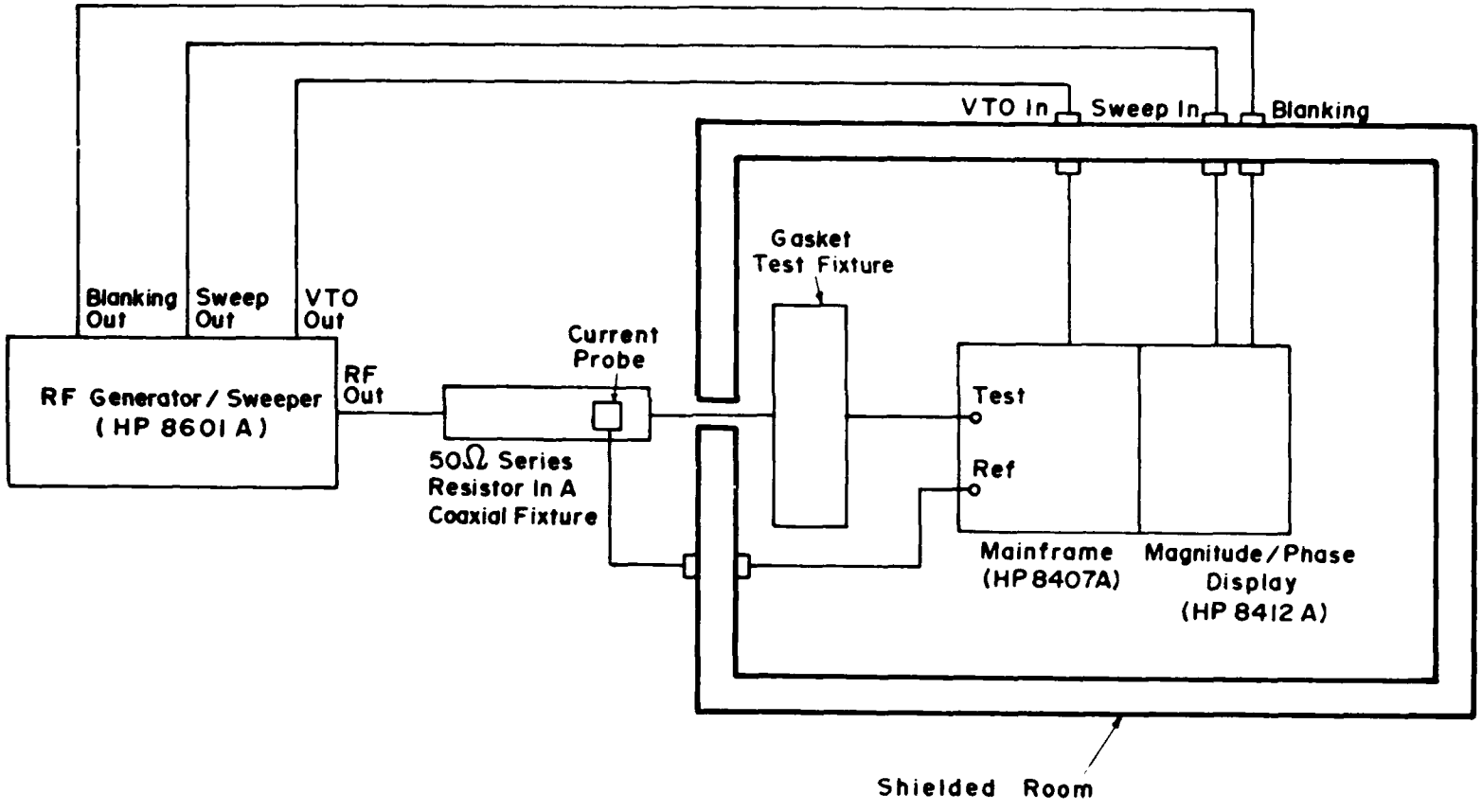

Figure 7-9. Swept-frequency test setup for gaskets.

gasket test fixture is mounted at the opening in the shielded room. The 50 Ω series resistor is mounted in a coaxial fixture with provision for monitoring the current flow. All interconnecting leads are coaxial cables.

7.4.4 Measurement Precautions

(a) The preferred arrangement of equipment shown in Figure 7-9 locates the RF source outside the shielded room and the measurement equipment inside. All signals coming into the shielded room should pass through appropriate feed throughs. The door should be closed tightly.

(b) The current probe and the network analyzer should be calibrated with a non-inductive 50 Ω load to establish that the response of their response is flat over the frequency range of interest (see References 3 and 4).

(c) The capacitance of the test fixture should be taken into account whenever the ohmic resistance between the contacting plates exceeds 3 Ω at low frequencies.

(d) The gasket under test should be properly lapped (see Figure 7-8).

(e) Symmetrically mount the gasket under test into the fixture and compress it uniformly by tightening alternate diagonal screws of the fixture.

(f) Determine the noise level of the measurement system (See Section 7.3.4 for suggestions.) Experience with swept frequency test equipment indicates that gasket transfer impedances down to the 0.1 mΩ level are measurable.

(g) Read and follow the operating instructions for the network analyzer. (See Reference 5)

7.4.5 Data Format

The characteristics of the gaskets studied should be described using a format similar to Table 7-1. Each photograph (or X-Y plot) of a measured gasket transfer impedance magnitude and/or phase should contain a list of the following:

1) Gasket type

2) Date of test

3) Spring Deflection

4) Applied Force

5) Frequency Range

6) Midscale values of magnitude and phase

7) Magnitude and phase scale factors

For ease in transcribing the data from a photograph of the display to other forms, at least three frequency ranges should be used. Experience shows that ranges of 0.1 MHz to 2.1 MHz, 1.0 to 21.0 MHz and 1.0 to 101.0 MHz are convenient.

It is recommended that a graphical presentation of the final data either Z_T or Z_{TN} be prepared in log magnitude vs log frequency and phase angle vs log frequency formats.

7.5 References

1. Chang, Hsi-Tien, "Interaction of Electromagnetic Radiation with an Airplane," Paper presented at Symposium on Electromagnetic Hazards, Pollution, and Environmental Quality, 1972.

2. "EMP Penetration Through Imperfectly Conducting Gaskets in Hatches, Part 1," Joint EMP Technical Meeting, First Annual Nuclear EMP Meeting, NEM, 1973, DNA 3609 P-3.

3. "Swept Frequency Impedance with the 8407A Network Analyzer, 0.1-110 MHz," Hewlett-Packard Application Note AN 121-2.

4. "Operating Note, Passive Probe Kit, 11654A," Hewlett-Packard, September 1970.

5. "Operating and Service Manual, Network Analyzer, 8407A," Hewlett-Packard, December 1971.

7.6 Bibliography

1. Air Force Weapons Laboratory, Electromagnetic Pulse Sensor and Simulation Notes series, June 1970.

2. Armour Research Foundation, EMC Lecture Series for WPAFB, August 1961, AF33(616)-8527.

3. Chang, Hsi-Tien, "Interaction of Electromagnetic Radiation with an Airplane," Symposium on Electromagnetic Hazards, Pollution and Environmental Quality, 1972.

4. Defense Nuclear Agency, EMP Awareness Course Notes, DASA01-69-C-0095, August 1973, Chapter VII.

5. Eckersley, A., "Transfer Impedance Across Interfaces Containing Conductive Gaskets," Joint EMP Technical Meeting, First Annual Nuclear EMP Meeting, NEM, 1973, DNA 3609 P-3.

6. Ehrreich, J.E., "Plastic RF Shielding Forms Based on a New Conductive Filler," Fifth National Symposium on Radio-Frequency Interference, Institute of Electrical Engineers, 4-5 June 1963, Philadelphia, Pennsylvania.

7. Good, T.M., "A Method of Evaluating the Effectiveness of Radio-Frequency Gasket Materials," Fifth Conference on Radio-Frequency Interference Reduction and Electromagnetic Compatibility, Armour Research Foundation, October 1959.

8. Schreiber, O.P., "RF Tightness Using Resilient Metallic Gaskets," Proc. of the Second Conference on Radio-Frequency Interference Reduction, Armour Research Foundation, March 1956.

9. Schumpert, T.H., "EMP Penetration Through Imperfectly Conducting Gaskets in Hatches," Part I, Joint EMP Technical Meeting, First Annual Nuclear EMP Meeting, 1973, DNA 3609-P3.

10. Awerkamp, D.R., "A New Idea for Determining RF Gasket Attenuation," Proceedings of the Eighth IEEE Symposium on EMC, San Francisco, California, 1966.

8. TEST PROCEDURES FOR EM VENT SHIELDS

TABLE OF CONTENTS

8. TEST PROCEDURES FOR EM VENT SHIELDS

8.1 Introduction

An EM Vent Shield is a fixture in the wall of an EMP shielded enclosure designed to allow the passage of air while preventing a significant penetration of electromagnetic pulses or other classes of electromagnetic waves below 100 GHz.

The purpose of this preferred test procedure is to measure the electromagnetic performance characteristics of a vent shield or screen which are of significance from an EMP viewpoint. Nonelectrical effects, such as the vent's ability to withstand weather, temperature changes, corrosion, and vibration, as well as other related environmental factors are not considered in this report, but must be taken into account by the design engineer concerned with the overall system.

The following procedure will give useful results in a number of areas, especially where the vent is considered as an individual component. Possible uses are envisioned as follows:

1. The design engineer may find the procedures a useful technique to evaluate the relative performance of various classes of vents.

2. For critical situations, the test procedure can be used as a guide for evaluating the vent performance for other expected environmental conditions.

3. The test procedure results can provide a system interaction analyst with a fairly realistic measure of the intrinsic performance characteristics of the EM vent.

4. Vent manufacturers should employ these or comparable uniform measurement procedures to optimize vent design for EMP purposes and to present results in data sheet format.

5. In conducting manufacturing quality control or part acceptance tests, the procedures can be used as a guide for simple quick-look tests.

6. In assessing EMP degradation with age, the procedure can be used as a guide to measure, on a relative basis, the aging characteristics of EM vents.

8.2 General

8.2.1 Characteristics of Vents and Screens

Air vents and screens permit field penetration in two ways. First, they allow some penetration of the external electric and magnetic fields. Second, their inclusion creates added defects such as seams and small apertures and, also, a region of reduced conductivity and permeability. It is important, therefore, in evaluating a vent or a screen to measure both the electrical and magnetic field penetration characteristics through the vent. The system designer, however, must assess the effects of reduced areas of conductivity and possible permeability as a result of including a vent or screen. This is a minor consideration if the vent size is small compared to the size of the shielding enclosure.

8.2.2 Construction of Vents and Screens

High-performance electromagnetic vent shields are usually of the "honeycomb" design, although other designs are also in use. An example of a honeycomb vent is illustrated in Figure 8-1. The cells of the honeycomb are made small enough so that they are operated essentially as "waveguides below cutoff." Materials utilized are typically the high-conductivity metals such as aluminum, brass, or steel.

The basic construction method of the honeycomb or screens is of prime importance. The better-performing honeycombs or screens have conductivity which is uniform or nearly so in all directions in the plane of the vent. This is usually achieved by welding, soldering, or galvanizing the honeycomb or screen assembly such that nearly uniform conductivity is achieved. Less expensive constructional methods are also employed, particularly for the aluminum type honeycomb panels. In this case, the aluminum honeycomb is formed by gluing overlapping layers of very thin aluminum sheets. As a consequence, in the plane of the panel, a higher conductivity exists in one direction than the other. Such glued-together aluminum

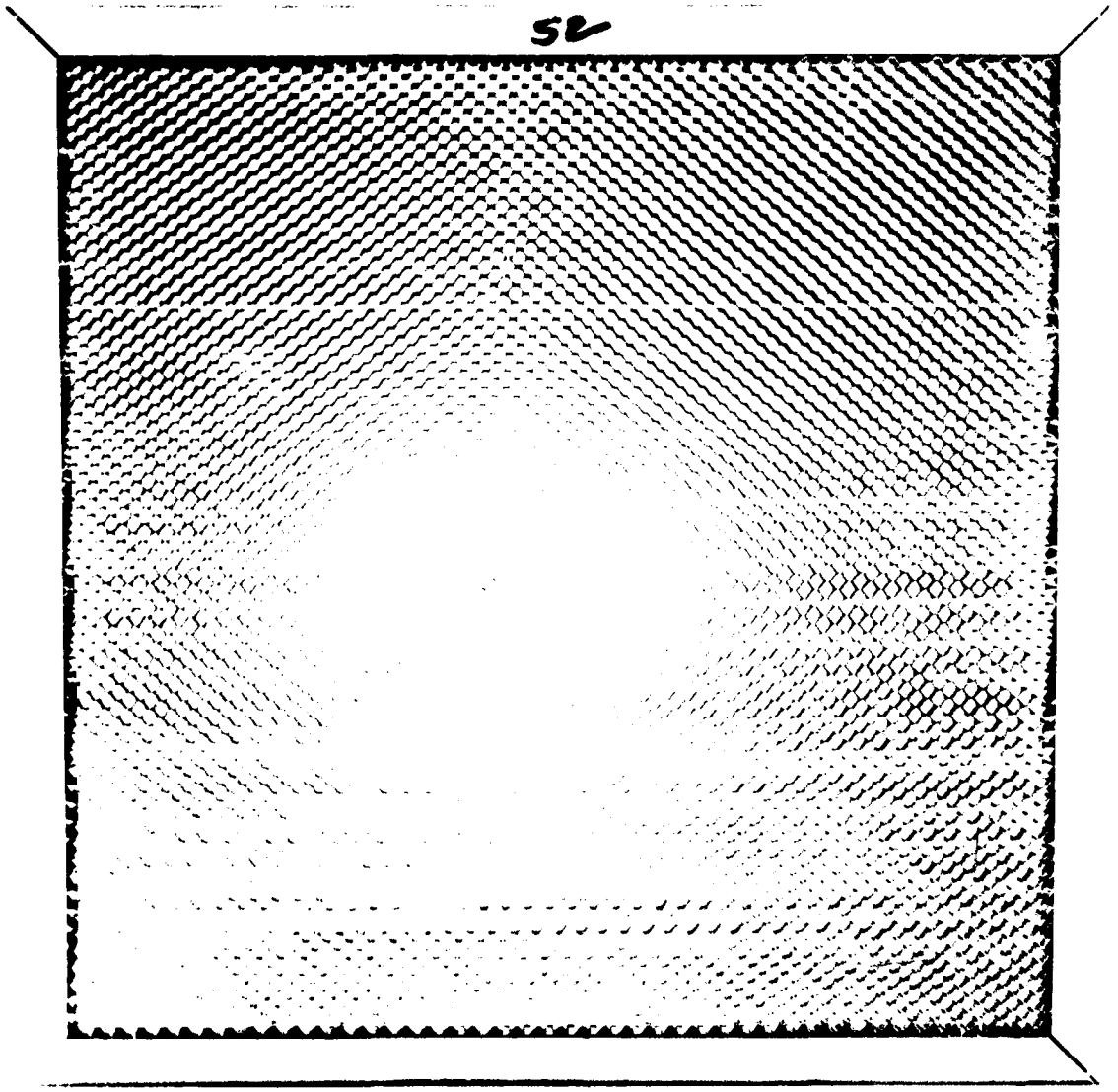

Figure 8-1. Typical honeycomb vent.

honeycomb screens are less expensive than the galvanized or soldered-after-fabrication type steel or brass vents. These aluminum vent screens exhibit noticeably poorer H-field protection and are sensitive to the direction of current flow across the vent.

Conceivably, vents or apertures could also be protected by ordinary wire screens. The best screen is one which is galvanized after weaving such that good conductivity exists at each wire contact point.

Also of prime interest is the way in which the honeycomb or screen is attached to the shielding enclosure. High-conductivity contacts between the vent shield or screen and the wall of the enclosure are highly desirable. This is often difficult to achieve in practice. Often the fabricator of the vent shield supplies it in some from of mounting bracket. The designer should examine the nature of the bracket to assure that high-conductivity contacts are made between the bracket and the vent shield.

8.2.3 Performance

In order to properly assess the performance of a vent shield as a simple component, it is necessary to understand how the vent shield performs in a shielded enclosure. Figure 8-2 shows the currents and fields on the exterior of an enclosure, a brief interval of time after this enclosure has been illuminated by an electromagnetic pulse. Note that there is a tangential H field and a perpendicular electric field. Scattered fields other than this are generally of little EMP interest. For example, a propagating wave impinging on the enclosure quickly sets up the tangential H and perpendicular E fields near the enclosure, at frequencies below 100 MHz.

Above 100 MHz, and particularly in the microwave region, the propagating wave concept may be applicable, where the wavelength of the propagating energy is small compared either to the vent size or size of the holes within the vent.

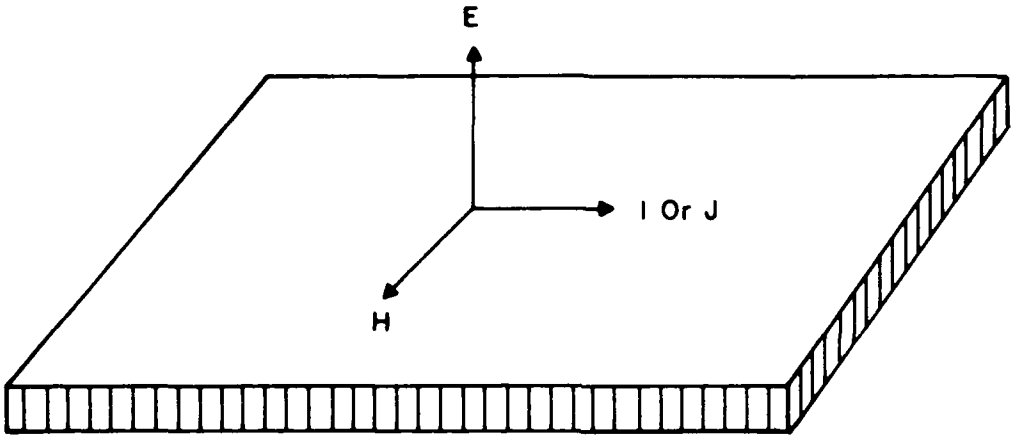

Figure 8-2. Orientation of fields very near a highly conducting surface.

Another case of interest is a magnetic field which, in the absence of a vent in the enclosure, would be nearly perpendicular to the enclosure wall or vent face. This does not usually occur in regions near vents except where fortuitously introduced by the presence of cable loops. Even if this does occur, the fields in the immediate vicinity of the vent are generally predominantly tangential H fields and perpendicular E fields, particularly in the case of high-performance enclosures and vents. Where the perpendicular magnetic field shielding characteristics appear to be of interest, this measurement may be made by modifying the small-loop test procedure described in Section 10.4.

Once a vent has been installed in the enclosure, the question arises as to how the installation of a particular vent material having a certain shape and size affects the performance of the enclosure. The insertion of an open aperture in the wall of the enclosure creates the presence of an equivalent electric or magnetic dipole which is a function of the perpendicular electric or tangential magnetic fields at distances a few mean diameters away from such an aperture. A mean diameter is defined as the diameter of a circle whose area equals the area of the vent. Assuming the aperture and enclosure to be electrically small, and the enclosure size large compared to the aperture, the fields introduced into an enclosure fall off exponentially. Thus, the introduction of a single small aperture well away from the sensitive equipment within the enclosure might not seriously affect the performance. It must be emphasized, however, that any equipment or cables appearing in the vicinity of the vent will be illuminated much more strongly than equipment located more distant from the vent.

The system or equipment designer should recognize that the major coupling effects arise from the time-varying nature of the penetrating fields. Therefore, performance measures must consider not only the magnitude of the penetrating fields, but the waveform or at least the rise time of these fields.

With the foregoing considerations in mind, it appear that the most desirable test procedure from an EMP viewpoint would be to test the vent's performance in response to tangential magnetic and perpendicular electric fields. In addition, different vent sizes will be encountered and some means to normalize the measurement for different sizes of apertures or vents appears to be desirable.

To accomplish these goals, the preferred test procedure creates tangential magnetic and perpendicular electric fields by means of a parallel plate or triplate line placed just outside of a test enclosure. When comparing the performance characteristics of different classes of vent materials, it is preferable to use the same size of shielding vents. Where this is impractical, it appears desirable to normalize the vent measurements. For minor variations in sizes, this may be approximated by making the measurement point for the penetrating fields on a line perpendicular to the plane of the vent shield through its center, at a distance equal to one-half the mean diameter. Figure 8-3 illustrates the basic measurement concept.

With the basic measurement arrangement as illustrated in Figure 8-3, vent performance is measured by developing, for a specified applied test waveform, the ratio of the time derivative of the magnetic field* appearing within this shielded room when the vent shield is absent to that which appears in the room when the vent is installed. Absolute values of the magnetic fields may also be measured, generally by a single frequency type of illumination rather than pulses. If modeling the performance from an analytical viewpoint is desired, then measurement of the exterior fields in the immediate vicinity of the vent is also necessary, along with the absolute calibration of the field sensors.

*The vector orientation of the magnetic vector is usually the same as the orientation in the absence of the vent. The sensor orientation should be changed in any event, to measure the maximum value.

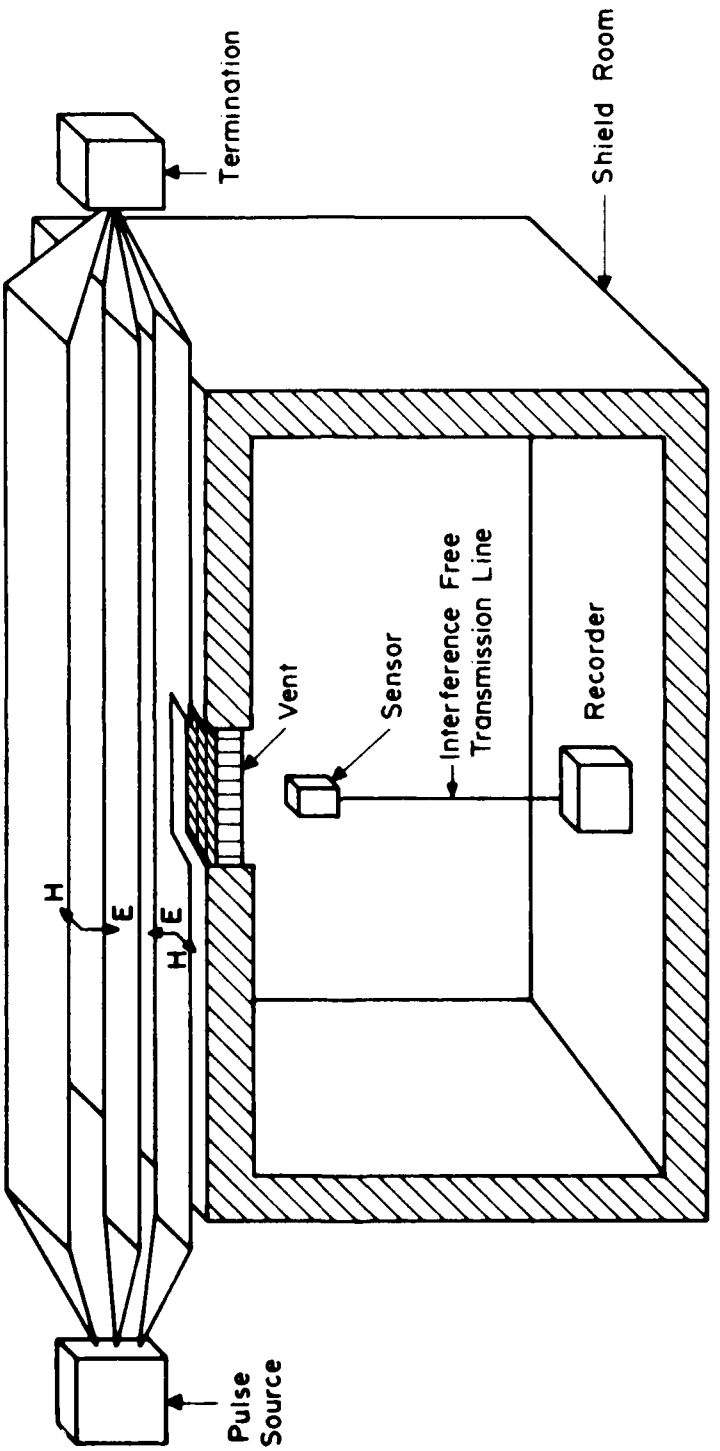

Figure 8-3. Basic measurement concept.

The ideal conditions for conducting this test require the mean diameter of the vent to be small compared with the smallest wavelength of interest. Ideally, the height of the center conductor of the triplate line should be equal to or larger than one-half the vent's mean diameter. In addition, the interior walls of the enclosure where the sensor is located should be six mean radii or greater away from the test area. Where relative performance of vents is being evaluated using the same test arrangement, the factors just mentioned may not be of importance. However, when comparing the performance of vents measured in different test facilities, significantly different variations in the aforementioned parameters should be considered when results are to be correlated.

The problem of cavity resonances has also been postulated as a possible source of comparison errors between measurements at two different facilities. Experimenters employing pulse techniques using measurement arrangements similar to that shown in Figure 8-3 have not encountered resonance problems when the sensor is always very close to the vent. In the case of CW measurements, resonance problems may be similarly suppressed, although longer dwell times at a single frequency may cause resonant buildups not encountered when pulse excitation is employed.

A simple transient test waveform is suggested where relative performance measurements are of prime interest. However, the test waveform may well have significant variation from the tangential magnetic and perpendicular electrical surface field waveform found on the exterior of an enclosure when excited by an EMP pulse. For example, the suggested double exponential test waveform is loosely related to the EMP from an exoatmospheric burst. The EMP from a near-surface burst may contain more low-frequency components. If this is the case, low frequency components can be added to the test waveform by increasing the fall time. In the case

of isolated enclosures, the surface fields are often in the form of very rapidly damped sinusoids. Moreover, the values and waveforms of the surface fields are different at different locations upon the surface. For example, the low-frequency fields are greatly enhanced near corners of a box-like enclosure. The proximity of nearby conductors, and the attachment of pipes or cables, will also affect the surface field waveforms. Therefore, unless a very complete and rigorous analysis or test of the composite structure containing a vent shield is made, it does not appear appropriate to use anything but the simplest form of a test waveform.

8.2.4 Definitions

A distinction must be made in defining the performance of a vent as to whether the fields measured are CW or pulse. If pulse, the general nature of the waveforms must be specified.

The CW relative shielding effectiveness of an EMP vent is defined as the ratio of the electric or magnetic fields appearing within the shield room when the hole for the vent is left open to that appearing when the vent is installed. It is assumed that the pickup sensor is located on a line perpendicular to the plane of the vent running through its center. The distance from the vent to the sensor is one-half the mean diameter 2a of the vent. It is convenient to express the shielding effectiveness in dB as given by the following formulas:

CW relative electric field shielding effectiveness

$$S.E.(\omega)_E = 20 \text{ Log}_{10} \frac{E_o(\omega)}{E_i(\omega)} \quad (8\text{-}1)$$

CW relative magnetic field shielding effectiveness

$$S.E.(\omega)_H = 20 \text{ Log}_{10} \frac{H_o(\omega)}{H_i(\omega)} \quad (8\text{-}2)$$

where $E_o(\omega)$ and $E_i(\omega)$ are the measured electric field intensities, respectively, without and with the vent and where $H_o(\omega)$ and $H_i(\omega)$ are the measured magnetic field intensities,

respectively, without and with the vent. The measurements apply to a single frequency CW-type illumination at a frequency of ./2=. The vent size is also small compared to a wavelength and the basic dimensions of the outside field excitation structure.

In the case of transient waveforms, other definitions are of interest, such as the peak electric field shielding effectiveness and the peak magnetic field shielding effectiveness. This is the ratio of the peak value of the field appearing within the shield room when no vent is present to that appearing when the vent is installed, for a specified pulse illumination. This definition is most appropriate for the electric field because this penetration is generally via small apertures such that the rise time of the interior field will closely approximate the rise time of the exterior field. These quantities are defined in dB as follows:

Peak electric field shielding effectiveness

$$(SE)_{E\text{-}P} = 20 \text{ Log}_{10} \frac{E_{o\text{-}P}}{E_{i\text{-}P}} \qquad (8\text{-}3)$$

Peak magnetic field shielding effectiveness

$$(SE)_{H\text{-}P} = 20 \text{ Log}_{10} \frac{H_{o\text{-}P}}{H_{i\text{-}P}} \qquad (8\text{-}4)$$

where $E_{o\text{-}p}$ and $H_{o\text{-}P}$ are the peak values of the fields measured in the absence of the vent and $E_{i\text{-}P}$ and $H_{i\text{-}P}$ are the peak values of the measured fields with the vent installed, using a specified illuminating test pulse waveform.

Another definition more appropriate for the magnetic field is the peak H-dot (or $\dot{H}$) shielding effectiveness (the time rate of change of the magnetic field shielding effectiveness). This is defined as the ratio of the peak value of time rate of change of the magnetic field within the shield room when no vent is present to that appearing when the vent is installed for the physical arrangement previously described. It should be recognized that the $\dot{H}$ shielding effectiveness under such a definition is a function of the waveform of the

applied field. Therefore, this definition should be used in the form of the test pulse waveform.

$$\text{Peak } \dot{H} \text{ shielding effectiveness} \qquad (SE)_{\dot{H}\text{-}P} = 20 \text{ Log}_{10} \frac{\dot{H}_{o\text{-}P}}{\dot{H}_{i\text{-}P}} \tag{8-5}$$

where $\dot{H}_{o\text{-}P}$ and $\dot{H}_{i\text{-}P}$ are the time rate of change of the observed magnetic field intensity, respectively, without and with the vent.

9

3.2.5 Equivalent Dipole Model

For a circular aperture of radius a, the components of the electric and magnetic fields inside a very large shielded space (see Figure 8-4) due to an exterior electric field, E_o, perpendicular to the metallic surface, and an incident magnetic field, H_o, parallel to the surface, are

$$E_r = \frac{2E_o a^3 \cos \theta}{3\pi r^3} \tag{8-6}$$

$$E_\theta = \frac{E_o a^3 \sin \theta}{3\pi r^3} \tag{8-7}$$

$$E_\phi = 0 \tag{8-8}$$

$$H_r = -\frac{4a^3 H_o}{3\pi r^3} \sin \phi \sin \theta \tag{8-9}$$

$$H_\theta = \frac{2a^3 H_o}{3\pi r^3} \sin \phi \cos \theta \tag{8-10}$$

$$H_\phi = \frac{2a^3 H_o}{2\pi r^3} \cos \phi \tag{8-11}$$

This same set of equations can be used to form an equivalent dipole model of the EMP fields that penetrate a vent. The adjustable parameter is the radius a, the effective aperture size. One value of a can be determined from a measurement

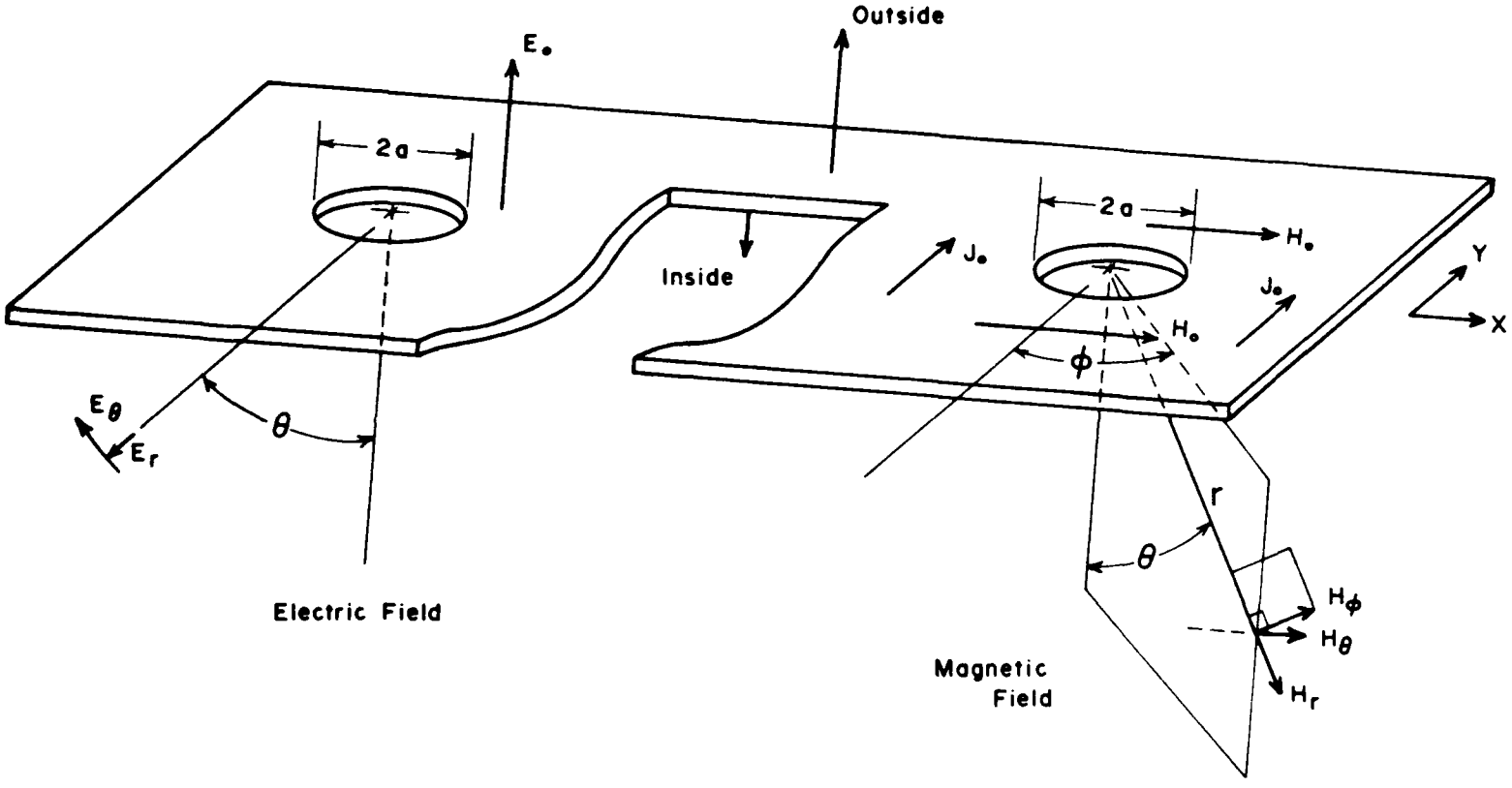

Figure 8-4. Geometric definition for quasi-static penetration through aperture.

of the electric field at a point r, θ, ϕ, such as $\frac{1}{2}D_m$, 0, 0. Another value of a can be derived from magnetic field measurements, since the vent is not expected to have the same effect on the external electric and magnetic fields. Furthermore, a third measurement of the magnetic field case should be made after the vent has been rotated by 90^o if the vent is expected to have asymmetric conductivity.

8.2.6 Types of Tests

Two types of test procedures are set forth--pulse and CW. The pulse tests are recommended as a preferred test procedure because of the transient nature of the EMP and because of their basic simplicity. This is consistent with most design and evaluation requirements. The basic procedure is also amenable to CW-type testing methods, and these are presented on an optional basis where detailed performance requirements warrant their use. Two pulse-type measurements are considered; that of the penetrating electric field and the time rate of change of the penetrating magnetic field. These provide a quick and simple measure of the performance of the vent shield under transient illumination. It must be noted, however, especially in the case of penetrating magnetic fields, that these measures of performance must be considered in the context of a specified illuminating type waveform. In the case of the CW measurements, the magnitudes of both the electric and magnetic field shielding are measured. If absolute measurement data are taken, the results can be used to model the interior fields as equivalent magnetic and electric dipoles.

8.3 Transient Test Procedure

8.3.1 Scope

This procedure is intended to develop on a rather simple quick-look type basis, the approximate shielding characteristics of typical vents and screens which might be used to provide shielding of apertures in shielded rooms. As such, it is assumed that the maximum dimension of the vent to be shielded is considerably smaller than the smallest wavelength of interest which is, generally, on the order of three meters. The procedures are readily amenable to developing the relative performance characteristics of different vents, and with care can be extended to absolute measures of performance. To facilitate relative performance comparisons on a transient basis, a standard type transient waveform is suggested. This waveform is relevant to the spectral components associated with the EMP from an exoatmospheric detonation. Where other than exoatmospheric detonations are likely, or where severe damped sinusoidal ringing can occur, other transient type test waveforms must be seriously considered.

8.3.2 Suggested Test Fixture

Figure 8-5 illustrates the basic details of the suggested test fixture. It shows one method of applying the E- and H-fields to the test vent. The test fixture uses what is often called a triplate line. This line can be excited from any number of pulse-type sources, and must be terminated in its characteristic impedance. The triplate line has the advantage of containing most of the fields to its interior, thereby minimizing shielding requirements. It is mounted on the outside of the shielded room as is shown in Figure 8-6. A shielded box or shielded enclosure is attached to one of the outer sheets of the triplate strip line as illustrated in Figure 8-5. A rectangular hole is cut into both the shielded enclosure and one side of the

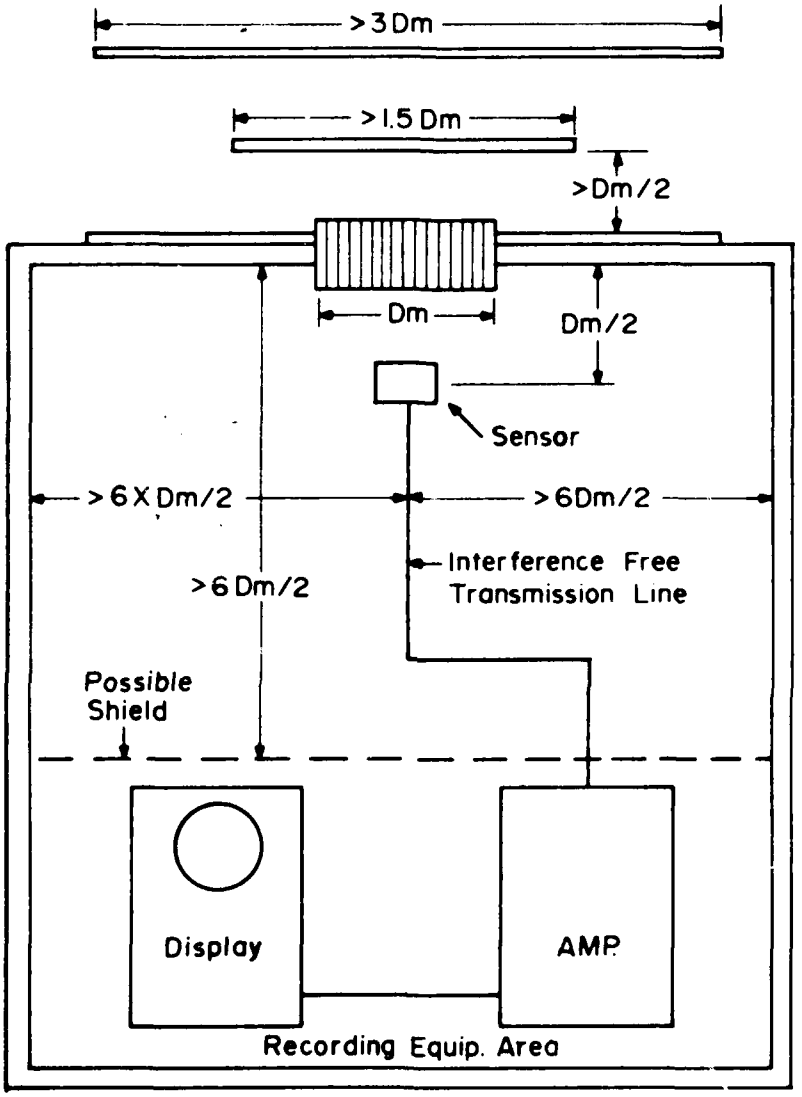

Figure 8-5. Suggested test fixture.

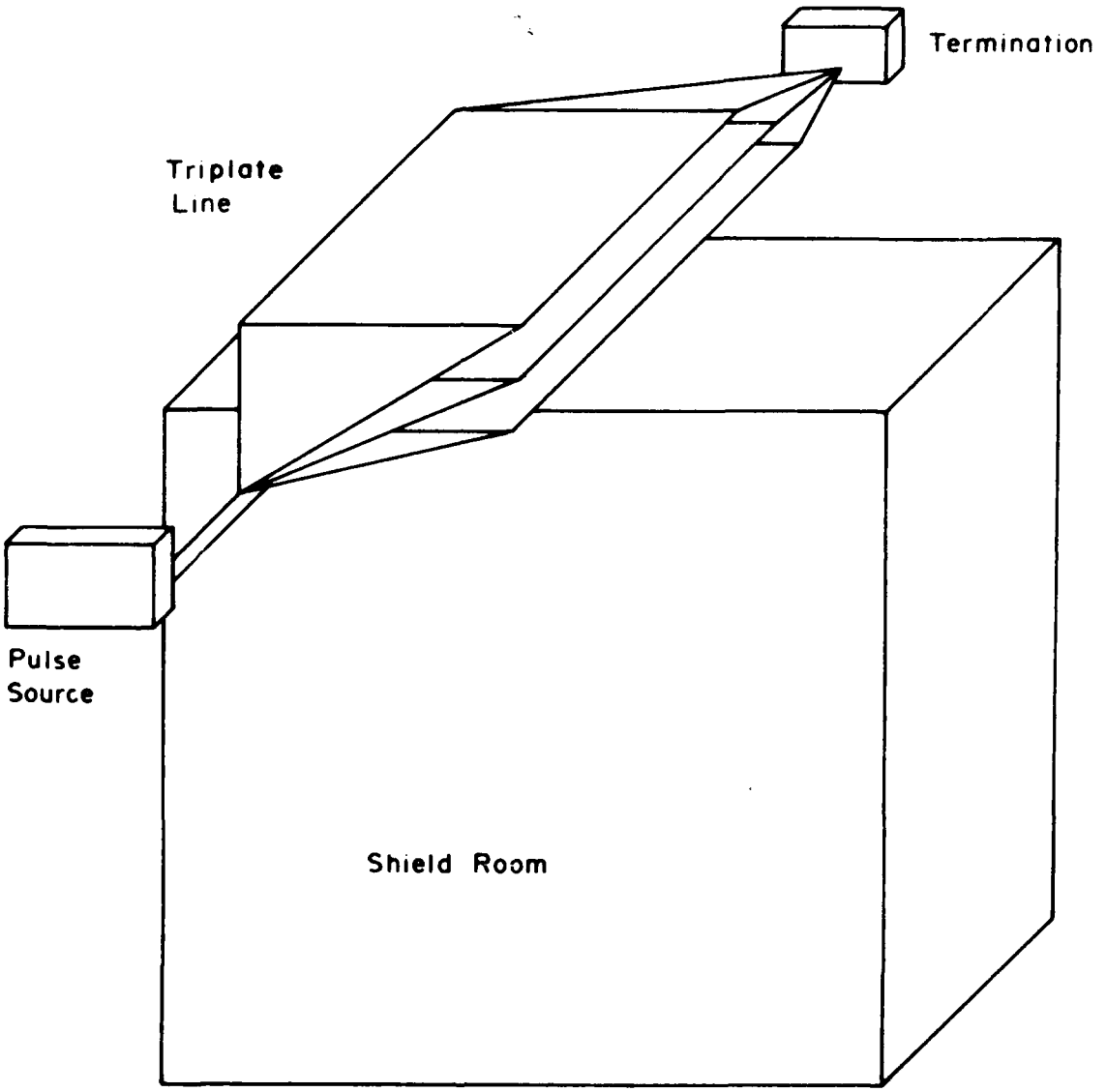

Figure 8-6. Suggested external test.

triplate line to accommodate the test vent. Ideally, the dimensions of the shielded enclosure should be such that the shielded wall is at least six mean vent radii away from the vent hole. In addition, the height of the triplate line should be at least one-half the mean vent diameter. Other restrictions on design are noted in Figure 8-5.

The dimensions of the triplate line shown in Figure 8-7 are chosen to give a 50-ohm characteristic impedance while being consistent with the size of vents to be tested (9" x 9"). Other impedance levels may also be chosen. It is important, in order to minimize problems in determining the field levels in the triplate line, that its characteristic impedance be well matched to the impedance of the dummy load. If reflections occur, they will distort the ratio of the magnetic-to-electric field in the vicinity of the vent. The reflections should be minimized by measuring the reflected wave with reflectometer techniques or by conventional methods. It should be emphasized that other dimensions of the triplate line, convenient to the particular measurement situation at hand, may also be used.

8.3.3 Measurement Equipment

The basic measurement equipment consists of two wide-band oscilloscopes having a 150-MHz response, an oscilloscope camera, broadband electric and magnetic field sensors along with suitable probes, line terminations, and cables.

The E-field sensor should be electrically floating with respect to ground, should be small and have no conducting cables attached to it. If such cables are attached to it, these cables will distort the penetrating electric field. Therefore, a battery-operated pickup device employing a fiber optic telemetry unit should be employed. Fiber optic telemetry systems are commercially available from Develco and other sources. The selected unit should have a 100 MHz bandwidth, although system with a 30 MHz bandwidth can be

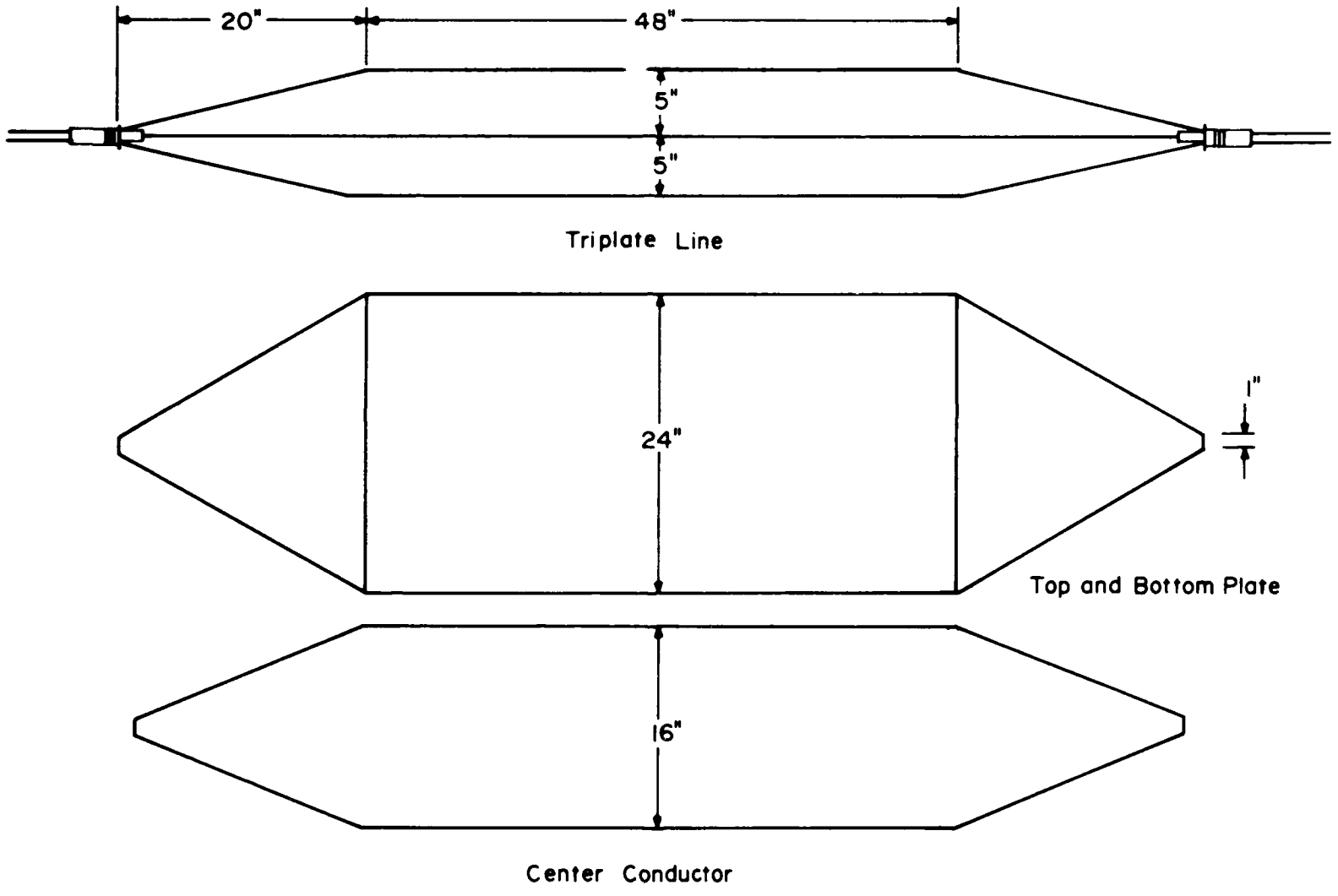

Figure 8-7. Possible 50Ω triplate.

used with some loss of high frequency data. The basic electric field sensor may be in the form of an electrometer.* The electrometer, as used for EMP purposes, often consists of an electrically short monopole operated with respect to a counterpoise or large ground plane. The output of the monopole is connected via a very short coaxial cable to a low capacitance, high input impedance amplifier. The amplified waveform is proportional to the time-history of the electric field for the higher frequency components where the input impedance of the amplifier is essentially capacitative. Balanced dipole versions are also possible. Fundamental descriptions of the operation of the electrometer appear elsewhere.[1,2,3] An essential requirement of the operation of the electrometer, is that the magnitude of the input impedance to the amplifier following the electrometer should be large, and the impedance must be essentially capacitive across the frequency band of interest. The fiber optic telemetry systems which are commercially available are readily modified into an electrometer configuration. One such configuration of a Develco unit is shown in Figure 8-8. It is desirable that the overall dimensions of this particular pickup device, including the telemetry transmitter, should be small compared to the dimensions of the vent. The pickup from the electrometer is relayed via the fiber optic link to a receiver, which need not be electrically floating. Obviously, the display devices, receiver, and other ancillary equipment within the shielded room should be located as far away from the vent as possible. A separation of at least three mean vent diameters is recommended. The output of the fiber optic received is connected to an oscilloscope, and provision is made for photographic recording of the output waveform.

As an alternate, a single-ended (non-floating) electrometer may be employed. In this case an unbalanced or monopole

*A dipole amplifier combination

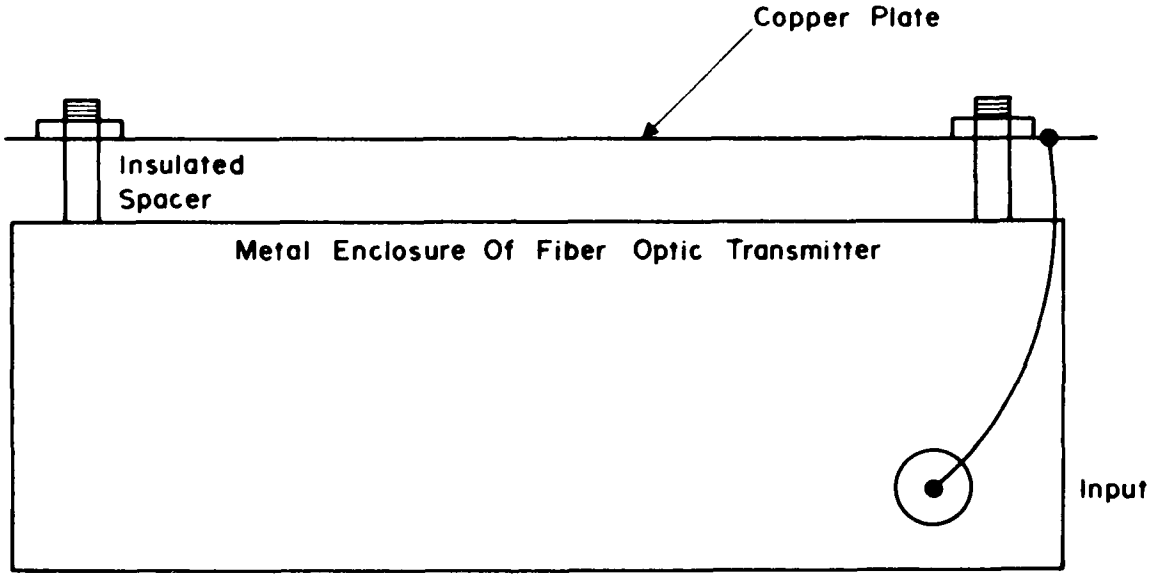

Figure 8-8. Suggested E-field sensor and fiber optic transmitter combination.

configuration can be employed. This sensor is placed next to the vent such that the counterpoise for the monopole is formed by the wall of the shielded room. The sensor is then connected to a broadband high impedance load such as the probe of a Tektronix 454 oscilloscope.

The H-field sensor can take any number of forms either as a magnetic field sensor or time-rate-of-change-of-magnetic-field sensor. In both cases, this sensor should be shielded against electric field pickup. The output of the magnetic field sensor can be connected via a hardwire link to a signal conditioning preamplifier and then to the recording oscilloscope previously described, using a high-performance, well-shielded cable. More complete descriptions of magnetic-field sensors are available elsewhere.[1,2,3]

Care should be taken to assure that the characteristics of a magnetic field sensor are well understood. A small loop sensor which is electrostatically shielded generally responds to the time rate of change of the magnetic field in the lower frequency regions, while the response is often proportional to the magnetic field in the higher frequency regions. It is possible to overcome this difficulty by more complex designs[1,2,3] or by reducing the size of the loop at the expense of sensitivity. Where the magnetic sensor takes the form of a simple loop, it may be desirable to compensate for the response variations with frequency (that is, deviation from a B-dot sensor or B-field sensor) by means of a compensating network[4] of by subsequent analysis of the observed waveforms.

The characteristics of the pulser are also of interest. A pulse source capable of measuring the characteristics of typical vents should have a peak output voltage on the order of 10,000 volts. The suggested test waveform for the quick-look evaluation of the performance of shielded vents should have a rise time of approximately ten nanoseconds and a fall

time of approximately one microsecond. Pulse sources approximating these requirements are commercially available. A repetitive mode of operation is also desirable.

The important characteristics of the dummy load which terminates the triplate line are its impedance, which should match the characteristic impedance of the triplate line, its peak power rating and, for convenience, provision for monitoring the voltage with conventional oscilloscope probes. Such dummy loads are commercially available.

Broadband oscilloscopes, having a bandwidth of 150 MHz, are commercially available. In the case of magnetic field measurements, using small loop-type sensors, a low noise (possibly balanced input) preamplifier may be advantageous. Provision for synchronizing the display with the pulse may be desirable to increase the dynamic range. Where very high dynamic range measurements are required, a signal integration oscilloscope, coupled with the use of a repetitive pulse source, may be needed.

8.3.4 Field Sensor Characterization

It is necessary that the E- ahd H-field sensors be tested to establish their frequency response, linearity and dynamic range. It is desirable, but in most cases not necessary, that an absolute calibration be performed. This may be done by inserting the sensor in the triplate or an equivalent parallel-plate line. This line must be terminated appropriately to avoid reflections. In the case of transient measurements, the EMP test waveform or similar waveform is applied to the particular line. The electric field in such lines is equal to the height of the line divided by the potential between the outer and inner plates or between two plates, as the case may be. The magnetic field is equal to the electric field divided by the characteristic impedance of free space. Such a calibration procedure may be done conveniently by removing the vent (as

shown in Figure 8-5) and inserting the E- or H-field sensor into the area between the inner plate and outer plate. The vent should be replaced by a solid shield having a hole for the cable to the sensor. Where this is done, the magnetic field sensor should be shielded against the electric field. The electric field shielding effectiveness of the sensor can be evaluated approximately by rotating the sensor in the field such that the plane of the sensor is parallel to the magnetic field within the triplate line (perpendicular to the axis of the line).

The frequency response is established by comparing the observed sensor output with the waveform present at the termination of the triplate or parallel-plate line. If the waveforms have identical shapes, then the sensor output can be used to measure the fields directly, no correction or compensation is needed. An H-dot sensor should accurately reproduce the derivative of the waveform seen at the termination of the test line. An absolute calibration requires that the sensor output be expressed as ratio to the E-, H- or $\dot{H}$-field in the line. For example, the E-field calibration would be expressed as volts per volt/meter.

It is important that the E-field sensor be operated within its linear range. This can be determined by varying the applied voltage to the triplate line in a known fashion and noting the linearity of the response of the E-field sensing system. Similar tests should also be conducted for the H-field sensor and related amplifiers. The dynamic range of the sensor is defined by the maximum signal for which the response is linear, or at least can be related to an impressed field, and the minimum detectable signal.

8.3.5 Measurement Precautions

It is important that the shielding effectiveness of the test enclosure mounted to the triplate line be relatively high to insure that leakage fields from the pulse

source, triplate line, related cables, and terminations do not adversely affect the measurements. The extent of this problem can be determined by replacing the vent by a solid plate and observing responses. The arrangement of the cables in the room and exterior to the room should be changed to see if the signals change. If such signals change, remedial action is required. To avoid reflections, all interconnecting cables should be terminated in their characteristic impedance, typically 50 ohms.

The dynamic range of the system should also be measured by removing the vent and gradually reducing the output of the pulse generator such that a minimum detectable system signal is noted within the test enclosure. In some cases, the dynamic range of the system can be improved by triggering the oscilloscope via the pulse source and employing pulse-to-pulse integration.

An additional precaution concerns the bond between the actual vent screen or honeycomb and bracket surrounding the vent which is clamped or soldered to the enclosure wall. Probing-type tests should be conducted to determine how well this bond is made. If this bond is not well made, excessive signals will appear in the vicinity of this interconnection. Consideration should be given to rectifying this problem, should this have a major influence upon the measurement.

8.3.6 Data Format

After a suitable test fixture has been constructed, appropriate test equipment has been found, the sensors have been characterized and the necessary precautions have been taken, data acquisition can begin.

All data should be summarized into a table which has all the essential data required to characterize the tests that were performed as well as the final results. The

following items are especially important:

1) the vent construction, material and size,

2) the position of the vent,

3) the sensor output without a vent,

4) the sensor output with the vent,

5) the calculated shielding effectiveness.

Two vent positions should be used which differ by 90^{o}. This is done because some vents conduct better in one direction than in others. The shielding effectiveness is expressed in dB and is computed using Equation 8-3, 8-4 or 8-5, as appropriate. Table 8-1 shows typical data in a suitable format.

The summary table should also contain supplementary information about the test conditions; specifically:

1) the system dynamic range,

2) the minimum detectable signal,

3) the pulse waveform characteristics.

Photographic records should be kept to show the following:

1) the voltage at termination of the triplate line,

2) the sensor output without a vent,

3) the sensor output with the vent in place.

If the pulse source has good stability, then voltage measurements at the termination of the triplate line are required only when an adjustment is made in the pulse amplitude or shape. The same applies to the sensor output without a vent. Note that if the sensor does not have a wide dynamic range, then it may be necessary to use different pulse amplitudes with and without the vent. If this is done, the sensor response without the vent should be scaled appropriately and a footnote on the summary table should indicate that this has been done.

Table 8-1. Shielding effectiveness.

	Vent (1)	Rotation of Vent (2)	Output of Sensor without Vent, mV.(7)	Output of Sensor with Vent, mV.	Peak Shielding Effectiveness dB
H-Field Data	Aluminum	0°	1400	20	36.9
	Aluminum	90°	1400	400	10.9
	Steel	0°	1400	15	39.4
	Steel	90°	1400	19	37.3
	Solid Steel Plate	-	1400	(5)	(6)
	Minimum Detectable Signals (3)	-	-	1	62.9 (4)
E-Field Data	Aluminum	0°	3825 (8)	(5)	(6)
	Aluminum	90°	3825 (8)	(5)	(6)
	Hardware Cloth (7)	-	3825 (8)	85	33.1
	Minimum Detectable Signal (3)	-	-	10	51.7 (4)

NOTES

(1) Vent size 10" x 10", honeycomb construction, 1/2" cell size.

(2) One position of the vent is arbitrarily selected as 0°.

(3) For this measurement, the output of the pulse source was reduced until a minimum detectable signal was measured in the shield room. No vent was used.

(4) This is the dynamic range of the system.

(5) Below the minimum detectable signal level of 10 mV.

(6) Beyond the dynamic range of the system.

(7) Characteristics of the double exponential pulse are a 10 nanosecond rise time and a 1 microsecond fall time.

(8) This number has been scaled by extrapolation from the linear range of the sensor.

8.4 CW Test Procedures

8.4.1 Scope

In general, CW measurements are not recommended, owing to the tedious nature of such measurement procedures, unless swept frequency CW measurement equipment is readily available. However, CW measurements can be considered where single frequency type illumination problems are important, such as where the external currents on the enclosure are in the form of a very long damped sinusoid or where the equipment to be shielded exhibits a strong susceptibility in a narrow frequency region. Specifically, the test procedures are restricted to cases where the size of the vent is considerably less than the smallest wavelength, generally on the order of about three meters. Both the relative magnetic and electric field penetration shielding effectiveness can be measured by this procedure. Where precise analytical results are required, the field transfer characteristics can also be measured in terms of equivalent electric and magnetic dipoles.

8.4.2 Test Fixture

The measurement fixture described in Section 8.3.2 may also be used for the CW tests.

8.4.3 Measurement Equipment

The measurement equipment for the CW measurement is conceptually similar to that described for the pulse measurements, as noted in Section 8.3.3. In the case of CW measurements, it is desirable to employ the same type of broadband electric or magnetic field sensors previously described in Section 8.3.3. However, in this case, the output data recording may be in the form of a radio frequency voltmeter rather than a photographic recording. A tuned RF voltmeter should be used which has a sensitivity of less than one

microvolt for an input impedance of 50-ohm and a bandwidth of approximately 100 Hz. The CW source should have an output capability on the order of a few hundred watts to ensure adequate dynamic range. The termination must also be capable of dissipating the continuous power supplied by the CW source.

A swept frequency configuration is also possible. Appropriate instruments are a RF sweeper/generator (e.g., Hewlett-Packard E601A) and a wide bandwidth, high power RF amplifier to drive the triplate line and a network analyzer (e.g., Hewlett-Packard 8407A) to monitor the sensor signal and the voltage at the termination of the triplate line.

8.4.4 Sensor Characterization

The frequency response, linearity and dynamic range of the sensor must be determined. This can be done using a procedure similar to that given in Section 8.3.4. Discrete or swept frequencies are supplied to the triplate or parallel-plate line and a RF voltmeter or network analyzer to record the sensor output.

It should be recognized that in the case of CW measurements the possibility exists for narrow band resonances* such as might be exhibited by the enclosure. Such resonances generally do not present a problem for the pulse type measurements because of the wideband distribution of the energy. For this reason, the calibration of the sensors should also be checked independently of the test fixture.

8.4.5 Measurement Precautions

Measurement precautions noted in the case of the pulse type measurements also apply in the case of the CW measurements. As noted previously, the possibility exists for spurious enclosure resonances which would not normally be excited in the case of the pulse type measurements. Care should be taken that the increased dynamic range sometimes

*See Section 10.2.4 and Figure 10-1.

offered by such CW measurements does not introduce additional spurious noise levels which might not be apparent in the case of pulse type approaches.

8.4.6 Data Format

The data format may be similar to that presented in Section 4.3.6 except that the dB values of the electric and magnetic shielding effectiveness at each test frequency are obtained from Equations 8-1 and 8-2, respectively. If many frequencies are measured, or if a swept frequency test is done, then graphs should be prepared which show sensor response (relative to the signal at the termination of the triplate line) versus frequency. The response with and without the vent in place should be given. If the graph is prepared using a log scale for the ratio of sensor to termination voltages, then the difference between the two is the shielding effectiveness.

8.5 References

1. Air Force Weapons Laboratory, Electromagnetic Pulse Sensor and Simulation Notes, Series EMP-I, Volumes I-10, June 1970.

2. Defense Nuclear Agency, EMP Awareness Course Notes, DNA 2772T, August 1973, Chapter VII.

3. Air Force Weapons Laboratory, Electromagnetic Pulse Sensor Handbook, Volume 1, June 1971.

4. Air Force Weapons Laboratory, Electromagnetic Pulse Instrumentation Handbook, Volume 1, October 1971.

8.6 Bibliography

1. Air Force Weapons Laboratory, Electromagnetic Pulse Sensor and Simulation Notes, Series EMP-1, Volumes 1-10, June 1970.

2. Albin, A.L., "Shielding Effectiveness of Electrically Conductive Protective Coatings for Magnesium and Aluminum Surfaces," Fifth National Symposium on Radio-Frequency Interference, Institute of Electrical and Electronics Engineers, June 4-5, 1963, Philadelphia, Pennsylvania.

12 3. Angelakos, D.J., "Radio Frequency Shielding Properties of Metal Honeycomb Materials and of Wire-Mesh Enclosures," Sixth Conference on Radio-Frequency Interference Reduction and Electromagnetic Compatibility, Armour Research Foundation, October 1960.

4. Defence Nuclear Agency, EMP Awareness Course Notes, DNA 2772T, August 1973, Chapter VII.

5. Jarva, W., "Shielding Efficiency Calculation Methods for Screening Waveguide Ventilation Panels, and Other Perforated Electromagnetic Shields," Seventh Conference on Radio-Frequency Interference Reduction and Electromagnetic Compatibility, Armour Research Foundation, November, 1961.

6. Schreiber, O.P., and Monroe, W.H., "A Standard Technique for Evaluation of EMI Shielding Components," Seventh National Symposium on Electromagnetic Compatibility, Institute of Electrical and Electronics Engineers, New York City, June 29, 1965.

7. Air Force Weapons Laboratory, Electromagnetic Pulse Sensor Handbook, Volume 1, June 1971.

8. Air Force Weapons Laboratory, Electromagnetic Pulse Instrumentation Handbook, Volume 1, October 1971.

9. TEST PROCEDURES FOR COAXIAL CABLES AND CONNECTORS

TABLE OF CONTENTS

9. TEST PROCEDURES FOR COAXIAL CABLES AND CONNECTORS

9.1 Introduction

Systems which could be exposed to EMP fields are frequently interconnected by cables. The outer conductor of coaxial cables and connectors is also a shield which reduces the energy appearing at the terminals. The shield can perform three functions:

1. Carry the currents induced on a conductor exposed to EMP.
2. Attenuate the electric field.
3. Attenuate the magnetic field.

In an overall nuclear hardening program, it is necessary to ensure that the EMP signal which appears at the terminations of cable runs will not cause permanent damage or harmful transient response in the system components. Whenever there is a real possibility of a system failure, a balanced hardening program will consider both additional shielding and/or terminal protection.

The purpose of this section is to describe three laboratory measurements which will characterize quantitatively the electromagnetic penetration behavior of shields for coaxial cables and connectors. The proposed tests are to be made on short lengths of coaxial cable but are a guide to procedures for testing more complex cable systems. For example, the shield of a multiconductor cable can be evaluated by joining all the conductors together. Additional tests or analyses are then required to determine how the induced EMP signal will divide among the conductors. Sample data will also be presented.

These test procedures have the following specific uses:

1. They supply system design engineers with useful techniques for evaluating the shielding performance of coaxial cables and connectors on either an absolute or a relative basis.

2. These test procedures provide EMP interaction analysts with empirical data regarding the response of coaxial cables to the EMP environment.

3. Cable and connector manufacturers can employ the recommended tests for evaluation of cable designs, data-sheet information and production quality control.

4. Equipment manufacturers can specify minimum characteristics for cable and connector components and then use these procedures for parts acceptance tests.

5. These test procedures can be used to measure changes in shielding characteristics of coaxial cables with age, handling or exposure to adverse environmental conditions.

EMP response calculations are often performed in the frequency domain and subsequently Fourier transformed into the time domain. When the inverse transformation is to be performed values of the cable shield transfer functions are needed at closely spaced frequencies. The frequency spacing and range can be determined from Nyquist sampling theory given the duration of the EMP response and the time resolution desired. The criterion which must be satisfied in the time domain is:

$$\Delta t < \frac{1}{2f_{max}} \qquad (9\text{-}1)$$

where Δt is the time spacing and f_{max} is the maximum significant frequency in the time waveform.

In terms of the frequency spacing the following criteria must be met:

$$\Delta f < \frac{1}{2t_{max}} \qquad (9\text{-}2)$$

where Δf is the frequency spacing and t_{max} is the pulse time duration of interest.

The minimum number of frequency samples, N, is determined from (9-1) and (9-2), giving:

$$N = \frac{f_{max}}{\Delta f} = \frac{t_{max}}{\Delta t} \qquad (9\text{-}3)$$

Typically one uses twice the minimum number of samples (N) to insure accuracy. For example a 2.5 μsec pulse can be reproduced with 5 nsec resolution if the calculation uses about (using 2N as the criteria) 1000 data points in the frequency domain (1024 would normally be used in practice). These frequency points would be spaced at 200 kHz intervals up to 100 MHz. The required data could be acquired at each frequency needed for the response calculations. However, this requirement for closely spaced information can be met far more efficiently and with no loss of accuracy if the data, acquired with these test procedures, is interpolated or used to determine coefficients in analytic expressions for the shielding transfer functions.

9.2 General

9.2.1 Characteristics of Coaxial Cables and Connectors

Analytical expressions can be used to calculate the performance of a solid wall shield for a coaxial cable. However, coaxial cables very frequently have flexible outer conductors with many openings where electromagnetic fields can penetrate. These cables must be evaluated empirically. For a cable with a single layer of braid, the size and composition of the wires, the optical coverage factor, the braid angle, and the cable diameter are all important parameters affecting the shielding characteristics. Thus, every time a significant change is made in one of these variables, there may be a corresponding change in the effectiveness of the shield. Cables are also made with multiple shielding layers, the most common of these has two layers of braid which are in contact. Also available are triaxial cables and cables with a thin metallic foil, usually aluminum, under a single braid. In the case of multiple layer shields, a change in the construction of any layer, their order or spacing, can have an impact on the shielding characteristics.

13

The performance of a connector is likewise dependent on a number of factors such as the design of the backshell, the torque on the nuts in the assembly, the design of the RF connections, etc. For instance, the backshell connection to the cable shield could be soldered, crimped or a clamped termination. Connectors are available which mate with threaded or bayonet structures or without a positive mechanical connection. In addition the performance of coaxial cables and especially connectors can be affected adversely by such factors as corrosion and manufacturing defects. Thus, for both cables and connectors, the shielding characteristics must be determined empirically.

9.2.2 Performance Criteria

In selecting quantities to describe cables and connector shields, performance is given to parameters which have wide applicability and which are easy to measure in the laboratory. In particular, fundamental quantities are emphasized since they are useful as absolute as well as relative criteria. Another advantage of the chosen parameters is that the final results are not dependent on the details of the test fixture. There is one test procedure for each of the three coupling modes: sheath current, radial electric field, and magnetic field. Appendix A treats the case when the sample cable is not electrically short. In this case only linear combinations of the first two parameters can be measured. The parameters which characterize the coupling are defined below.

9.2.3 Definitions

In many cases, sheath currents caused by both electric and magnetic fields are the predominant mode of coupling. The surface transfer impedance, $Z_T(\omega)$, quantitatively relates the voltage drop (per connector or per unit length of cable) appearing on the inside of the shield to current flowing on the outside of the sheath. Consider first an incremental length, Δx, of shielded cable. The current, $I(x,\omega)$, flowing on the outside of the sheath causes an incremental voltage, $\Delta V(x,\omega)$, to appear along Δx on the inside of the sheath. This voltage is given by:

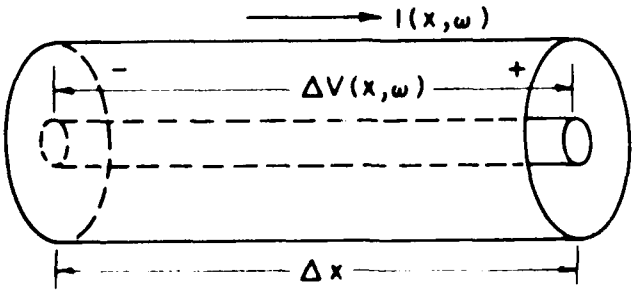

$$\Delta V(x,\omega) = Z_T(\omega)\ I(x,\omega)\ \Delta x \qquad (9\text{-}4)$$

For a length, ℓ, of cable short compared with the wavelength of the current, the current, $I(\omega)$, is uniform and $Z_T(\omega)$, is given by:

$$Z_T(\omega) = V(\omega)/(I(\omega) \cdot \ell) \qquad (9\text{-}5)$$

where $V(\omega)$ is the voltage along the inside of the outer sheath. For a cable which is longer than one-tenth the wavelength of $I(\omega)$, correction factors are required which depend on the surface transfer admittance, the test fixture geometry, and terminating impedances. A general derivation of these factors is given in Appendix A. For a connector, the surface transfer impedance is given by

$$Z_T(\omega) = V(\omega)/I(\omega) \qquad (9\text{-}6)$$

where $V(\omega)$ and $I(\omega)$ have the same meaning as for a short cable. Small values of Z_T are synonymous with good shielding.

Radial electric field coupling is caused by partial penetration of the shield and results in a current source between the shield and the inner conductor. The <u>surface transfer admittance</u>, $Y_T(\omega)$, quantitatively relates the equivalent shunt current generated to the external radial electric field. Over an incremental length of cable the current generated is

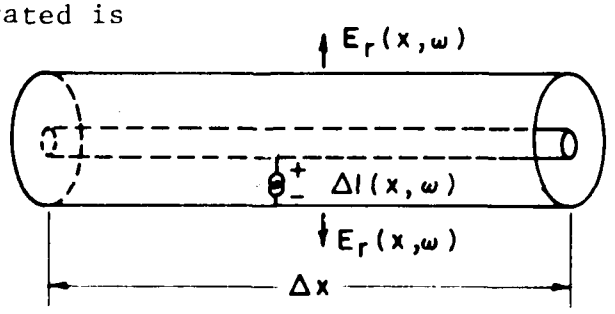

$$\Delta I(x,\omega) = Y_T(\omega)\ E_r(x,\omega)\ \Delta x \qquad (9\text{-}7)$$

where $E_r(x,\omega)$ is the radial electric field. For a test fixture which is electrically short, $E_r(\omega)$ is constant over the whole sample and thus

$$Y_T(\omega) = I(\omega)/(E_r(\omega)\cdot\ell) \qquad (9\text{-}8)$$

From the above equations it is apparent that the shunt currents generated are proportional to the value of Y_T for a particular cable. Radial electric field coupling often is not the predominant mode of EMP penetration. This is especially true for high performance shields with high optical coverage which have low impedance terminations.

For some applications another test for magnetic field coupling is needed. The shielding performance of the outer conductor is expressed in terms of an equivalent B-dot ($\dot{B}$) coupling loop area. The voltage generated per unit of cable length is

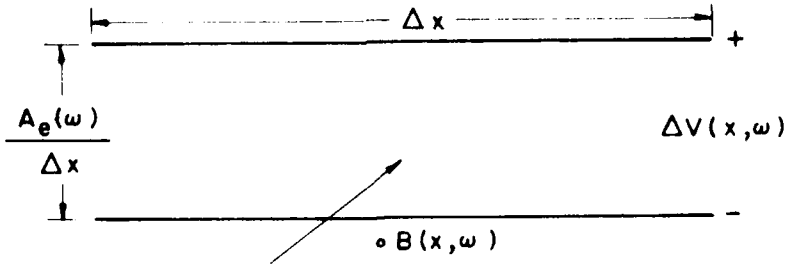

$$\Delta V(x,\omega) = +A_e(\omega)\ \dot{B}(x,\omega)\ \Delta x \qquad (9\text{-}9)$$

where $\dot{B}(x,\omega)$ is the time derivative of the magnetic field and $A_e(\omega)$ is the equivalent B-dot ($\dot{B}$) area per unit length.

Again for an electrically short cable of length, ℓ, the field is constant and the equivalent $\dot{B}$ area is given by

$$A_e(\omega) = +V(j\omega\mu H_o\ell) \qquad (9\text{-}10)$$

where V is the peak amplitude of the induced signal and where the functional representation of the magnetic field is $B = \mu H_o e^{j\omega t}$. Geometrically, the equivalent $\dot{B}$ area can

be related to such factors as the center conductor and the outer conductor not having a common axis, twisted center conductor(s) and spiral-wrapped (rather than braided) outer shields.

An effective shield is one which significantly reduces A_e below the value it would have if the outer conductor offered no shielding to magnetic fields. Clearly magnetic field pickup can also be diminished by improvements in cable design and manufacturing tolerances.

9.2.4 Types of Tests

To fully characterize any one of these three coupling parameters, amplitude and phase measurements should be made in the frequency domain from 10 kHz to over 100 MHz. In practice it is often possible to obtain a good representation of these parameters using a fraction of this frequency range.

For the surface transfer impedance the recommended test procedure measures the current applied to the shield and the induced voltage in a sample of cable which is about one meter long. A simple triaxial test fixture is required. Measuring equipment can be either a sophisticated swept frequency signal generator and a network analyzer or a variable frequency signal generator and a tuned RF voltmeter. The equipment should operate at frequencies from 100 kHz to 10 MHz, and at higher and lower ones if possible. An alternate test procedure can be performed in the time domain using a square pulse of current. Both the current and the induced voltage are monitored with an oscilloscope. The data obtained with this method are limited but it can be useful when the sample has an uncomplicated variation in $Z_T(.)$ with frequency.

For the transfer admittance measurements the cable sample is placed into a triaxial test fixture and a sinusoidal potential is applied between the shield and exterior

cylinder of the test fixture. This potential produces the radial electric field. The applied potential and the voltage appearing across 50 Ω termination as a result of the induced current are both measured using either a swept frequency network analyzer or a tuned RF voltmeter. Because the frequency dependence of the transfer admittance is generally simple, i.e., increasing linearly, measurements at a few fixed frequencies can be sufficient.

To determine the magnetic field coupling, a sample cable is placed in the magnetic field generated by either a large solonoid or a parallel plate transmission line. The signal which is induced on the center conductor should be transmitted to a well-shielded tuned RF voltmeter via a fiber optic data link or some other method which has no electromagnetic field pickup. It is recommended that the orientation of cable in the magnetic field be chosen such that the observed signal is a maximum. At low frequencies (up to about 10 kHz), the equivalent area will in general be constant and be a consequence of the cable construction. The cable sheath provides some magnetic shielding at higher frequencies which tends to increase as the frequency is increased.

9.3 Surface Transfer Impedance Test Procedure for Cables

9.3.1 Scope

The surface transfer impedance is determined by the construction of the outer coaxial conductor. Analytical expressions are available for solid shell coaxial cables. However, the geometry of braided outer conductors is very difficult to analyze in detail, so their surface transfer impedance is most easily determined experimentally. Data from 10 kHz to 100 MHz are desired. The surface transfer impedance can be measured by placing a known current on the sheath of a cable and then observing the voltage at one of the terminals. This is done by making the cable part of the inner conductor of a large triaxial or quadraxial test fixture. For the recommended measurement procedure, a triaxial fixture is specified and measurements are made in the frequency domain from 100 kHz to about 10 MHz. An alternate technique performed in the time domain is discussed later. Appendix A outlines a method which can be used at frequencies above 10 MHz to determine Z_T and Y_T. These procedures apply only to shields which respond linearly to the intensity of electromagnetic fields.

Before describing how to measure Z_T, a brief explanation is given of how it is used in EMP calculations. The frequency domain representation of the EMP waveform is used to calculate the sheath current distribution using the geometry of the cable and the shield's terminations to ground. This sheath current distribution is combined with the measured values of Z_T to get the continuous distribution of incremental voltage sources. The current distribution on the inside of the cable is calculated using the superposition integral and expressions for the current and voltage at any point in the line with arbitrary loads for an

arbitrary location of a series voltage generator. The time history of the load current is obtained by application of the inverse Fourier transform.

9.3.2 Test Equipment

The cable sample is placed in a triaxial test fixture. The sample is the inner coaxial line. The cable shield and a larger solid cylinder form the outer coaxial system. At one end the outer coaxial line is driven by a sine wave generator and the sample cable is shorted. At the other end, the induced voltage is measured and the large cylinder is shorted to the cable sheath. This configuration has been used by most, but not all, investigators who have determined surface transfer impedances. Other configurations which are electrically equivalent to the recommended test fixture should give identical results. For example, a rectangular trough used in place of the larger cylinder would make sample changing easier.

Figure 9-1 shows a test setup using a three-inch diameter outer conductor (actually a part of a large diameter solid coax), for frequencies up to about 20 MHz. This outer conductor can be up to three or four feet long. Above 20 MHz, it is necessary either to shorten the length of this fixture to about 10 inches, or rely on certain correction factors presented in Appendix A. For the practicing engineer, the shortened test fixture is the recommended approach since computational correction can be tedious and subject to error at certain "pole" and "null" frequencies. Type N connectors have been employed successfully for many measurements. Certain sheath designs may introduce interface problems at the connector, such that soldering the sheath directly to the backshell of the connector or directly to the fixture is required. Note the RF gasket and clamps used to attach the end plate to the cylinder. All the parts are easy to obtain and are also easy to assemble.

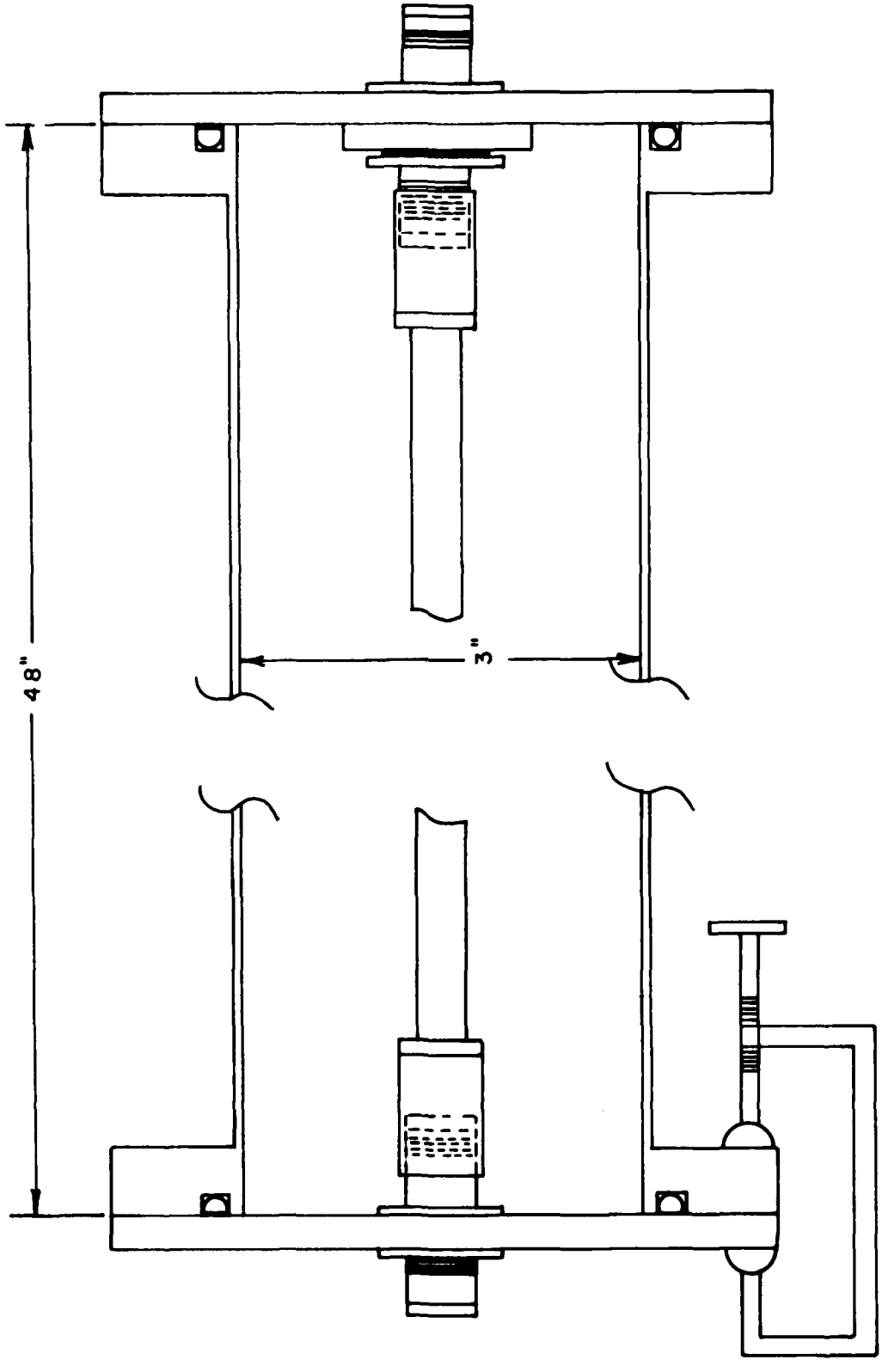

Figure 9-1. Triaxial test fixture for surface transfer impedance measurements.

Surface transfer impedance measurements can be performed at specified frequencies using the setup shown in Figure 9-2. In this mode, the most important instrument is a tuned RF voltmeter or field intensity meter with microvolt sensitivity. Examples are the NM20B, the EMC 25, and the NF105, which are radio receivers manufactured by Empire Devices, Fairchild, and Stoddart, respectively. A more automatic system can be assembled using a swept frequency generator and a network analyzer. The latter subtracts the logarithms of the input current and the induced voltage, giving the log of Z_T. The phase of Z_T can also be determined. An example of a swept frequency system is shown in Figure 9-3, using the Hewlett-Packard 8601A generator/sweeper and the 8407A network analyzer. The output of the current probe goes to the reference channel and the induced voltage is measured at the test input. In general, the swept frequency system is recommended over a discrete frequency one since the data, which includes both the amplitude and the phase, is acquired quickly in permanent form (i.e., a photograph).

The International Electrotechnical Commission (IEC) recommends a triaxial fixture similar to the one described for the preferred test procedure but with the shorted test cable termination replaced by a matched load. There is no particular advantage to this. Note that the IEC test procedure specifies a test fixture which is very difficult to construct and use since the test cable is soldered into the fixture.

A quadraxial test fixture has not been recommended for general purpose tests. Both radial electric field and sheath current coupling occur simultaneously--a result of the matched terminations used in this test fixture. However, the values of Z_T and Y_T can be determined using two independent measurements (see Appendix A). When using the

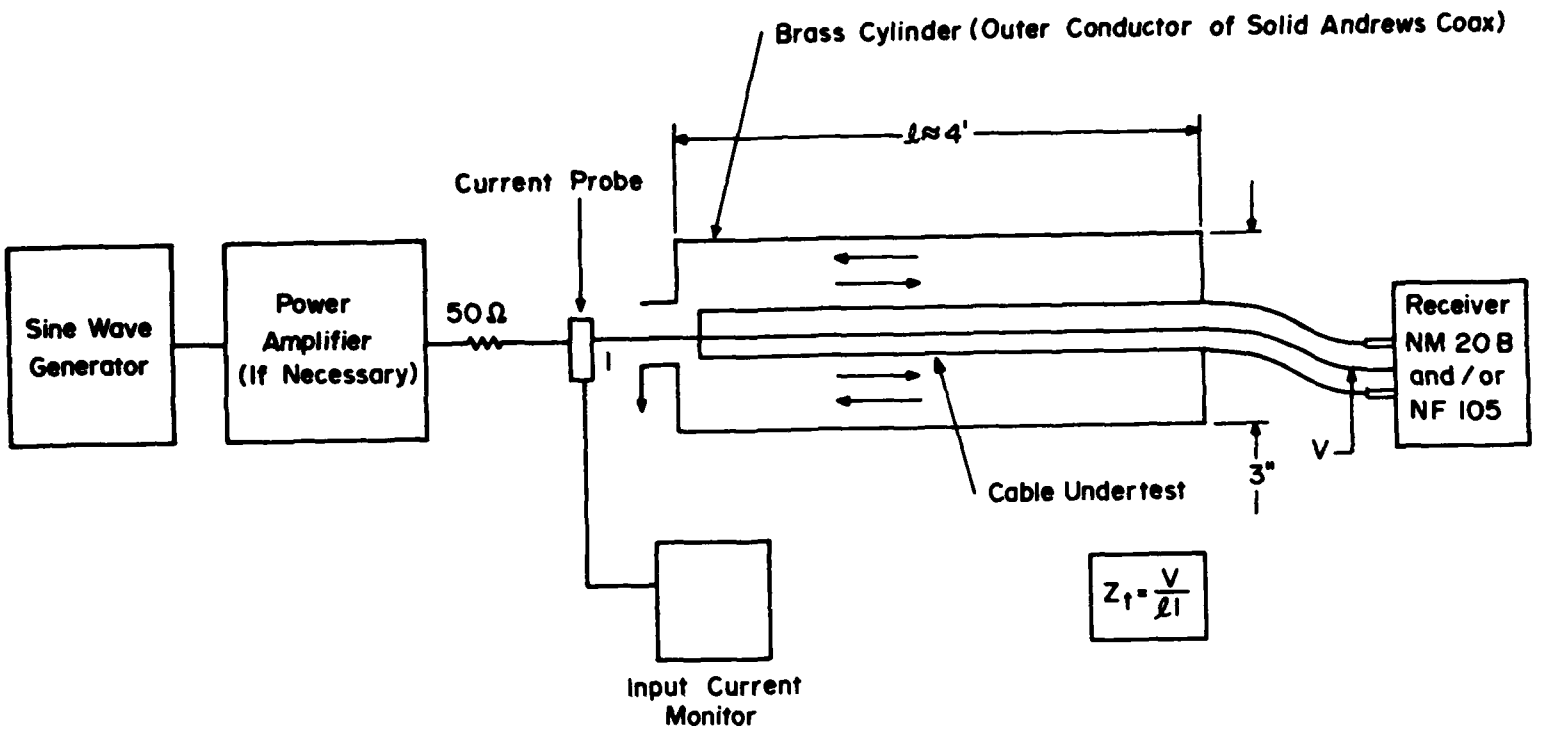

Figure 9-2. Transfer impedance measurement, test setup.

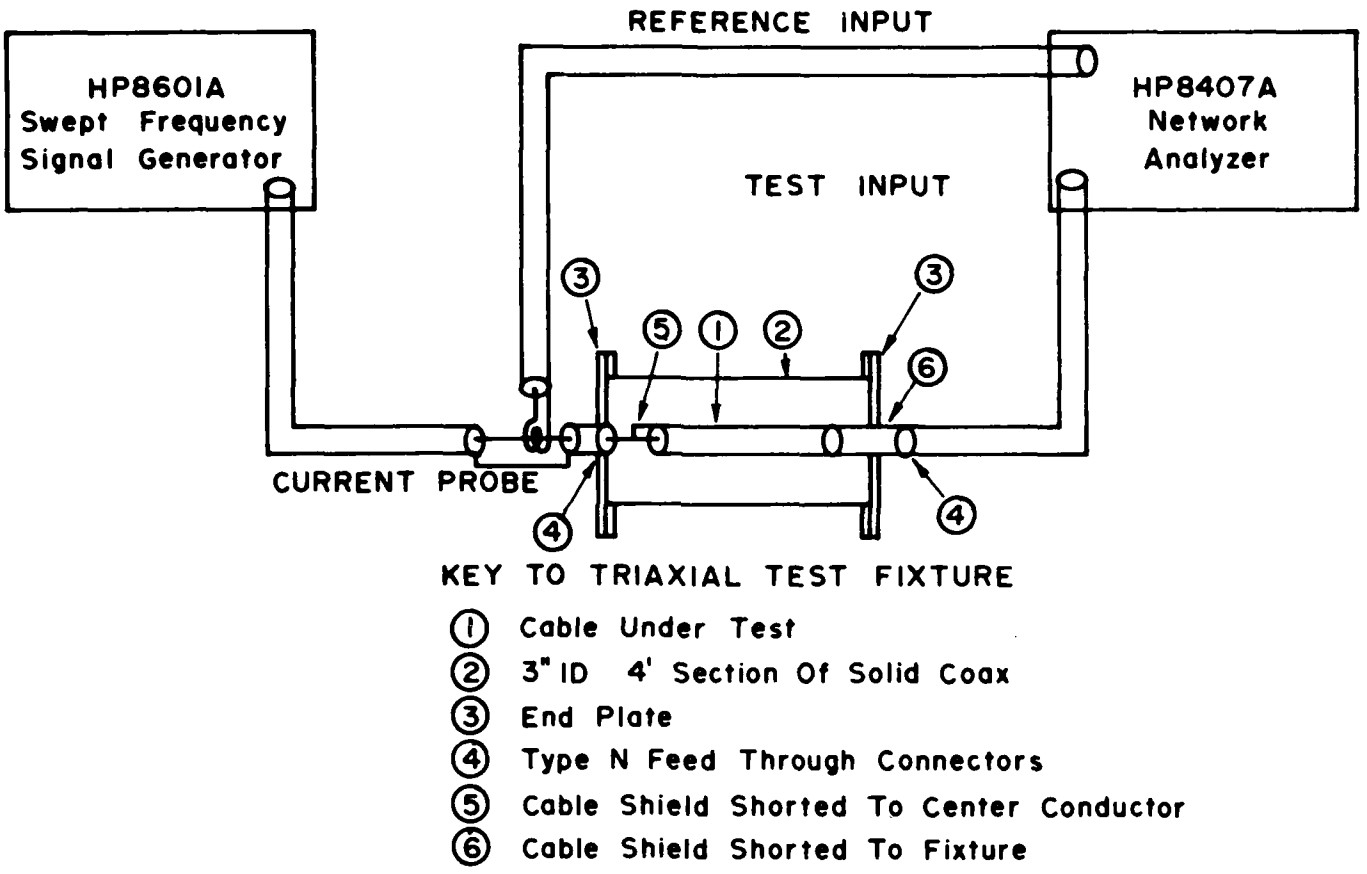

Figure 9-3. Test setup for surface transfer impedance measurements.

quadraxial test fixture the characteristic impedances of each pair of conductors must be used or correction factors applied (see Appendix A). For frequencies up to at least 10 MHz, the overall accuracy with which Z_T (and especially Y_T) can be determined using a quadraxial fixture often is inferior to the results obtained with the recommended fixtures. In the case of high-performance cable with very good optical covering factors (>95%), the quadraxial test fixture should give satisfactory measurements of transfer impedance for all electrically short test conditions.

9.3.3 Precautions

The equipment used for the surface transfer impedance measurements should be calibrated. For the swept frequency system the basic calibration is to replace the test fixture with a 50 Ω termination as in Figure 9-4. The network analyzer is then adjusted to read 0.5 Ω and 0^o of phase angle at low frequencies. Since the measured voltage is attenuated by 40 dB, the calibration is in effect 0.5 Ω. The frequency response of the network analyzer should be flat over its full working range. If this is not the case, simple corrections can be applied to the cable data based on the measurements of the 50 Ω termination. Discrete frequency systems are somewhat harder to calibrate primarily because they are not designed to have a linear or logarithmic response to all frequencies.

It is very important to use well-shielded interconnecting cables, such as RG-55B/U, to keep stray pickup at a minimum. In its nominal impedance measuring mode, a network analyzer is noise limited at a fraction of an ohm, but for surface transfer impedance measurements using the arrangement shown, the noise level is about 0.1 mΩ. With careful selection of components for the fixed frequency mode, measurements can be made at the 10 μΩ level.

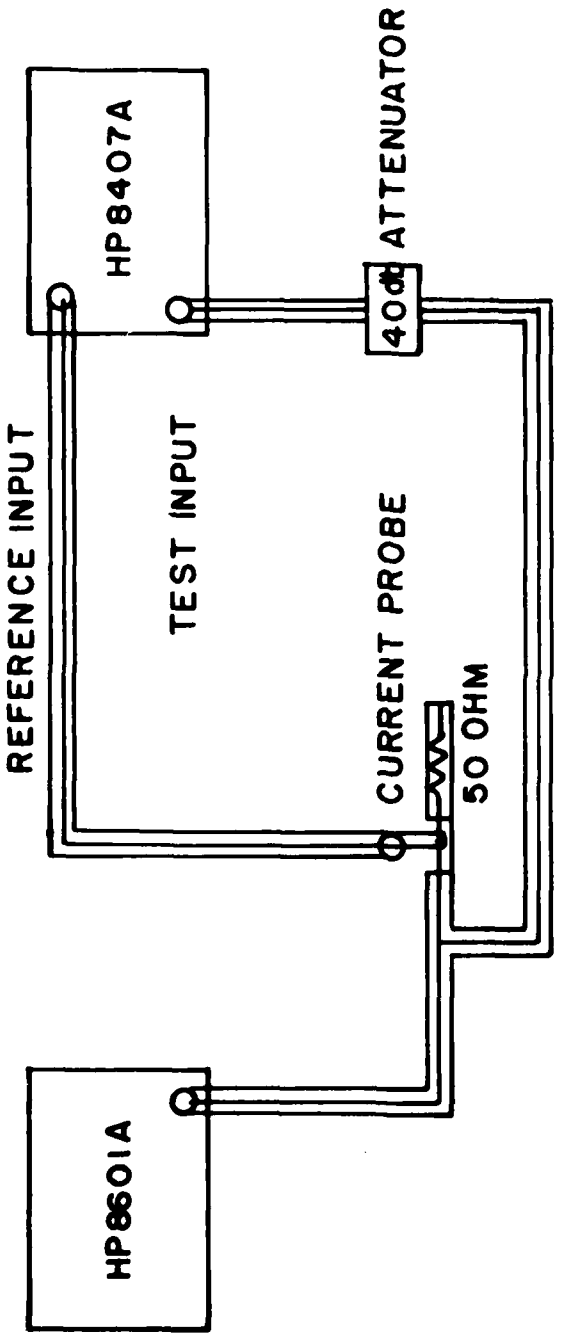

Figure 9-4. Calibration of swept frequency system.

An excellent check of the noise level is to measure a cable with a piece of copper tube as the shield. (For example, use RG-9B/U cable inside a 3/8" pipe.) The use of type N or equivalent connectors is strongly recommended since a bayonet connector such as a BNC increases the system noise level to about 1.0 mΩ.

9.3.4 Data Format

The basic data to be recorded are the magnitude and the phase of the surface transfer impedance as a function of frequency. Measurements should be made over at least a two-decade frequency range from 100 kHz to 10 MHz. In this range significant changes in Z_T are observed usually. For typical braided cable shields, Z_T is constant below 100 kHz and is increasing monotonically at 10 MHz. However, to better cover the EMP spectrum, measurements should be extended down to 10 kHz and up to 100 MHz. Above about 15 MHz the sample is no longer electrically short compared to the wavelength of the current. This requires the use of either a shorter test fixture or the methods described in Appendix A. Numerical data should be tabulated at logarithmic intervals; for example, at 0.125, 0.25, 0.5, etc., MHz. Graphically, the data should be presented as log Z_T and ϕ_T vs log frequency.

For the purpose of illustration, surface transfer impedance measurements have been made on samples of RG-8A/U, RG-9B/U, and RG-58A/U. All are 50 Ω coaxial cables; RG-8A/U and RG-58A/U each have a single braid layer while RG-9B/U has a double layer of braid. Figure 9-5 shows the magnitude and the phase of Z_T from 0.1 to 10 MHz for two samples as measured with the network analyzer. Note the wide dynamic range of the display. The magnitude data has been plotted on a log-log scale in Figure 9-6. Also shown on this figure is the transfer impedance of a thin solid

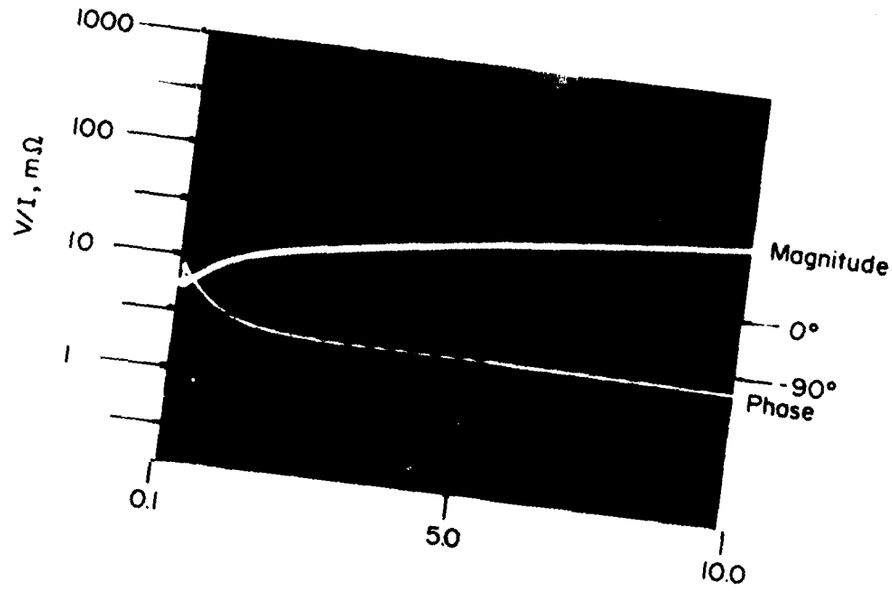

a) RG-8A/U

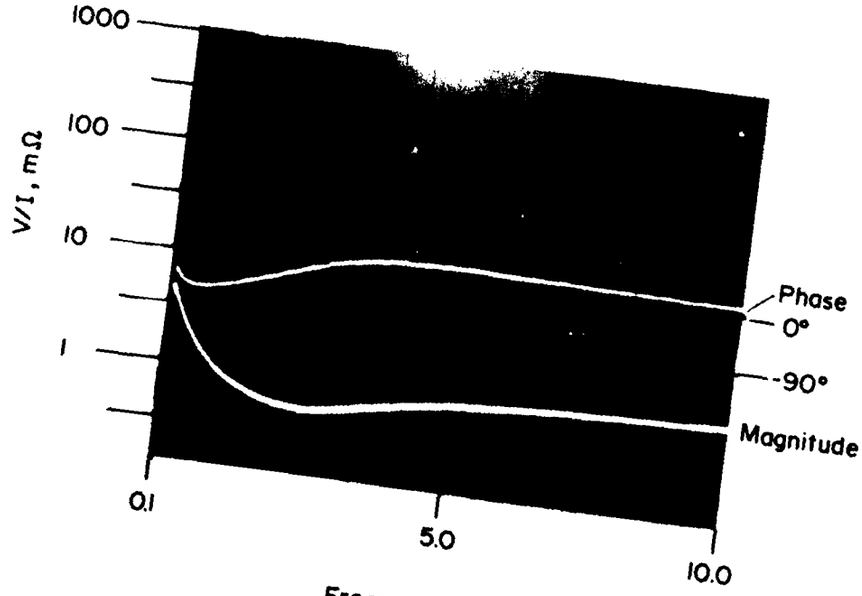

b) RG-9B/U

Figure 9-5. Surface transfer impedance, sample test data.

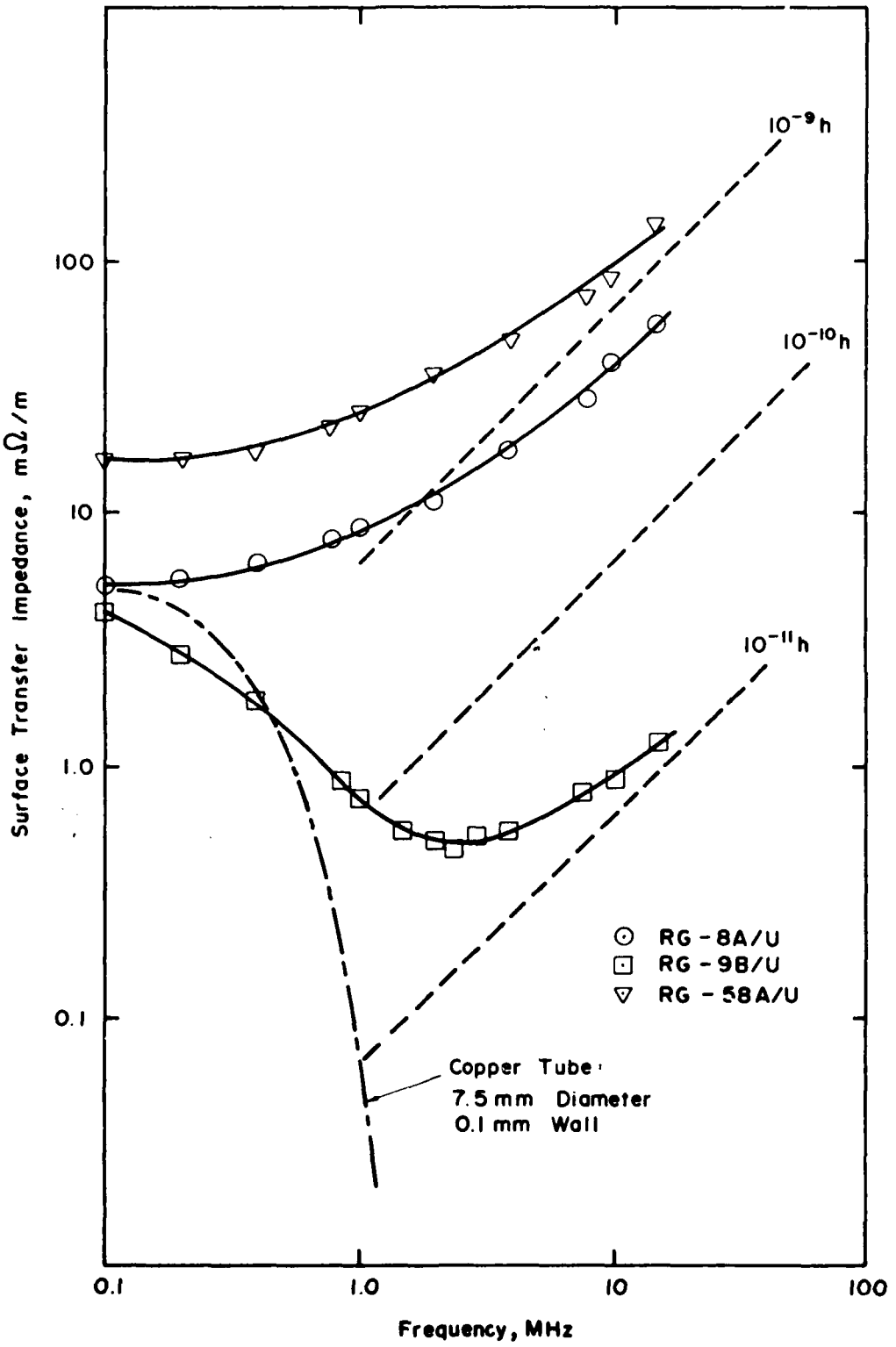

Figure 9-6. Surface transfer impedance, sample data.

wall sheath and the impedance of various inductors. These typical measurements show that the surface transfer impedance of ordinary braided shielded cables increases linearly with frequency above one or two MHz. Thus Z_T can be represented by the empirical equation

$$Z_T = R_T \pm j\omega M_T \qquad (9\text{-}11)$$

where R_T is the low frequency value and M_T represents a mutual inductance between the interior and the exterior of the braid. The negative sign in this equation applies for single braid cables and the positive sign for double braids.

For the cables tested, the variation in R_T from 4 to 15 mΩ/m can be attributed to differences in the quantity of copper in the braid. For the cables with a single braid, a typical value for M_T is 1.0×10^{-9} h/m, while for the double shield cable M_T is about 2.0×10^{-11} h/m.

9.3.5 Time Domain Measurements: An Alternate Procedure

The determination of the real and the imaginary parts of the surface transfer impedance in the frequency domain requires either measurements at a large number of frequency points or a sophisticated swept frequency network analyzer. On the other hand, by working in the time domain, it is possible to obtain a crude quantitative estimate of Z_T. A pulse is applied for which the sample is electrically short at the highest significant frequency. The response of a cable to this test pulse then consists of an initial and final spike attributed to the mutual inductance component of Z_T and a plateau which is related to a purely resistive component. Thus, it is possible to obtain quantitative estimates for the two constants in the empirical equation

$$Z_T = R_T \pm j\omega M_T \qquad (9\text{-}12)$$

which often characterizes the transfer impedance in the EMP frequency range.

Time domain measurements of the surface transfer impedance can be performed with the experimental setup shown in Figure 9-7. The signal induced on the test cable and the pulse waveform are recorded directly on an oscilloscope (Tektronix 454 or similar). The pulse generator output goes through a 50 Ω series impedance and current probe (Tektronix Model CT-2) to the reference channel in the oscilloscope. It is necessary to terminate the cable from the test cable output to the oscilloscope in 50 Ω so that the observed induced signal does not ring at high frequencies. An appropriate pulse has an amplitude of 1.0 ampere and a duration of 2.4 microseconds.

In Figure 9-8, for example, the observed plateau responses are 5.5 mV for RG-8A/U and 17 mV for RG-58A/U. Thus the resistive component, R_T, is estimated to be 5 mΩ/m and 15 mΩ/m for these two coaxial cables (ℓ = 1.14 m). These results compare very favorably with the measurements in the frequency domain at about 200 kHz, the lowest frequency in the test pulse. The rate of rise for the pulse is 10^7 a/sec and the rate of decrease at the end of the pulse is approximately 2×10^7 a/sec. The cables have an initial spike with amplitudes of 10 mV and 20 mV from which estimates of 9×10^{-10} h/m and 1.8×10^{-9} h/m are made for the mutual inductances. Again, these results agree quite well with the model M_T's at a frequency of about 2 MHz corresponding to the highest frequency in the test waveform. Note that the negative initial voltage spike correlates with the observed -90^o phase angle which is characteristic of a negative mutual inductance.

The problem with this method is that Z_T is essentially measured in only two broad frequency bands. By changing the pulse width or the rise time, the frequency of a band may be changed. However, it is very difficult to accurately reproduce the detailed Z_T data that is easily acquired using a swept frequency measurement.

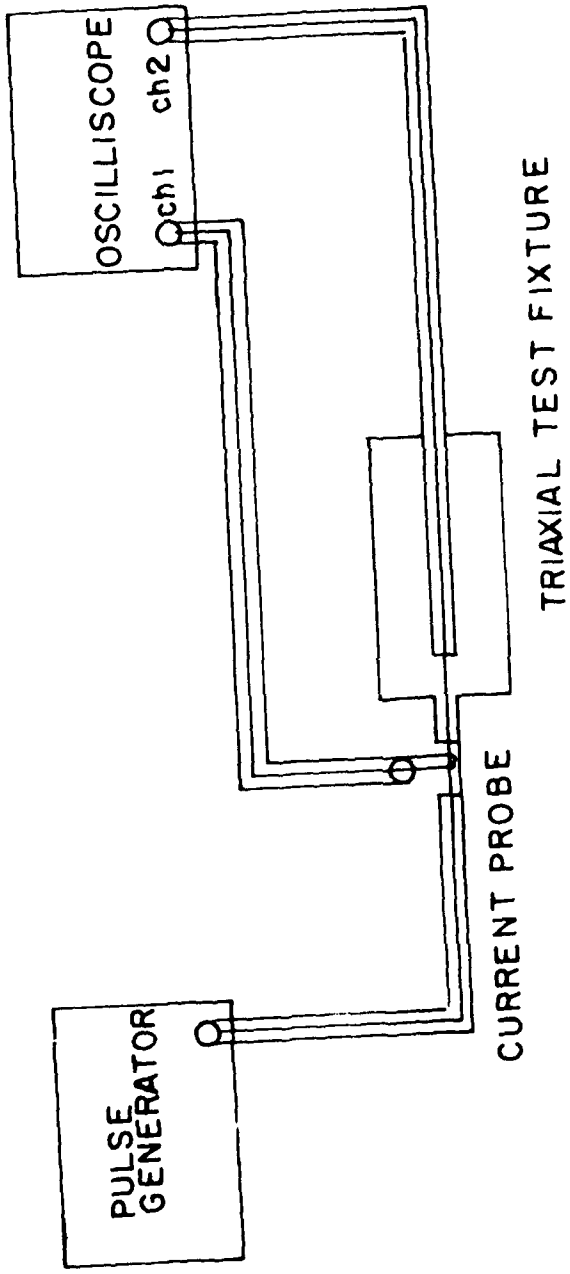

Figure 9-7. Surface transfer impedance measurement test setup for time domain.

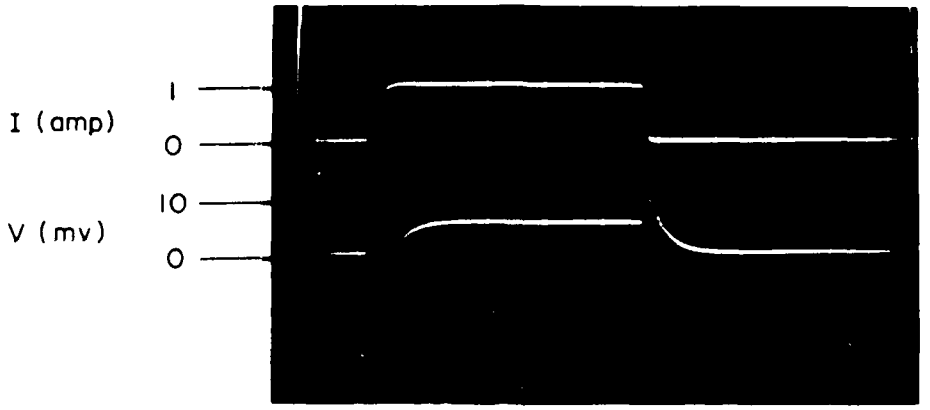

Time (0.5 μSec / div)

a) RG-8A/U

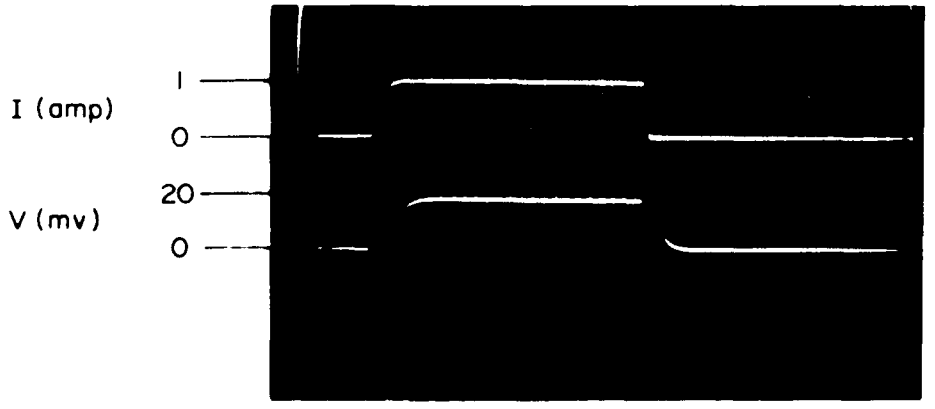

Time (0.5 μSec / div)

b) RG-58A/U

Figure 9-8. Surface transfer impedance, sample test data.

9.4 Surface Transfer Admittance Test Procedure for Cables

9.4.1 Scope

The radial component of the electric field can partially penetrate through the braid of cable shields. This is especially true of shields which do not have an optical coverage near 100 percent. The model for this mode of penetration is a distributed shunt current source whose magnitude is given by the product of the transfer admittance and the applied radial electric field. The recommended test procedure applies a known radial electric field to the outer conductor of a coaxial cable. Frequencies between 100 kHz and 10 MHz are used.

When a cable is illuminated by an EMP waveform with a transverse electric field component, there is a net radial electric field at the shield. A transmission line analysis, similar to that employed for sheath current coupling but with distributed shunt current sources, can be used to predict the waveform at the ends of the cable.

9.4.2 Test Equipment

Again the sample of cable goes in a triaxial fixture. The radio frequency signal generator is connected to both ends of the outer coaxial line. The radial electric field at the cable sheath is

$$E_r = Q/(2\pi\varepsilon a\ell) \qquad (9\text{-}13)$$

where Q is the charge on the sheath, a and ℓ are its radius and length and ε is the permittivity of free space. However the charge is directly proportional to the product of the capacitance, C, of the outer coaxial line and the applied voltage, V'. Since

$$C = 2\pi\varepsilon\ell/\ln(b/a) \qquad (9\text{-}14)$$

where b is the radius of the outer cylinder, the radial field is

$$E_r = V'/(a \ln(b/a)) \qquad (9\text{-}15)$$

This radial electric field gives rise to a shunt current, I, and produces a voltage, V, which appears across the combined parallel impedance, Z, of the measuring equipment, Z_{in}, and the total cable capacitance, C_c. Thus the equivalent circuit is

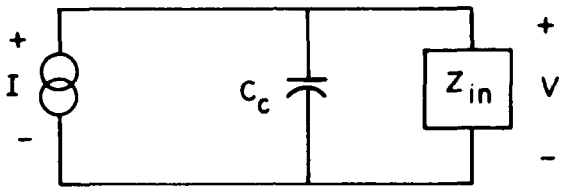

$$I = Y_T \cdot E_r \cdot \ell$$

and the current is given by

$$I = \frac{V}{Z} = V \left(\frac{1}{Z_{in}} + j\omega C_c \right) \qquad (9\text{-}16)$$

Substituting Equations (9-15) and (9-16) into (9-8) yields for the surface transfer admittance

$$Y_T = \frac{Va}{V'\ell} \ln(b/a) \left(\frac{1}{Z_{in}} + j\omega C_c \right) \qquad (9\text{-}17)$$

To minimize the stray external capacitance, one end of the coaxial cable being tested should be connected to the measuring equipment with a short shielded cable and the other end left as an open circuit but capped by an end-shield (see Figure 9-9).

Some current will flow along the cable sheath as voltage on the cylindrical capacitor formed by the sheath and the outer cylinder changes. Connecting both ends of this cylindrical capacitor to the signal generator reduces the sheath current. At frequencies below 10 MHz there usually is no significant signal as a result of sheath current coupling. At higher frequencies, these two coupling modes must be considered together as in Appendix A.

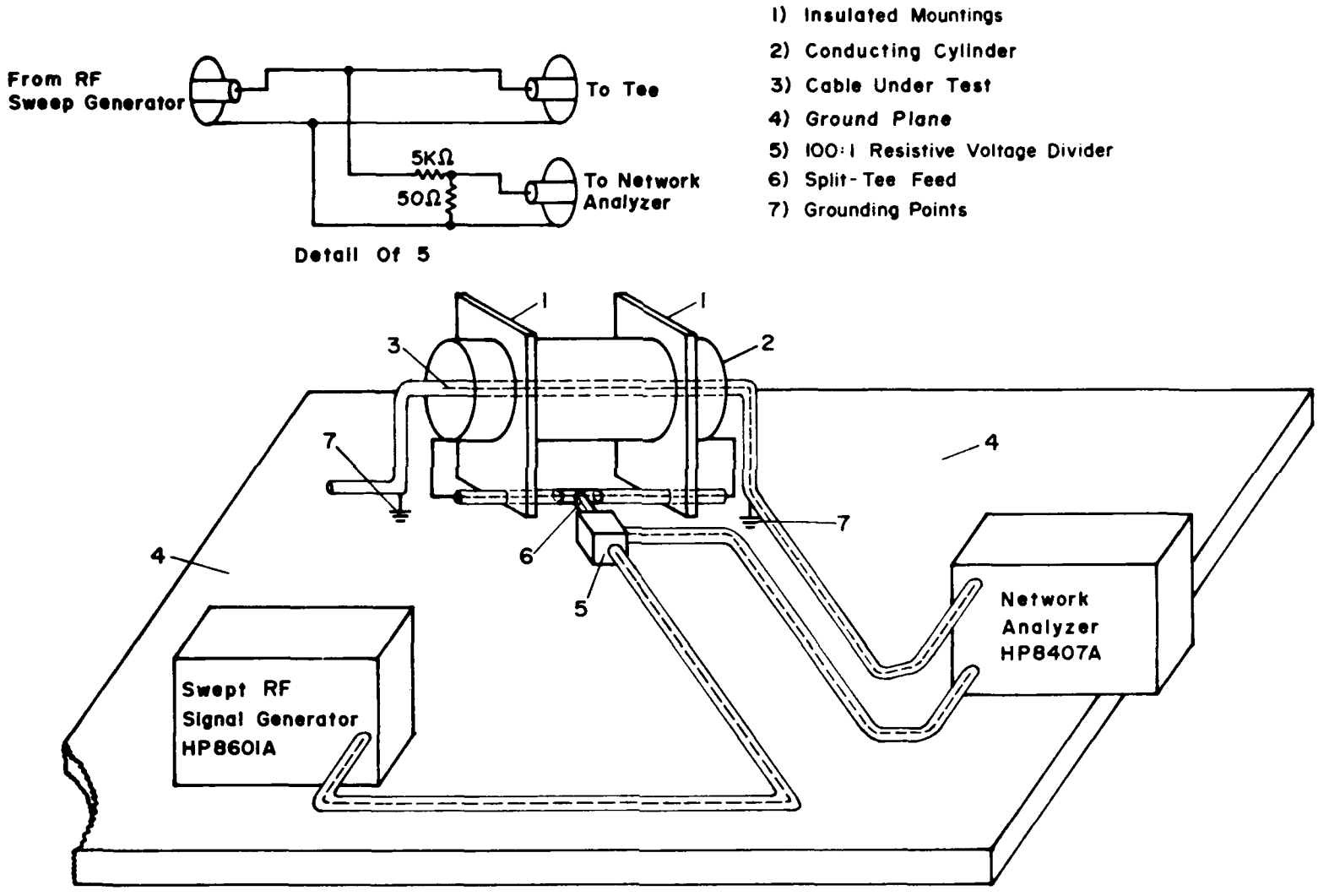

Figure 9-9. Surface transfer admittance measurement test setup.

Specific instrumentation which can be used for this test procedure is shown in Figure 9-9. The swept frequency signal generator and network analyzer are the same ones used for the measurement of Z_T. The signal goes to the reference channel input through a 40 dB attenuator. If a 100:1 resistive divider is used, there will be more voltage on the cylindrical capacitor than with a 50 Ω input impedance attenuator. The induced voltage goes directly into the 50 Ω test channel input. These measurements can also be performed with a tuned RF voltmeter. A calibrated radio receiver can be used such as the NM20B, the EMC 25 or the NF105 which are made by Empire Devices, Fairchild, and Stoddard, respectively. New insulation ends for the test fixture are needed. Note that the outer cylinder of the test fixture has a three inch diameter and is connected to the center conductor of the cable from the signal generator. Since the sample cable shield is the common ground for the system, it is a good idea to provide an additional ground strap, which is parallel to the signal cable, between the ends of the fixture. This function could also be performed by the outer conductor of a quadraxial test fixture.

9.4.3 Precautions

Several precautions have already been mentioned; namely the ground strap, driving the cylindrical capacitor from both ends, the resistive voltage divider, and the short cable for the induced signal. Calibration of the system is important. With a swept frequency analyzer, the generator output is fed into both channels through 40 dB attenuators and adjusted for zero amplitude and zero phase. For discrete frequency systems the calibration is more time consuming since such systems are not designed for identical response to all frequencies.

Using well shielded cables and good electrical contacts are important. With some care induced voltages can be observed which are about 125 dB below the applied voltage. This is equivalent to a transfer admittance of about 3×10^{-10} mhos/m. Again the noise level can be checked using a solid copper shield.

9.4.4 Data Format

The basic data to be recorded are the magnitude and the phase of Y_T as a function of frequency. The observed voltage ratio must be multiplied by the other factors in Equation (9-17). Measurements should be made over the two-decade frequency range from 100 kHz to 10.0 MHz. In this range Y_T generally increases linearly although the observed V/V' ratio may fall off due to the cable capacitance. Ideally data would be taken from 10 kHz to over 100 MHz. However, this is not easily accomplished since below 100 kHz the signal is generally too small to be measured and above 10 MHz the recommended fixture is too long. If the contributions by Z_T and Y_T are about equal then both can be determined above 10.0 MHz using the methods suggested in Appendix A.

Numerical data could be tabulated at logarithmic intervals; for example at 0.10, 0.31, 1.0, 3.1, and 10.0 MHz. A graph of log $|Y_T|$ and its phase could be drawn as a function of log frequency. Figure 9-10 shows data taken on RG-8A/U which has a single layer of braided shield with about 95 percent optical coverage. For this cable the induced signal is below -120 dB up to a frequency of 1.0 MHz. The phase angle is constant at $+90^{\circ}$. Log $|Y_T|$ vs log frequency is plotted in Figure 9-11. A linear relationship between $|Y_T|$ and frequency is apparent. Also shown is the surface transfer admittance of the outer braid of a triaxial cable (Belden 8232) which has 80 percent optical

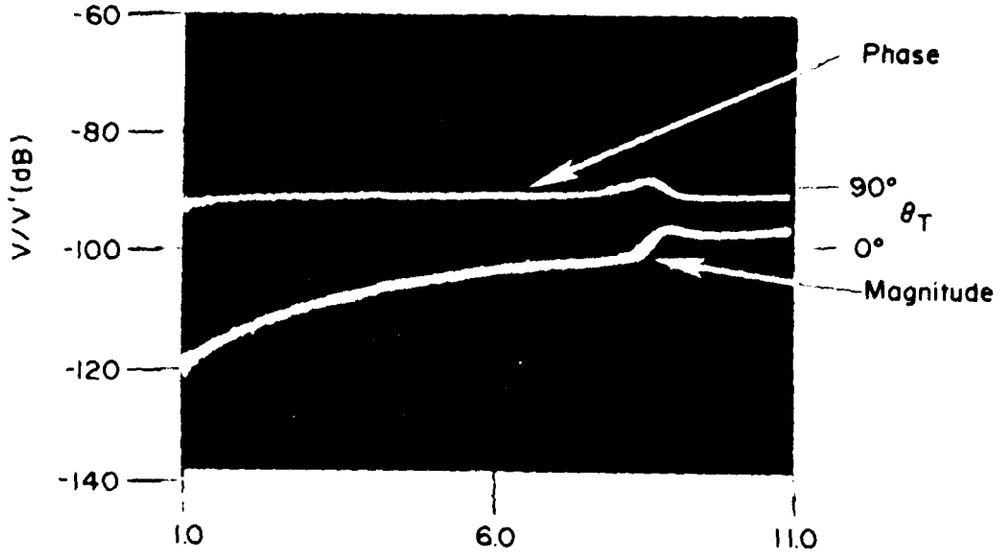

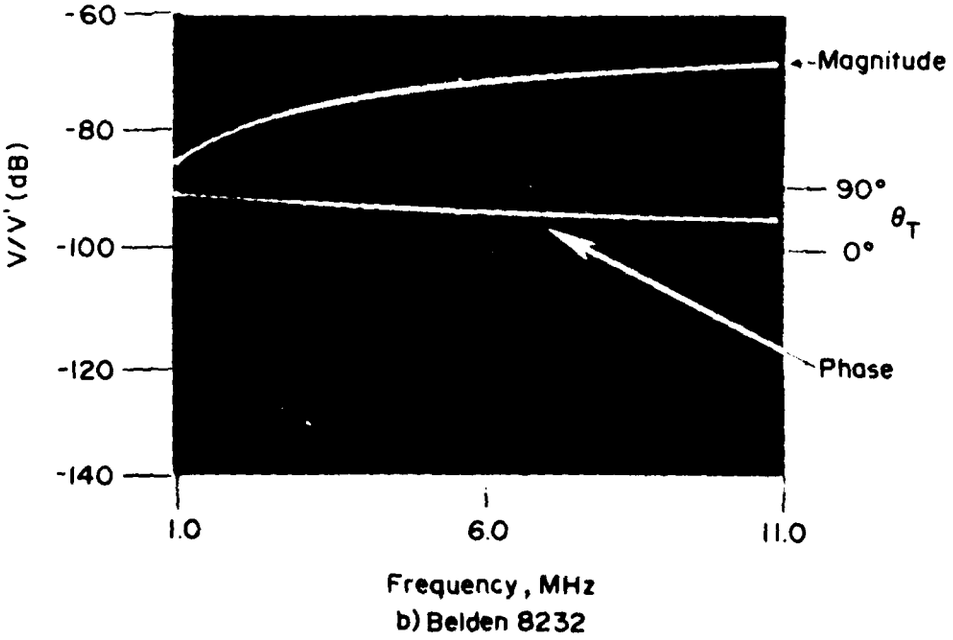

Figure 9-10. Surface transfer admittance, sample test data.

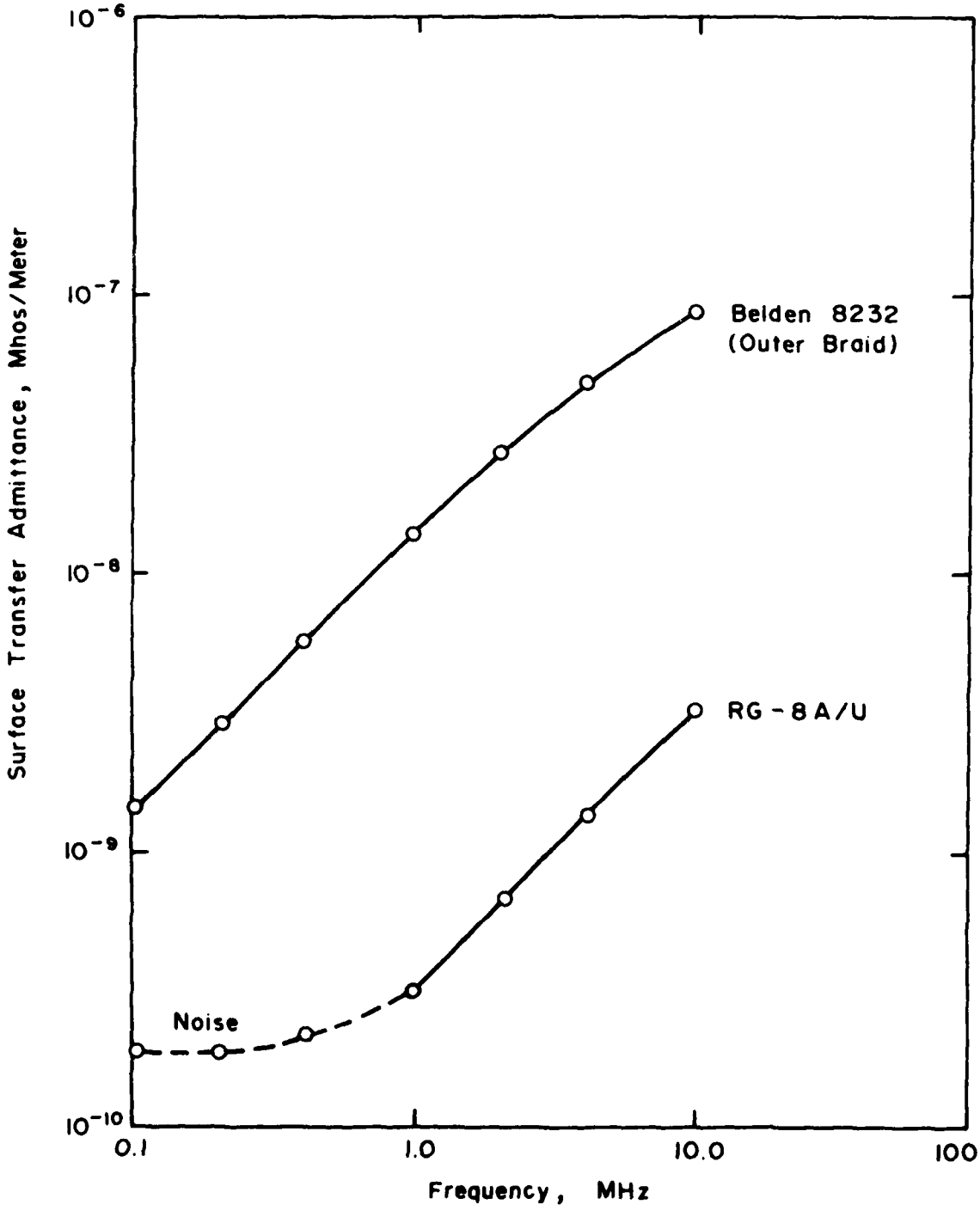

Figure 9-11. Surface transfer admittance, sample data.

coverage. The inner braid and outer braids were the center conductor and shield of a very low characteristic impedance coaxial cable. The observed pickup is much larger. The roll off at frequencies above 1.0 MHz is caused by the high cable capacitance (about 10^{-9} farads).

Considering the simple uncomplicated behavior of Y_T vs frequency, the data reporting can be greatly simplified. All that is required is the value of Y_T at a specific frequency, ω_o, say 1.0 MHz, and the value at any other frequency, ω, can be determined from the simple relationship

$$Y_T(\omega) = Y_T(\omega_o) \quad (\omega/\omega_o) \qquad (9\text{-}18)$$

The phase is $+90^o$ so an alternative way of specifying Y_T is to compute the equivalent capacitance, C_T so that

$$Y_T(\omega) = j\omega C_T \qquad (9\text{-}19)$$

For the two cables tested, the model capacitances are:

Cable	C_T
RG-8A/U	5.0×10^{-17} farads/meter
Belden 8232	2.2×10^{-15} farads/meter.

9.5 Equivalent B-dot ($\dot{B}$) Area Test Procedure for Cables

9.5.1 Scope

The equivalent $\dot{B}$ area is measured by placing a short length of coaxial cable in a magnetic field generated by either a parallel-plane transmission line or a solenoid. The induced voltage which appears between the conductors of the coaxial cable is the direct result of a time varying magnetic field penetrating the outer conductor or shield and acting on an equivalent area. This area can be due to a number of geometric factors including separate axes for the inner and outer coaxial cable conductors, a twisted pair center conductor, and spiral-wrapped shields.

Measurements should be made over a wide frequency range beginning at about 1.0 kHz and extending beyond 100 kHz. At the lowest frequencies the response will be determined largely by the cable design and the manufacturing tolerances. The equivalent area generally decreases with increasing frequency when the cable sheath can become effective in reducing the magnetic fields within the cable. Since neither the geometric or the magnetic shielding properties of cables can be treated analytically, an experimental measurement following the recommended test procedure is the best way to characterize cable response to magnetic fields. However, this procedure, as described, applies only to shields for which the attenuation is independent of the amplitude of the magnetic field. Many ferromagnetic materials violate this constraint.

9.5.2 Test Equipment

The cable sample is placed in a uniform magnetic field. Such a field can be found inside a large solenoid or between the plates of a parallel-plane transmission line. In the transmission line, both E and H fields exist so that both types of pickup may occur simultaneously. Ideally, when

the cable is placed flat on one of the plates in the line and is pointed in the H or P direction, there will be only axial or loop pickup from the H-field, respectively (the P direction is the direction of propagation). Axial currents induced on the line may introduce transfer impedance pickup if cable ends are grounded to the plate. A spherical coil could also be used; it minimizes the energy requirement and the field fringing but is more difficult to construct.

Due to the geometric factors governing magnetic field coupling, it is not possible to predict which cable orientation will produce the largest induced voltage. Thus it is necessary to provide for rotating the cable sample for maximum signal pickup or to measure the pickup at orthogonal orientations. The length of the test cable should be approximately one meter, so the dimensions of the structure for generating the magnetic field must be several times larger, but still about room size. To minimize spurious effects and eliminate field perturbations a non-hardwire fiber optic telemetry system is recommended for relaying the induced voltage from one end of the cable to the tuned RF voltmeter. Both ends of the cable should be terminated in the characteristic impedance.

No specific recommendations are given concerning the geometry and instrumentation to be used for generating the uniform magnetic field. The non-hardwire telemetry system should have low noise and wide bandwidth and operate on battery power. A calibrated radio receiver, such as the NM20B or the EMC 10, can be used as the tuned RF voltmeter to determine the amplitude of the induced voltage. The amplitude of the magnetic field can be determined using the same RF voltmeter to measure the voltage generated in a small coil. The magnetic field can then be monitored by measuring the input to the field generating structure.

9.5.3 Precautions

The RF voltmeter and the fiber optic telemetry unit must be well-shielded from both magnetic and electric fields. Both of these instruments must be well-calibrated. The overall noise and sensitivity of the system is determined by the rate of change of the magnetic field and either the sensitivity of the RF voltmeter, the noise in the telemetry link or leakage into the system. The best results are obtained by decreasing the voltmeter bandwidth and using good shielding, a low noise preamplifier in the telemetry unit and the largest practical amplitude for the magnetic field. A good check on the noise is to use a triaxial cable that is inside a piece of iron pipe.

17

9.5.4 Data Format

It is recommended that data be taken from about 1.0 kHz to over 100 kHz at logarithmically spaced frequencies. If it is possible to make measurements above 100 kHz, this should be done. However, at these frequencies, it is difficult to expose the cable to a uniform magnetic field and to exclude other coupling modes, including those associated with electric fields, which contribute to the observed signal. Thus, data above 100 kHz are useful only if it can be demonstrated that the dominant source is magnetic field penetration.

All data should be reduced to effective areas using Equation (9-10) and tabulated. A graph should be prepared on log-log paper of A_e as a function of frequency. Either the cable orientation should be varied for maximum pickup or data should be taken with orthogonal cable positions and the maximum signal determined by taking the rms value.

Typically, A_e decreases at higher frequencies as the ability of the cable shield to attenuate magnetic fields improves. There is no analytical model for the behavior of A_e with frequency which could be illustrated with sample data.

9.6 Test Procedures for Coaxial Connectors

9.6.1 Scope

Connectors can sometimes be an important source of EMP pickup This discussion of test procedures for connectors will cover sheath current coupling which is again characterized by the surface transfer impedance Z_T. In the case of well-designed* coaxial connectors, the transfer admittance and B-dot coupling mode are not expected to be important. The test procedures described below apply to coaxial connectors including the backshell to braided cable shield connection. The frequency range of primary interest is 100 kHz to over 10 MHz with extensions to 10 kHz and 100 MHz being of secondary concern. These procedures apply only to coaxial connectors whose pickup is linearly related to the sheath current.

A current, I, is injected along the connector sheath and through the backshell to braid interface. The voltage, V, induced along the sheath is measured and Z_T calculated by dividing V by I at each frequency. Z_T can be measured in the frequency or time domain. Because the test procedures for coaxial connectors are very similar to those for coaxial cables, many of the details which can be found in Section 9.3 are not duplicated here.

9.6.2 Test Equipment

The connector tests can be performed in the triaxial test fixture described in Section 9.3.2. The connector (or several connectors) is attached to a cable in the normal manner. Then a piece of solid copper tube is placed over the cable and soldered to the cable shield. This is done so that the cable shield makes no significant contribution to the observed signal.

*This implies a continuous coaxial type backshell. Both sides of the connector should not exhibit apertures and the interior design should be axially symmetric. The wall thickness should be at least 0.05 of an inch thick.

A simple alternative is to place uniformly connecting clamps on the cable shield which are very close to the connector. The signal generator output is connected to the two clamps to provide the required current on the shield. The voltage between the center conductor and the shield is observed on one side of the connector and the other end is shorted.

The drive current is measured with a current probe. Test equipment (i.e., signal generator and tuned RF voltmeter, network analyzer or oscilloscope) requirements are identical to those for the cable test procedures. See Section 9.3.2 for more detail on the frequency domain test and Section 9.3.5 for the time domain discussion.

9.6.3 Precautions

It is important that well-shielded interconnecting cables such as RG-55B/U be used. The noise level is about 0.1 mΩ for the swept frequency system and with care is lower for a discrete frequency setup. The system noise can be determined by replacing the connector with an equivalent length of copper tube soldered to a cable. Calibration is to be performed using a 50 Ω termination as described in Section 9.3.3.

9.6.4 Data Format

The basic data to be obtained are the magnitude and the phase of the surface transfer impedance as a function of frequency. When using a swept frequency system, measurements should be made over at least a two-decade frequency range from 100 kHz to 10 MHz. In this range significant changes in Z_T may be observed. Numerical data should be tabulated at logarithmic intervals; for example, at 0.125, 0.25, 0.5, etc., MHz. Graphically, the data should be presented as log Z_T and ϕ_T vs log frequency. With a time

domain measurement it is possible to obtain quantitative estimates for the constants in the empirical equation

$$Z_T = R_T \pm j\omega M_T \qquad (9\text{-}20)$$

which often characterizes the surface transfer impedance in the EMP frequency range.

9.7 Bibliography

1. Bridges, J.E., and Miller, D.A., "Standard EMC Cable Parameter Measurements," in 1969 IEEE Electromagnetic Compatibility Symposium Record.

2. Bridges, J.E., and Zalewski, R.A., "Magnetic Field Pickup by Flexible Braid Coaxial Cables," IEEE Trans. on Electromagnetic Compatibility, vol. EMC-10, pp. 130-134, March 1968.

3. Frankel, S., "Terminal Response of Braided-Shield Cables to External Monochromatic Electromagnetic Fields," IEEE Trans. on Electromagnetic Compatibility, vol. EMC-16, pp. 4-15, February 1974.

4. Kaden, H., Wirbelstroeme und Schirmung in der Nachrichten Technik, (Berlin: Springer-Verlag, 1959.)

5. Knowles, E.D., and Brossier, J.C., "Measuring Connector Shielding Effectiveness During Vibration," IEEE Trans. on Electromagnetic Compatibility, vol. EMC-16, pp. 24-28, February 1974.

6. Knowles, E.D., and Olson, L.W., "Cable Shielding Effectiveness Testing," IEEE Trans. on Electromagnetic Compatibility, vol. EMC-16, pp. 16-23, February 1974.

7. Krugel, L., "Abschirmwirkang von Aussenleitern Flexibler Koaxialkabel," Telefunken-Zeitung, vol 29, pp. 256-266, December 1956.

8. Miller, D.A., and Toulios, P.P., "Penetration of Coaxial Cables by Transient Fields," 1968 IEEE Electromagnetic Compatibility Symposium Record.

9. Schelkunoff, S.A., "The Electromagnetic Theory of Coaxial Transmission Lines and Cylindrical Shields," Bell Syst. Tech. J., vol. 13, pp. 532-579, October 1934.

10. Vance, E.F., "Shielding Effectiveness of Braided-Wire Shields," IEEE Trans. on Electromagnetic Compatibility, vol. EMC-17, pp. 71-77, May 1975.

11. Whitmer, R.W., "Cable Shielding Performance and CW Response," IEEE Trans. on Electromagnetic Compatibility, vol. EMC-15, pp. 180-187, November 1973.

18

10. UNIFORM TEST PROCEDURE FOR SHIELDED ENCLOSURES

TABLE OF CONTENTS

10. UNIFORM TEST PROCEDURE FOR SHIELDED ENCLOSURES

10.1 Introduction

A shielding enclosure is a completely enclosed thin wall structure used to suppress an electromagnetic field either outside or inside the structure. A high-performance shielding enclosure is constructed of very high conductivity and sometimes of permeable materials in such a way that it is capable of suppressing, by orders of magnitude, electromagnetic fields. It is usually constructed from metallic conducting sheets or screens with provisions for continuous electrical contact between sheets, screens, and other features, such as doors. Its function may be to provide an EMP-field-free space for sensitive electronic equipments, or to contain the intense fields associated with a high level pulse source.

One of the purposes of the series of test procedures described here is to establish a uniform basis for comparing the relative shielding effectiveness of different enclosures. The tests are designed to be conducted within typical laboratory areas using conventional, readily available equipment. The use of readily available laboratory equipment limits these procedures to narrow band characterization. Wide band and pulse illuminating facilities, including EMP simulators, are not easily constructed and those that have been built at government and contractor facilities are not generally available, except for the testing of specific critical systems. The procedures are restricted to trailer size and somewhat smaller enclosures. For either larger structures such as buildings, or very small enclosures, such as cabinets, these test procedures form a useful guide.

As such, these procedures are aimed toward evaluating the shielded enclosure as a component, or a shielded enclosure door and sill. These test procedures have the following special uses:

1. They provide the design engineer with a useful technique to assist him in evaluating the relative performance of shielded enclosures and related elements, such as doors, and sills, which can only be evaluated in situ.

2. For critical situations, the test procedures can be used as a guide for evaluating the electromagnetic responses of the shield to other environmental conditions, such as vibration and corrosion.

3. The results of detailed tests across the frequency band of interest provide the system interaction analyst with experimentally developed data which is of assistance in analytically modeling the transient behavior of the shield.

4. Shielded enclosure and shielded door supplier may employ the procedures in hardware design improvement and in data sheet sales literature.

5. Those conducting quality control or part acceptance tests can use the procedures as a guide for simple quick-look evaluations.

6. Those assessing the degradation of performance with age may use the procedures as a guide to measure shielding performance degradation.

7. Those concerned with very large shielded structures, or very small enclosures, may use the procedures as a guide for test procedures unique to the system enclosure.

10.2 General Background on Shielded Enclosures

10.2.1 Characteristics of Shielded Enclosures

The ideal behavior of shielded enclosures is controlled by the wall thickness and the electromagnetic parameters of the shielding material. With the exception of audio frequency H-fields or very light-weight shields, the EMP performance is determined by other factors. Typically, the controlling factors are the defective joints or bonds which generally appear at the interconnection between the conducting sheets, or the apertures which occur in vents (see Section 8) or between a door and sill. Still another problem is the penetration of wires and cables into the walls of an enclosure.

The effects of low frequency magnetic and electric fields can be considered separately where the enclosure size is quite small compared to the smallest wavelength of interest. When this is not the case, the combined effect of both components must be considered.

In the frequency range below 10 kHz, the magnetic field shielding effectiveness is controlled by the thickness, conductivity, and permeability of the walls. The greater these values, the lower the "turning point frequency." Below this frequency, the shielding is very small and above it the shielding increases with increasing frequency. For idealized enclosures, as the frequency is further increased, the performance improves greatly (because of the "skin effect") to a point where penetrating fields are not measured easily. For practical enclosures, the performance increasingly tends to become independent of frequency until enclosure or aperture resonances are encountered.

In the case of low frequency electric field penetrations, an idealized enclosure having a metallic wall thickness in excess of 0.001 inch exhibits such good performance

that it is very difficult to measure any appreciable penetration. In the case of practical enclosures, the electric field penetration in the low frequency region is controlled almost entirely by defects, bonds, apertures, or cable penetrations. Most high-performance enclosures can be made to exhibit very good electric field performance. In addition, effects of electric field coupling to equipment are often small or insignificant in this low frequency region. Therefore, electric field penetration measurements are not of general interest and should be considered only where very unusual susceptibilities to low frequency electric fields can occur.

One is often not interested in the nonlinear behavior of the electromagnetic parameters of the shielding material. In this case, single-frequency tests provide reasonable estimates of performance. However the specific CW excitation level may change the permeability and shield effectiveness. Intense excitation levels with a high low-frequency content and thin wall enclosures employing highly permeable materials are likely to exhibit saturation effects. These test procedures can be supplemented by tests employing fields and currents similar to those that might be experienced during an EMP event.

10.2.2 Performance Criteria

The performance of the shielded enclosure generally is specified in terms of "shielding effectiveness," which is defined as the ratio of the fields without the enclosure being present to the field with the enclosure installed. This concept is satisfactory only for monochromatic (CW) fields. This shielding effectiveness also must be qualified in terms of a measurement procedure, such as how the enclosure was illuminated, the amplitude of the illumination, the divergence of the illuminating fields, and the position of the sources and sensors. As such, the concept or criterion must be regarded as an "insertion-loss" criterion, dependent on the method of measurement.

Pulse response tests would be highly desirable, but appear extremely inconvenient to implement on a laboratory basis except for the smallest of enclosures. Moreover, very accurate measurement of both illuminating and penetrating waveforms would be required to characterize analytically the response over a wide frequency range. Measurement of peak pulse value of rate-of-change of peak value might prove worthwhile, but would require selecting a test waveform, redefining criteria, and large illuminating structures. The required illuminating structures and associated pulse sources are available, even for room or van size enclosures. These illuminating structures require taking the enclosure to be tested to the simulator.

Where pulse waveform penetration of restricted regions, such as small apertures in the wall of the shielded room, is of interest, the procedures for vents given in Section 8 can be extended to evaluate penetration effects for wide spread spatial distributions of apertures by employing a two plate or triplate line field exciter which uses the wall of the enclosure as one of the conductors as shown in Figure 8-3 of Section 8. Such test procedures are not commonly employed and appear to be of a special purpose nature.

Another test method which has acquired wide use measures the magnetic field penetration of a single MF frequency (usually about 100 kHz) near the seams. While such a procedure is useful during assembly of an enclosure, it has been shown to omit sensing some of the more obscure, but no less important, penetration modes.

Other criteria must also be considered; it is assumed that most systems which are EMP hardened by exterior shields would employ a single-point interior ground. Where this is not the case, the possibility of wall potentials developing between separated grounding points must be considered.

No procedure is provided for the measurement of wall potentials. Other specialized criteria exist; such as, the conversion of exterior quasi-static electric fields into interior magnetic fields, or, conversely, exterior quasi-static magnetic into interior electric fields. These two are--by past experiences and current practices--generally not considered.

Another consideration is the degradation in performance with age and other environmental factors. These must be considered on a specific basis.

It should be emphasized that shielding performance, except for the lowest frequencies or where weight and size are at a high premium, is either very good or very bad. This arises because the performance is controlled by defects. Thus, the major efforts should be to control these defects. These are best revealed by measurements made in the UHF band. The measurement results of this procedure--as well as any other recognized test procedure--are "insertion loss" tests; that is, they produce accurate results only for similar test situations. Therefore, some "safety margin" may be desirable if shielding effectiveness performance becomes a critical factor.

10.2.3 Definitions

In general, fields penetrating a shielding enclosure arise from both the electric and magnetic components of the electromagnetic energy impinging upon the enclosure. If the penetrating magnetic or electric fields are measured separately, each can be demonstrated to be a function of both the electric and magnetic components of the impinging waveform. In addition, the applied fields are altered radically in penetrating a high-performance enclsoure, and the measured penetrating waveforms are affected by the position of the sensor. As a consequence, measurement results

are highly sensitive to the test procedures employed, and simple amplitude ratios between any external and internal electric field vectors (or the magnetic field vectors) alone do not correctly characterize the shielding phenomenon. For similar considerations, simple measurements of power flow ratios in the conventional sense cannot be employed without reference to a standardized test procedure. As a result, a definition of a measure of enclosure performance is set forth and must be associated with a specific test and procedure. This measurement is termed "shielding effectiveness."

In the low-frequency region (200 Hz to 20 MHz), shielding effectiveness* can be expressed by

$$S_H = 20 \log_{10} (H_1/H_2) \qquad (10\text{-}1)$$

where

19

H_1 = magnetic field in absence of enclosure

H_2 = magnetic field within the enclosure.

For the UHF range (300-1000 MHz), the shielding effectiveness* is expressed by

$$S_E = 20 \log_{10} (E_1/E_2) \qquad (10\text{-}2)$$

where

E_1 = electric field in absence of enclosure

E_2 = electric field within the enclosure.

10.2.4 Type of Tests

10.2.4.1 General Procedures

Uniform procedures are provided to determine the continuous wave effectiveness over frequency ranges from 100 Hz to about 20 MHz and from 300-1000 MHz. Where only a general

*NOTE: This definition applies only to a specific measurement procedure described in subsequent sections.

estimate of effectiveness is desired, single frequency tests are recommended within three standard frequency ranges:

14-16 kHz
13-18 MHZ*
850-950 MHz*

Measurement results for these three standard frequency ranges form a uniform basis to compare the performances of various shielding enclosures.

For the lower frequency ranges (100 Hz to 20 MHz), magnetic loops are employed. In the the UHF range (300-1000 MHz), dipoles are employed.

In the lower frequency ranges, tests using both small and large loops are employed. The small-loop test procedures simulate, in some degree, the fields from sources near the enclosure walls. This test also provides an in situ measure of the effectiveness of certain constructional features, such as bonds between adjacent panels or gaskets. This procedure may also be used to measure the effectiveness of shielding doors. The small-loop test procedure covers the frequency range from 100 Hz to about 20 MHz.

The large-loop test procedure simulates, in some degree, a magnetic field encompassing the entire enclosure. As such, it provides a measure of the overall performance in the low-frequency region from 100 Hz to 200 kHz. Provisions for two large-loop tests are made, but the one involving the entire enclosure, where access to all walls of the enclosure is possible, is recommended. Where limited access exists, an alternate test is delineated which requires access to only one wall.

For the UHF range (300-1000 MHz), dipole-to-dipole tests are delineated. The effect of a nearby source on all

*Frequencies employed for dielectric heating or cooking are desirable, (I S M Frequencies).

portions of accessible wall areas is determined by one test procedure. The effect of distant sources is assessed by combining measurement results on all accessible portions of the enclosure.

The single-frequency measurements in the three above-mentioned recommended frequency ranges should provide a good guide for the relative performance of enclosures, or doors, in all ranges. However, tests using other frequencies pertinent to the specific installation should be considered. No recommended test procedures are noted for frequencies between 20-300 MHz, owing to the sensitiveness of the test results to small variations in measurement procedures. Large resonant type antennas are required. Enclosure cavity resonances in this region, as shown in Figure 10-1, often give rise to uncorrelatable results. Where tests in this region are desired, the practices noted for the small-loop tests or the UHF tests may be used as a guide.

10.2.4.2 Low-Frequency Loop Tests

The preferred large-loop test immerses the shielding enclosure in a magnetic field oriented to induce appreciable components of current throughout the shield. In the large-loop test, a significant portion of the seams is subjected to shielding currents by encircling the enclosure with a transmitting loop in order to obtain a gross measure of performance. The magnitude of the magnetic field generated at the center of this loop is determined indirectly from a measurement of the loop current and the enclosure dimensions; whereas the resulting field at the center of the enclosure is measured directly. A supplementary benefit of the test setup is the ease with which some of the shielding defects can be located by an exploring loop. To minimize effort, only one large-loop position is recommended as a basis for a uniform measurement procedure. A more complete

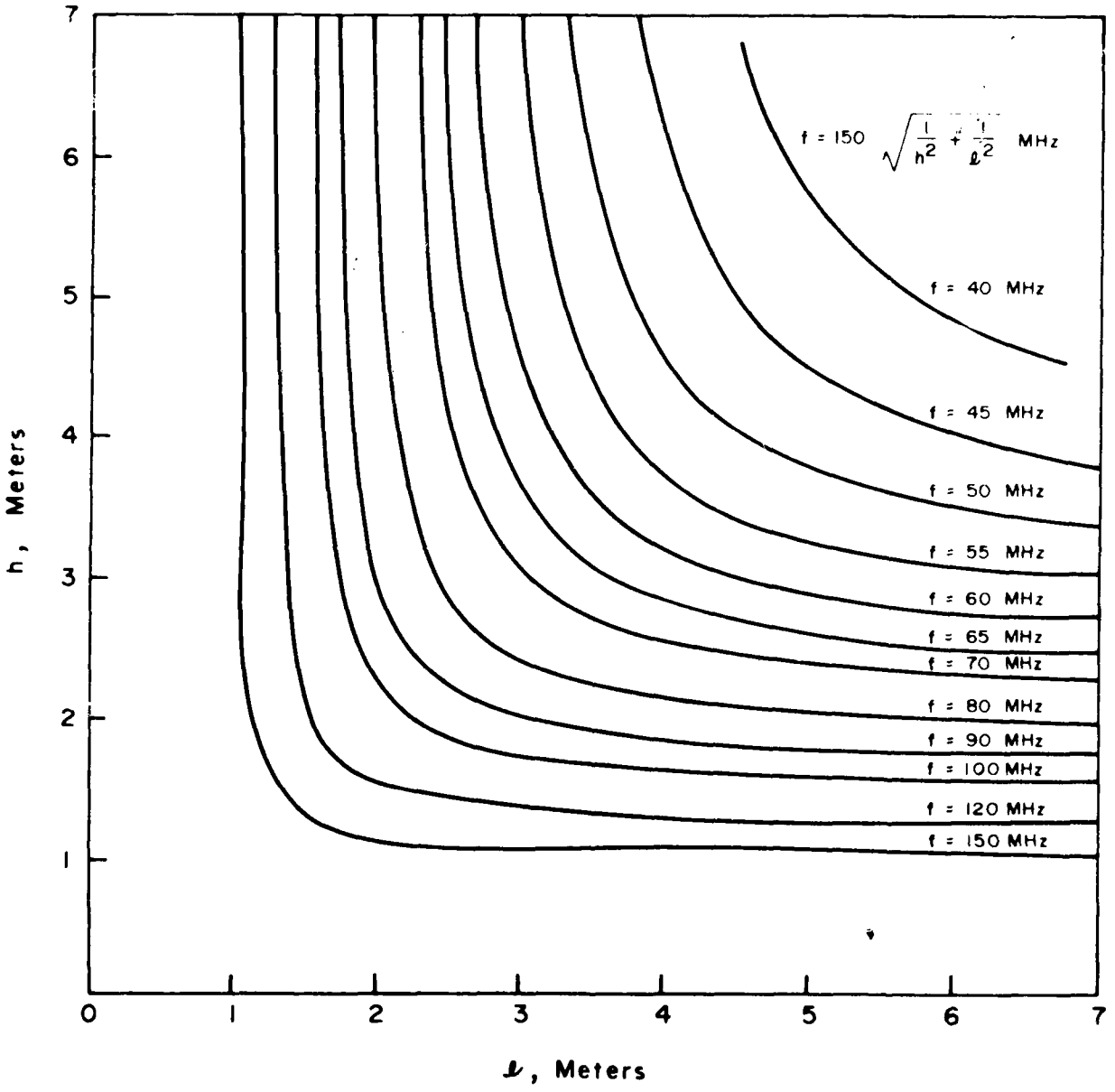

Figure 10-1. Lowest natural resonant frequency chart.

test would use this procedure as a guide and might employ at least three loop positions in planes approximately perpendicular to each other. The large-loop test may be modified to measure the performance of very small enclosures. The large-loop test procedure is usable anywhere in the frequency range from 0.1 kHz to 200 kHz.

The small-loop test, insofar as it is practical, evaluates the performance of the enclosure to sources near the enclosure walls. It is especially useful to determine, on a separate basis, performance of doors and sills as well as of enclosure seams and bonds. The small-loop test provides a uniform test procedure from 100 Hz up to about 20 MHz (instead of an upper frequency of 200 kHz, as for the large-loop tests).

10.2.4.3 UHF Tests

To simulate the effect of nearby sources, a UHF test procedure is provided to measure the shielding effectiveness of a portion of the surface of a typical room-sized enclosure, having a height not exceeding 3 meters. The effect of a distant source is assessed by combining the results of tests on all accessible portions of the enclosure. The UHF test procedures are designed to measure, insofar as possible, the general overall performance of the enclosure in the UHF region, and to assess the lower frequency performance in the 20-300 MHz range.

Since the general performance of an enclosure is often a function of certain constructional features, such as seams, bonds, or doors, the UHF test procedure may be used, on a preliminary basis, to evaluate the relative effectiveness of these constructional features. For many enclosure designs, measurements of seam, door, or bond performance can also be made in the 100 Hz to 20 MHz region using small loops. However, many shielding experts regard the UHF test as more revealing of the presence of apertures and other defects.

UHF test procedures are provided for a frequency range from 300 MHz to 1000 MHz. In all cases, the frequency range of the source must be chosen to be well above the lowest natural resonant frequency of the enclosure. For a rectangular parallelepiped (the usual shape of the enclosure), the lowest natural resonant frequency, provided the width, w, is small compared with the height, h, or the length of the longest side wall, ℓ, is approximately given as:

$$f_r = \frac{150}{h}\sqrt{1 + \left(\frac{h}{\ell}\right)^2} \qquad (10\text{-}3)$$

where f_r is in MHz, and h and ℓ are in meters. Alternatively, this frequency may be obtained from Figure 10-1.

The UHF test procedure may be modified to evaluate the performance of very small enclosures. If a frequency is selected in the 900-1000 MHz region, small exciters and sensors are possible. The small size permits ease of installation of the sensor within the enclosure.

10.3 Large Loop Test

10.3.1 Test Equipment and Setup

All signal sources, pickup devices, and measuring equipment, as well as their arrangement with respect to the shielding enclosure, shall be in accordance with the following paragraphs and Figure 10-2.

10.3.2 Source of Magnetic Field

The test magnetic field is generated by current in a large planar loop encircling the enclosure at a spacing of at least one inch from the outer shielding material. Such a loop around a rectangular parallelepiped forms a parallelogram. As shown in Figure 10-2, the obtuse angle vertices are positioned away from the floor and ceiling by distances C and D which are proportional to the horizontal distances form the respective acute vertices:

$$C = \left(\frac{w}{\ell + w}\right) h \qquad (10\text{-}4)$$

$$D = \left(\frac{\ell}{\ell + w}\right) h \qquad (10\text{-}5)$$

It may be noted that C = h - D and D = h - C. In these equations, ℓ, w, and h are the enclosure dimensions of length, width and height respectively. The large loop consists of a single turn of stranded, insulated copper wire, preferably No. 18 AWG "hook-up" wire. The loop wire can be fastened by means of rubber suction cups, masking tape, or both. This wire can be fastened to the exterior surface of the enclosure or to nearby objects, such as building walls, so that the wire is at least 2.5 centimeters (1 inch) away from the outer wall of the enclosure.

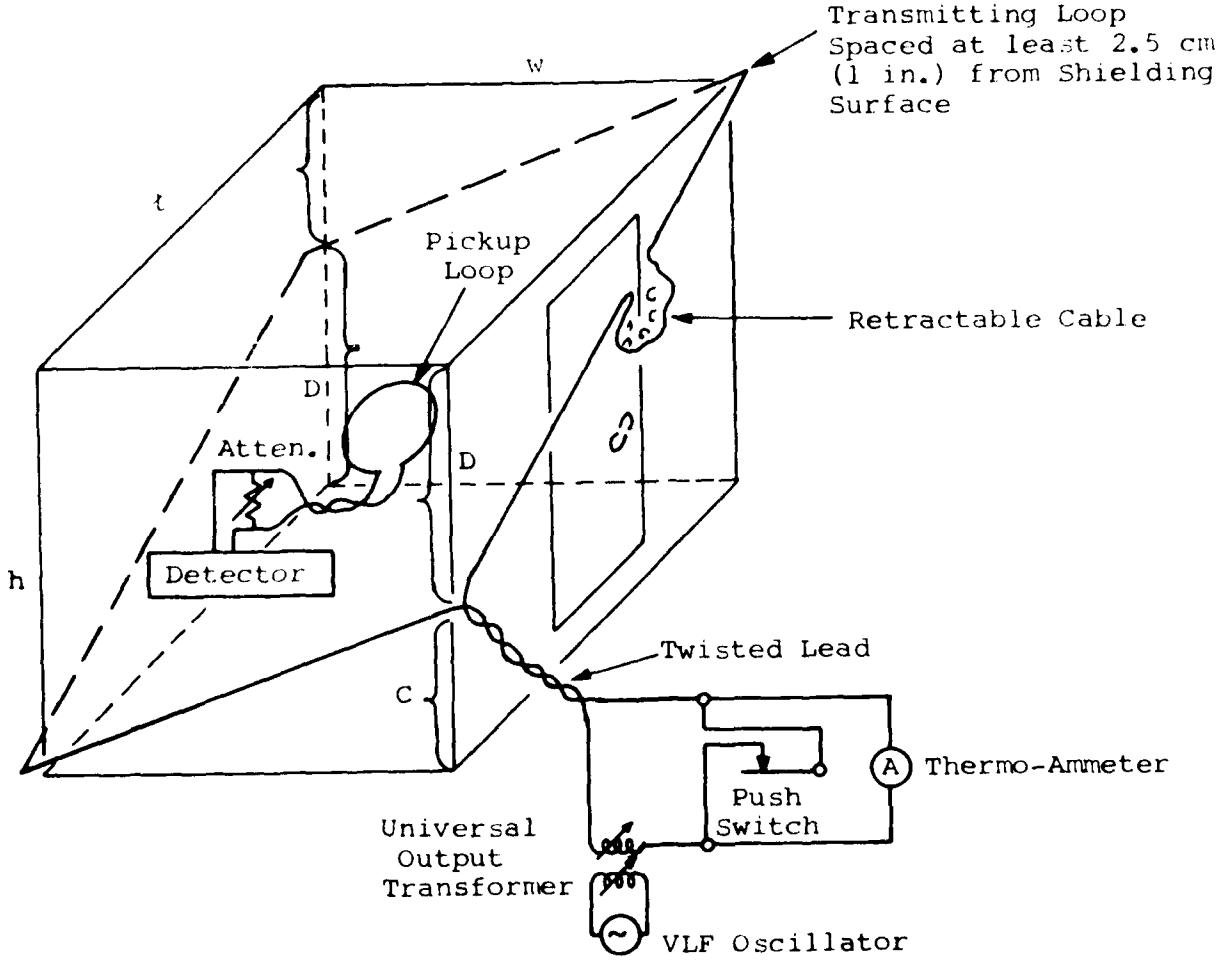

NOTES: $C = \frac{W}{t+W} h$

$D = \frac{t}{t+W} h$

Pickup loop in plane of large loop or center of enclosure

ALSO $C = h-D$

$D = h-C$

Figure 10-2. Large-loop test setup.

In order to avoid obstruction of the door by the large loop, a retractable cable such as a test prod lead or telephone cord may be utilized as part of the loop at the jamb edge of the door, as shown in Figure 10-2. For maximum convenience, the large-loop orientation can be selected so that this cable is placed on the upper portion of the door.

A conventional one-watt output RC oscillator is usually adequate to supply the loop current in the VLF band, provided the impedance mismatch is minimized at the lower frequencies by a step-down transformer, such as a universal output transformer. Higher power sources and resonant matching may be required at higher frequencies. Current through the large loop may be measured by the voltage drop across a known carbon resistor or by using a thermo-ammeter, with a parallel momentary-open switch to protect it against overload.

10.3.3 Detector

20

The detector may be either a field-strength meter equipped with a pickup loop for the measurement of magnetic fields, or a combination of pickup loop and high input impedance RF voltmeter. The detector should be capable of indicating 300 microvolts.

For a field strength meter, the calibration and meter readings are normally given in terms of an equivalent electric field E_{eq2} on the basis of plane-wave propagation. The corresponding magnetic field H_2 is then obtained from the expression

$$H_2 = \frac{E_{eq2}}{\eta} = \frac{E_{eq2}}{120\pi} \qquad (10\text{-}6)$$

where η is the wave impedance of free space, and for the numerical form, H_2, is expressed in amperes per meter when E_{eq2} is given in volts per meter.

If a pickup loop, high-impedance voltmeter combination forms the detector, the pickup loop should consist of 11 turns of closely spaced insulated wire on a 0.762 meter (30-inch) diameter form. The loop should be connected to a voltmeter (or amplifier-voltmeter combination) of high input impedance only. The input impedance must always be large compared to the inductive reactance of the loop.

For the high-impedance voltmeter detector, the field H_2 in amperes-per-meter at the center of the enclosure is given by

$$H_2 = \frac{V_{induced}}{2\pi f N_1 A \mu} \qquad (10\text{-}7)$$

and for the suggested loop, Equation 10-7 reduces to:

$$H_2 = 2.5 \times 10^4 \left(\frac{V_{induced}}{f} \right) \qquad (10\text{-}8)$$

where

$V_{induced}$ = induced voltage in volts

f = frequency in hertz

N_1 = number of pickup loops (11)

A = area of pickup loops (0.456 square meters)

μ_o = permeability of air ($4\pi \times 10^{-7}$ henry/meter).

10.3.4 Preliminary Procedures and Precautions

Metallic equipment or metal-containing equipment, such as internal cables, chassis, chairs, and cabinets, should be removed prior to conducting tests. A power-line filter can be used to supply energy for internal lighting and the detection equipment, if large enclosures are being tested. Where the enclosure is to be tested as a component, the power line filter outputs should be capped with a shield, and power be supplied by batteries and converters. All cables and pipe entry points should be capped for shielding evaluation of the enclosure itself.

10.3.5 Basic Measurement Procedure

Both signal source and detector should be arranged as shown in Figure 10-2. All the measurement equipment must be connected and warmed up until stabilized. The detector loop is positioned at the geometric center of the enclosure, and the plane of this loop is oriented for maximum signal. Both the signal source oscillator and detector tuning (if tunable) should be adjusted to the measurement frequency.

The oscillator output is adjusted until adequate for the measurement; the current in the transmitting loop can be indicated by a thermo-ammeter. Currents on the order of 20-200 milliamperes have been found satisfactory in the VLF band.

With all shielding-enclosure entrances securely closed, the detecting equipment is tuned to the source (if narrow band) and the meter reading noted. The received field is then calculated with aid of either Equation 10-6 for a field strength meter or Equation 10-8 for a high-impedance voltmeter.

10.3.6 Simulation of the Field in Absence of Enclosure

For the rectangular parallelepiped enclosure, the magnetic field H_1 produced at the center of the loop by this source can be calculated from

$$H_1 = \frac{2I}{\pi w} \Bigg/ \sqrt{\frac{1 + (\frac{w}{\ell})^2}{1 + (\frac{h}{\ell + w})^2}} \qquad (10\text{-}9)$$

where H_1 is expressed in amperes per meter when

I = coil current in amperes

h = enclosure height in meters

ℓ = enclosure length in meters

w = enclosure width in meters.

The relation given by Equation 10-9 is an approximation which assumes a zero-diameter wire filament.

10.3.7 Data Reporting and Reduction

Shielding effectiveness is determined by Equation 10-1 from the results of 10.3.4 and 10.3.5. The positions or conditions (e.g., capped) of all cables, power lines, and other conductors normally entering the shielding enclosure should be noted.

10.4 Small Loop Test

10.4.1 Introduction

All signal sources, pickup devices, and measuring equipment, as well as their arrangement with respect to the shielding enclosure, should be in accordance with the following paragraphs and Figure 10-3.

10.4.2 Source of Magnetic Field

The test magnetic field is generated by current in an 0.30 meter (12-inch) diameter transmitting loop. The loop may be constructed from a single turn of No. 6 AWG copper wire. A conventional laboratory test oscillator is usually adequate to supply the loop current by a suitable step-down transformer such as a universal output-to-voice-coil transformer in the VLF band. Higher power sources and resonant matching may be required at higher frequencies.

10.4.3 Detector

The detector may be a field strength meter or a high impedance voltmeter which measures the voltage induced in a pickup loop identical to the 0.30 meter (12-inch) transmitting loop.

10.4.4 Measurement Precautions

Metallic or metal-containing equipment, such as chassis, interior cables, and cabinets, should be removed prior to conducting tests. A power-line filter may supply energy for internal lighting and the detection equipment, but a battery supply (DC to AC converter) is preferred, along with capping all exterior cable entry points.

Prior to making the measurement, especially for newly installed enclosures, it is desirable to scan the available areas of the enclosure in order to disclose serious defects, particularly those near seams. This is done by raising or

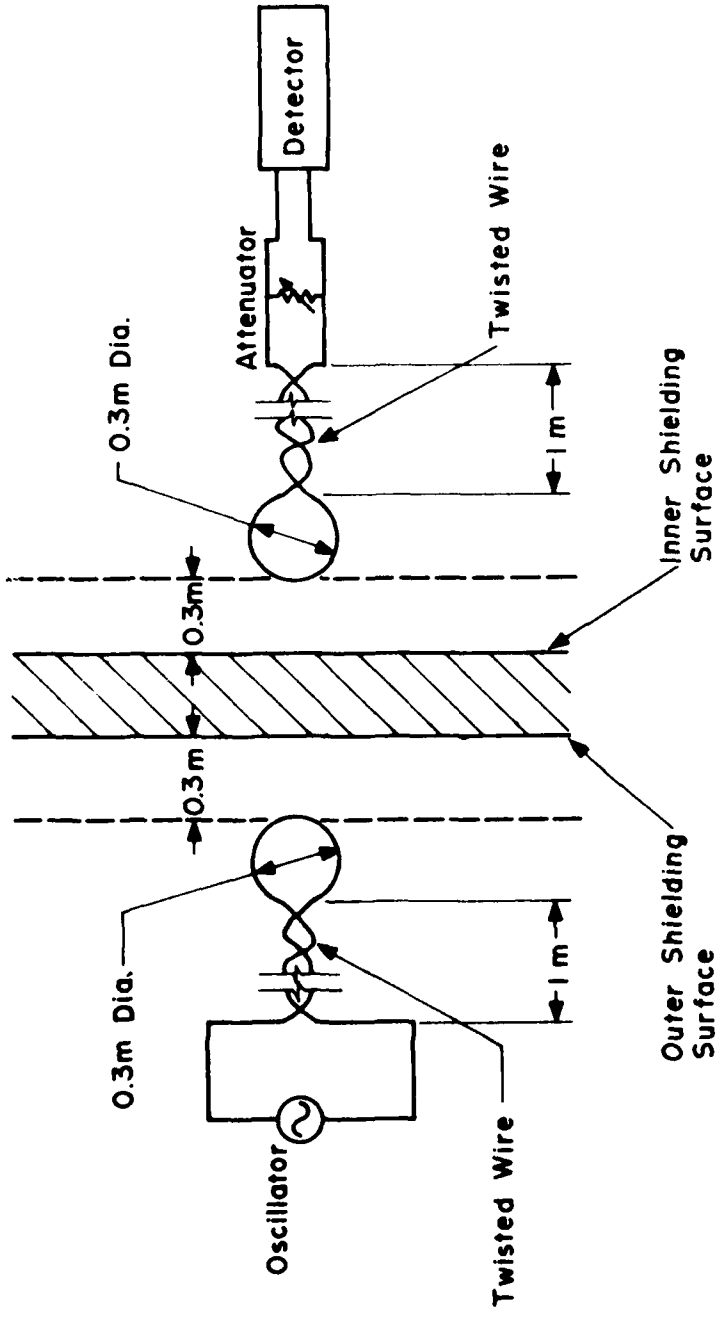

Figure 10-3. Small-loop test setup.

lowering the source and receiving loops simultaneously, so that the dimensions indicated in Figure 10-3 are held, while noting the reading of the output meter for any significant increase over or above that normally experienced. Worst-case areas should be noted and a uniform measurement, insofar as possible, should be conducted and reported for these areas as outlined in the following paragraphs. Tests should be made to ensure that no case leakage exists at the meter. When the detector pickup is disconnected at the case, or when the loop itself is "shorted" near the excited detector loop, the meter should read substantially below the smallest measured value.

10.4.5 Measurement Procedure

The measurements are made using the configuration shown in Figure 10-3 with transmitting and receiving loops coplanar, and each spaced 0.305 meters (12 inches) away from a shielding barrier in a plane perpendicular to a metal seam.

Measurement should be made near door contacts, panel seams or joints, power-line filters, and air inlets. For doors, small-loop tests are to be conducted at six loop positions as indicated in Figure 10-4. The plane of the loop is perpendicular to that of the door and panel being tested, and perpendicular to the line of the door contact. For the horizontal portion of the door, the loop should be located equidistant from the edges. For the vertical contact regions, the loop centers should be located one-third the distance from either the top or the bottom. The top and bottom vertical contacts should be tested as indicated in Figures 10-4a and 10-4b, provided the facilities permit such tests. Should the facilities preclude such tests, loop positioning as indicated in Figure 10-4d should be used.

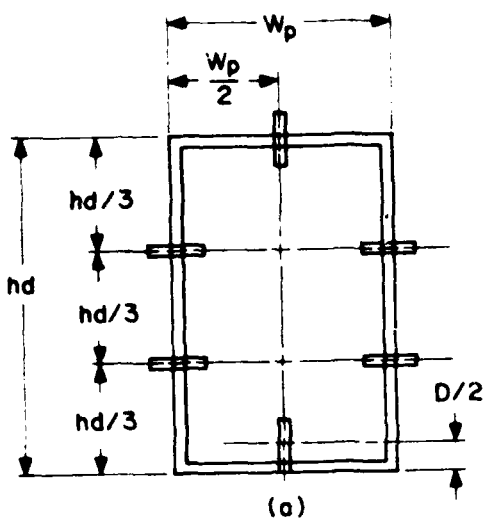

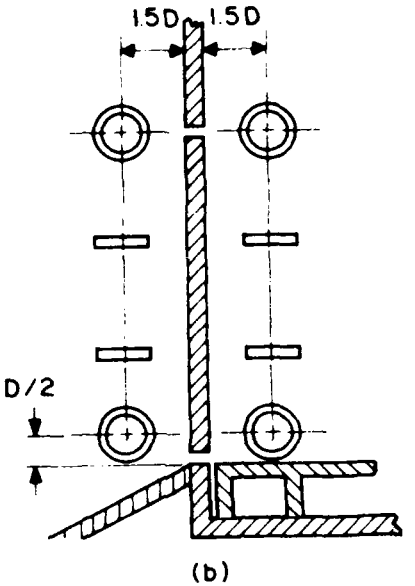

(a), (b) Loop Positions For Door Measurements

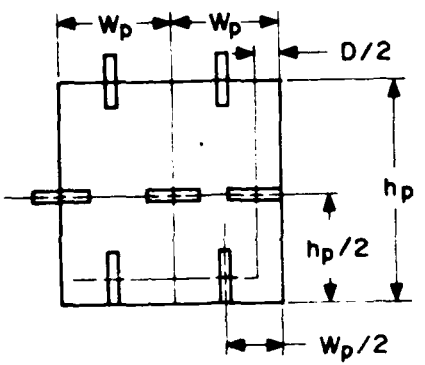

(c) Loop Positions For Panel Seam Measurements

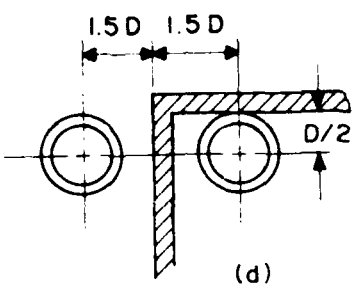

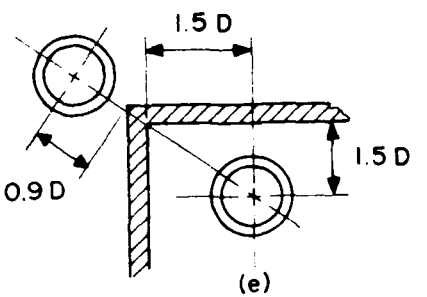

(d) Partially Or (e) Fully Accessible Loop Positions For Corner Seam

Figure 10-4. Standardized positions for small loop-tests.

Wherever the shielding enclosure construction is discontinuous, tests should be made in the region of the discontinuity or seam. Discontinuities include regions where modular portions are joined together by a clamp or bolt assembly, or by a soldered or welded joint. The tests to be conducted are similar to those for doors, except that centers of the loops should be located only at the midpoints of each seam or joint. Corner seams should be tested as in Figures 10-4d or 10-4e. Where the corner is fully accessible, tests using the arrangements of Figure 10-4e should be conducted.

An air vent or similar penetration point should be treated similarly to a seam. The plane of the loop should be perpendicular to the panel and seam formed between the panel and air vent, and located so that the plane of the loop passes through the midpoint of the seam formed by the vent. The plane nearest the edge of the loop should be located 12 inches from the panel. Ancillary equipment, such as blowers and fans, which are not an integral part of the shielding enclosure should be removed while performing these tests. (Tests should also be considered with ancillary equipment in place.)

21

To facilitate the tests, it is permissible to locate the positions of the external and internal loops only approximately, insofar as the coplanar positions of the source and detector loop are concerned. During all measurements, the detector is re-oriented and raised or lowered (at least one-fourth the seam distance) to ensure that a worst-case measurement has been realized. For each position, the maximum indication of the detector reading is to be used.

10.4.6 Simulation of the Field in Absence of Enclosure

The field, H_1, in the absence of the shielding enclosure, is obtained by direct measurement. The pickup loop is spaced from the transmitting loop by 0.610 meters (24 inches) center-

to-center plus the thickness of the shielding barrier, the same total loop-to-loop distance utilized when a shielding barrier intervenes. This spacing is critical in two respects: the magnitude of reflection of the incident wave from the shielding surface and, transmission through the shield as a function of source-to-shield spacing. Furthermore, the received fraction of the emitted energy (real and reactive) depends on the coil-to-coil spacing.

10.4.7 Data Reduction

If the detector is a field strength meter calibrated to read equivalent electric field (volts per meter), the magnetic field strength in the absence of the enclosure is given by Equation 10-10a (where the definition of terms used in Section 10.3.3 are employed) and the magnetic field strength in the presence of the enclosure is given by Equation 10-10b.

$$H_1 = \frac{E_{eq1}}{\eta} = \frac{E_{eq1}}{120\pi} \qquad (10\text{-}10a)$$

$$H_2 = \frac{E_{eq2}}{\eta} = \frac{E_{eq2}}{120\pi} \qquad (10\text{-}10b)$$

When a high-impedance voltmeter is used, the magnetic field strengths can be calculated from Equation 10-11. For the pickup loop used, this becomes

$$H_1 = V_1 \, (N_2 A \mu 2\pi f)^{-1} = 1.7 \times 10^6 \left| \frac{V_1}{f} \right| \qquad (10\text{-}11a)$$

$$H_2 = V_2 \, (N_2 A \mu 2\pi f)^{-1} = 1.7 \times 10^6 \left| \frac{V_2}{f} \right| \qquad (10\text{-}11b)$$

where V_1, A, μ, and f are as defined in Section 10.3.3 and N_2 is the number of turns used for the small-loop test of Section 10.4. For the suggested loops, $N_2 = 1$, $A = \frac{1}{4}\pi(0.3)^2 \; \pi/4$ and $\mu = \mu_o = 4\pi 10^{-7}$ henries/meter. V_1 and V_2 are in volts measured in the absence and presence of the shielding enclosure respectively, and f is the frequency in hertz.

The shielding effectiveness may now be computed by Equation 10-1 for the minimum value and by Equations 10-12 and 10-1 for the average value.

The condition of the enclosure should be noted with respect to power cables, vents, and internal equipments. Where average shielding effectiveness values are to be computed, these should be based on the average amplitudes so that

$$(H_2)_{ave} = \frac{1}{K} \sum_{n=1}^{n=k} (H_2)_n \qquad (10\text{-}12)$$

Figure 10-5 presents typical results for a 25 gauge steel bolted panel (not welded) enclosure using the large-loop test procedure in the ELF and LF bands. Figure 10-6 shows the test positions (as noted in Figure 10-4) on the same enclosure for the small loop test. Figure 10-7 shows one method of presenting small loop test data. The fundamental resonance of the enclosure was above 30 MHz.

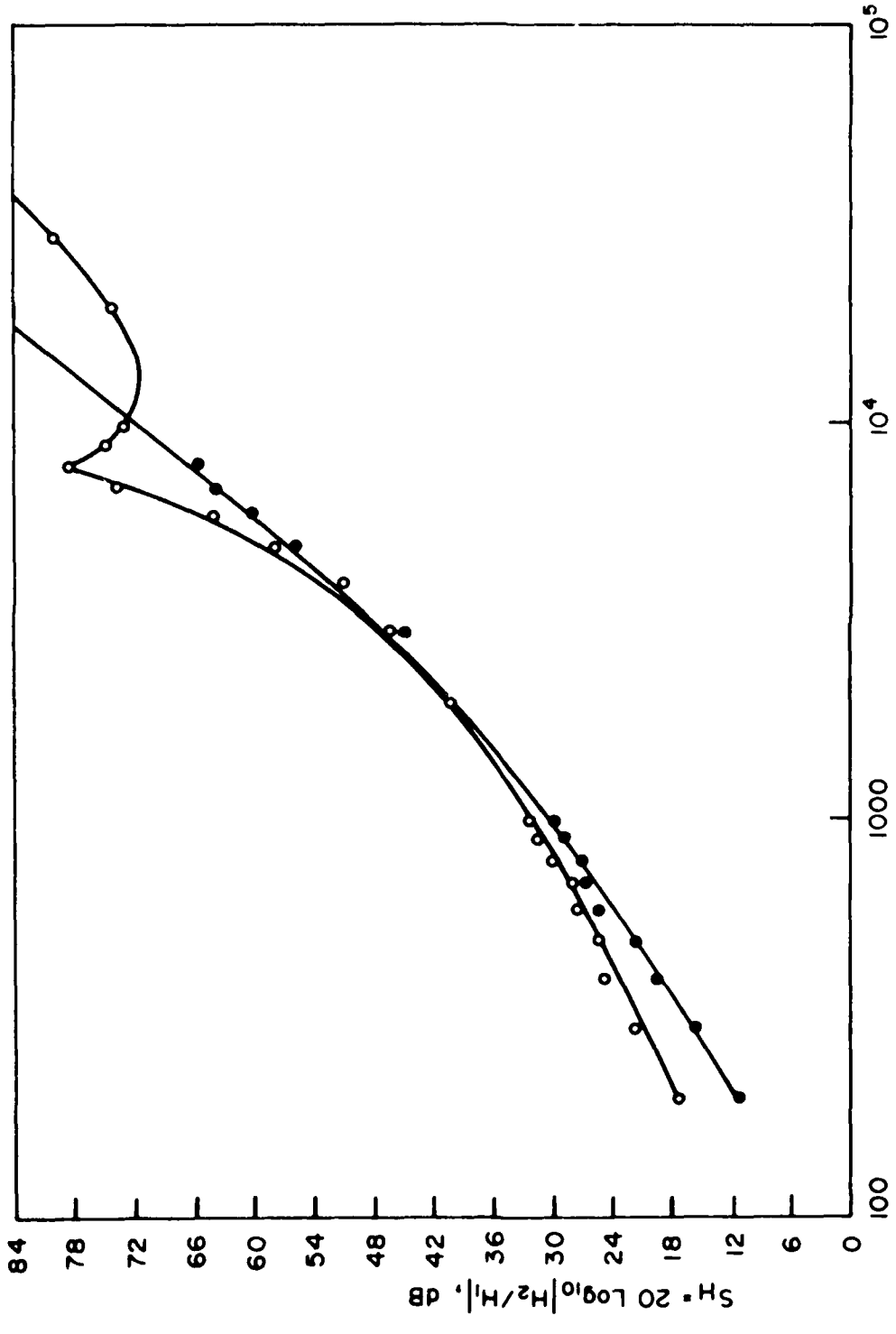

Figure 10-5. Typical results of large-loop tests on 25 gauge steel bolted panel enclosure.

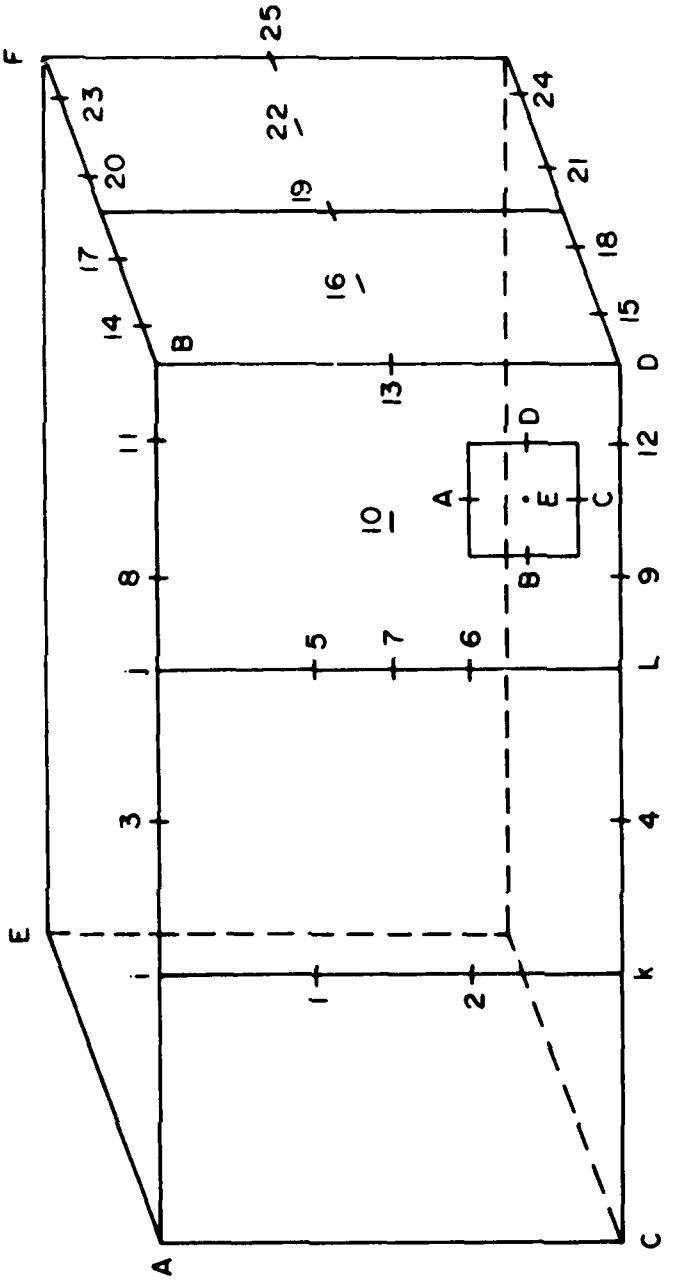

Figure 10-6. Diagram of shielded room showing labeled seams and position numbers for small-loop tests.

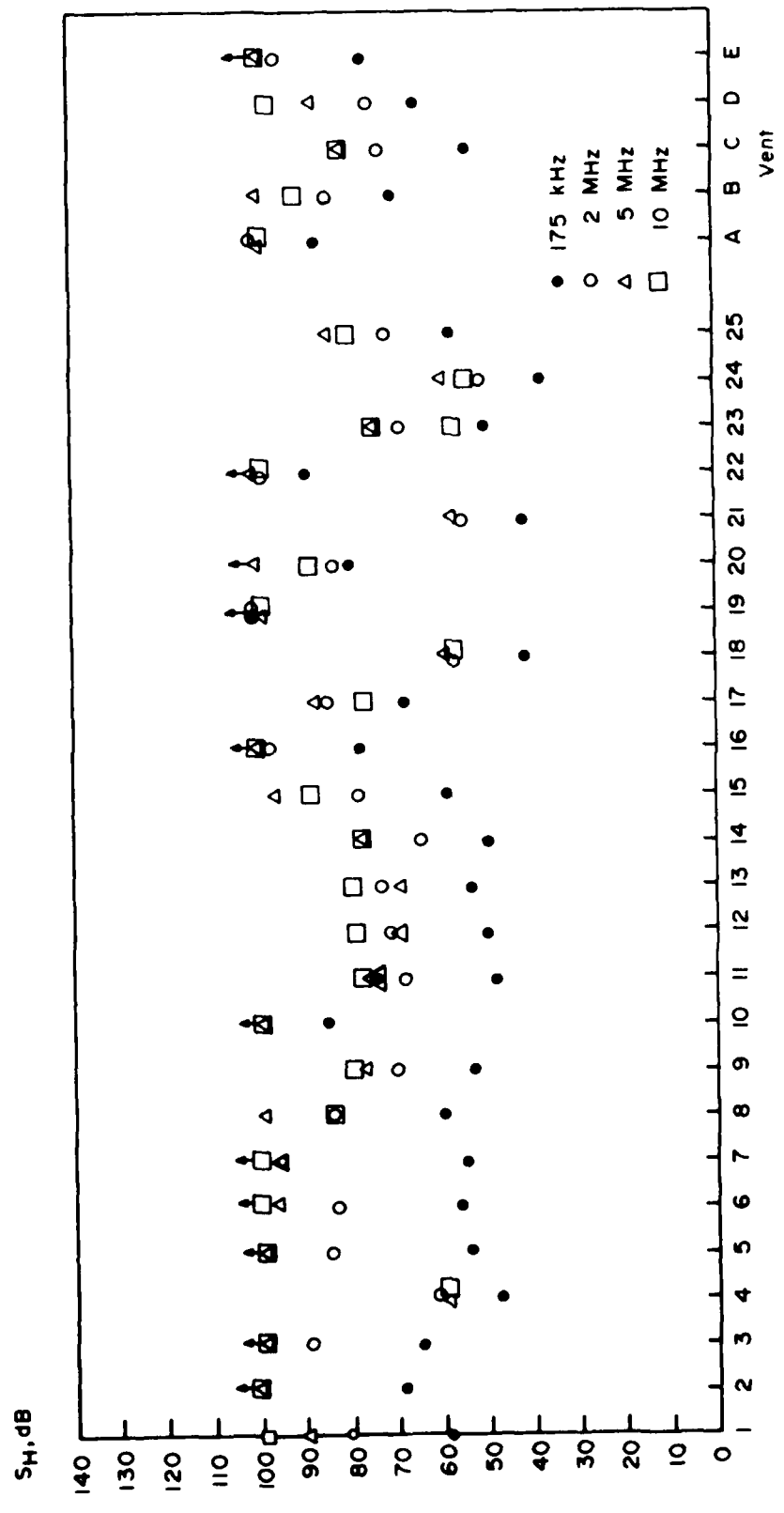

Figure 10-7a. Small-loop shielding effectiveness on 25 gauge steel bolted panel enclosure.

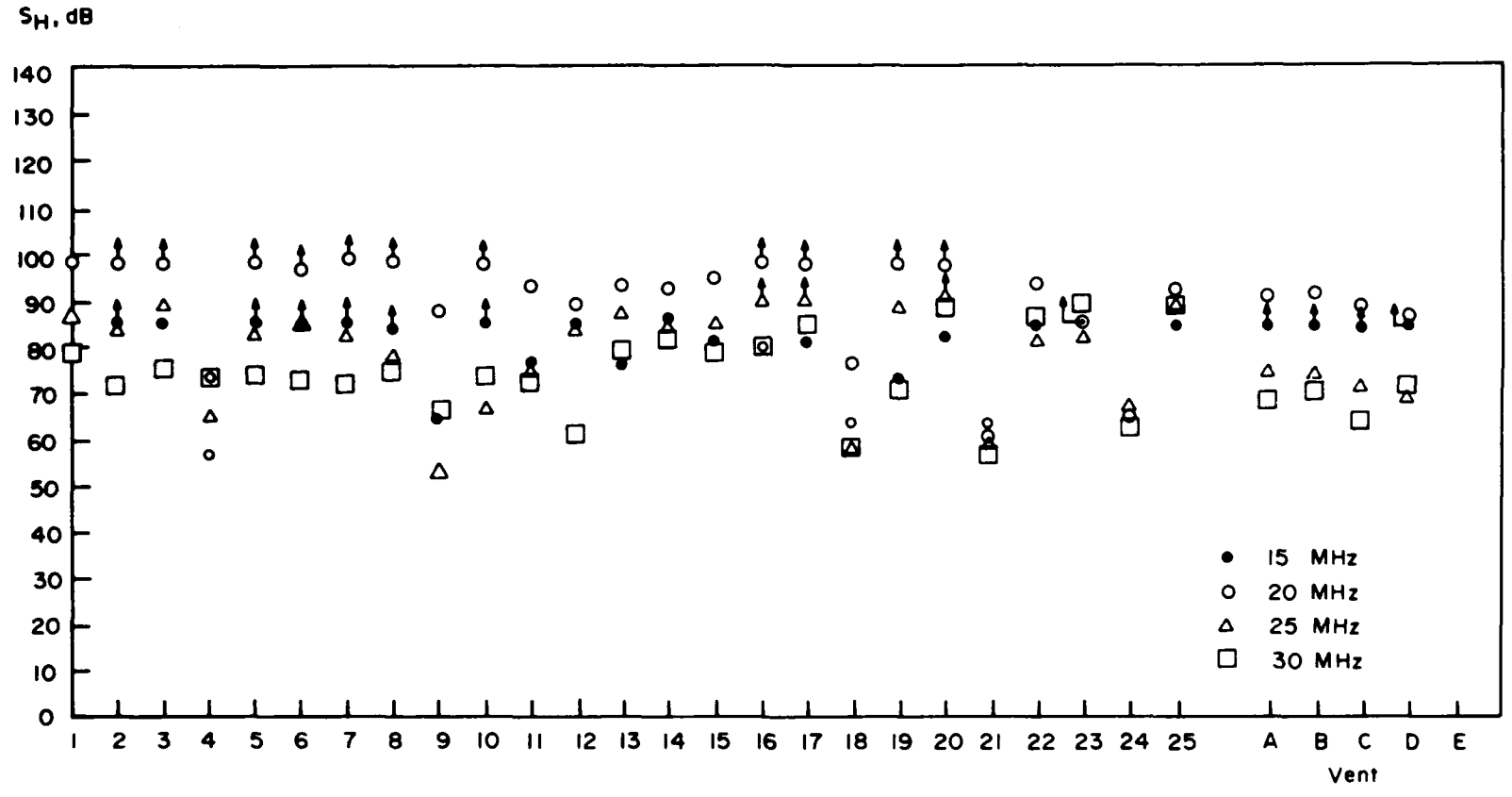

Figure 10-7b. Small-loop shielding effectiveness on 25 gauge steel bolted panel enclosure.

10.5 UHF Test Procedure

10.5.1 Introduction

All signal sources, pickup devices, and measuring equipment, as well as their arrangement with respect to the shielding enclosure, should be in accordance with the following paragraphs and Figures 10-8 and 10-9.

10.5.2 Source of UHF Electromagnetic Field

Because of the high attenuation usually introduced by the shielding enclosure, a signal generator capable of delivering at least 10 watts into a matched load may be required. The generator should be connected to a 75-Ω unbalanced to a 300-Ω balanced transformer. The output of the 300-Ω side of the transformer should be connected to a half-wavelength, balanced, folded dipole antenna which is resonant at the test frequency. Other forms of providing a balanced drive, and which preclude radiation from the cable, are acceptable but should be described in the test report. The cable should be perpendicular to the dipole and should be at least two meters or two wavelengths long, whichever is the greater.

22

10.5.3 Detector

The detecting antenna is an electric dipole whose overall electric length is one-eighth of a wavelength (so as to minimize impedance change problems at the test frequency). The output of the receiving antenna is connected through a balanced-to-unbalanced transformer (balun) via an antenna cable, such as RG-9 or equivalent. The antenna cable is connected to a field strength meter. The field strength meter should be preceded by an attenuator, if one is not contained within the field strength meter. The field strength meter should be located well away from the vicinity where the tests are being conducted. The coaxial cable,

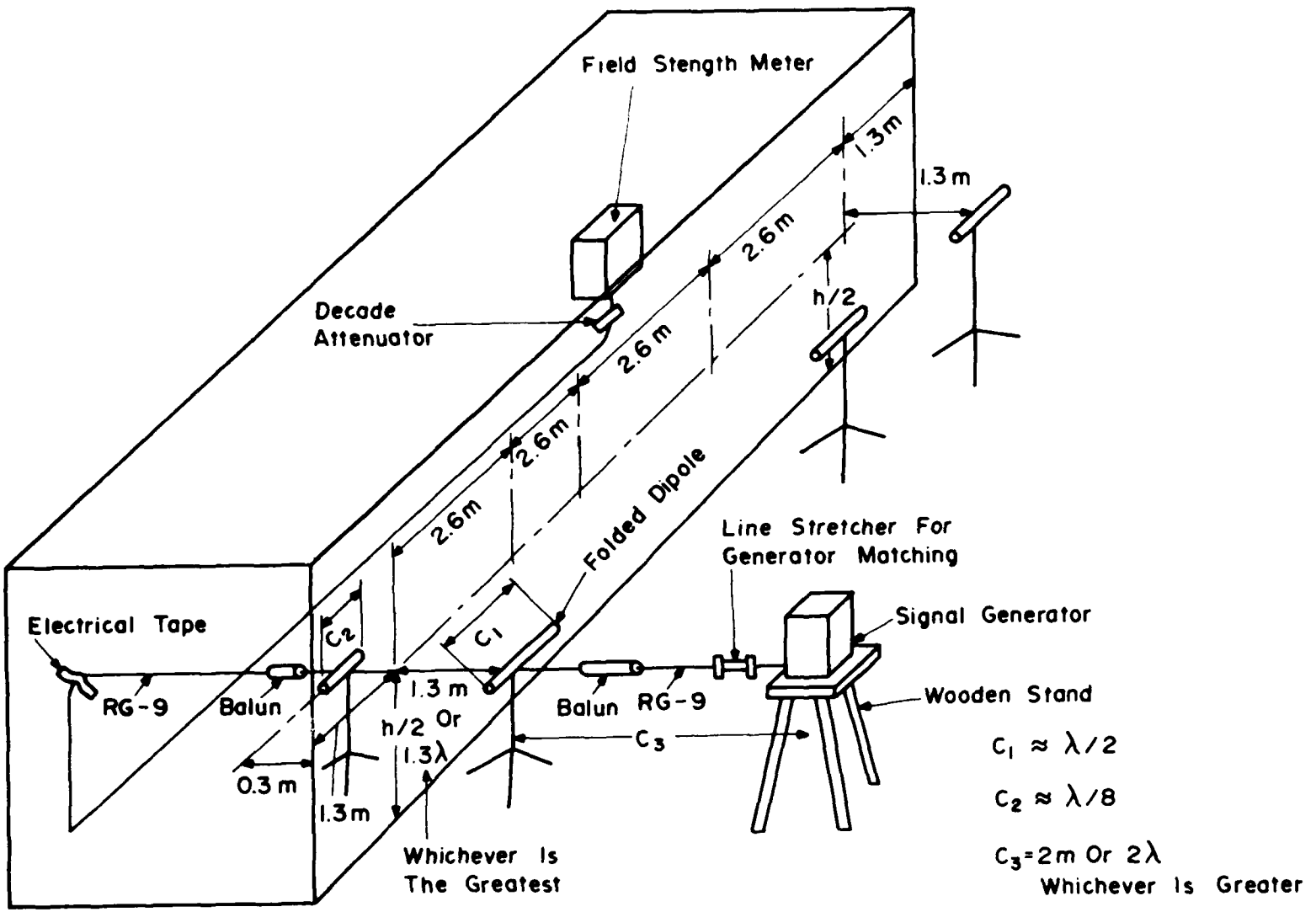

Figure 10-8. UHF measurement setup.

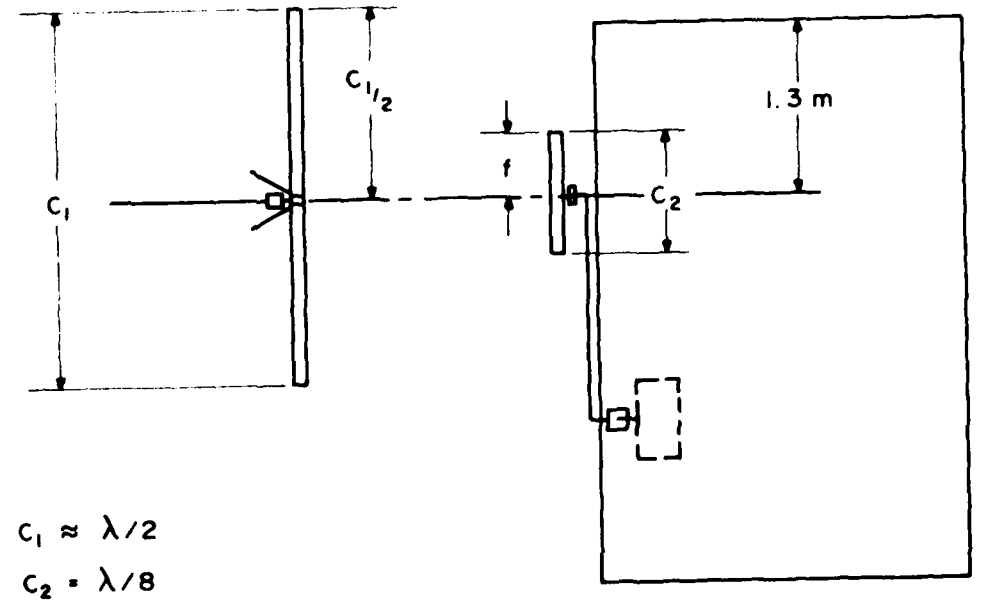

(a) Plan View

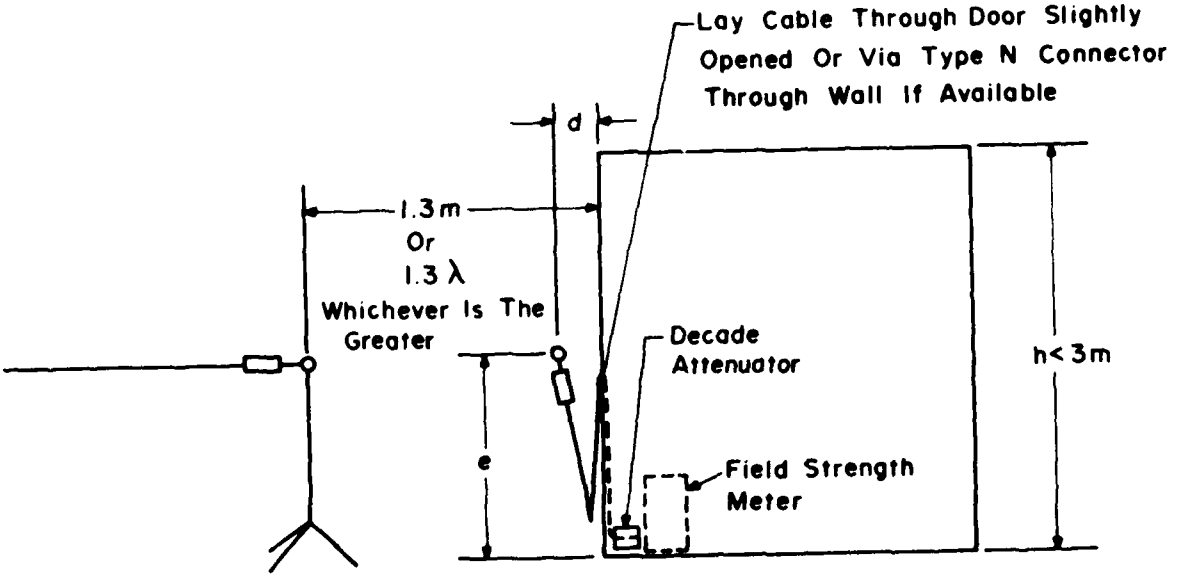

$d = 0.3\ m\ (\pm \lambda/4$ By Movement)
$e = h/2$ (At Least $\pm \lambda/4$ And $< h/4$)
$f = C_2/2\ (\pm \lambda/4$ By Movement)

(b) Side View

Figure 10-9. Setup for simulating free field.

except in regions very close to the walls or floors of the enclosure, must always be perpendicular to the axis of the electric dipole. The field strength meter should have a sensitivity of -80 dBm or better, and should be insulated from the conductive portions of the enclosure.

10.5.4 Precautions

It is suggested that preliminary measurements be made to detect shielding defects, such as poor door and seam contacts or bad joints around power-line filters and air inlets, especially for newly installed enclosures prior to actual measurement. Shielding defects noted may be repaired before measurement.

Metal-containing equipment, such as chassis, cable runs, and cabinets should be removed prior to conducting tests. A power-line filter may supply energy for internal lighting and the detection equipment, but a battery and DC to AC converter is preferred. All cables, power lines and other utilities normally entering the enclosure should be in place when tests are conducted.

To locate shielding defects in a given region, the transmitting antenna is approximately positioned opposite this region as shown in Figure 10-8. The receiving antenna is used as a probe primarily to locate areas of maximum penetration. Items which should be checked are door seams, power-line or air filter panels, air vent areas, panel seams and cable fittings. The receiving antenna may be positioned to within a quarter wavelength of the area under investigation, and its position and polarization orientation varied so as to note any pickup maximum. Preferably, all seams and bonds should be scanned by this procedure. Once a given region (approximately within $\pm$ 1.3 meters away from the projected center of the transmitting antenna as noted in Figure 10-8) has been explored, the transmitting antenna is repositioned to permit exploration of an adjacent region

as suggested in Figure 10-8. If the performance of the enclosure appears inferior, remedial measures are suggested prior to tests. Regions of excessive penetration should be noted on the test reports.

10.5.5 Measurement Procedure

In many situations, it is impractical to illuminate an entire side of an enclosure. For this reason, a measurement procedure is delineated where smaller areas are succesively illuminated. The distance of the transmitting antenna to the enclosure is chosen on the basis of providing reasonable uniform illumination for typical room-sized enclosures not exceeding 3 meters, in height, of a small area, which is approximately 2.6 meters by 2.6 meters. Any penetration of the enclosure can result in standing waves having different polarizations within the enclosure. To take this into account, the test procedure requires that the receiving antenna be positioned over $\pm \lambda/4$ distances to minimize the effect of standing waves, and the orientation varied to explore all possible polarizations.

The transmitting antenna should be located in the plane parallel to the face of the enclosure wall undergoing tests. The distance of 1.3 meters was chosen to be at least 5/4 of the longest UHF wavelength to minimize antenna loading effects and to provide uniform illumination. (If the UHF test is extended into the VHF region, this distance should be 5/4 of a wavelength.) The center of the transmitting antenna should also be located 1.3 meters from the corner of a height of h/2. Initially the receiving antenna should also be located within the enclosure in a plane parallel to the enclosure wall. It should be separated from the enclosure by 0.3 meter (so as to exceed a quarter wavelength at the lowest UHF frequency) at the same height as the transmitting antenna and with the same separation of 1.3 meters from the corner.

Tests are conducted with the source antenna horizontally polarized, and then repeated with a source vertically polarized. For each transmitter polarization, the polarization of the receiving antenna is rotated from horizontal to vertical. Simultaneously, the receiver antenna is moved horizontally in all directions at least $\lambda/4$, and vertically at least $h/4$, so as to intercept any maxima in the event of standing waves. The maximum reading should be noted.

A similar test is conducted 1.3 meters from the other corner of the face. It is repeated every 2.6 meters so that the entire face has been exposed to tests every 2.6 meters or closer. Two test results are required: the maximum field strength indication and the average amplitude of the field strength indications. Similar tests are also repeated on all accessible panels. It is suggested that a decade attenuator preceding the field strength meter be employed to achieve a scale multiplication. This will insure that the output meter operates in the same nonlinear region through the test.

10.5.6 Simulation of the Free Field in Absence of Enclosure

The ideal way to simulate the free-field environment would be to employ similar test spacings, but in a reflection-free environment. This is not practical, however, so a procedure is delineated which utilizes an outside wall of the enclosure to provide a reasonably consistent reflecting surface. When illuminated, the reflection from the enclosure creates a standing wave and the average value of this standing wave in a small region is a measure of the far field in a reflection-free environment. By means of this approach, the free field can be reasonably simulated within typical facilities as noted in the following paragraphs.

To simulate the free field without the presence of the enclosure, the following test procedure is set forth. It is designed to be conducted within typical facilities

housing shielding enclosures and with a minimum reliance on long-term calibrations. For every test position indicated in Figure 10-8, the free field condition is simulated by placing the detector antenna approximately 0.3 meter (so as to exceed $\lambda/4$ at the longest UHF wavelength) outside the shielded enclosure as shown in Figure 10-9.

The coaxial cable to the electric dipole should be perpendicular to the axis of the dipole, except in the immediate vicinity of the shielding enclosure. The cable from the detector dipole may be attached to the field intensity meter via a coaxial cable fitting often found on the walls of the enclosure. If this is not available, the door is opened slightly to permit running the cable to the field intensity meter. In some cases, calibrated attenuators prior to the field intensity meter should be included with the reading of the field meter increased by the appropriate amount.

Employing horizontal polarization for both antennas, the receiver detector dipole is moved up and down at least h/4 but not more than the height of the enclosure. It is also moved horizontally away and toward the source at least $\lambda/4$ so as to intercept any maxima or minima in the event of standing waves. During this procedure the maximum and minimum readings of the field strength meter are noted. Field strength without the the presence of the enclosure is simulated by taking the average of the amplitude of the maximum and minimum readings.

These test procedures require multiple measurements of a similar performance feature at different locations or polarizations. For a given procedure, the minimum and average shielding effectiveness should be reported. The average shielding effectiveness shall be based on an average amplitude.

Minimum and average values of shielding effectiveness should be calculated for any group of measurement positions and polarizations using the following definition:

$$S_E = 20 \log_{10} (E_1/E_2) \qquad (10\text{-}12)$$

where E_1 is the free field signal. For the minimum shielding effectiveness value, E_2 is the maximum observed signal for the set of measurement sites. The average value of S_E is computed using the average of K measurements of the amplitude of E_2 in the position group; i.e.,

$$E_2 = \frac{1}{K} \sum_{n=1}^{n=K} (E_2)_n \qquad (10\text{-}13)$$

The test condition of the enclosure should also be noted, i.e., condition of interior penetrating and exterior cables. Typical data taken for EMP purposes at UHF may consider only a single frequency. The purpose of this single frequency UHF test is to assess the constructional condition of the enclosure with respect to apertures. In the case of the bolted panel enclosure previously cited in Section 10.4.7, measurements were made before and after the bolt and nuts fastening the panels were tightened. This tightening degrades with age, so that the the measurements for the untightened condition represent, in this case, aging effects over a three year period. Results at other frequencies are included for comparison in Table 10-1.

Table 10-1. Comparison of shielding effectiveness before and after tightening the 25 gauge, steel panel enclosure.

	HF - 30 MHz Worst Case		UHF - 950 MHz		Microwave - 9.7GHz	
	North Side	South Side	North Side	South Side	North Side	South Side
Before (3 Years of Aging)	58 dB	–	54 dB	61 dB	59 dB	58 dB
After Tightening	90 dB	–	63 dB	62 dB	69 dB	72 dB

23

11. TEST PROCEDURES FOR CONDUIT AND COUPLINGS

TABLE OF CONTENTS

11. TEST PROCEDURES FOR CONDUIT AND COUPLINGS

11.1 Introduction

The test procedures described in this chapter are for the purpose of determining shielding performance of conduit or solid cylindrical shields for cabling including degradation due to corrosion of connectors, inadequately tightened couplings, flaws in shield/connector manufacture, and poor electrical contact between shield sections. The tests are designed primarily for laboratory evaluation; however, they can be modified for in-situ tests on existing installations.

These procedures are designed to be of use to the following classes of individuals:

1. engineers designing systems using conduit as a shield to provide a measure of EMP hardening;
2. engineers writing specifications for or supervising the installation of conduit for shielding cables;
3. manufacturers of conduit, couplers, etc.

The procedures described in this chapter can provide accurate measures of comparative shielding effectiveness with a relatively modest investment of test equipment and manpower.

These tests are designed to identify localized faults in conduit assemblies. Some examples are:

- improperly tightened connectors;
- mechanically stressed and cracked connectors;
- improper joint sealing at connectors;
- corroded joints.

The tests also are useful in determining shielding effectiveness for different types of conduit construction. One example would be the comparison between different materials, sizes, etc., of conduit shields. Another example would be the comparison between different coupling constructions.

11.2 General

11.2.1 Definitions of Fundamental Shield Transfer Functions

A commonly used measure of shielding performance is the surface transfer impedance, $Z_T(\omega)$, which is a complex frequency domain quantity. The surface transfer impedance is the property of a shield which quantitatively relates the voltage drop (per unit length of conduit or per coupling) appearing in the inner surface of the shield to the current flowing on the outside of the conduit structure. For an incremental length of conduit, Δx, which has a current, $I_s(x,\omega)$, flowing on the outside, an incremental voltage, $\Delta V(x,\omega)$, will appear along Δx on the inside of the shield. This is shown in Figure 11-1a. For a length, ℓ, of conduit which is short compared with the wavelength of the current, $I_s(\omega)$ is uniform over ℓ, and thus Z_T is given by:

$$Z_T(\omega) = V(\omega)/(I_s(\omega) \cdot \ell) \qquad (11\text{-}1)$$

where $V(\omega)$ is the total voltage along the inside of the sheath. The units of $Z_T(\omega)$ are ohms per meter.

For a coupling, point defect or flaw, the value of $Z_T(\omega)$ is given by:

$$Z_T(\omega) = V(\omega)/I_s(\omega) \qquad (11\text{-}2)$$

where $V(\omega)$ is the voltage along the inner surface of the coupling or defective section of conduit (see Figure 11-1b). The units of $Z_T(\omega)$ for couplings and flaws are simply ohms.

The surface transfer admittance, $Y_T(\omega)$, of a shield is dependent on the external surroundings of the cable as well as the properties of the shield. The transfer admittance results in a distributed current source, $\Delta I(x,\omega)$, between the shield and the internal wire(s) which is proportional to the voltage, $V_s(x,\omega)$, between the shield and its surroundings (see Figure 11-2). For a

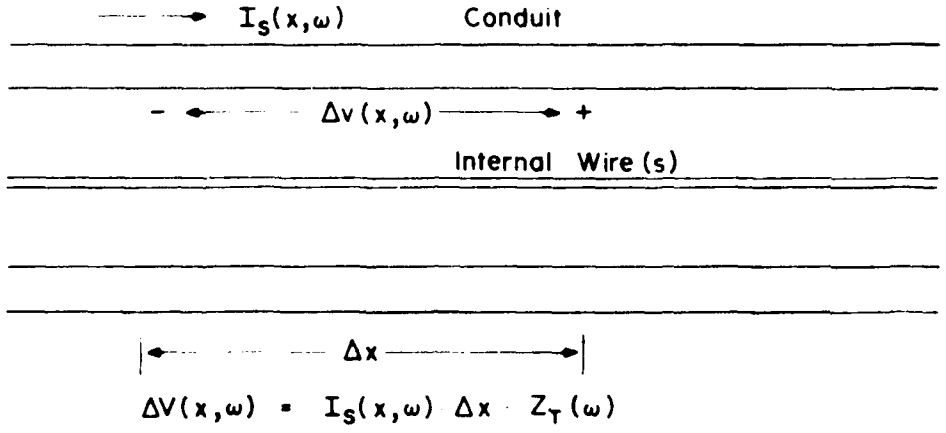

a) For Solid Conduit

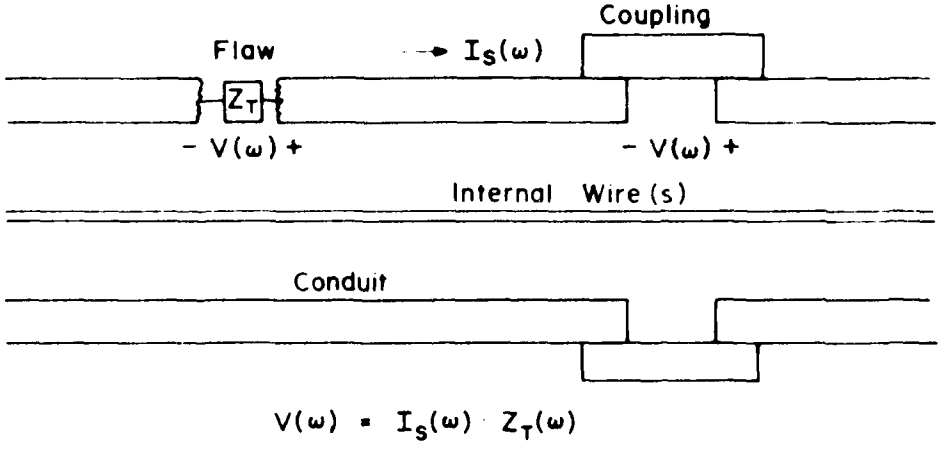

b) For A Coupling Or Flaw

Figure 11-1. Surface transfer impedance definitions.

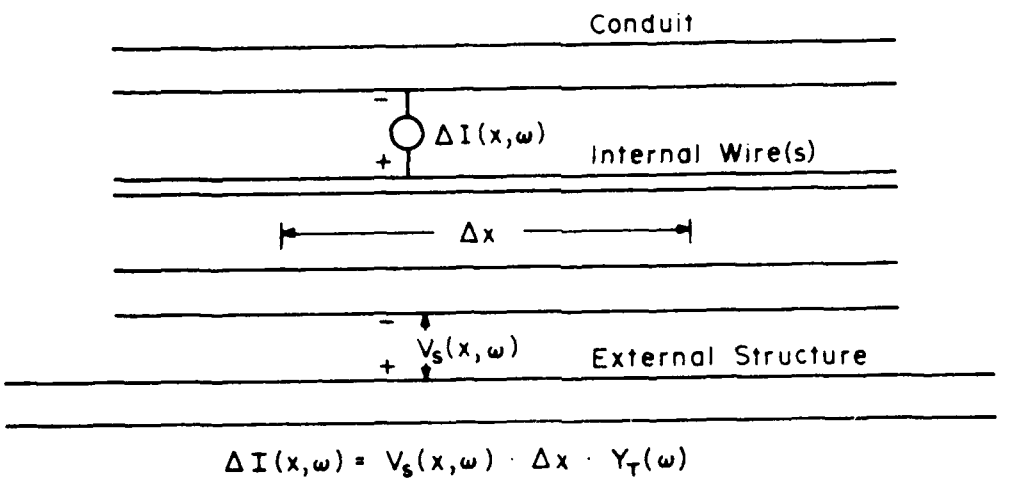

Figure 11-2. Definition of surface transfer admittance.

short length, ℓ, of conduit, $Y_T(\omega)$ is given by:

$$Y_T(\omega) = I(\omega)/(V_s(\omega) \cdot \ell) \qquad (11\text{-}3)$$

where $I(\omega)$ is the total shunt current generated along the length of conduit. $Y_T(\omega)$ is a complex frequency domain quantity with units of $(\text{ohm-meters})^{-1}$. Similarly, for a coupling or flaw, the value of $Y_T(\omega)$ is given by:

$$Y_T(\omega) = I(\omega)/V_s(\omega) \qquad (11\text{-}4)$$

where $I(\omega)$ is the shunt current in the vicinity of the coupling or flaw.

11.2.2 Characterization of Conduit Shielding

A conduit is a thin-walled tubular shield. Ideally this metal tube has a uniform diameter and wall thickness. Coupling can occur only by diffusion of electromagnetic fields through the conduit wall. The surface transfer impedance always has a diffusion component because shield materials have finite conductivity; i.e., the electric field cannot be zero inside a conductor which is carrying current. The surface transfer impedance for the thin-walled tube, derived by Schelkunoff,[1] is

$$Z_T(\omega) = \frac{1}{2\pi a \sigma T} \frac{(1+j)\ T/\delta}{\sinh\{(1+j)\ T/\delta\}} \qquad (11\text{-}5)$$

where a is the shield radius, T its thickness and σ the conductivity. The skin depth, δ, in the material is given by:

$$\delta = (\pi f \mu \sigma)^{-\frac{1}{2}}$$

where μ is the permeability of the shield, and f is the frequency.

Several assumptions are made to obtain this result:

1) The diameter is much larger than the wall thickness;

2) The diameter is much smaller than the smallest wavelength of interest;

3) The shield is a good conductor (metal) so that the displacement current is negligible.

In addition to the diffusion terms, a leaky shield with a flaw or defect has a mutual inductance term that accounts for the penetration of magnetic fields through the apertures. A coupling is characterized by a contact resistance and may have a mutual inductance term too.

Thus, at low frequencies (not more than 10 kHz for steel conduit), the surface transfer impedance of a typical section of conduit is equal to the dc resistance, R_o. As the frequency increases past the point, f_δ, where the skin depth in the material is the same as the thickness of the tubular wall, then Z_T decreases very rapidly toward zero (see Figure 11-3). For a unit length of conduit which contains either a coupling or a flaw, Z_T has a significant value at high frequencies. For a coupling with contact resistance only, Z_T is independent of frequency, while for a flaw, Z_T is expected to be proportional to frequency (i.e., inductive behavior).

An ideal conduit structure has no surface transfer admittance. When there is a flaw there is leakage of the external electric field through the aperture. Usually Y_T is proportional to frequency since mutual capacitance accounts for the coupling between the internal conductors and the external structure that causes the shunt current to flow.

11.2.3 Performance Criteria

The shielding performance of a conduit structure is characterized completely by the surface transfer impedance and surface transfer admittance. Note that the above criteria are fundamental quantities which means that they are useful as both relative or absolute values. These two parameters should be known for all significant frequencies in the EMP induced current on the exterior of the conduit--typically for frequencies between 10 kHz and 100 MHz. Both the absolute magnitudes and the phase angles should be determined.

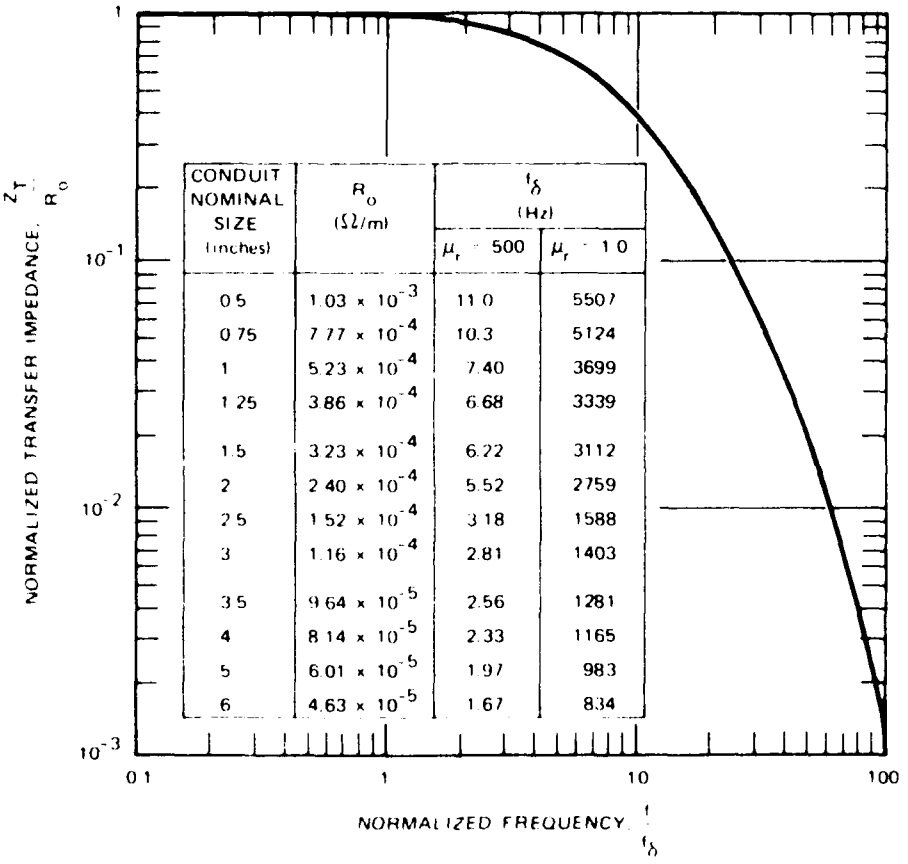

CONDUIT NOMINAL SIZE (inches)	R_o (Ω/m)	f_δ (Hz) $\mu_r = 500$	f_δ (Hz) $\mu_r = 10$
0.5	1.03×10^{-3}	11.0	5507
0.75	7.77×10^{-4}	10.3	5124
1	5.23×10^{-4}	7.40	3699
1.25	3.86×10^{-4}	6.68	3339
1.5	3.23×10^{-4}	6.22	3112
2	2.40×10^{-4}	5.52	2759
2.5	1.52×10^{-4}	3.18	1588
3	1.16×10^{-4}	2.81	1403
3.5	9.64×10^{-5}	2.56	1281
4	8.14×10^{-5}	2.33	1165
5	6.01×10^{-5}	1.97	983
6	4.63×10^{-5}	1.67	834

Figure 11-3. Magnitude of the transfer impedance of rigid steel conduit ($\sigma = 6 \times 10^6$ mho/m).

The process of characterizing a conduit system can be broken into two separate problems. First, the low frequency (less than 10 kHz) behavior of the surface transfer impedance, which is the property of an ideal conduit described in the previous section, must be determined experimentally or analytically. The second step is to determine whether there are penetrations at higher frequencies (10 kHz to 100 MHz). Such electromagnetic penetrations are often associated with the couplings, unions, etc., used to join sections of conduit or with flaws in the conduit wall.

For many purposes, complete characterization is not necessary. For example, a simple procedure which can estimate the mutual inductance term in Z_T would be useful for studying flaws, and one for measuring contact resistance would be useful when working with couplings.

Shielding effectiveness is a frequency domain measure of relative shielding. Figure 11-4 shows the quantities of interest. If I_s is the sheath current, and I_L is the current in the load, then shielding effectiveness is defined as

$$SE = 20 \text{ Log } \frac{|I_L|}{|I_S|} \text{ dB} \qquad (11\text{-}6)$$

This quantity is a function of the length of the test section, ℓ, and the terminating impedance of the sense wire-conduit transmission line. Note that under matched conditions, $Z_i = R_i$, the shielding effectiveness can be related to the transfer impedance through the relation

$$SE = 20 \text{ Log } \frac{|Z_T \cdot \ell|}{|2R_i|} \text{ dB} \qquad (11\text{-}7)$$

where R_i is the characteristic impedance of the conduit-sense wire line. R_i is a pure resistance for low loss conduit. Equation (11-7) assumes that there is no surface transfer admittance to contribute to the load current.

The shielding effectiveness does not have to be defined for

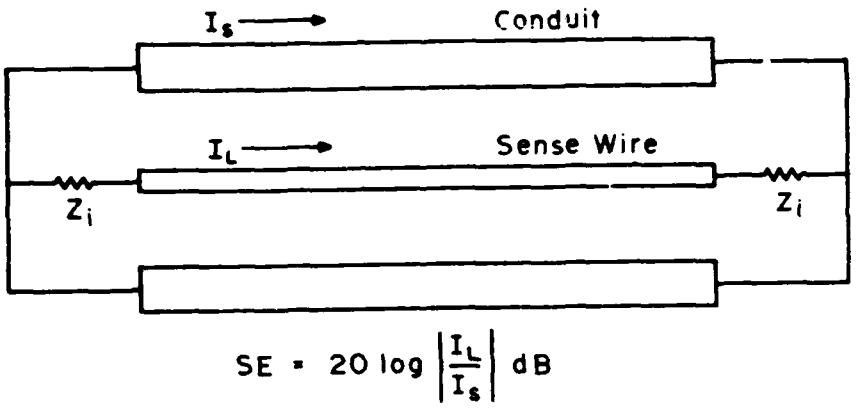

Figure 11-4. Shielding effectiveness definition.

matched conditions however. Any load can be used for Z_i. A frequent choice is a short circuit. A disadvantage of not using the matched case is that it makes the shielding effectiveness sensitive to frequency and line length, since an unmatched line reflects a frequency sensitive impedance back to the test line. In addition, it is more difficult to relate SE to a fundamental shielding parameter (Z_T) if $Z_i \neq R_i$.

11.2.4 Types of Tests

Since the surface transfer impedance, the transfer admittance and shielding effectiveness are all frequency domain quantities, a recommendation to perform the measurements using a frequency domain procedure is a natural one. However, there are two reasons why a time domain test procedure is also useful. First, it is always possible to use a Fourier transform to reconstruct frequency domain information from time domain measurements. Secondly, it is often possible to use the time domain measurements directly to obtain the coefficients of analytic expressions for shielding performance. Thus, both time and frequency domain test procedures are described. The choice between them should be made after comparing the type of data desired with the dynamic range and measurement accuracy of available test equipment.

The ideal test procedure for measuring the surface transfer impedance places a known uniform current on the test section of conduit and allows easy determination of the resulting voltage developed along the inner surface of the shield. Three types of test structures are considered for carrying the current:

1) parallel transmission line;
2) balanced transmission line;
3) coaxial transmission line.

A parallel line is employed to obtain sample test results. The detection is performed by placing a sense wire in the middle of the piece of test conduit, thus forming a coaxial transmission line.

Similarly, the ideal procedure for measuring the surface

transfer admittance applies a known voltage between the test section of conduit and an exterior surface which permits observation of the induced current. It is possible to use the same physical arrangements for both Z_T and Y_T measurements providing that the exterior and interior transmission lines are terminated properly. Specifically, for an electrically short test fixture, if the exterior line is terminated in a short circuit, then current flows on the test section as required for measuring Z_T and no voltage appears that would cause Y_T effects. With the exterior line terminated in an open circuit, the voltage, desired for Y_T measurements, is developed and no current flows.

At higher frequencies, when the fixture is not small compared to a wavelength, any measurement yields a linear combination of Z_T and Y_T. Values for Z_T and Y_T at a given frequency are obtained from two independent measurements, i.e., different terminating impedances for the exterior and/or interior transmission lines, according to procedures discussed in Section 9 (especially its Appendix).

The test procedures recommended here are for determining the surface transfer impedance and do not seek to evaluate the transfer admittance. This is done because the only time when a section of a conduit structure has a measureable Y_T is when there is a crack or similar flaw. In this case there is always a mutual inductance term in the characteristics of Z_T, so that there is adequate warning of the possibility for transfer admittance effects. A procedure for determining Y_T for coaxial cable shields is described in Section 9. This frequency domain procedure is easily adapted for use on conduit systems using a modification of the test setup shown below for transfer impedance measurements.

11.3 Time Domain Test Procedure

11.3.1 Scope

The parallel transmission line method is suggested as the preferred simplified test procedure. When properly used, the results obtained with this method are as accurate as with the more elaborate balanced transmission line and triaxial methods.

The test procedure is suitable for testing rigid conduit sections up to approximately ten feet in length or sections of this length containing conduit couplers. Both transfer impedance and shielding effectiveness can be obtained using Fourier transforms. This test procedure can be used to measure these performance criteria at frequencies between 10 kHz and 10 MHz.

11.3.2 Test Fixture and Equipment

The sheath current is placed on the test section of conduit by the parallel transmission line method which uses a piece of identical, but uncoupled and unflawed, piece of conduit as the second half of a transmission line (see Figure 11-5). The transmission line is driven by a pulsed high voltage source which produces the desired sheath current. For this time domain procedure, the transmission line formed by these two parallel pieces of conduit is terminated in its characteristic impedance, R_1. For low loss conduits, R_1 is a pure resistance. The magnitude of R_1 is given by

$$R_1 = 120 \ln (b/a + \sqrt{b/a-1}) \qquad (11\text{-}8)$$

where a is the diameter of the conduit and b is the center-to-center spacing. The characteristic impedance is used so that the driving pulse is not reflected by an unmatched termination.

The advantages of the parallel transmission line method are its simplicity and lower cost compared to other ways of exciting a test section of conduit. (Examples of other methods are the balanced transmission line and triaxial line which are described

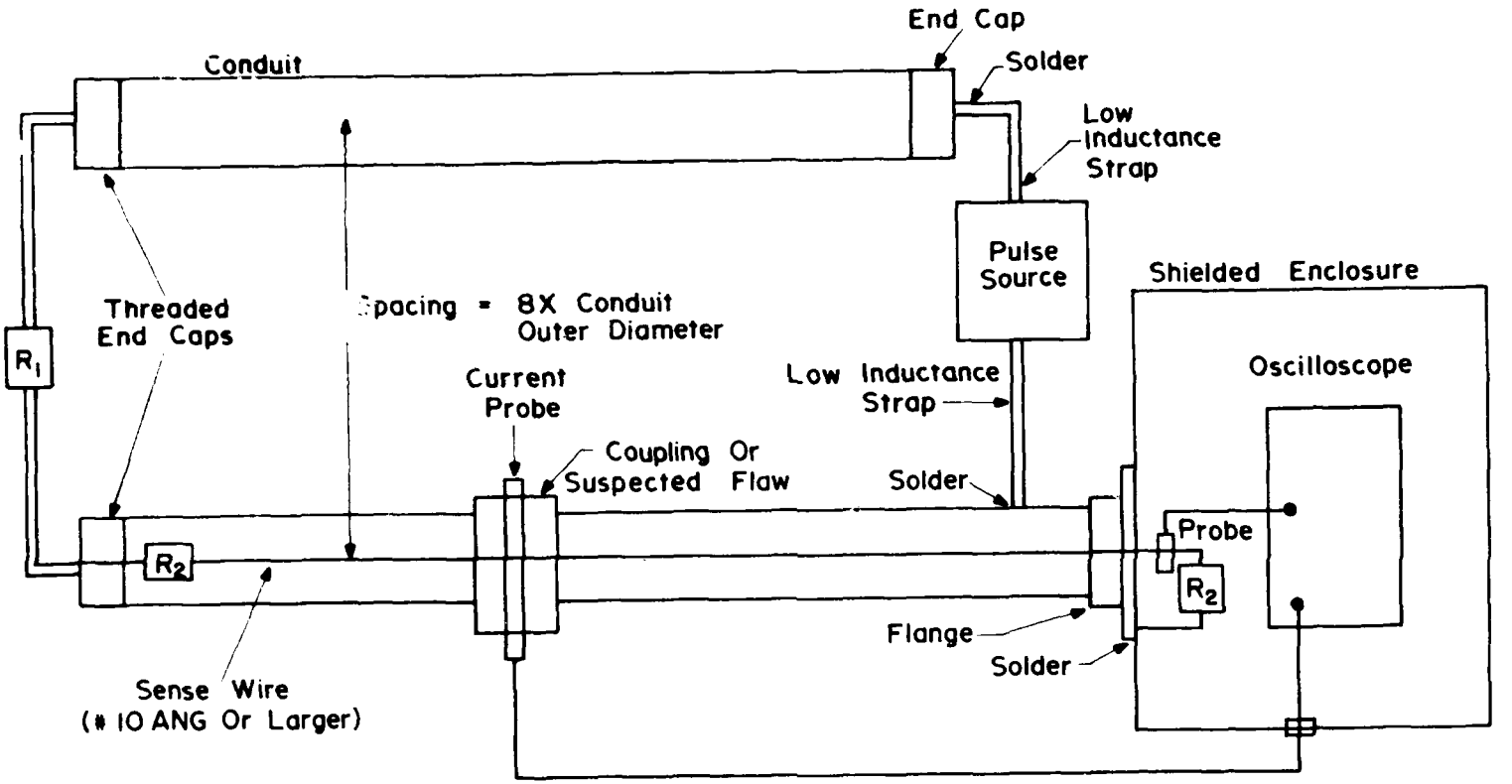

Figure 11-5. Schematic representation of parallel transmission line test.

below.) A disadvantage of this method is the lack of symmetry in the parallel line structure which causes a nonuniform distribution of current density on the conduits. That is, there is a greater current density on the side of the test section facing the other parallel conduit than on the side opposite the other conduit. If the spacing between the two parallel conduits is more than eight times the conduit diameter, then the current density is uniform within one percent.

A second disadvantage of this method, and for any transmission line method that is terminated in its characteristic impedance, is that there is a significant voltage between the test section of conduit and the external structures. This means that there is a possibility for transfer admittance coupling to the sense wire inside the conduit under test in addition to the desired transfer impedance coupling. This problem exists whenever electromagnetic fields can penetrate through apertures (i.e., cracks, slots, etc.). In general, apertures are not found in conduit structures. Since penetration through apertures is greater at higher frequencies, an adequate indication of aperture effects is given by a measured Z_T which is proportional to frequency.

In order to overcome the effects of the nonuniform current distribution, a third conductor can be added to the parallel transmission line just described. A schematic representation of this method is shown in Figure 11-6. The asymmetry is reduced considerably with this method and as a result, the spacing is not as critical as for the simpler parallel line. A disadvantage of the balanced line method is the requirement that the currents in the two halves be identical in order to achieve the balance.

The next step of complexity in achieving uniform current distribution on the test conduit is to make the test conduit the inner conductor of a coaxial line. This provides complete axial symmetry and gives a highly uniform current distribution. Such a system is shown schematically in Figure 11-7. The disadvantage with this system is the complexity and consequently the cost, of

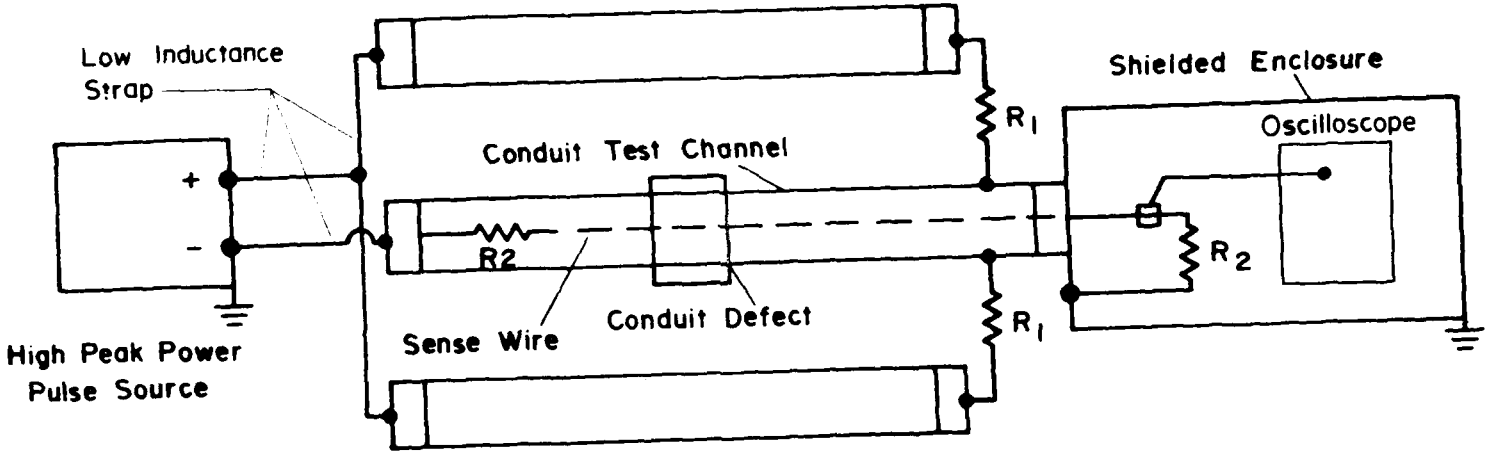

Figure 11-6. Balanced transmission line setup.

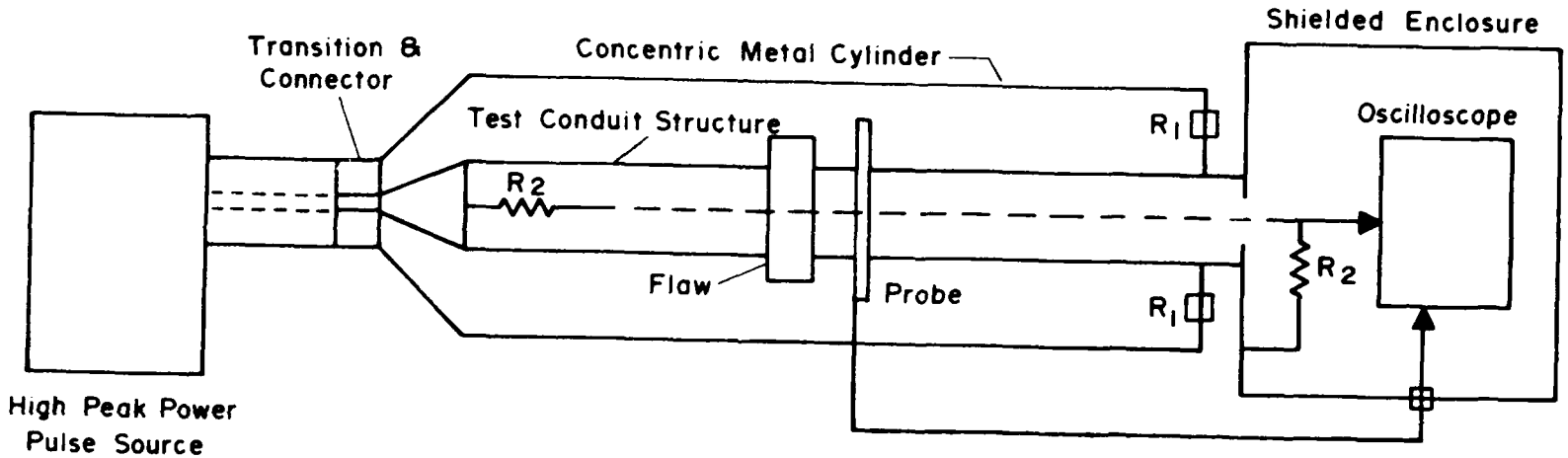

Figure 11-7. Schematic diagram representing concept of triaxial/quadraxial methods.

the test fixture. This is especially true if large samples are to be tested.

The sense wire is a coaxial wire in the center of the test section of conduit. For measurements of the surface transfer impedance, the sense wire should be terminated to each end of the conduit by identical resistors, R_2. These resistors should be equal to the characteristic impedance of the transmission line formed by the sense wire and the conduit. The value of R_2 can be computed from

$$R_2 = 60 \ln (b'/a') \qquad (11\text{-}9)$$

where b' is the inner diameter of the conduit and a' is the outer diameter of the sense wire. One half of the induced voltage appears across each of the two terminating resistors, R_2. Thus, the voltage measured across one resistor must be multiplied by two to get the open circuit voltage needed for computing Z_T. When making shielding effectiveness measurements, the value of I_L is maximized if the sense wire is connected directly to the ends of the section of conduit; that is, the transmission line is terminated with short circuits. If this is done, Equation (11-7) cannot be used to derive Z_T from the measured shielding effectiveness.

The pulse source shown in Figure 11-5 should provide a broadband excitation of large amplitude. A simple method for obtaining such a pulse waveform is to close a switch which discharges a capacitor into the resistive load. (A parallel transmission which is terminated in its characteristic impedance, R_1, is a resistive load.) This produces a double exponential pulse of current, $I_s(t)$, given by

$$I_s(t) = \frac{V_o}{R_1} \left[e^{-(R_1/L)t} - e^{-t/(R_1C)}\right] \qquad (11\text{-}10)$$

The peak current determined by the magnitude of V_o, the voltage

on the charged capacitor, and by R_1, the load impedance. (It is assumed that the capacitor and the switch have small series resistance compared to R_1.) The rise time is established by the ratio of R_1 to the circuit inductance, L. Both the capacitor and the switch may contribute to L. The fall time is determined by the R_1 and C.

To make the desired measurements at frequencies between 10 kHz and 10 MHz, the rise time of the pulse (given by L/R_1) should be less than a microsecond and the fall time (given by R_1C) should be several tens of microseconds. R_1 is 330 ohms, if in Equation (11-8) the ratio b/a is taken as 8.0 as recommended for current uniformity. Consequently, C should be 0.1 μF or larger and L should be less than 0.3 mH. The value of the charging voltage is determined by the desired minimum measurable coupling. For example, a surface transfer impedance (for a point defect) of 10^{-5} ohms can be detected when a one millivolt signal can be measured if the maximum current is 100 amperes. This means that V_o should be at least 30 kV. Power supplies and switches (or triggered spark gaps) with 30 kV ratings are commercially available.

The response of the current probe(s) should be flat within 3 dB over the desired frequency range of 10 kHz to 10 MHz. In addition, the current probe measuring the sheath current must have linear response up to an amplitude of over 100 amperes. The sheath current and either I_L or the induced voltage across R_2 should be displayed on an oscilloscope(s) with a bandwidth greater than 10 MHz. Photographs of the oscilloscope traces become the permanent record of the measured quantities.

11.3.3 Precautions

It is first necessary to establish baseline data for a known, good piece of conduit. This is accomplished by using a continuous, flawless piece of conduit in the test channel. The excitation and response are measured and photographed. The recorded data can then be digitized and the Fourier transforms can be computed.

In order to obtain meaningful, repeatable results, care has to be exercised in setting up the system. Some points that must be considered are discussed.

The sense wire of the conduit under test should be AWG #10 or larger. The sense wire should be centered to maintain the coaxial configuration as closely as possible. This requires the wire to be under considerable tension. When measuring $Z_T(\omega)$, the sense wire should be fastened to the ends of the conduit under test through two identical, noninductive, terminating resistors, R_2. The value of R_2 can be obtained from Equation (11-9).

The termination resistor, R_1, of the parallel transmission line should be connected to the end caps of the conduit sections using heavy straps to minimize the inductance of the leads. The resistor should be noninductive, its value can be obtained from Equation (11-8).

All threaded connections on the conduit should be tightened with a pipe wrench. Since torque measuring pipe wrenches are not a standard shop item, the number of turns used to tighten each connection should be recorded to guarantee that the measurements are repeatable. Prior to assembly, all threaded joints should be cleaned and wire-brushed to ensure an adequate electrical contact.

The high voltage pulse source should be connected to the two pieces of conduit with heavy, low inductance straps. These should be soldered to the conduit.

The primary power for the oscilloscope must be supplied through an inverter-battery combination to prevent signals from the pulse source feeding through the primary power line. The oscilloscope must be shielded from the pulse source and the parallel transmission line.

11.3.4 Data Format

There are two aspects of data recording that must be considered. The first is the data required to duplicate the measurements. The suggested data format for this purpose is shown in

Table 11-1 in which the detailed information about the equipment, conduit and pulse source used in the experiment and a summary of the measured response is properly recorded such that a repeatable measurement can be made, if necessary.

The second set of data gives the detailed results of the measurement. For this purpose, it is suggested that the time domain waveforms of the current on the test conduit and the voltage across the terminating resistor be photographed. In addition, the transfer impedance and/or shielding effectiveness for the conduit under test should be presented on appropriate logarithmically scaled papers. The plots of transfer impedance and shielding effectiveness versus frequency, therefore, provide a measure of the performance in the conduit structure over the frequency range of interest.

To illustrate the data format desired, a measurement is made to the surface transfer impedance of a rusty coupling joining rusty conduits. The conduit current and the sense wire voltages are shown in Figure 11-8. The dimensions of the galvanized steel conduit are 5.1 cm inside diameter, 0.4 cm wall thickness and a length of 3.2m. The peak conduit current is about 170 A.

It is apparent, that while the conduit current rises slowly to its peak at about 4 μs, the sense wire voltage rises rapidly to its peak at about 40 ns. The slow rise of the conduit current and the fast rise of the sense wire voltage implies that the high frequency content of the leakage signal is significant. Hence, the shielding performance is expected to be badly degraded at high frequencies.

The calculated transfer impedance obtained by standard Fourier transform techniques is shown in Figure 11-9. Also shown is a quick estimate obtained by fitting double exponential functions to the conduit current and sense wire voltage waveforms. Using these approximations, the frequency domain magnitude of the conduit current and shield-sense wire voltage can be calculated

Table 11-1.

REPORT OF CONDUIT TEST

Sample Identification_____ Date_____

Equipment:

Oscilloscope _____

Sheath Current Probe_____

Load Current Probe_____

Pulse Source:

Peak Voltage_____

Peak Current_____

Rise Time_____

Decay Time_____

Conduit:

Outside Diameter_____

Separation_____

Parallel Line Termination_____

Coaxial Line Termination_____

Response:

Peak Voltage

Peak Current_____

Rise Time_____

Decay Time_____

End Caps:

Tightness_____Turns

Coupling Tightness_____Turns

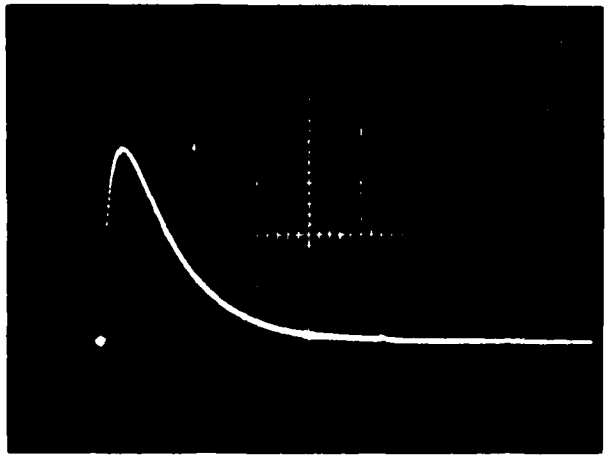

(6a) Conduit Current

45.4 Amp/Div.
10 μsec/Div.

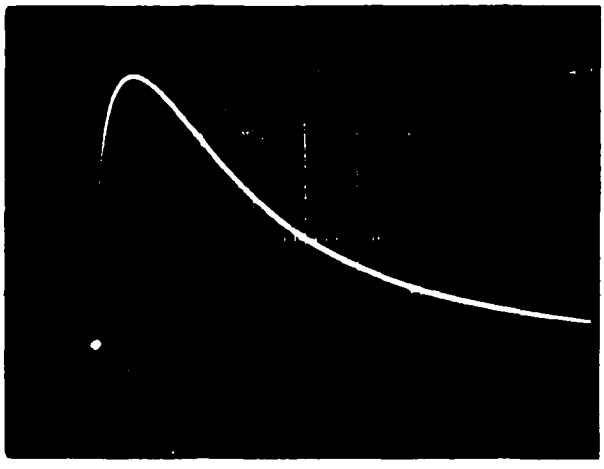

(6b) Sense Wire Current
SC Mode

200 mA/Div.
10 μsec/Div.

(6c) Sense Wire Voltage
50 Ω Mode

1 V/Div.
0.1 μsec/Div.

Figure 11-8. Rusty coupling joining rusty conduits (wrench tight medium).

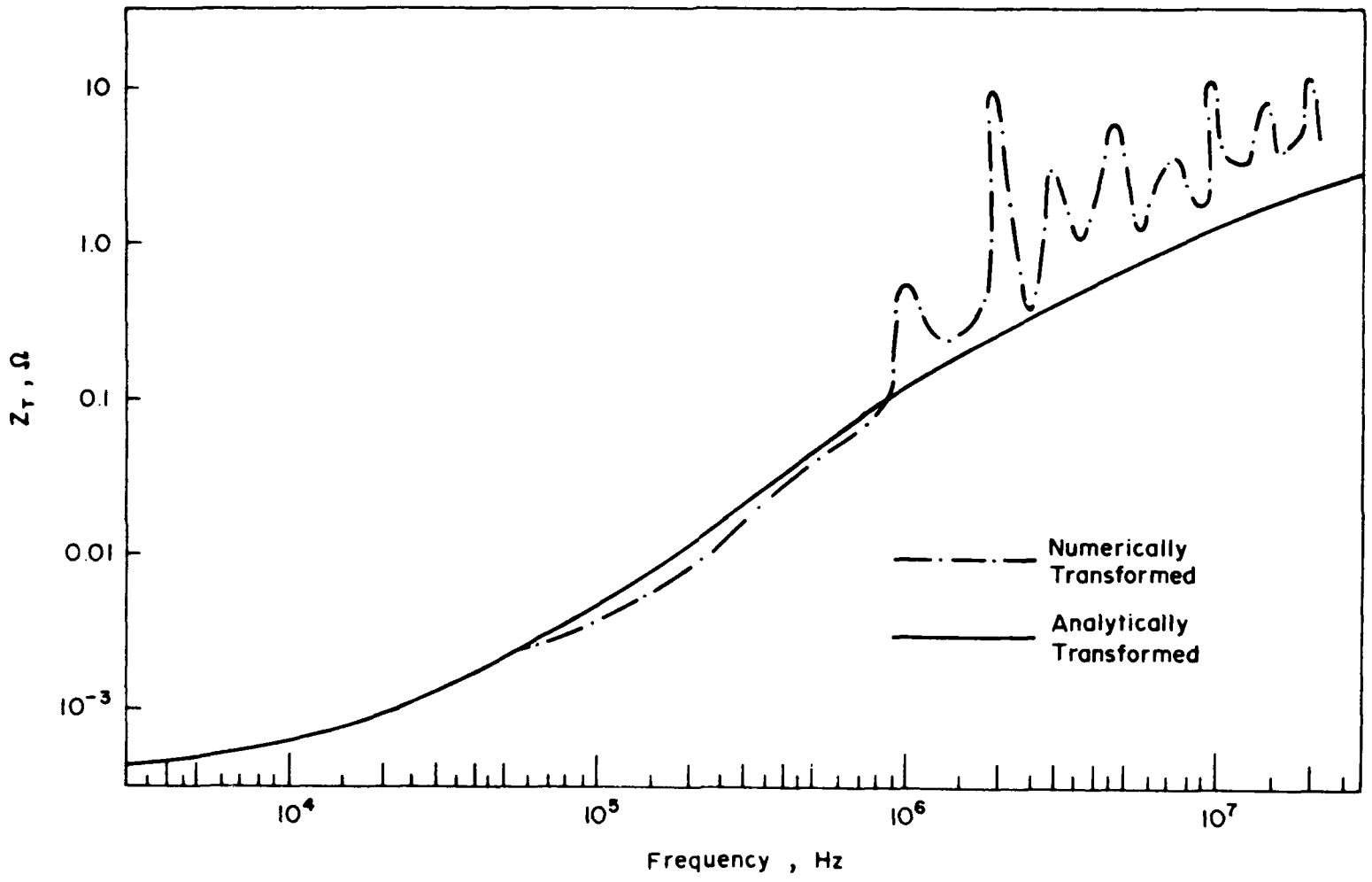

Figure 11-9. Transfer impedance versus frequency for rusty coupling joining rusty conduits.

by taking analytical Fourier Transformation. The transfer impedance is then obtained from the ratio of the calculated voltage to the current. A comparison of the two curves reveals that the transfer impedances obtained from the two methods discussed agree fairly well for low frequencies, but that they differ by an average of about 10 dB for frequencies higher than 1 MHz. This is expected because the analytic expression used to approximate the observed voltage could not take the high frequency oscillations into account.

Figure 11-10 shows the results obtained from a similar test performed on a conduit structure that included a clean coupling joining two clean conduits. The sense wire current response, measured under a short circuit condition, is used to find the shielding effectiveness shown in Figure 11-11. The shielding effectiveness is calculated by fitting exponential function waveforms.

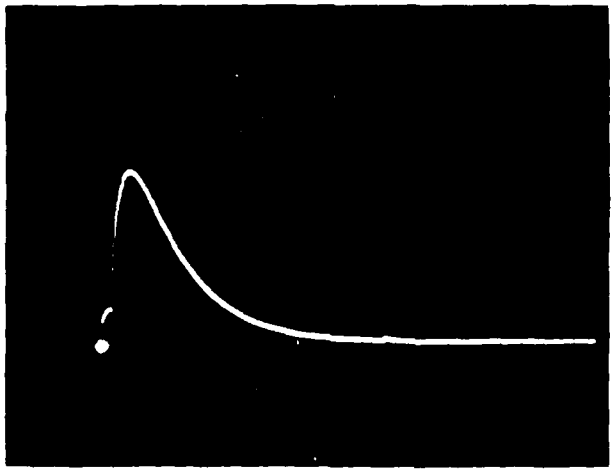

(5a) Conduit Current

45.4 Amp/Div.
10 μsec/Div.

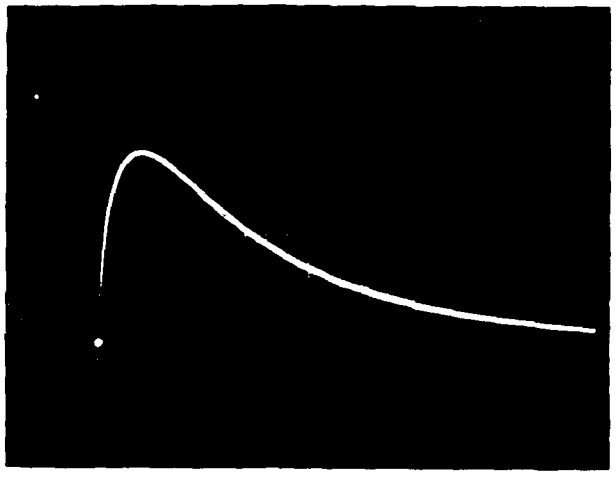

(5b) Sense Wire Current
SC Mode

5 mA/Div.
10 μsec/Div.

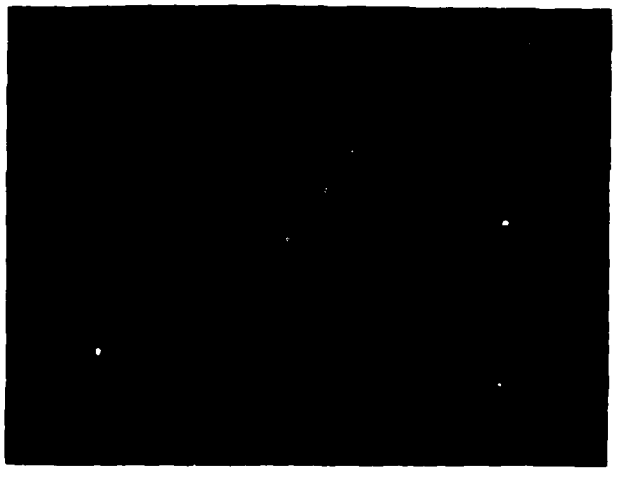

(5c) Sense Wire Voltage
50Ω Mode

50 mV/Div.
0.1 μsec/Div.

Figure 11-10. Clean coupling joining conduits (wrench tight medium).

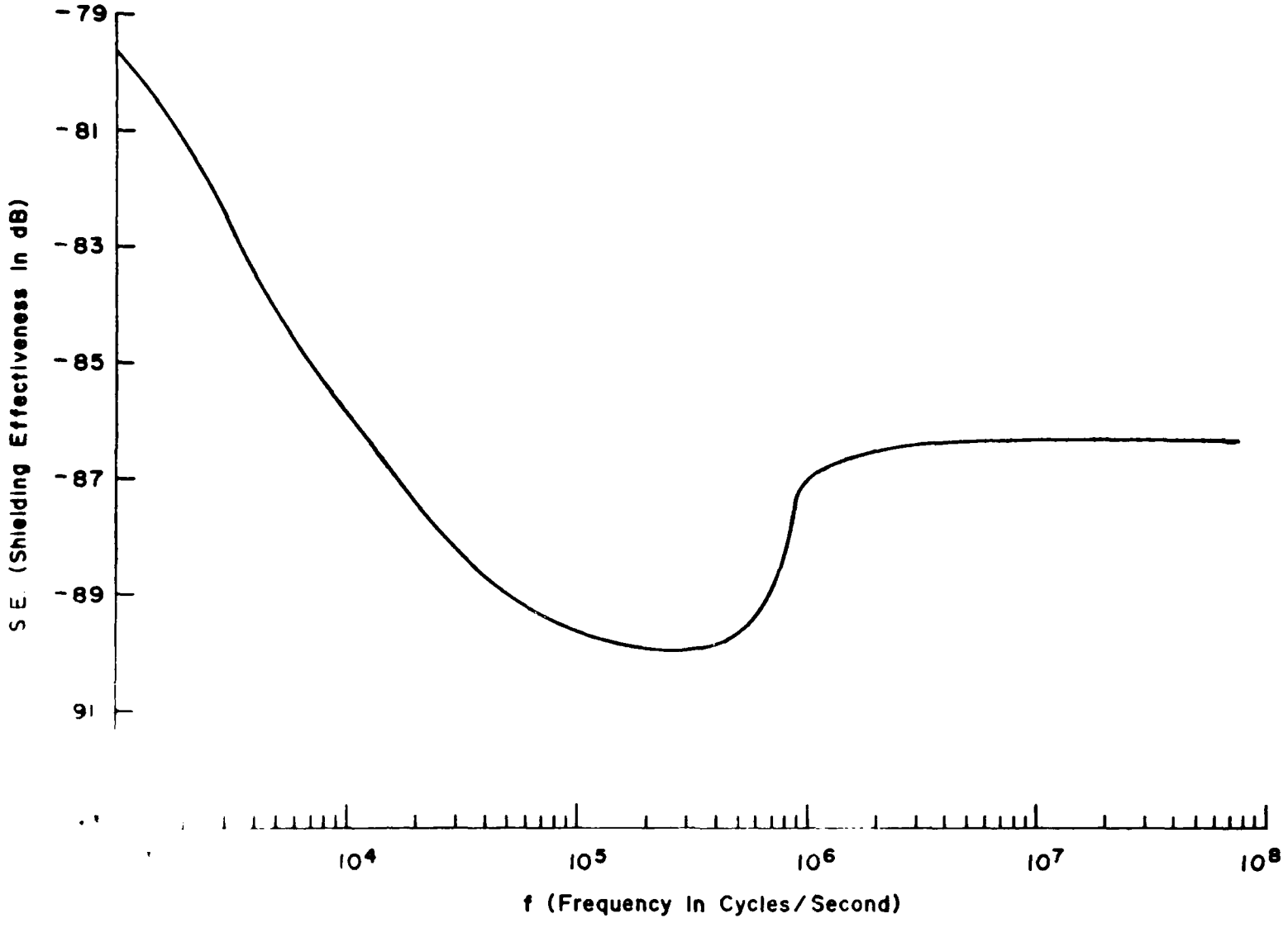

Clean coupling (medium wrench tight) S.E. versus frequency (S.C. mode).

11.4 Frequency Domain Test Procedures

11.4.1 Scope

In general, frequency domain tests for determining faults in the shielding integrity of conduit structures are recommended only if swept frequency CW measurement equipment is readily available. However, frequency domain tests may be used where the susceptibility is confined to a single frequency or a narrow frequency band. The test procedure that is presented is restricted to cases where the length of the test conduit is shorter than the smallest wavelength of interest which, from an EMP viewpoint, is a wavelength of about three meters. For long conduits, the test results may be used with appropriate correction factors included. Both the transfer impedance and shielding effectiveness can be measured with this test procedure.

This test procedure is similar to that given in Section 9.3 for coaxial cables except that the test fixture is similar to that described in Section 11.3.2, above. These sections should be consulted for details not included here.

11.4.2 Test Fixture and Equipment

The test fixture for frequency domain measurements is again designed for determining the transfer impedance and shielding effectiveness. The test fixture may be considered to be composed of two sections. The conduit section consists of the section of conduit under test and a mechanism for providing the shield current. The detection section, which is in an electrically shielded enclosure, consists of the necessary instrumentation for monitoring the shield current and for detecting the leakage signal induced on the sense wire.

The parallel transmission line fixture discussed in Section 11.3.2 is used to excite the conduit shield current; however, the balanced transmission line method and the triaxial method may also be used as the conduit drive section. The sense wire configuration is also the same as for the time domain procedure.

For frequencies where the test fixture is electrically short, the interpretation of the results is easy even if the transmission lines are not terminated in their characteristic impedances. At higher frequencies the comments in Section 9.3.2 and Appendix A apply.

The pulse source is replaced by an oscillator and a broadband power amplifier which are used to drive current on the conduit shield. It is suggested that a swept frequency signal generator be used as the oscillator. The voltage across the resistor, R_2, or the induced sense wire current is then measured inside the electrically shielded room by a high sensitivity voltmeter or a current probe.

The power amplifier should have a one hundred watt rating. The resistor terminating the parallel transmission line, R_1, should be chosen so that the current on the test conduit is large and so that there is a reasonable match between the amplifier output impedance and the load impedance. For example, a 100 watt audio amplifier can drive 12 amperes into an 8 ohm load. The response of the current probe(s) used to measure the shield current (and the induced current) should be known at all measurement frequencies. If the current probe response is independent of frequency, then a network analyzer can be used to measure I_s and the induced voltage and compute the transfer impedance. Similarly, if the two current probes have similar responses as functions of frequency, then the output of the network analyzer can be shielding effectiveness.

The induced signals should be measured by a device with sufficient sensitivity that a transfer impedance of 10^{-5} ohms or a shielding effectiveness of 100 dB can be determined. This requires a meter sensitivity of 0.06 mV for the induced voltage (recall that only half the voltage is across each terminating resistor, R_2) when the shield current is 12 amperes. Since most current probes have a 1.0 mV/ma response, a meter sensitivity of 0.12 mV is required to make shielding effectiveness measurements at the 100 dB level.

Both manual and automatic instruments are available with the stated sensitivities for frequencies up to about 100 kHz. The measurements are particularly easy to process if a swept frequency generator is used to drive the power source, a gain/phase meter (e.g., Hewlett-Packard 3575A) is used to measure signals and take the ratio and the output is taken on an X-Y plotter or oscilloscope. Above 100 kHz, the measurements can be made with RF voltmeters or a network analyzer with a typical sensitivity of 1.0 μvolt (see Section 9.3.2).

11.4.3 Precautions

All of the precautions concerning noninductive termination resistances, low inductance leads to the power source, low impedance connections and shielding for the instrumentation which are described in Section 10.3.3 should be followed here, too. It is necessary that the probes be calibrated and that a baseline be established. A good calibration procedure for surface transfer impedance measurements is given in Section 9.3.3. The baseline consists of a measurement of the Z_T or SE for an uncoupled and unflawed section of conduit. It is important that the measurement frequencies be much less than the frequency for which the parallel transmission line is 0.25 wavelengths.

11.4.4 Data Format

The data format needed for repeatable measurements and suggested in Table 11-1, should be followed so that the measurement equipment, conduit structure and power source used for the measurement are properly recorded.

The basic resultant data to be recorded for frequency domain measurements are the magnitude and phase of the surface transfer impedance or the shielding effectiveness as a function of frequency. Measurements should be performed over the frequency range of interest. The data should be presented graphically, on logarithmically scaled paper with frequency as the independent variable.

To illustrate the type of data obtained and the proper format, test results are presented for a faulty conduit structure. This structure has longitudinal and transverse cracks near the coupling which joins two pieces of conduit. The dimensions of the cracks are 5" x 3/16" for the longitudinal crack and 3" x 3/16" for the transverse one. The inside diameter of the conduit is 2 inches and the wall thickness is 0.16 inches.

Shown in Figure 11-12 is the surface transfer impedance of this faulty conduit structure. At low frequencies, the effects of the cracks on the transfer impedance is insignificant. The shielding performance below 0.3 kHz is almost identical to that of a solid conduit. At higher frequencies, however, the Z_T of this faulty conduit increases as frequency increases, as would be expected.

The data obtained for the shielding effectiveness is shown in Figure 11-13. The induced sense wire current measured at each frequency is the short circuit current. Because of the leakage through the cracks, the shielding effectiveness deteriorates with increasing frequency.

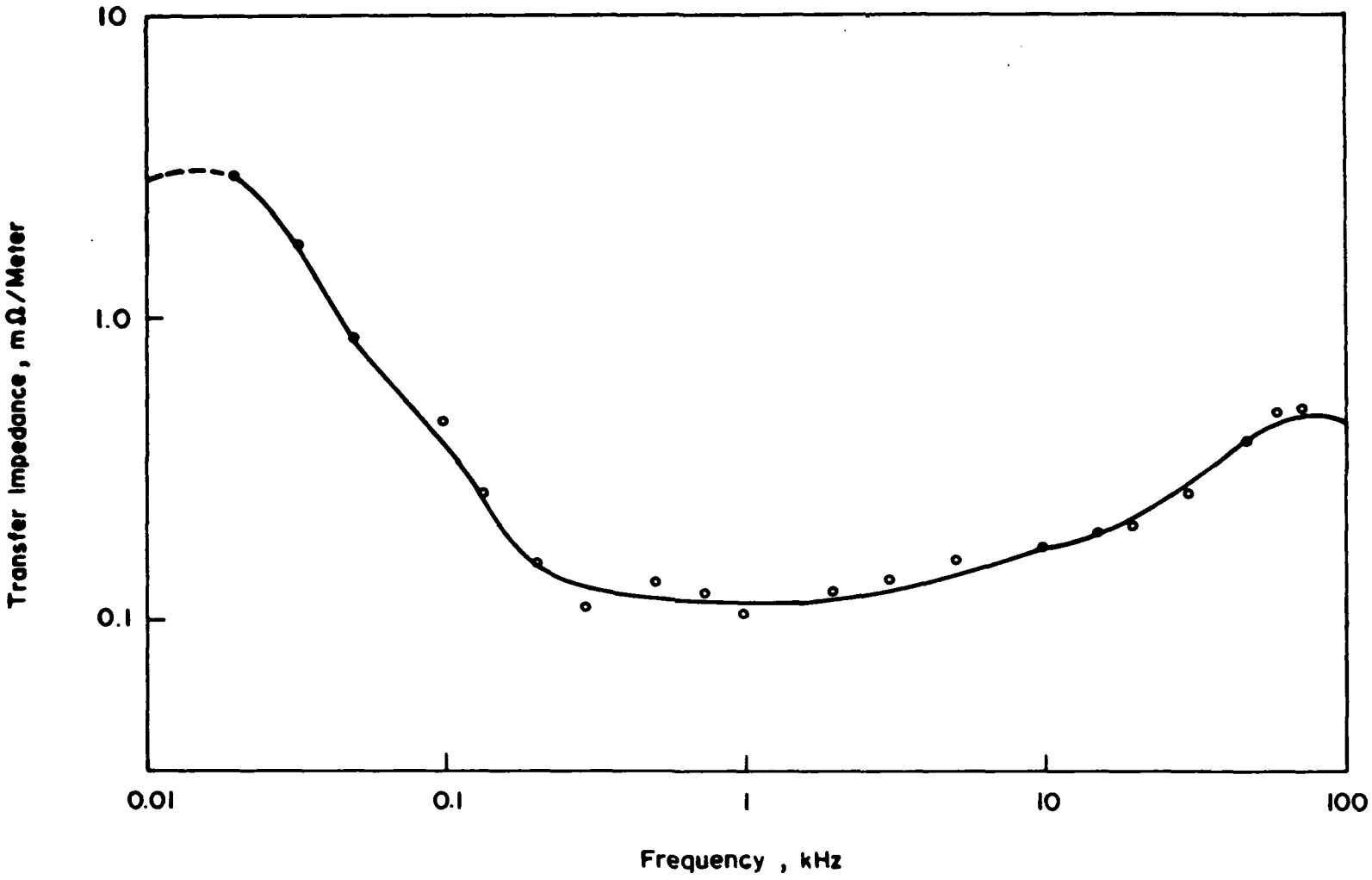

Figure 11-12. Transfer impedance of a faulty conduit with longitudinal and transverse cracks.

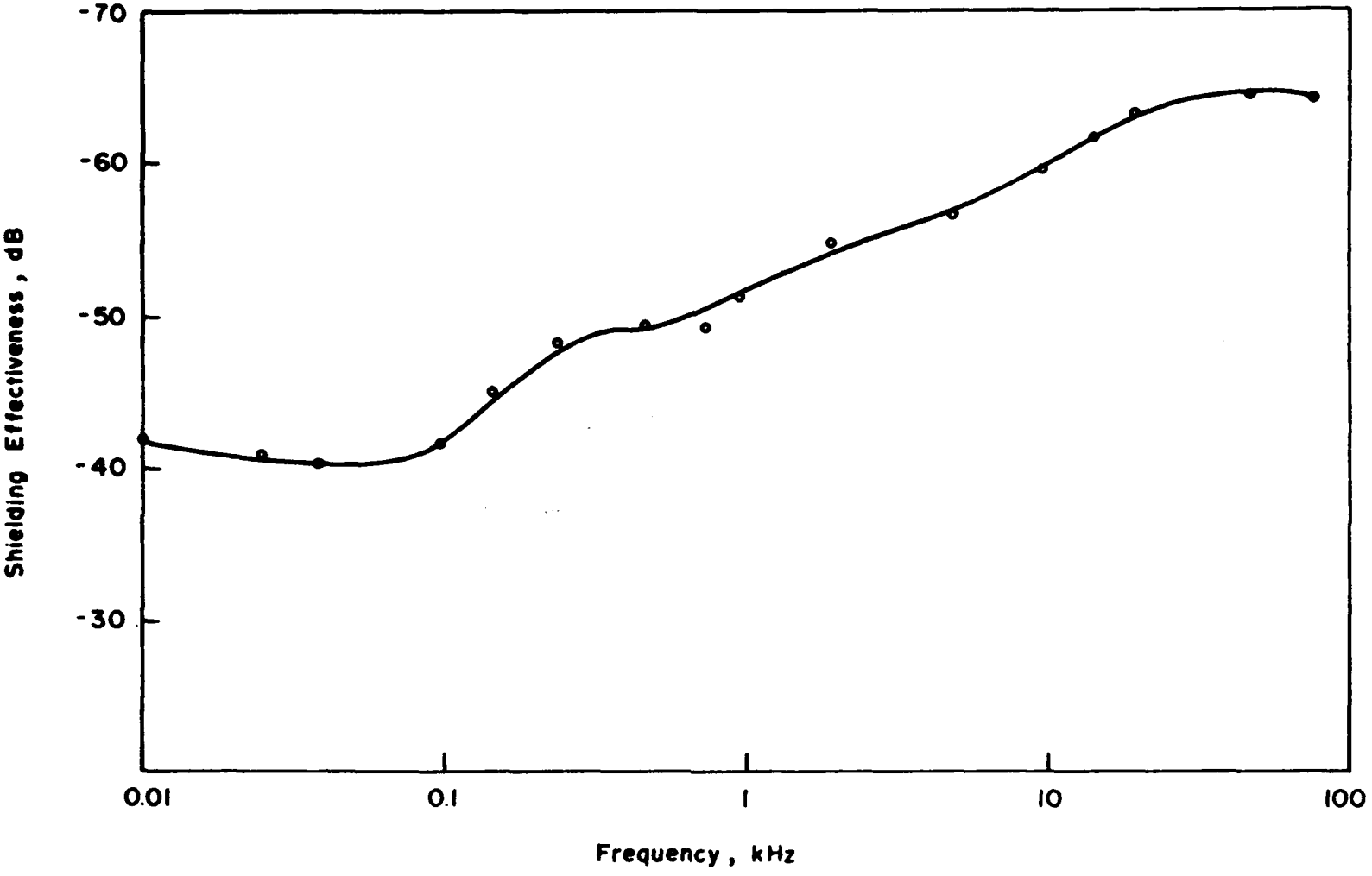

Figure 11-13. Shielding effectiveness of a faulty conduit with longitudinal and transverse cracks.

12. EMP PREFERRED TEST PROCEDURES FOR TRANSFORMERS AND INDUCTORS

TABLE OF CONTENTS

12. EMP PREFERRED TEST PROCEDURES FOR TRANSFORMERS AND INDUCTORS

12.1 Introduction

12.1.1 General

This chapter is concerned with establishing test procedures for transformers, baluns and inductors which may be used to terminate antennas or long exposed cables. The purpose of these tests is to determine the ability of the elements to impart hardening and to resist functional damage from EMP. They are intended to provide information concerning the important performance characteristics of the elements and procedures for measuring their characteristics.

The primary sources of information employed in establishing the procedures include the RETMA Standard RS-174 for transformers,[1] MIL-T-27B for transformers and inductors,[2] and brochures provided by transformer manufacturers which describe test procedure applicable to their products.[3]

12.1.2 Types of Elements

As indicated previously, the test procedures developed in this chapter are concerned with transformers, baluns, and inductors of the type used to terminate cables and antennas. There are, of course, a wide variety of such elements. For example, transformers, include pulse transformers, RF impedance matching transformers, baluns, and wideband transformers and for each of these, a variety of winding configurations. They may or may not employ shields, be encapsulated, or have a direct connection between windings. There is also a substantial variation in transformer power handling capabilities and their ability to resist voltage breakdown.

It is not possible to specify a detailed test procedure for every available transformer configuration; however, in those cases where a particular configuration is not specified, the test procedures can serve as a guide in formulating an appropriate procedure.

12.1.3 Element Applications

Transformers (one type of which is termed a balun) and inductors can be part of an overall hardening system when used as cable terminating elements. Several properties of these systems are considered briefly to provide background for the test procedures.

Common-Mode Rejection

A shielded twisted-pair represents a reasonable compromise between economy and non-susceptibility to moderately intense electromagnetic fields. Figure 12-1(a) depicts such a cable where the twisted pair is shown as a pair of parallel conductors to facilitate the discussion. Currents induced by EMP are I_{i1} and I_{i2}, where the return path for these currents is a ground path, part of which is the cable shield. The signal current is I_s. Figure 12-1(b) shows the cable terminated by an isolation transformer and 12-1(c) by a balun. The operation of the transformer or balun is straightforward, at least in the ideal case when I_{i1} and I_{i2} are identical. Because of the directions of I_{i1} and I_{i2}, it is evident that they produce no net magnetic flux in the ideal isolation transformer or balun. Conversely, the signal current, I_s, does produce a net flux and, in this manner, the signal current is transferred through the transformer or balun while the induced currents are not. This property of the transformer to reject the induced current when used with a balanced cable (twisted pair) is called common-mode rejection.

Resistor R in Figure 12-1(b) is often added to dissipate the energy in the induced currents, and the transformer may or may not be equipped with a shield to reduce capacitive coupling between the primary and secondary windings.

A transformer can also be used as a common-mode choke to preserve the dc components and to provide common-mode rejection as shown in Figure 12-2. Because of the equality of the signal current, I_s, in the two transformer windings and the transformer polarity, I_s produces no net flux and there is, therefore, no impedance to the flow of this current. Conversely, the flux

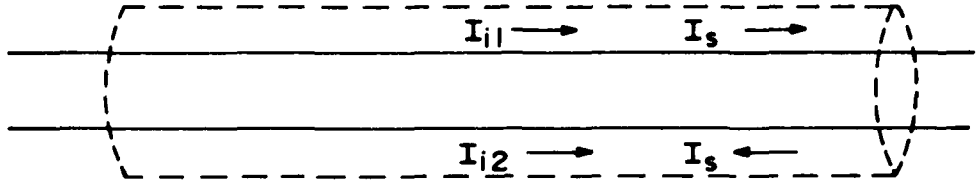

Figure 12-1a. Twisted pair.

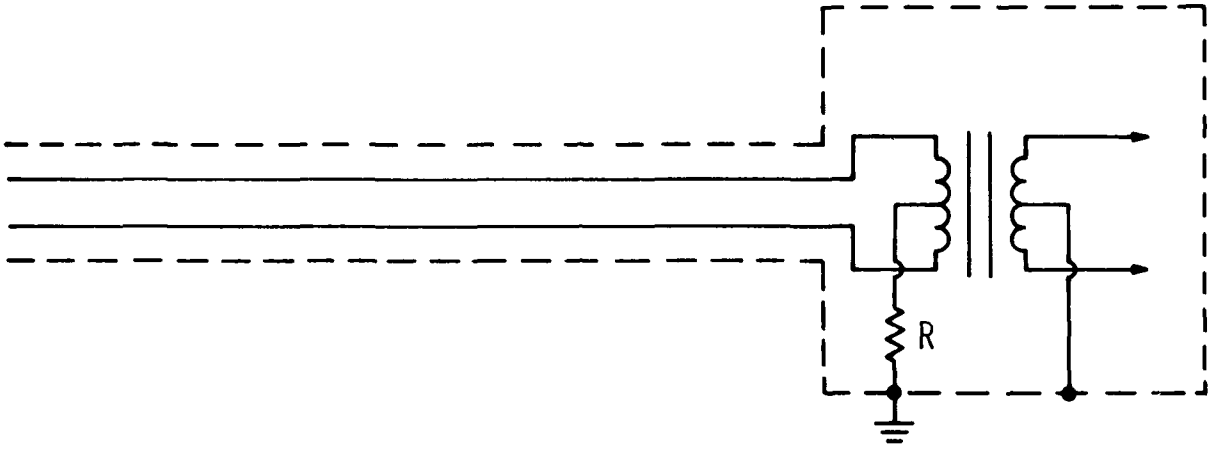

Figure 12-1b. Isolation transformer.

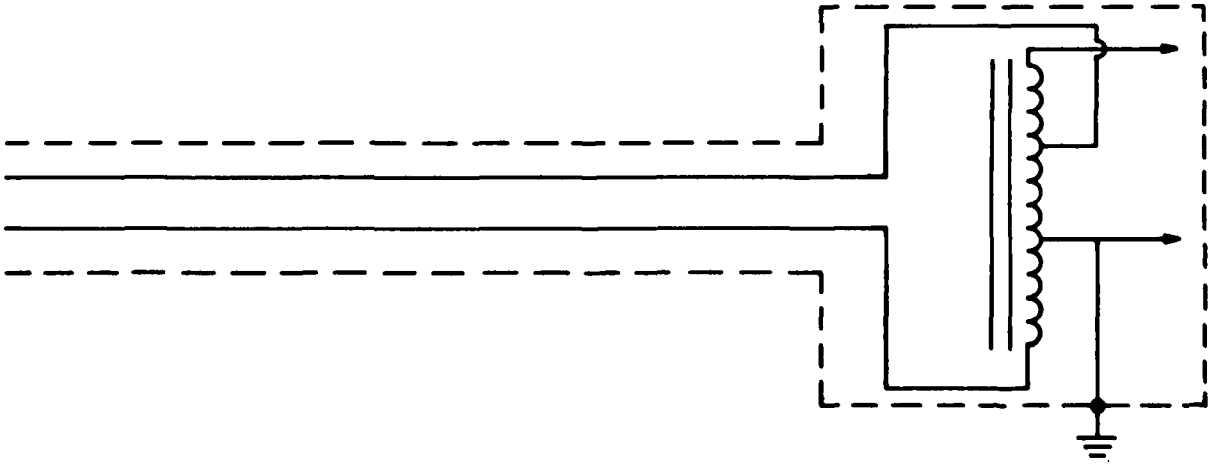

Figure 12-1c. Balun.

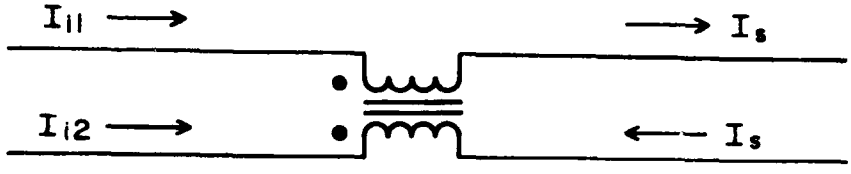

Figure 12-2. Common-mode choke.

produced by induced currents I_{i1} and I_{i2} is additive with a resulting impedance to the flow of induced currents.

Limited Frequency Response

A transformer can act as a filter to pass a signal which is within its bandpass but not pass an EMP pulse which is rich in high-frequency components. This property, referred to as frequency response, can provide a modest amount of hardening.

A series inductor can provide hardening by acting as a low-pass filter to pass a signal and not pass the high-frequency components of the EMP pulse. Distributed capacity can cause the inductor to act as a parallel resonant circuit and thereby function as a narrow-band filter when used to terminate a cable.

Saturation

A large number of inductive devices employ ferromagnetic materials as cores and such materials are subject to saturation. Saturation of the core due to an EMP pulse can be both detrimental and beneficial. It can result in functional upset in a system because of the resulting distortion in the signal component due to saturation by the EMP pulse. Conversely, saturation of the core may result in the EMP pulse being reduced at the output of the transformer and thereby provide hardening in the sense of reducing equipment damage.

12.1.4 Users of Procedures

The test procedures developed in this document should prove useful to a variety of users including:

1) System and circuit designers who require quantitative data on hardening components.
2) System engineers and project officers who formulate acceptance criteria and performance specifications.
3) Component manufacturers who can provide data having EMP significance.

It should be noted that the test procedures described in this document pertain only to the electrical behavior of the

element and do not include mechanical or environmental tests. Furthermore, they are not "cookbook" acceptance procedures but are intended to provide the basis for such procedures and military specification. They represent, in short, the first phase in a process which can result in mil-specs and procedures.

12.2 Element Characteristics, Definitions and Failure Modes

12.2.1 General

Two types of tests are considered in these test procedures. One type involves low-level tests to determine how well the component performs its hardening function. Such tests are designed to measure those performance characteristics of the element which are important to hardening and are performed at signal intensity levels within the design limits of the element. The second type, high-level tests, are concerned with permanent damage to the element as a result of EMP.

In this section, tests normally employed to measure the performance characteristics of interest are considered briefly and their shortcomings, from an EMP point of view, are identified. Forthcoming sections present preferred test procedures intended to remove these shortcomings.

12.2.2 Transformers

The purpose of this section is to identify those electrical characteristics of transformers or baluns which are of particular interest to EMP and thereby establish a basis for the test procedures.

Common-Mode Rejection

It has been indicated that transformers and baluns provide hardening by common-mode current rejection. This property of the transformer has been, in part, characterized by the common-mode rejection ratio and the longitudinal balance. Figure 12-3 provides a definition of the common-mode rejection ratio.[3] The measurement is performed with a sinusoidal waveform at a specified frequency with R equal to the terminating impedance of the winding. This test suffers from two shortcomings from an EMP point of view. Since it is performed at a single frequency, it does not indicate how well the transformer provides common-mode current rejection over the broad band of frequencies present in an EMP pulse.

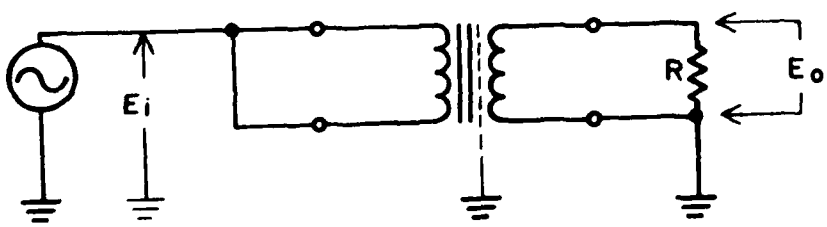

$$\text{Common-Mode Rejection Ratio} = \frac{E_i}{E_o}$$

Figure 12-3. Common-mode rejection ratio.

Furthermore, it does not take into account the effect of the source impedance or terminating impedance for the common-mode currents.

Figure 12-4 provides a definition of longitudinal balance[1] and again the measurement is made with a sinusoidal waveform at a specified frequency. In this case, as before, performing the measurement at a single frequency is not considered to be satisfactory for EMP purposes. Furthermore, it is desirable to terminate the transformer in its proper winding impedance to more nearly duplicate normal operating conditions. This is especially important for frequencies which are outside of the design limits of the transformer, but present in an EMP pulse.

As indicated earlier, a test which is intended to overcome the shortcomings in these two tests is given in Section 12.4.

Frequency Response

It has been indicated that the frequency response of a transformer might provide a modest amount of hardening by virtue of the fact that the transformer may not pass many of the high-frequency components in EMP. Frequency response is defined in Figure 12-5 where R_s and R_L are the appropriate terminating impedances, and where E_{of} and E_{or} are the output voltages at an arbitrary frequency and at a reference frequency respectively. Tests for frequency response are well documented[2] and are normally performed over the design bandwidth of the transformer. However, the band of frequencies over which the test is performed should be extended to cover frequencies contained in an EMP pulse rather than the design bandwidth. Furthermore, the frequency response, as defined in Figure 12-5, provides a relative indication of the ability of the transformer to pass or not pass frequencies. That is, the response at a given frequency is relative to that at a specified frequency. It is desirable to have an absolute indication of the response and a modified definition of frequency response which provides this is given in Section 12.4.

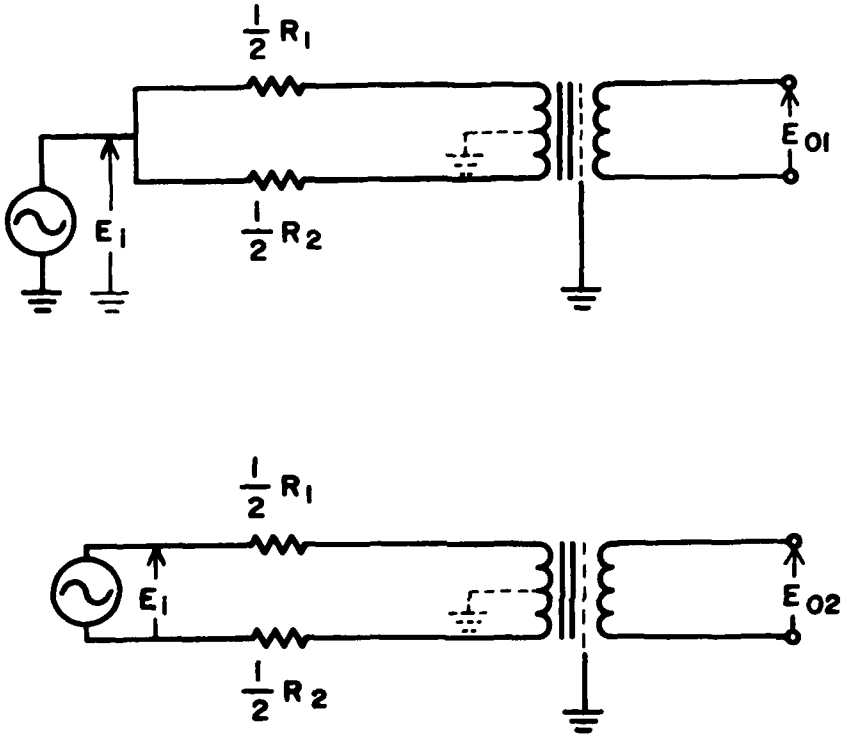

$$\text{Longitudinal Balance} = 20 \log \frac{E_{02}}{E_{01}} \quad \text{dB}$$

Figure 12-4. Definition of longitudinal balance.

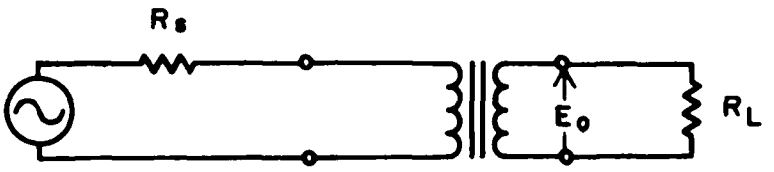

$$\text{Frequency Response (dB)} = 20 \log \frac{E_{of}}{E_{or}}$$

Figure 12-5. Definition of frequency response.

Insulation Breakdown

A high-intensity EMP pulse can result in arcing between windings, between a winding and the shield and/or case, or across a winding. This arcing can puncture the insulation or, in extreme cases, result in destruction of the wire to the extent of causing an open winding. In the case of an encapsulated transformer, the energy in the arc may be sufficient to explode the case. Experience has shown that a low-energy arc may puncture the insulation with no discernable change in the performance of the transformer except that the insulation may breakdown at a lower voltage after arcing. Thus, the nature of damage that can be done to the transformer depends upon the characteristics of the EMP pulse which produces breakdown.

Conventional insulation breakdown tests[2] are, in some cases, performed at the highest operating frequency of the transformer, or in the case of a pulse transformer, using a representative pulse. In other cases, the test is performed using a dc voltage or a 60 Hz sinusoidal voltage. Breakdown is usually characterized by an abrupt change in the current waveform due to arcing. Evidently, for EMP purposes, the test should be performed with a waveform which duplicates as closely as possible an EMP pulse. Such a high-level test is discussed in Section 12.6.

Saturation

The role of saturation in hardening has been mentioned in an earlier section. A quantity which is used to characterize saturation in pulse transformers is the ET-Constant[3] (voltage-time constant). When a flat-top voltage pulse is applied to the primary of a transformer whose secondary is open circuited, the current rises nearly linearly with time until the onset of saturation at which time the current increases more rapidly. The "time-to-saturation" is the time taken for the current to reach 1.5 times a linear extrapolation of the current curve prior to saturation; see Figure 12-6. The product of the amplitude of the voltage pulse and the "time-to-saturation" is the ET-Constant.

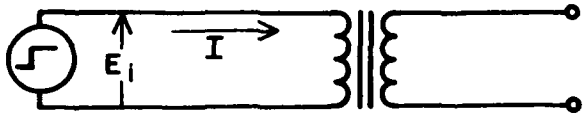

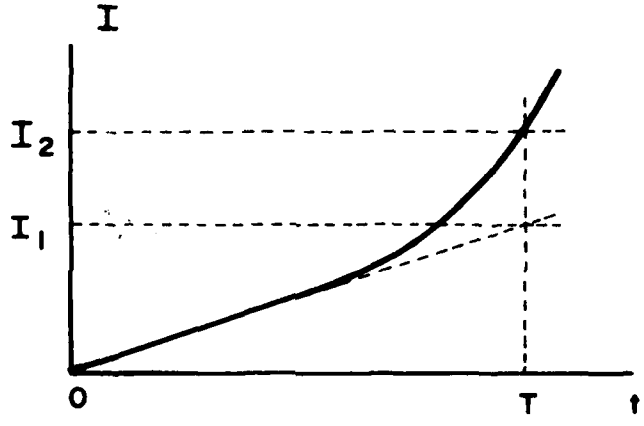

$I_2 = 1.5\ I_1$

T = Time To Saturation

ET - Constant = $E_1 T$

Figure 12-6. Definition of ET-constant.

An alternate method for measuring saturation is to apply a sinusoidal voltage across the primary of a transformer whose secondary is open-circuited. The voltage is increased until the primary current becomes non-sinusoidal indicating the onset of saturation. Saturation tests are high-level tests in the sense that they are made with signals whose intensities are beyond the design limits of the transformers.

The ET-Constant test for saturation is normally applied to pulse transformers and is useful when the transformer is used with rectangular or near rectangular pulses. On the other hand, the test which makes use of distortion in a sinusoidal waveform is usually applied to audio and power transformers. An EMP pulse is typically a damped sinusoid and, therefore, neither test is truly representative. Furthermore, it is difficult to obtain signal sources which deliver pulsed sinusoids of sufficient intensity to duplicate an EMP pulse. For these reasons, it has not been possible to formulate a preferred test procedure for saturation which is meaningful and which does not require great sophistication. Further work is required to formulate a satisfactory test for saturation due to an EMP pulse.

12.2.3 Chokes (Inductors)

It has been indicated that chokes can provide hardening by virtue of their frequency selective properties, that is, as a low-pass filter or parallel resonant circuit. Usually a choke is characterized by its inductance, its loss factor (Q at a given frequency), and its self-resonant frequency. All of these properties of the choke are embodied in its complex impedance given as a function of frequency and test procedures are discussed for measuring this impedance. Such tests are low-level tests since they are performed at signal levels consistent with the design limits of the element.

Permanent damage can occur in a choke when a high voltage pulse is applied across the choke. As in the case of a transformer, arcing can occur which may be of sufficient magnitude to

locally destroy the wire and open-circuit the choke. If the choke is encapsulated, the arcing may explode the case. There is also a possibility that arcing may produce shorted turns and thereby produce a high loss choke. Tests performed to determine these kinds of failures are, of course, high-level tests and are discussed in greater detail in Section 12.6.

12.3 Test Philosophy

Two low-level tests have been emphasized in the previous section, one concerned with common-mode rejection and the other with frequency response. Such tests are normally performed at frequencies which are within the design bandwidth of the element. When testing for EMP purposes, the test should be performed over the frequency band extending from 10 KHz to 100 MHz to take into account the broad range of frequencies contained in EMP.

Typical EMP waveforms are exponentially damped sinusoids which are difficult to generate at the required voltage and frequency. As a result, high-level tests are normally performed using pulses obtained by discharging a capacitor or transmission line. When a capacitor is discharged into a resistive load, the voltage waveform appearing across the resistance is a double exponential pulse characterized by a peak voltage, rise time and fall time. Decay times extending from 50 ns to 15 μs are appropriate with rise times 10% or less of the decay time where possible. It should be emphasized that if a capacitor is discharged into a transformer or choke, the voltage pulse appearing across the element is, in most cases, not a double exponential because of the inductance of the element. In order to obtain a specified pulse, which is reasonably independent of the element, it is necessary to use a resistor in series or in parallel with the element to stabilize the waveform.

If a section of transmission line is discharged into its characteristic impedance, it produces a voltage pulse across that impedance which is nearly rectangular and whose duration is determined by the length of the line. If the transmission line is discharged into a choke or transformer containing inductance, the voltage waveform appearing across the element is no longer rectangular and it may be necessary to use a stabilizing resistor to obtain a specified voltage pulse.

Because of the wide variety of transformers, baluns, and chokes which are available, test fixtures are not specified in

this report. Frequently, the manufacturer of the element specifies the fixture to be employed with his product. It is, of course, necessary to insure that this fixture is suitable for use over the range of frequencies extending from 10 kHz to 100 MHz. This means that there must be no significant lead inductance in series with the test item and no significant stray capacitance in parallel with it.

12.4 Test Procedure For Common-Mode Rejection Ratio and Frequency Response

As described previously, the hardening capability of the transformers can be evaluated by determining their common-mode rejection ratio and the frequency response. This test procedure therefore, covers various aspects of these measurements.

12.4.1 Scope and Experimental Details

12.4.1.1 Common-Mode Rejection Ratio Tests

A modified common-mode rejection ratio (CMRR) test is recommended for transformers and baluns where the CMRR (in dB) is defined in Figure 12-7 for a variety of transformer configurations. The test should be performed with a sinusoidal voltage and over the band of frequencies extending from 10 kHz to 100 MHz. E_i is the rms applied voltage and E_o is the rms voltage appearing across the resistor R_L. R_L is the proper terminating impedance for the loaded winding and R_S the proper source impedance for the excited winding. When the grounded side of the output winding is not specified, the test should be performed with first one side of the winding grounded and then repeated with the other side grounded.

Although the excitation can be provided by a signal generator and the voltages measured using a voltmeter having the correct frequency response, such a measurement procedure is likely to be time consuming if employed for the complete range of frequencies from 10 kHz to 100 MHz. Swept-frequency instruments are available which simplify the measurement. For example, the HP8407A Network Analyzer provides a visual display or, when used with a recorder, a graphical record of the CMRR over the frequency range of 0.1 MHz to 100 MHz. Figure 12-8 depicts a typical test arrangement employing the HP8407A where voltage probes are used to measure E_o and E_i.

For the frequency range extending from 10 kHz to 100 MHz,

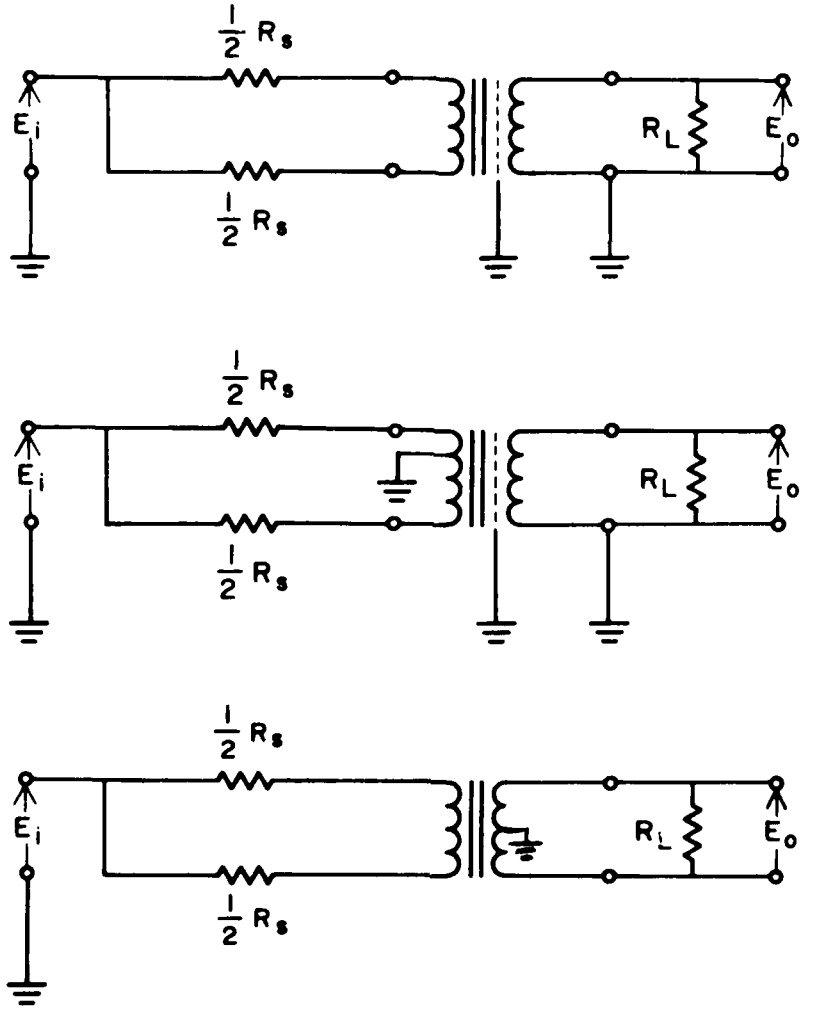

$$CMR = 20 \log \frac{E_o}{E_i}$$

Figure 12-7. Common-mode rejection test.

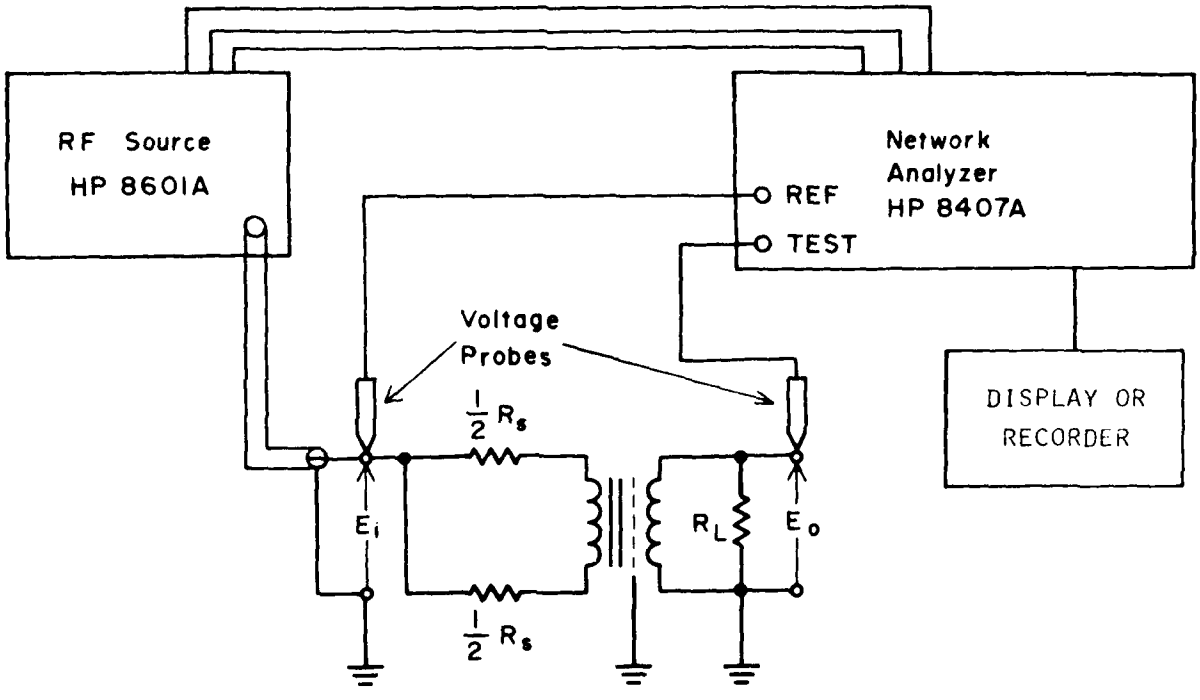

Figure 12-8. CMRR test using HP8407A (See page 16, transmission measurements HP application note 121-1).

a signal generator and voltmeter can be used to perform supplemental tests.

12.4.1.2 Frequency Response Test

A modified frequency response test is recommended for transformers and baluns where the frequency response (in dB) is defined in Figure 12-9 for a variety of winding configurations. A sinusoidal voltage should be used to perform the test and the frequency response should be measured over the range of frequencies from 10 kHz to 100 MHz. E_i is the rms voltage applied to the excited winding whose terminating impedance is R_S, while E_o is the voltage appearing across the loaded winding whose terminating impedance is R_L. The transformer should be connected, as regards shield, case, and taps, to duplicate normal operating conditions as closely as possible.

Although the test can be performed using a signal generator and voltmeter, it can be done more conveniently in the frequency range from 0.1 MHz to 100 MHz using the HP8407A Network Analyzer or similar device. Figure 12-10 depicts a typical test arrangement employing this instrument where voltage probes are used to measure E_i and E_o. The HP8407A provides a visual display of the frequency response or, when used with a recorder, a graphical record. A signal generator and voltmeter can be used to perform supplemental measurements in the region from 10 kHz to 100 MHz.

12.4.2 Precautions

Certain precautions should be observed in making these measurements.

(1) The CMRR can take on values as low as -80 dB which may make it necessary to shield the source of excitation from the device used to measure E_o.

(2) Good practices regarding lead lengths, stray capacities, inductive loops, grounding, etc., should be observed in performing the test.

(3) If the CMRR and frequency response are measured on a point-by-point basis with respect to frequency, ten measurements should be made per frequency decade.

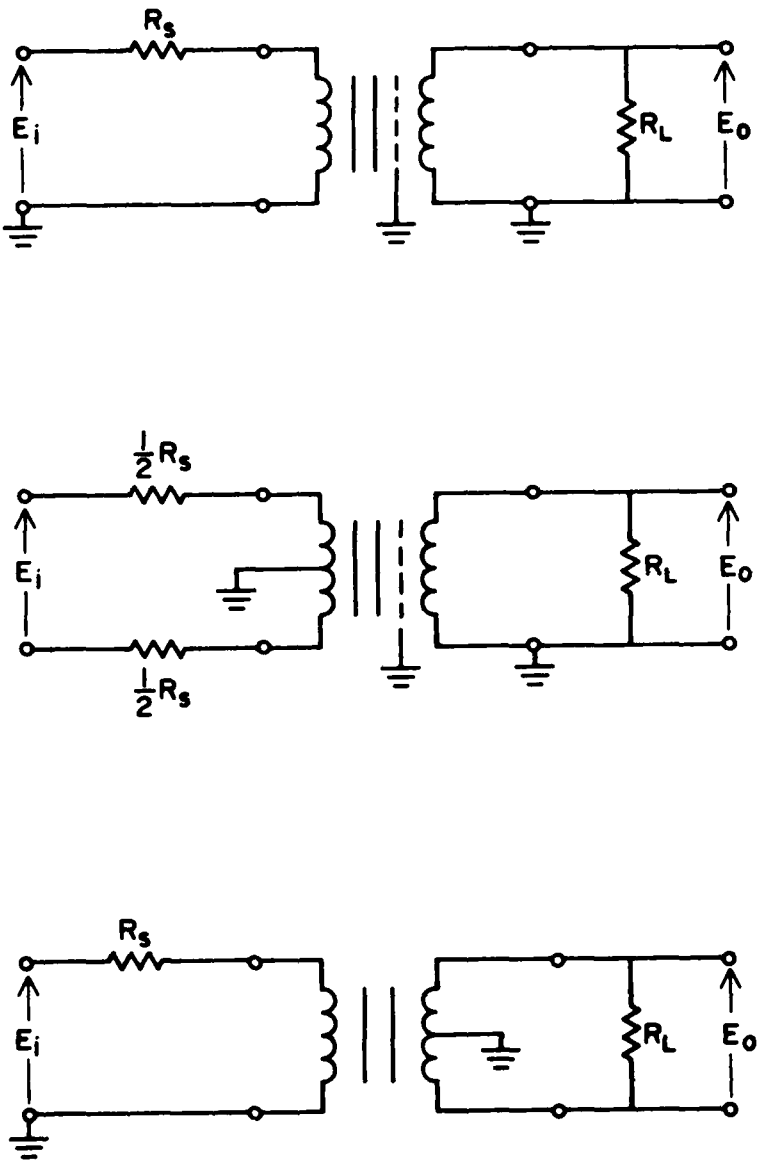

$$\text{Frequency Response} = 20 \text{ Log} \frac{E_i}{E_o}$$

Figure 12-9. Frequency response.

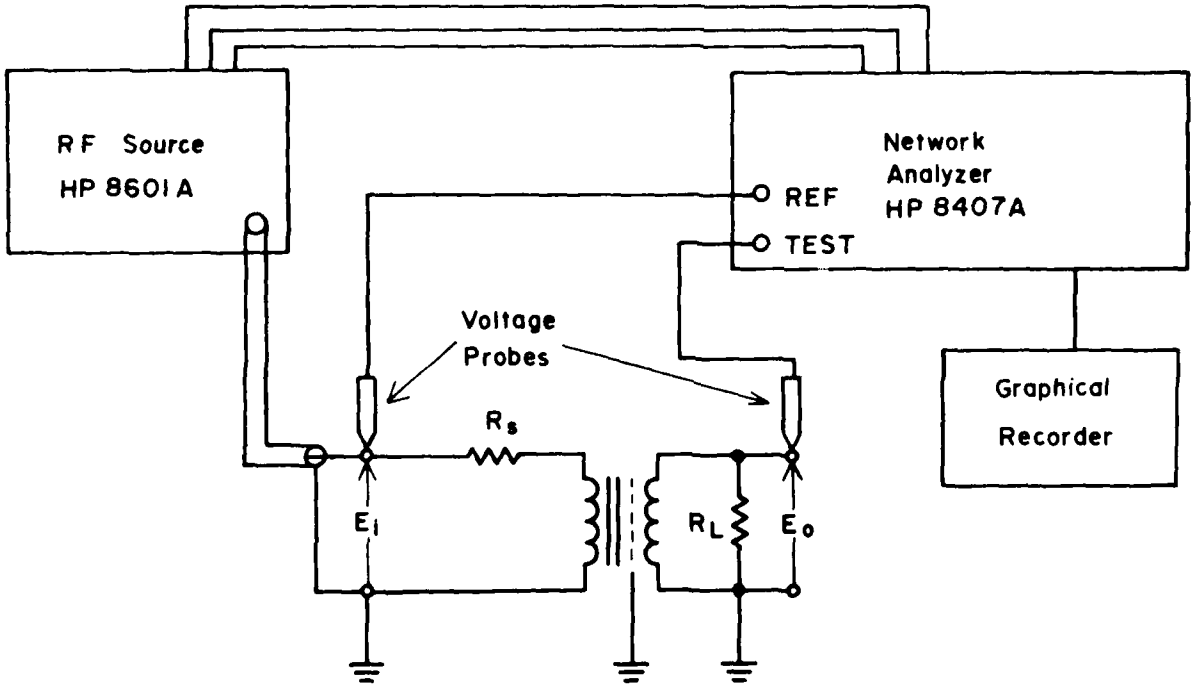

Figure 12-10. Frequency response test using HP8407A (See page 16, transmission measurements HP application note 121-1).

Any abrupt variations in either with frequency should be noted.

12.4.3 Calibration

The network analyzer and the test fixtures should be calibrated. The basic calibration consists of replacing the test item with a short circuit so that E_o and E_i are equal. E_o is measured across a 50 Ω resistor. The display should be flat, indicating that the resistor and the fixture do not have reactive impedances at the test frequencies. The display is then adjusted to provide a 0 dB reference at the top of the display.

12.4.4 Data Format

The basic data to be presented are the CMRR and frequency response (or differential mode response) over the frequency range of 100 kHz to 100 MHz. The best format is a graph of each property on semi-log arithmic paper. However, photographs of the network analyzer display are easier to obtain and contain the same information. However, the frequency axis is often linear so that several photographs are needed to provide adequate detail over the full three decade range in frequency.

Each piece of data should describe the test item and the configuration of the input and output terminations used. Examples of typical test results for one frequency range are given here for a balun, a wideband transformer and a pulse transformer.

A Cambion Balun Type 555-7167-07 was tested for common-mode rejection and frequency response with the balun connected as shown in Figure 12-11. This balun, designed for a 50 ohm source impedance and a 50 ohm load impedance with an advertised frequency response of 60 kHz to 30 MHz although the test data shows reasonably flat response to 100 MHz. The common-mode rejection becomes poor at the highest frequencies. It should be noted that the roles of the input and output of the balun were reversed in performing the frequency response test. This was done for convenience in measurement and is valid because of the reciprocal properties of the balun.

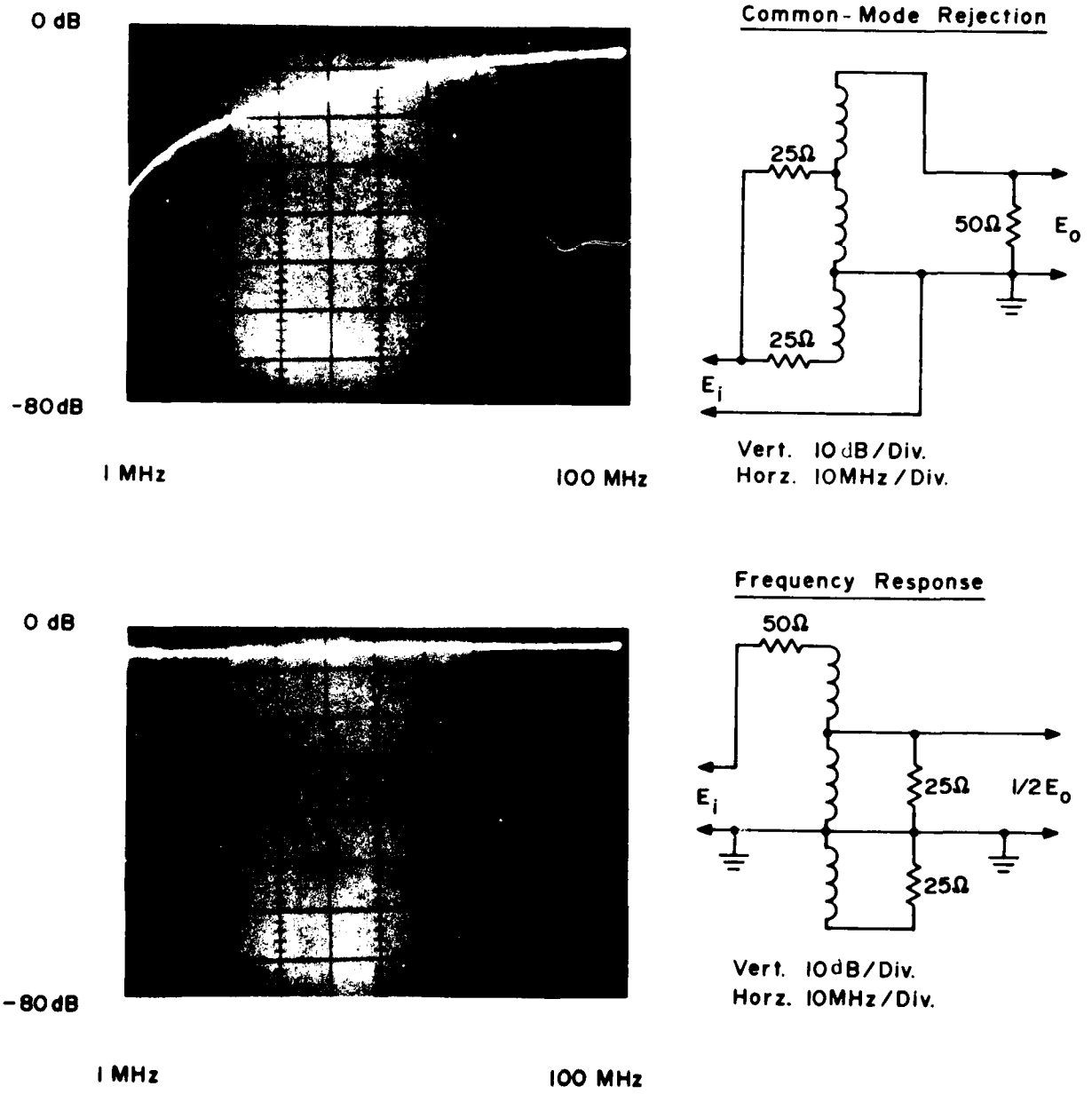

Figure 12-11. Test results for cambion balun - 07.

Figure 12-12 shows test results obtained from a Vari-L Co., Inc. wideband transformer Type LF428 with the transformer connected as shown. It should be noted that here, as in the case of the baluns, the foles of the input and output of the transformer have been inverted to simplify the frequency response measurement. This is valid because of the reciprocal properties of the transformer. This is an impedance matching transformer for 50 ohms to 200 ohms with an advertised frequency response of 10 KHz to 50 MHz. The drop-off of frequency response at the higher frequencies is evident, as is a deterioration in CMRR performance.

Figure 12-13 shows the results for a common-mode rejection test performed on a Pulse Engineering Type 5154 pulse transformer with and without the electrostatic shield connected. The shield does provide additional CMRR. The frequency response of this transformer is also shown in Figure 12-13. The transformer has a one-to-one winding ratio; however, frequency response normally is not quoted for pulse transformers. The measured frequency response is far from being independent of frequency.

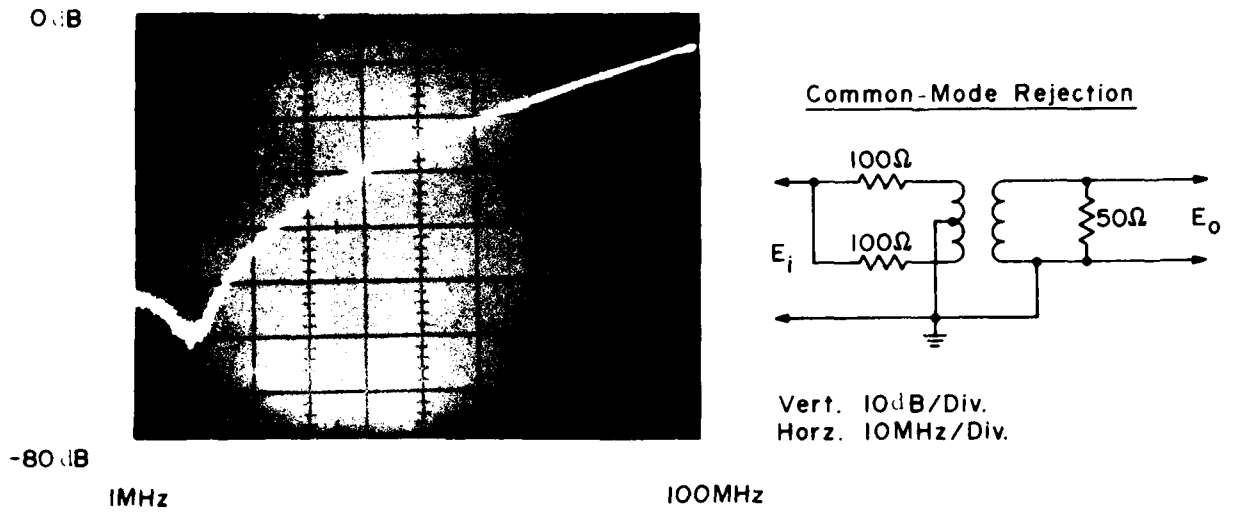

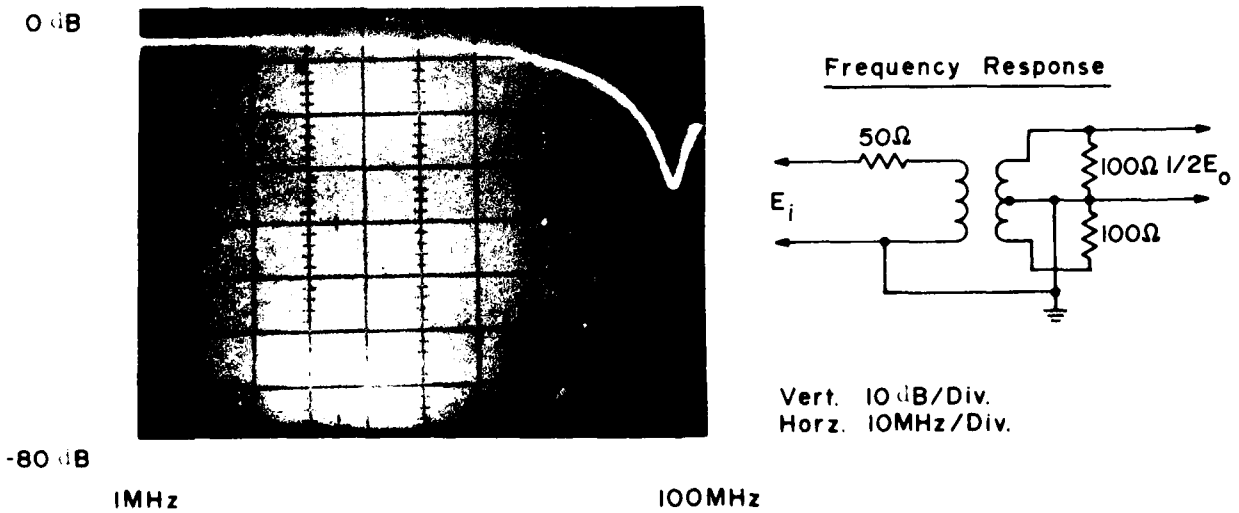

Figure 12-12. Test results for vari-L type LF428 transformer.

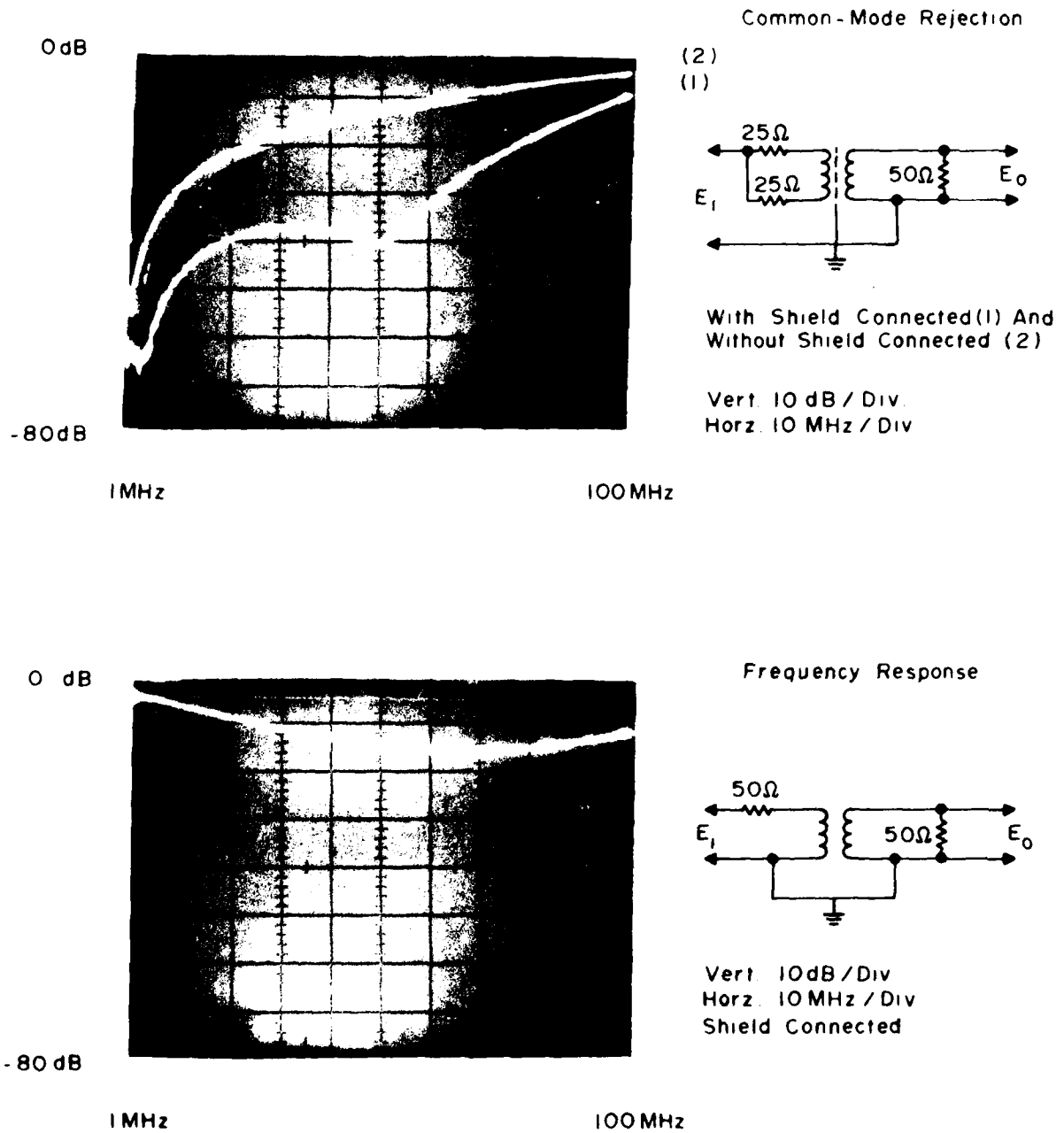

Figure 12-13. Test results for 5154 pulse transformer.

12.5 Complex Impedance Test Procedure

12.5.1 Scope and Experimental Details

It is recommended that a complex impedance test procedure be used for evaluating inductors (or chokes) over the frequency range extending from 10 kHz to 100 MHz. The impedance can be measured with a variety of instruments including impedance meters, vector voltmeters, and Q-meters. Some of these instruments are swept frequency devices with read-outs which can be used to obtain a photographic record with an oscilloscope or a graphical record with a pen recorder. This measurement can also be performed with the HP8407A Network Analyzer using the arrangement shown in Figure 12-14.

12.5.2 Precautions and Calibration

Good practices should be observed regarding lead lengths, stray capacities, inductive loops, grounding, etc. The calibration of the HP8407A Network Analyzer is performed by using a 50 Ω resistor rather than the test item shown in Figure 12-14. Precautions should be observed in the initial calibration and usage.

12.5.3 Data Format

Complex impedance measurements on chokes should be presented in graphical forms. However, photographs are easier to obtain and contain all essential information. Figure 12-15 shows the ease with which the self-resonant frequency of the choke can be located by a rapid variation in the amplitude and phase displays. These traces are illustrative and not calibration and thus not quantitative. For further details on measurements of complex impedance, see discussions in the literature.[4,5]

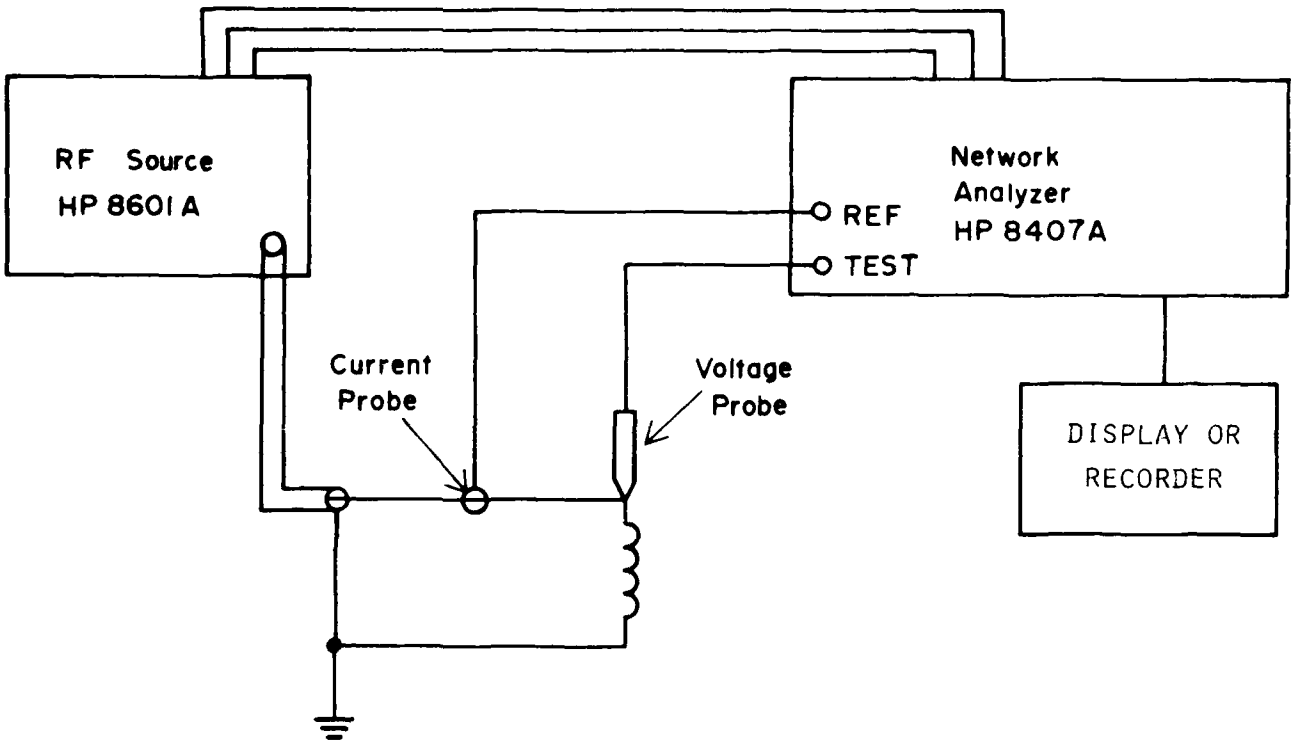

Figure 12-14. Complex impedance measurements using HP8407A.

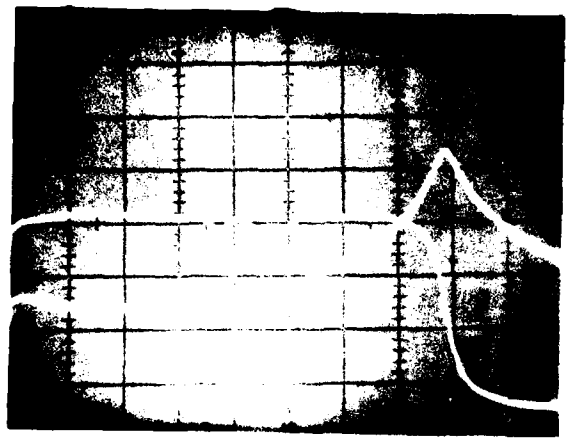

Nytronics Type 90 537-25
10 μH Choke

AMPLITUDE

PHASE

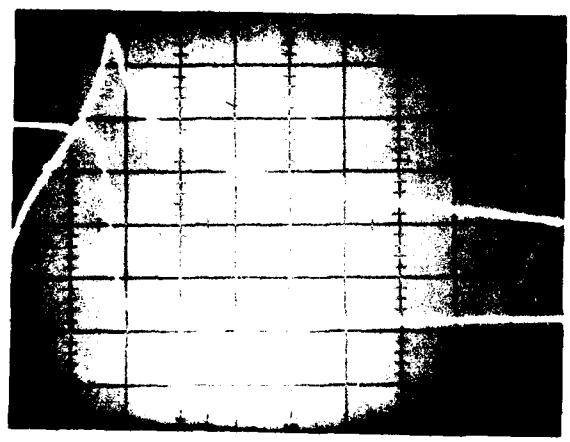

Nytronics Type 90 537-37
100 μH Choke

AMPLITUDE

PHASE

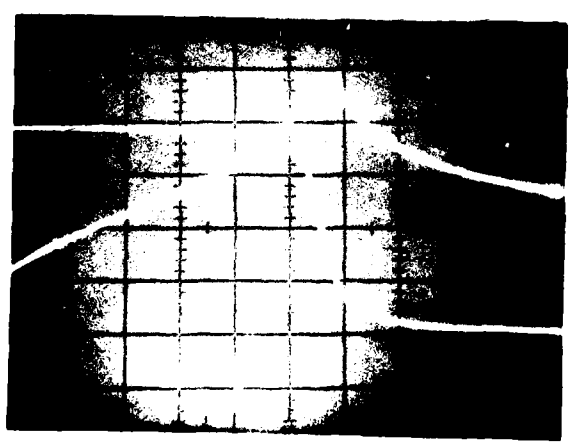

Nytronics Type 90 537-49
1000 μH Choke

AMPLITUDE

PHASE

0.1MHz

10 MHz

Figure 12-15. Complex impedance of chokes

12.6 High Voltage Pulse Tests for Insulation Breakdown

12.6.1 Scope and Experimental Details

Interwinding and inrawinding breakdown tests are recommended for transformers, baluns, and chokes where applicable. Figure 12-16(a) depicts a typical interwinding test, and 12-16(b) an intrawinding test. A capacitor discharge pulse source, as shown in Figure 12-17(a) or a transmission line pulse source, Figure 12-17(b), may be employed. If the test item is a resistor, the capacitor pulse source would produce a double exponential voltage pulse whose fall time is determined by the size of the storage capacitor and the test resistor, rise time by the characteristics of the switch and distributed capacity, and peak value of the pulse by the high-voltage source. If the test item were a resistor equal to the characteristic impedance of the transmission line, the transmission line pulse source would produce a nearly rectangular pulse whose duration is twice the transmission time of the line and whose amplitude is one-half the voltage delivered by the high-voltage source.

In either of the two cases, since the test item is assumed to be resistive, the waveform of the current through the resistance is the same as the voltage waveform. Unfortunately, both of these situations are highly idealized and, in either the intrawinding or interwinding test, the transformer, balun or choke constitutes a complex load on the pulse source. This causes the voltage and current waveforms to be complicated in shape, both prior to and after breakdown; and for this reason, these waveforms should be monitored.

In most cases, the pulse waveform obtained with the transmission line source is somewhat less sensitive to the test item and this source generally is preferred when the pulse amplitude and duration requirements can be met with a line of reasonable length.

The current waveform can be stabilized partially by adding a resistance in series with the test item, while the voltage

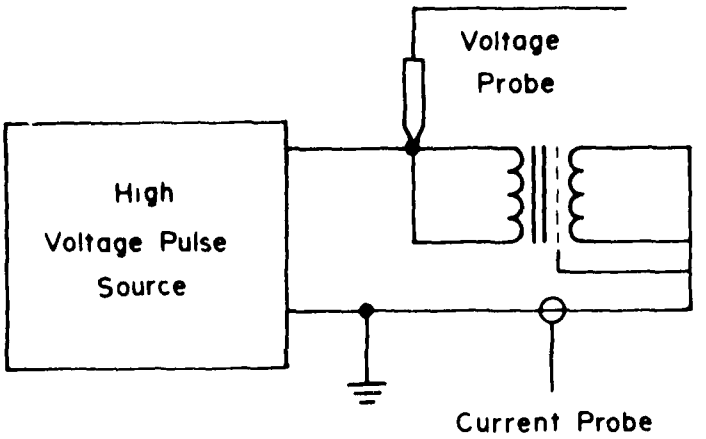

(a) Interwinding Pulse Test

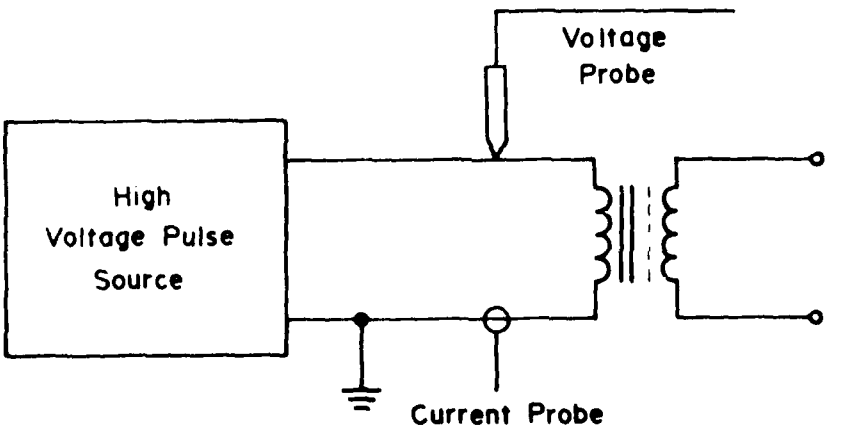

(b) Intrawinding Pulse Test

Figure 12-16. Insulation breakdown tests.

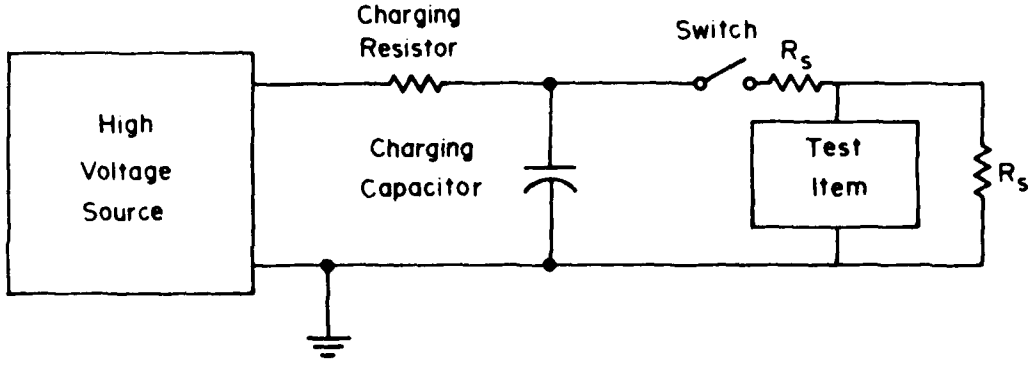

(a) Capacitor Pulse Source

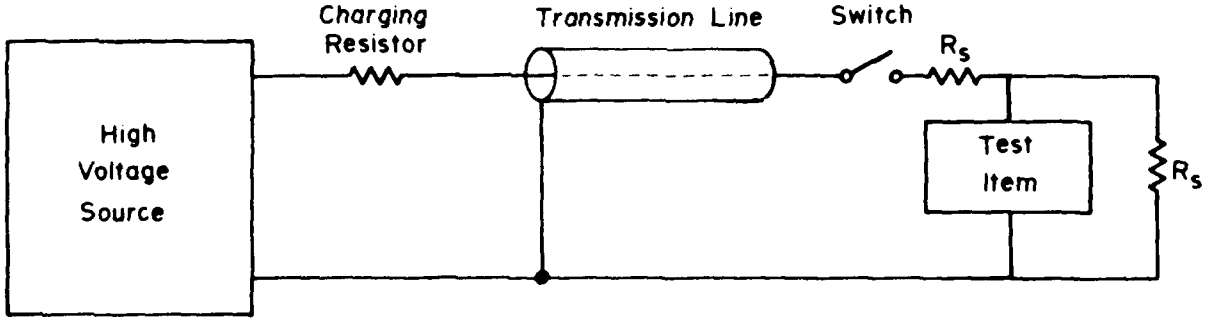

(b) Transmission Line Pulse Source

Figure 12-17. High voltage pulse source.

waveform can be stabilized partially by employing a resistance in parallel with the test item. The addition of the stabilizing resistors means that the voltage and current waveforms are similar to the ideal (resistive) case and are relatively independent of the test item impedance. The size of the parallel or shunt resistance, R_S, required to obtain partial stabilization depends upon the impedance of the test item.

A current probe provides one means of determining when breakdown has occurred since there is an abrupt change in the shape of the current waveform at the onset of arcing. The current can also be monitored by observing the voltage across a resistor through which the current flows. In some cases, an attenuator connected across the test item can serve as both a stabilizing resistor and a voltage probe.

12.6.2.2 Precautions

If the transformer is encased in a metallic case, the case should be connected as is the shield. All chokes should be tested for intrawinding breakdown; and for chokes encased in a metallic case, a winding to case test is applicable. The current and voltage waveforms should be appropriately stabilized by connecting series and parallel resistors with the test item.

12.6.2.3 Sample Data

Figure 12-18 provides data of interwinding breakdown by a voltage measurement. It should be noted that the 26 dB Bird Attenuator in this configuration is playing the dual role of a voltage stabilizing resistor and a voltage measuring device (probe). The 50 ohm resistor is included to provide a degree of current stabilization or, more precisely, current limiting. When breakdown occurs most of the pulse voltage appears across this resistor because of the low resistance of the arc appearing across the windings.

The test item in Figure 12-18 is an open construction toroidal pulse Transformer Type PE52120, produced by Pulse

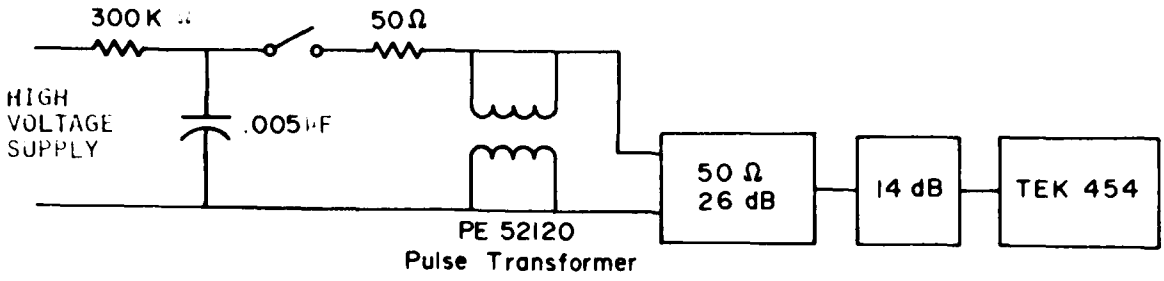

500 V/Div.
0.2 μs/Div.

Before Breakdown
SUPPLY VOLTAGE 3kV

500 V/Div.
0.2 μs/Div.

Breakdown
SUPPLY VOLTAGE 5kV

Figure 12-18. Interwinding breakdown test.

Engineering, Inc., which has an interwinding capacitance of 10 pF. The voltage appearing across the transformer is observed on the oscilloscope. The upper trace shows the voltage appearing across the transformer before breakdown; it closely resembles that without the transformer present as is to be expected, since the interwinding capacity is small. The lower trace shows the voltage across the transformer when insulation breakdown occurs. This method of measuring breakdown voltage is convenient since the form of the voltage wave remains the same as the supply voltage is increased until the onset of breakdown.

Intrawinding breakdown is demonstrated in Figure 12-19, in this case, by current measurement. As suggested earlier, the current is measured by observing the voltage drop it produces across the resistance of the 26 dB attenuator, although a current probe can also be used. The test item is a Nytronics Type DD-100 choke which has an inductance of 1,000 μH. For supply voltages of 2.5 kV and 5.0 kV, breakdown does not occur as is evident from the two curves having the general form of a heavily damped sinusoid. These curves imply, as would be expected, that initially the full voltage of the storage capacitor appears across the choke since that observed across the attenuator is very nearly zero. Breakdown is evidenced by a radical change in the current waveform due to arcing. Once again the measurement technique is convenient since the form of the current waveform remains the same as the supply voltage is increased until breakdown. Although it is not the objective of this program to investigate breakdown mechanisms, based upon the construction of the choke, breakdown is believed to have occurred from one end of the winding to the ferrite core and to the other end of the winding.

The techniques for measuring breakdown voltages discussed above are by no means exhaustive and are intended only to present some general ideas pertaining to this subject. For example, transmission line pulse sources can be employed and currents and voltages measured with probes rather than with an attenuator.

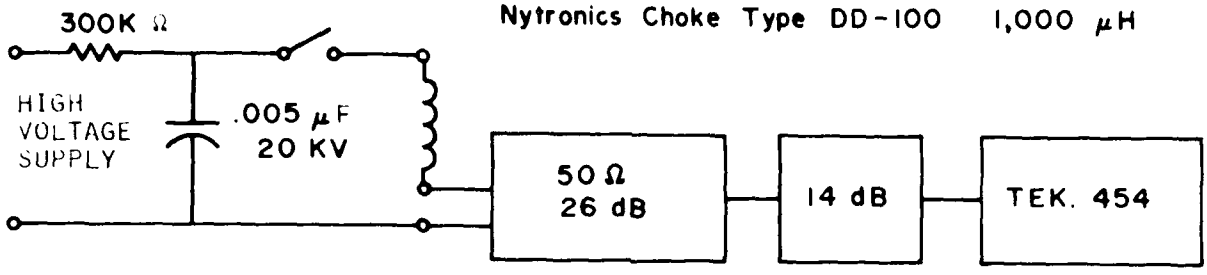

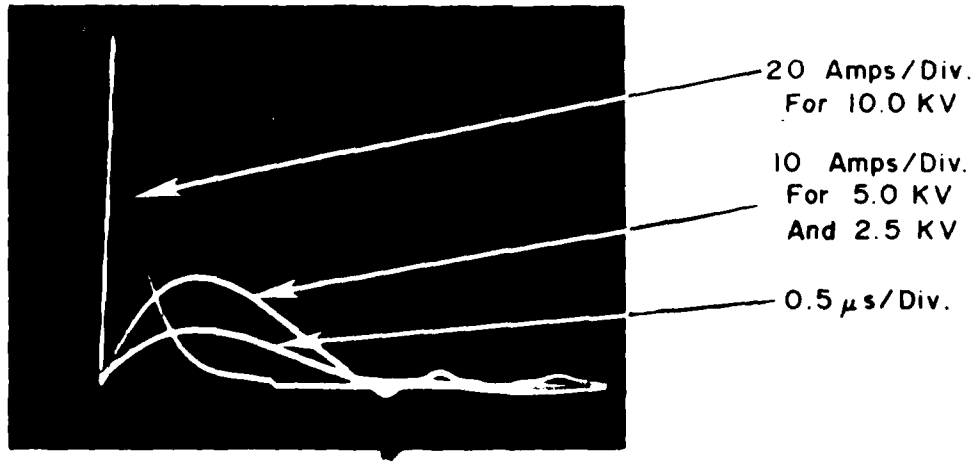

33

Figure 12-19. Intrawinding breakdown test.

What represents the most convenient method depends upon the characteristics of the element under test and the availability of test equipment.

12.7 References

1. "Transformer and Inductor (Audio, Power and High Power Pulse), General Specification for MIL-T-27D, 15 April 1974.

2. "Audio Transformers for Electronic Equipment," Electronic Industries Association, Recommended Standard RS-174.

3. "Catalog - Handbook for Delay Lines, Pulse Transformers and Inductors," Pulse Engineering, Inc., September 1973.

4. "Network Analysis with the HP8407A," Application Note 121-1, Hewlett-Packard, February 1970.

5. "Swept Impedance with the 8407A Network Analyzer," Application Note 121-2, Hewlett-Packard, June 1970.

13. EMP PREFERRED TEST PROCEDURES FOR RESISTORS

TABLE OF CONTENTS

13. EMP PREFERRED TEST PROCEDURES FOR RESISTORS

13.1 Introduction

This test procedure is developed for all resistive components which are to be used in EMP hardened electronic circuits. This includes discrete resistors of the metal films, carbon composition, and wire wound varieties with power ratings from 1/8 watt upward and resistances from a few ohms to many megohms. In general, integrated circuit (IC) resistors cannot be tested in this manner because of the interconnections with other components which would affect the results. However, IC manufacturers with the capability of isolating the resistive elements and connecting auxiliary leads may consider using this procedure also.

Frequently, resistors are used at the interface between cables and electronic circuits to terminate the line in its characteristic impedance, reduce the current or voltage into or from a line, act as the first element in an RC or RL filter, or apply a dc bias current to a component on the other end of the line. Such a resistor would be stressed by an EMP waveform. The short term effect can be an increase or decrease of resistance or a change in its noise figure. The criticality of a resistor's failure is dependent upon the circuit sensitivity and its application. In many cases, the failure of a resistor, which became an open circuit following an EMP event, would result in a failure of the electronic system. However, other degradations such as moderate resistance changes, increased resistor noise, and temperature-humidity coefficient changes may result in degraded system performance without complete failure. The extent to which these factors need be considered must be evaluated for each application.

The test procedures described in this section are methods for obtaining the safe EMP levels at which a resistor may operate. This procedure uses a capacitor discharge through a triggered spark gap to simulate a double exponential pulse. Since each application has a unique cable coupled EMP waveform, resistor requirements, such as a safe voltage and pulse width, cannot be universally defined.

It is intended that these procedures can be used, with appropriate modifications for the specific application, by many individuals, including:

1) Engineers designing an EMP hardened system;

2) Systems engineers who must validate the hardness of resistors used in a system design;

3) Manufacturers interested in specifying and/or improving the EMP hardness of their components;

4) Scientists interested in developing a practical model for resistor response to pulsed stresses.

5) Engineers interested in pre-testing resistors to their design limits.

13.2 General

13.2.1 Characteristics

Brief descriptions of pertinent resistor parameters are given in the following paragraphs. Depending upon the application, these parameters may or may not be important to the design engineer. For instance, long term humidity effects may not be of interest if the engineer is concerned only with the immediate effects of EMP exposure. Such effects are presented to remind the engineer that they could become important. Other test procedures for passive components, including resistors, are presented in EIA Standard RS-186-D.[6]

Measurement of Resistance

Resistance is the property of a conductor which determines the current resulting from a given potential difference across the conductor. Measurements of resistance normally are made using a dc potential applied for a period of five seconds or less to limit the temperature rise. The recommended test voltages for each type of resistor can be found in appropriate EIA Standards.[3,4,5]

Temperature Coefficient of Resistance

This is a measure of the sensitivity of a resistor to changes in temperature. The temperature coefficient (TC) of a resistor, referred to a reference temperature of 25°C, is computed as follows:

$$TC = \frac{100\Delta R}{R\Delta T} \qquad (13\text{-}1)$$

where R is the resistance at 25°C, ΔR is the change of resistance from the resistance at the reference temperature for a temperature difference of ΔT from 25°C. The procedure is quoted in several EIA Standards.[3,4,5]

34

Voltage Coefficient of Resistance

This is a measure of the change of resistance of a resistor with applied voltage. This is normally negligible with wire

wound and metal film resistors but must be considered for carbon composition resistors. The voltage coefficient, VC, is obtained by measuring the resistance, R_2, at its maximum working voltage, E, and at 1/10 of that voltage, R_1. The voltage coefficient (VC) is computed as follows:

$$VC = \frac{100}{0.9E} \left(\frac{R_2 - R_1}{R_1} \right) \qquad (13\text{-}2)$$

Noise Level

All resistors generate a voltage across an open circuit due to the thermal agitation of the electrons of the resistor (Johnson noise). In addition, a noise voltage is developed across composition resistors when they carry currents which is called "resistance fluctuation" noise. This noise is due to the effects of the myriads of connections between the discrete particles of the resistive element. EMP may have a large effect on this phenomenon. If a resistor is to be used in a low signal level circuit, the circuit should be duplicated with resistors that have been exposed to EMP test waveforms of various levels and the circuit performance checked with the noisier resistors.

13.2.2 Definitions

Definitions of terms as applied to resistor testing are presented below.

Test Waveform

For the purpose of this test procedure, a double exponential pulse is used to simulate an EMP exposure pulse. Rise time from 10 to 90 percent levels should be less than 30 nanoseconds and fall time should be 0.1 to 20 microseconds. Other acceptable waveforms for these tests are square top and short exponentially damped sinusoids.

Pulse Width

For an exponentially decaying pulse resulting from an RC discharge, approximately 86 percent of the energy is dissipated

when the voltage drops to 1/e or 37 percent of the peak. For all practical purposes, the pulse width (T) is determined by the RC product where R is the resistance in ohms and C is the capacitance in farads and time is in seconds.

Safe Voltage

The safe voltage is the peak pulse voltage level at which the test waveform does not change the short term resistor characteristics outside predetermined limits after a minimum number of pulses. From the safe voltage, a safe current or power level is easily determined.

Average Power Level

The average power (P_a) to which the test resistor is exposed to is given by

$$P_a = n(\tfrac{1}{2} CV_p^2) \qquad (13\text{-}3)$$

where

n = number of pulses in one second period

$1/2CV_p^2$ = energy stored in the capacitor for each pulse.

For maintaining test resistor body near ambient temperature, it is suggested that average power be less than 1/10 of the dc rated power of the component.

Number of Exposures

The safe voltages of resistors are sensitive to the number of exposures. It has been reported[1] that the sensitivity of the safe voltage of the test resistor to the number of applied pulses asymptotically reaches a constant level after about 10^4 applied pulses.

This number of applied pulses does not represent a realistic situation and it may require considerable time to perform such a test. A typical EMP exposure would probably consist of a few pulses. Therefore, it is suggested that fifteen test pulses be

applied to a component. This is a compromise between the time to perform the resistor test and the number of possible exposures in a real environment.

Failure Criteria

The resistance change must exceed the resistor tolerance. This includes the possibility that the resistor is physically destroyed. Other criteria might be considered depending upon the resistor application.

13.2.3 Test Philosophy

This test was developed to provide an engineer with a sensitive test procedure to ascertain the maximum safe EMP voltage at which a resistor may be operated. The test procedure is to be simple and inexpensive to implement but the test conditions are realistic. More elaborate equipment can be considered if large quantities of resistors are to be tested on a production line basis with this procedure used as an example from which the automated equipment could be designed.

This procedure should be capable of investigating the following possible relationships:

1) Maximum safe voltage levels vs resistance value;

2) Pulse width vs peak pulse power or maximum safe voltage levels;

3) Steady state dc power dissipation vs maximum safe voltage level;

4) Maximum safe voltage vs resistor type (metal film, carbon composition, etc.).

Only two of the listed factors are known to be significant. They are the pulse width and the resistor types. It has been shown that the steady state dc dissipation does not affect the maximum safe level.[1] There is no accepted empirical relationship between the resistance value and the maximum safe voltage but there probably is a relationship between internal construction and the maximum safe voltage level.

Four modes of EMP failures have been observed;[1] they are:

1) External arcing around the resistor case;

2) External arc penetrating the case;

3) Internal arc along the resistive element;

4) Change of resistance.

The first failure mode causes no serious change in the resistor characteristics and, in fact, limits the resistive element stresses. This failure mode in itself might be considered advantageous because it acts like a protective spark gap but can lead to the second failure mode if case defects are present. The second failure mode is due to an arc along the case entering into the resistive element through a case defect. The external arc path has a lower resistance than the resistive element. Therefore, the current flow through the remaining portion of the resistor is larger than would be experienced normally. This excessive level can open the resistive element and cause the case to split. The third failure mode results in the element opening without any observable external arc but could be due to an internal arc. The fourth failure mode is due to the pulse energy damaging the resistive material.

The voltage level necessary to cause some carbon composition resistors to fail can cause arcing around the component. Since the relative humidity and atmospheric pressure can determine the air gap breakdown level, the resistors can be immersed in oil to increase the high voltage testing capability without regard to room humidity. This option is left open to the engineer designing the test but it is recommended that the worst case environment be considered and used during the resistor testing. This worst case condition may be high humidity or low pressure where arcing around the case could possibly damage the components the resistor is supposed to protect.

During the development of the test procedure, a few of the carbon composition resistors explosively disintegrated upon

application of simulated EMP. This occured at voltages slightly above the maximum safe voltage determined by the test. The phenomena causing these explosions were not investigated further but may have been due to cracks in the resistor case. A volatile substance could be present inside the resistor which was vaporized during the pulse. The resulting pressure could have destroyed the case. In most instances, only bare leads were left hanging. A few examples of damage to the test resistor are demonstrated in Plate 13-1.

The failure criteria used by Sandia Laboratories[1] was a measurable resistance change during application of 100 pulses at a given level. A failure criteria suggested by Dale Electronics[2] is a temperature increase of the resistive element to +350°C without heat loss to the core or coating. Other possible failure criteria are:

1) A resistance change greater than the resistor tolerance;
2) Increase in the resistor noise factor;
3) Change of the voltage coefficient;
4) Change of the temperature coefficient;
5) Increased sensitivity to humidity or salt water corrosion.

The failure criteria must be selected by the investigating engineer to match the resistor circuit application. One large variable that will be noted during testing is the unit-to-unit variation of the maximum safe voltage between identical resistors purchased in a group. This large scatter of safe voltage has two effects on testing. First, if a very good resistor is tested initially to roughly determine the failure level, many decremental steps may be necessary before a nominal safe level is determined for the average resistor. Second, a large number of resistors must be tested to ensure that the lower limit for a poor resistor is obtained. Of course, a screening test using this procedure could be performed upon incoming resistors to ensure that a poor resistor is not used. The simulated EMP used in the screening process might lower the threshold of nominally good resistors.

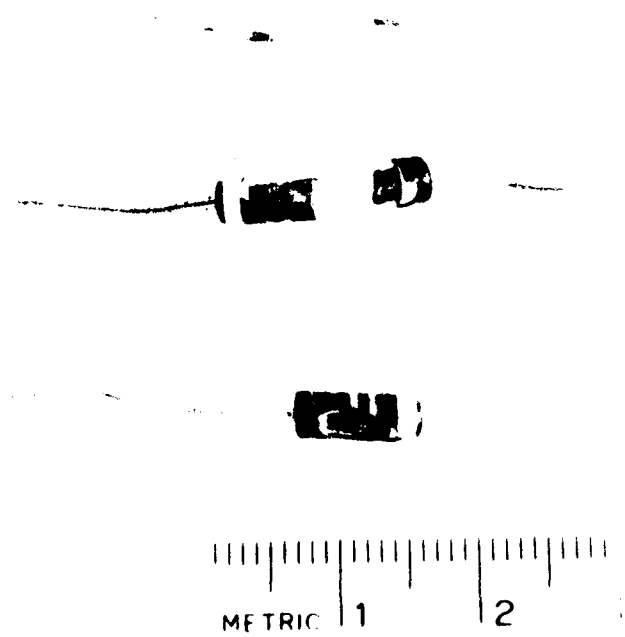

Plate 13-1. Examples of resistor damage.

13.3 Test Procedure

13.3.1 Scope

This test procedure is a guide for an engineer in developing a procedure specific to his requirements. The equipment and procedures described may be used on resistors ranging from about ten ohms to many megohms with power ratings up to 100 watts. The major limitation of the procedure is the voltage range obtainable with triggered spark gaps (about 50 kV). Pulse widths up to milliseconds can be generated by proper selection of the energy storage capacitor.

13.3.2 Test Fixture

Two special test fixtures need to be built for this procedure. One fixture, Figure 13-1, contains the triggered spark gap; the fast switch, and the energy storage capacitors. There are several firms selling spark gap switches that can be used for the source. This fixture operates in the following manner. A high dc voltage is applied through the connector (1), for charging the energy storage capacitors (2). The voltage potential on the capacitors at the time the switch closes is approximately the peak simulated EMP voltage. When a low voltage (20-500V) pulse is applied to the trigger transformer (3) through connector (4), a positive high voltage pulse (8-20kV) is applied to the trigger electrode of the spark gap (5) through dc blocking capacitors (6). This trigger pulse initiates the discharge of the storage capacitors through the spark gap to the output connector (7).

A triggerable spark gap is needed to provide the fast switching times for the high peak currents and voltages encountered in EMP testing. Spark gaps normally operate over a limited input voltage range of about 3:1. Therefore, provisions need be made to use several spark gaps to cover the voltage range from 1 kV to 40 kV. Each spark gap may have different trigger pulse requirements. Laser triggered spark gaps are commercially available which produce subnanosecond pulses but the cost of such an apparatus is high. An electrically triggered gap requires a trigger pulse of 5 kV to

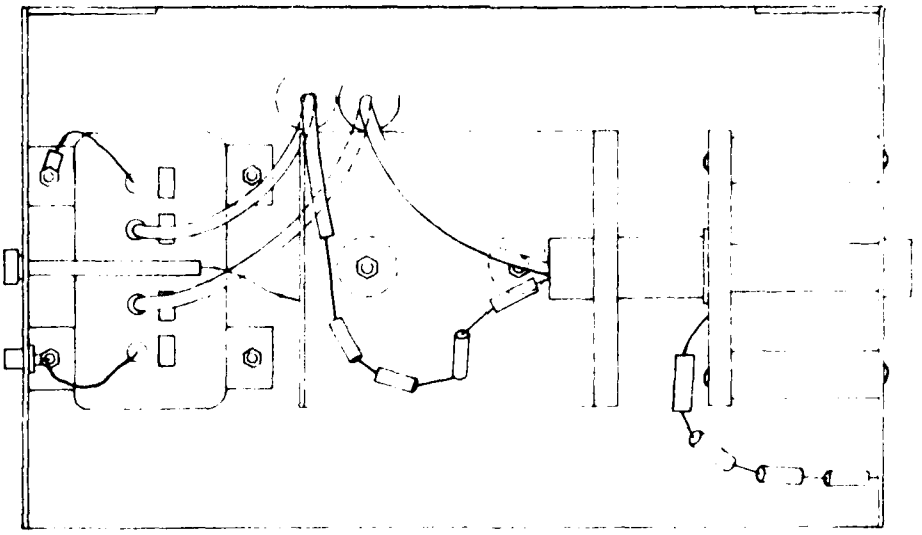

1	DC Input Connector	5	Spark Gap
2	Energy Storage Cap.	6	100pF 30kV Cap.
3	Trigger Trans.	7	Output Connector
4	Trigger Input	8	Shunting Resistor

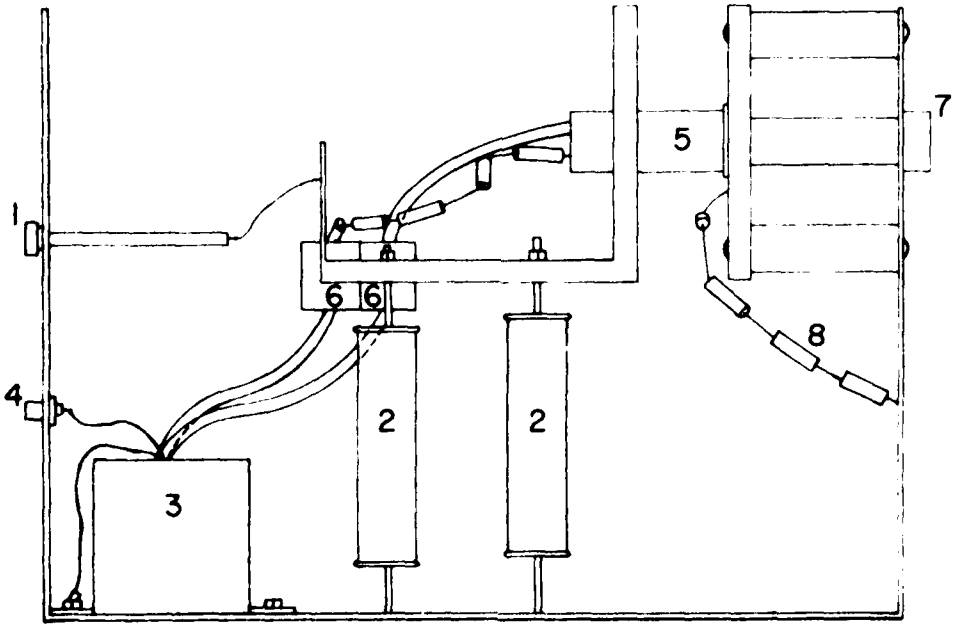

Figure 13-1. Illustration of high voltage switch.

20 kV. If several gaps are to be used, the maximum trigger requirements should be determined and a trigger transformer purchased to meet these requirements. The primary voltage, supplied by the lower voltage power supply, can be adjusted to lower voltages to accomodate the gaps with lower trigger requirements.

The capacitor must be rated at the highest voltage to which it is to be charged. Since the rise time of the simulated EMP is a major consideration, the internal inductance, L, of the capacitor should be minimized. It is desirable to obtain rise times of 5 nanoseconds or less than the inductive time constant. If the load (R) is 50 ohms, we find that from the approximate time constant formula that L must be less than 0.2 microhenries. This also clearly illustrates the need for minimum length and maximum diameter for all leads.

Figure 13-2 shows a low inductance fixture for holding the resistor under test. This unit was designed with the requirement of being adaptable to different sized components. Therefore, a connector (2) to the component mounted between two bars (3) and (4). An insulator (5) provides mechanical strength necessary for mounting and removing the resistor to bar (3).

If the resistor under test has a resistance other than 50 ohms, there is an impedance mismatch at the cable termination which causes pulse distortion. For the case where the resistor under test is larger than 50 ohms, an impedance match may be accomplished by shunting the pulse input connector (2) with an appropriate resistor. This shunting resistor can be made up of four to six 1 watt carbon composition resistors in series. For the case where the resistor under test (RUT) is less than 50 ohms, a series resistor should be used to match the cable impedance. While this forms, in effect, a voltage divider reducing the voltage to the RUT, the impedance mismatch created by not using a series impedance matching resistor also results in a low voltage across the RUT. In addition, an improperly terminated cable rings causing multiple application of pulses. Therefore, it is recommended that series

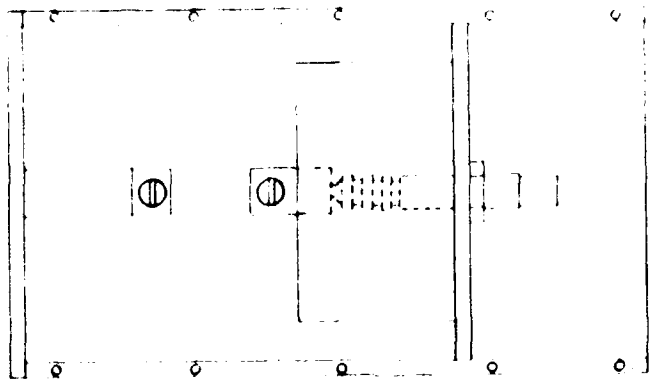

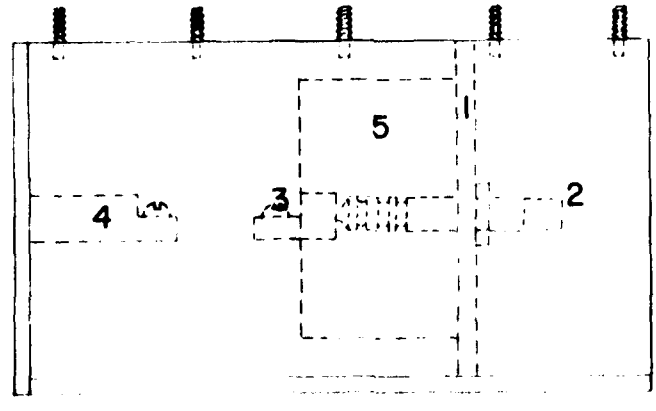

1 Adjustable End Plate
2 Pulse Input Connector
3 Support Bar
4 Support Bar
5 Insulator

Figure 13-2. Component support fixture.

or shunt resistances be used to fix the resistance at approximately 50 ohms. The applied pulse should be monitored to determine its true amplitude. The voltage probe should have minimum shunting effect.

The load resistance, R, and the capacitance of the energy storage capacitor, C, determine the pulse decay constant given by the RC product. This identifies another advantage for maintaining a constant load of 50 ohms. The pulse shape is independent of the resistance under test.

Some resistor applications involve a resistor shunting a transmission line in the middle of the line. Resistors to be used for these applications might be more realistically tested by replacing the component test fixture, Figure 13-2, with a "T" test fixture shown conceptually in Figure 13-3. For resistances much greater than 50 ohms, the voltage applied to the RUT may be measured at the line termination. Resistances less than 100 ohms cause a significant impedance mismatch at the "T" resulting in pulse reflections in the 50 ohm transmission line. For example, a 100 ohm resistor reflects 10 percent of the incident power. Therefore, this test fixture is not recommended for low value resistors.

13.3.3 Equipment

The equipments necessary to perform this test procedure are a high voltage supply to charge the storage capacitor, a low voltage supply to generate a trigger pulse, a high frequency oscilloscope to monitor the applied voltage and the resultant current, a high voltage probe, a current probe and the test fixtures discussed above. A circuit diagram showing the interconnection of these items is given in Figure 13-4. The requirements of each item are discussed in the following paragraphs.

The power supply should be capable of generating up to 40 kV at up to 5 mA. The current capability should be as high as possible to reduce the charging time for the storage capacitor. However, the spark gaps continue to operate (simmer) if the

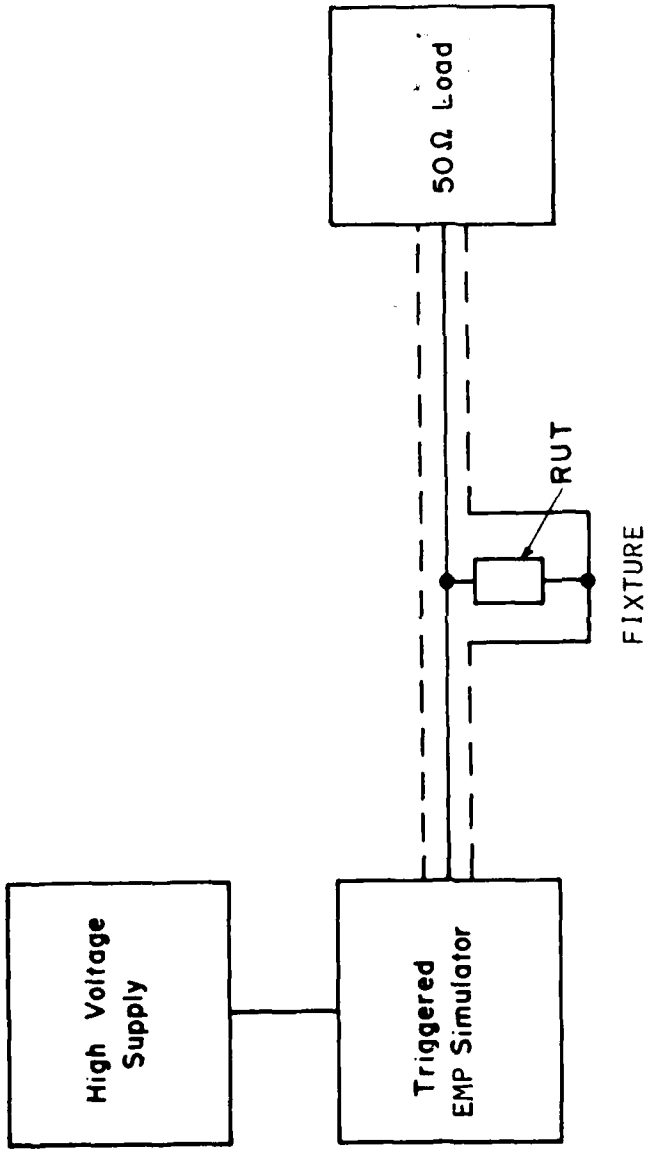

Figure 13-3. Pulse test setup.

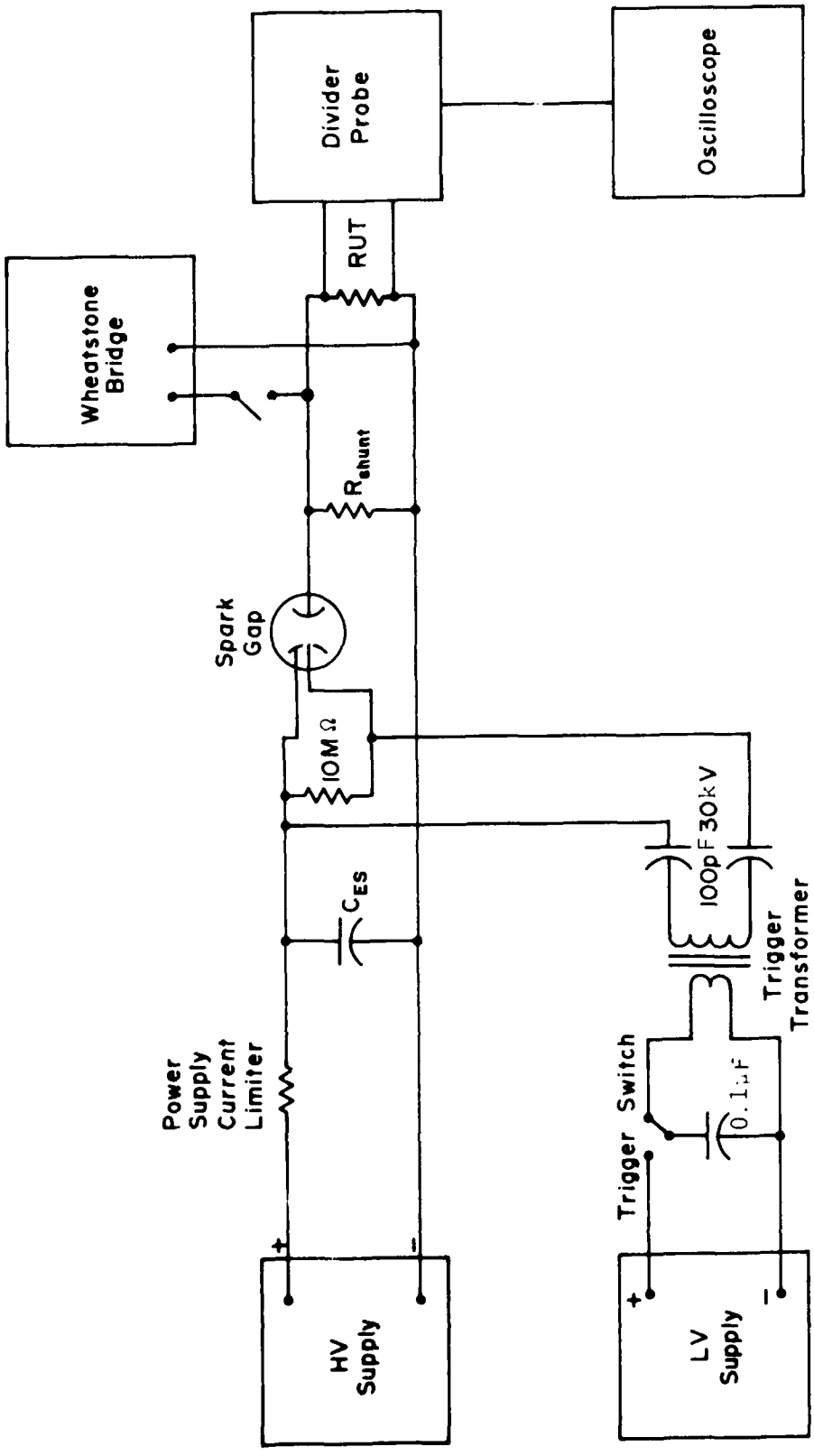

Figure 13-4. Experimental setup showing component interconnection.

supply can provide in excess of 5 mA. Regulation of $\pm$ 5 percent is sufficient for this application. Since the low current supplies are less expensive, they might seem attractive. However, if the supply provides a peak current of one milliampere at 40 kV, then a series current limiting resistor of 4×10^7 ohms is needed between the storage capacitor and the power supply. For a 10 μsec wide pulse working into a resistance of 50 ohms, the storage capacitor must be 0.1 μfd. The charging time constant is therefore 4 seconds, i.e., the time required for the capacitor to charge 63 percent of the supply voltage. The capacitor voltage will reach 95 percent of the supply after 3 time constants or 12 seconds. Therefore, a compromise must be made by the engineer designing the test fixture between the power supply cost, the time required to charge the storage capacitor, the desired pulse width, and the degree of cable impedance mismatch.

This power supply provides the voltage that charges the capacitor used in generating the trigger pulse which fires the spark gap. The voltage required is dependent upon the trigger transformer turns ratio and the trigger voltage needed to fire the spark gap. In general, this supply should be adjustable between 200 and 500 volts with an output current of 100 mA being adequate. There are no regulation requirements so an unregulated supply may be used.

An oscilloscope is required to monitor the voltage and current waveforms applied to the resistor during the time the tests are being initiated and each time the voltage level is changed when testing the resistors. Where peak power failure models are of concern, it might be useful to have a dual beam scope to look at both voltage and current simultaneously. The scope amplifiers must have a rise time of less than 5 nanoseconds and sweep rates of 50 nsec/cm or less to observe accurately the early part of the simulated EMP. Since peak voltages can reach 40 kV, a high voltage divider probe is needed to reduce the observed voltage to the scope input voltage. The current probe must be capable of measuring up to about 100 amps with rise times of 5 nanoseconds or less.

Any of the several types of resistance measuring instruments commercially available can be used to measure the resistance of the resistor under test. The instrument should have better than 1 percent resolution and repeatability, and at least 1 percent accuracy over the resistance range of interest.

There should be a single pole double throw (SPDT) switch rated at 40 kV between the instrument and the resistor under test to protect the instrument from the high voltages and prevent the instrument from loading the generator.

13.3.4 Precautions

The high voltages used in this procedure are very dangerous and great care should be exercised when working with this equipment. The fixture housing the storage capacitors and spark gap should be completely enclosed. Provisions should also be made to short circuit the energy storage capacitors to ground when resistors are removed from or installed in the component test fixture.

As illustrated earlier, inductances as small as 0.2 μH can degrade the pulse rise time. All leads including ground leads should have minimum length feasible and be as heavy as practical to minimize inductances.

The current measuring instruments should be capable of measuring currents to about 100 amps, although during breakdown around the resistor the peak currents can reach a few thousand amps. The probe must be capable of experiencing the fields associated with these currents without physical damage or calibration shifts.

Fields from currents of 10-100 amps can also affect the oscilloscope trace. Even shielded scopes are inadequately shielded for fields of this amplitude. These fields can cause strange effects in the display such as a right to left sweep observable during the rise time of the pulse. The scope, or conversely the equipment, must be placed in a screen room to adequately isolate the scope from the stray fields.

13.3.5 Measurement Procedure

The step stress method should be used to obtain the safe level for resistors. Steps less than 10 percent are not used because the resistor-to-resistor variation causes inaccuracies of about this magnitude. The stress step method is performed as follows:

1) With the resistor installed in the test fixture, apply five pulses at an arbitrary initial voltage level. Measure the resistance. If the resistor remains within tolerance, increase the voltage by 25 percent and pulse the same component again. Repeat this process until the measured resistance is outside its tolerance limits or the resistor fails catastrophically.

2) Reduce the applied voltage by 10 percent and test five new resistors at five pulses each. Measure their resistance. If the resistance of any resistor is outside its tolerance, repeat this step.

3) Test ten additional resistors at this level with 15 pulses. If any resistor fails, repeat Step 2, otherwise record this voltage as the safe voltage.

13.3.6 Data Format

Table 13-1 gives the recommended data format. All pertinent information is included in this table. Under the environment column, the conditions to which the resistor is subjected during the test should be indicated. Two types of environments that may be used are typical ambient and oil immersion. In the typical ambient case, no attempt is made to control the barometric pressure, the temperature, or the humidity. These factors can affect the voltage level at which external arcing around the component and case-damage occurs. For determining the intrinsic level of internal breakdown, the resistors can be immersed in oil to suppress the ambient effects. It should be recognized that many applications require the resistor to be potted in epoxy, RTV,

Table 13-1. Resistors tested on capacitor discharge EMP simulator.

Manufacturer	Type/ MIL.SPEC	Resistance	Wattage	Environment	Failure Mode	Maximum Safe Voltage	Pulse Width	Number of Pulse
Corning	C5/RL20S	51K	1/2W	Ambient	Internal Arc-Opened Resistor	3.5 kV	20 μsec.	15
Corning	C5/RL20S	10K	1/2W	Ambient	Internal Arc-Opened Resistor	4.0 kV	20 μsec.	15
Corning	C5/RL20S	1K	1/2W	Ambient	Internal Arc-Opened Resistor	2.7 kV	20 μsec.	15
Allen Bradley	EB/RC20	5.1K	1/2W	Oil Immersion	5% ΔR	18.0 kV	20 μsec.	15
Allen Bradley	EB/RC20	1K	1/2W	Oil Immersion	5% ΔR	14.0 kV	20 μsec.	15

or other similar materials and these tests should be conducted in this environment. In the failure mode column, the manner in which components failed at 10 percent above the safe voltage should be recorded. The criteria of resistor failure are determined by the type of application for which it is used. For example, in the case where an external arcing is observed, this may be a safe condition if the resistor is to be used as a shunt element to ground, but would be considered a failure when the resistor's function is to limit the current to more sensitive components. A resistor that fails because of an increase of the noise level, the voltage coefficient, etc., for one application may not be considered a failure for another application.

The Corning resistors indicated here are metal film resistors with 1 percent tolerance. The Allen-Bradley resistors are carbon composition resistors with 5 percent tolerance. Failure criteria for these resistors were resistance changes greater than 1 or 5 percent, respectively, after 15 pulses. In general, the metal film resistors failed by explosive disintegration of the film. From this limited data, the only trend that can be determined is an increase in safe voltage with increasing resistance.

Data on 1/2 watt metal film resistors' is presented in Table 13-2 to illustrate the range of safe voltages for this type of resistor. The differences in safe voltage values from those in Table 13-1 is attributable to the differences in their construction. The safe voltage was obtained by a similar step stress testing method; however, the resistor was subjected to 100 pulses or more. If the resistance did not change after exposure, the voltage was considered a safe voltage.

The effect of dc operation level on the resistor failure level was briefly evaluated. This effect was investigated using the test procedure outlined in Section 13.3, but the resistor was biased at 0 percent, 50 percent, and 100 percent of its rated dc power level from a high impedance current source. The results indicated that the bias effects were smaller than the experimental

Table 13-2. Metal film resistors tested by Sandia Laboratory on a rectangular pulse EMP simulator.

Manufacturer	Type	Nominal Resistance	Wattage	Maximum Safe Voltage	Pulse Width
IRC	MEC	100Ω	1/2W	400V	20 sec.
IRC	MEC	200Ω	1/2W	600V	20 sec.
IRC	MEC	300Ω	1/2W	600V	20 sec.
IRC	MEC	600Ω	1/2W	700V	20 sec.
IRC	MEC	1000Ω	1/2W	800V	20 sec.
IRC	MEC	1620Ω	1/2W	1500V	20 sec.
IRC	MEC	3160Ω	1/2W	1500V	20 sec.
IRC	MEC	5900Ω	1/2W	2000V	20 sec.
IRC	MEC	8600Ω	1/2W	2000V	20 sec.
IRC	MEC	50kΩ	1/2W	6kV	20 sec.
IRC	MEC	100kΩ	1/2W	7kV	20 sec.
IRC	MEC	464kΩ	1/2W	16kV	20 sec.
IRC	MEC	750kΩ	1/2W	16kV	20 sec.
IRC	MEC	909kΩ	1/2W	16kV	20 sec.

error resulting from resistor-to-resistor variations. Therefore, the test procedure was simplified by not including resistor biasing equipment.

13.4 References

1. Lennox, C. R., "Experimental Results of Testing Resistors Under Pulse Conditions", Protection Engineering and Management Note #6, Lawrence Livermore Laboratory, Albuquerque, N. M., Nov. 1967.

2. Robinson, D., "Pulse Handling Capabilities of Wire Wound Resistors", Dale Electronics, Inc., Columbus, Nebraska.

3. "Fixed Film Resistors - Precision and Semi-Precision", Electronic Industries Association (EIA) Standard RS-196-A, September, 1970.

4. "Fixed Composition Resistors", EIA Standard RS-172-A, June 1969.

5. "Fixed, Wire-Wound, Precision Resistors", EIA Standard RS-229-A, May 1965.

6. "Standard Test Methods for Electronic Component Parts", EIA Standard RS-186-D.

14. EMP PREFERRED TEST PROCEDURES FOR CAPACITORS

TABLE OF CONTENTS

14. EMP PREFERRED TEST PROCEDURES FOR CAPACITORS

14.1 Introduction

Three test procedures, presented herein, are developed as a guide to testing the capacitors used in low voltage electronic circuits. These procedures are intended for capacitors with dc voltage ratings from a few volts to a few hundred volts and capacitances up to 10 μF. The upper capacitance range is limited by the very low reactance of capacitors for fast pulses.

Capacitors are used to isolate ac from dc components, to differentiate between different frequencies, to bypass ac frequencies imposed on a dc voltage without affecting the dc, and to store electrical energy. Selection of a bypass capacitor with a self-resonance (series resonance) of 10 MHz might seem quite adequate for applications up to 2 or 3 MHz. However, when this unit is exposed to EMP, which has significant energy up to 100 MHz, the series inductance, internal to the capacitor, presents a high impedance to the high frequency components of EMP. Therefore, the high frequencies are not shunted through the capacitor and some other component must absorb this energy. Of course, internal breakdown could result in large leakage currents which could short circuit a power supply when the capacitor is used as a bypass element; or the increased leakage could change the operating point of a tube or transistor when used as a coupling element.

The testing procedure described in Section 14.5 of this report presents a method of obtaining the safe pulse operating level for capacitors. Sections 14.3 and 14.4 both present low level procedures for determining the self-resonant frequency of a capacitor. These procedures are presented as a guide for the engineer designing an EMP hardness test. Some applications for which these test procedures might prove useful are

1) identification, during the design phase, of capacitors that can be used in a system;

2) stock screening of selected capacitors to ensure that they meet quality control requirements;

3) improving the hardness of capacitors by design changes, such as substituting dielectric materials of high or dielectric strength;

4) development of a capacitor breakdown model;

5) testing a completed system for its EMP hardness.

14.2 General

14.2.1 Characteristics

A capacitor is basically composed of two plates separated by an insulator. Unfortunately, the plates are not ideal conductors and so they exhibit resistance and inductance. The insulator likewise is not ideal and it therefore has some resistance and a dielectric constant, both of which are functions of temperature and humidity. Dielectric breakdown occurs under excessive voltage conditions.

A brief discussion of some of the more important capacitor parameters is presented in the following paragraphs. The importance of these parameters relative to EMP hardness for a particular application is left to the judgement of the engineer. Test procedures for measuring some of these parameters as well as mechanical tests for capacitors and other passive components are described in EIA Standard RS-186-D.[2]

Capacitance

Capacitance is determined by the area of the plates, the separation between them, and the dielectric constant of the insulating material. The electrical unit of capacitance, C in farads, is defined in terms of the quantity of charge on the plates, Q in Coulombs, and a voltage differential, V in volts, across the plates. The mathematical relationship is

$$C = Q/V. \qquad (14\text{-}1)$$

The capacitance is usually measured by a bridge. The bridge operating frequency is normally identified in the EIA standard[3] relating to a specific capacitor type and ranges from 60 Hz to 1 MHz. A procedure is described in MIL-STD-202, Method 305,[4] also.

Temperature Coefficient

Ambient or core temperature affects the dielectric constant and, hence, causes changes in the capacitance. The coefficient is normally expressed as so many parts per million per

degree centigrade. The coefficient may be positive, negative or zero. The calculated temperature coefficient is often a function of the temperature differential and so it is normally quoted for a specific temperature range. Consequently, a capacitance change of 5 percent over a 50°C temperature differential (1000 ppm/°C) does not imply a 4 percent change over a 40°C differential. The two extreme temperatures at which the capacitance is measured in order to obtain the temperature coefficient is dependent upon the type of capacitor. Refer to the appropriate EIA standard for exact measurement information.

Dielectric Strength

The dielectric strength of the insulator between the plates is a measure of the insulator's ability to withstand a dc voltage and is usually expressed in volts per mil thickness. The dielectric strength of the insulator times its thickness determines the maximum voltage at which a capacitor can be operated. Practical, or commercial, capacitors normally cannot be operated at this level because of contamination during the fabrication process and pinholes or other anomolies in the dielectric material. The dielectric withstanding voltage is normally tested by applying 150 percent of the rated voltage to the capacitor for periods of less than five seconds. This measurement is normally performed at 25°C unless specified otherwise.

Electrolytic capacitors are normally tested by application of a surge voltage, about 130 percent of the rated voltage, for 30 seconds then discharged for 5.5 minutes. This process is normally repeated for 1000 cycles. This measurement is normally made at the capacitor's maximum rated temperature.

Power Factor (Dissipation Factor)

The power factor (P.F.) is a measure of all the energy loss in the capacitor due to dielectric absorption and ohmic losses in the leads and conducting plates. The dielectric losses appear as a resistive loss in parallel with the capacitance and ohmic losses appear as a series resistance loss. The power factor

times the volts-amperes in the circuit is proportional to the heat generated internally. For small power factors, less than 0.1 percent, the effective series resistance (R_s) which includes both types of loss into an effective loss and is in series with a capacitance (C_s), is

$$R_s = P.F./(\omega C_s) \tag{14-2}$$

or the effective parallel resistance (R_p), which also combines both types of loss into an effective one, and is in parallel with a capacitance (C_p), is

$$R_p = [\omega C(P.F.)]^{-1} \tag{14-3}$$

where ω is the angular frequency. The dissipation factor (D) is equal to the power factor, if P.F. <0.1, and is the reciprocal of the quality factor (Q)

$$D = P.F. = \frac{1}{Q} \tag{14.4}$$

Impedance as a Function of Frequency

An ideal capacitor has a reactance that is inversely proportional to frequency. This is generally true at low frequencies where the series resistance and lead inductances are negligible. An equivalent circuit for a capacitor, including the non-ideal parts, is shown in Figure 14-1. A wide band impedance measurement of a capacitor normally reveals a series resonance phenomena as low as a few kilohertz up to hundreds of megahertz depending upon capacitance, lead length and internal construction. This parasitic resonance is caused by the combination of the capacitance and the self-inductance of the conductive plates and the connection leads. The ac resistance of the leads and the plates is also found to change with frequency due to skin and proximity effects. The dielectric losses may increase or decrease with frequency, depending upon the dielectric material. In addition to the series resonance, additional parallel resonant frequencies are independent of the leads and are due to the capacitor acting like a cavity resonator or a longline resonator of fairly high Q.

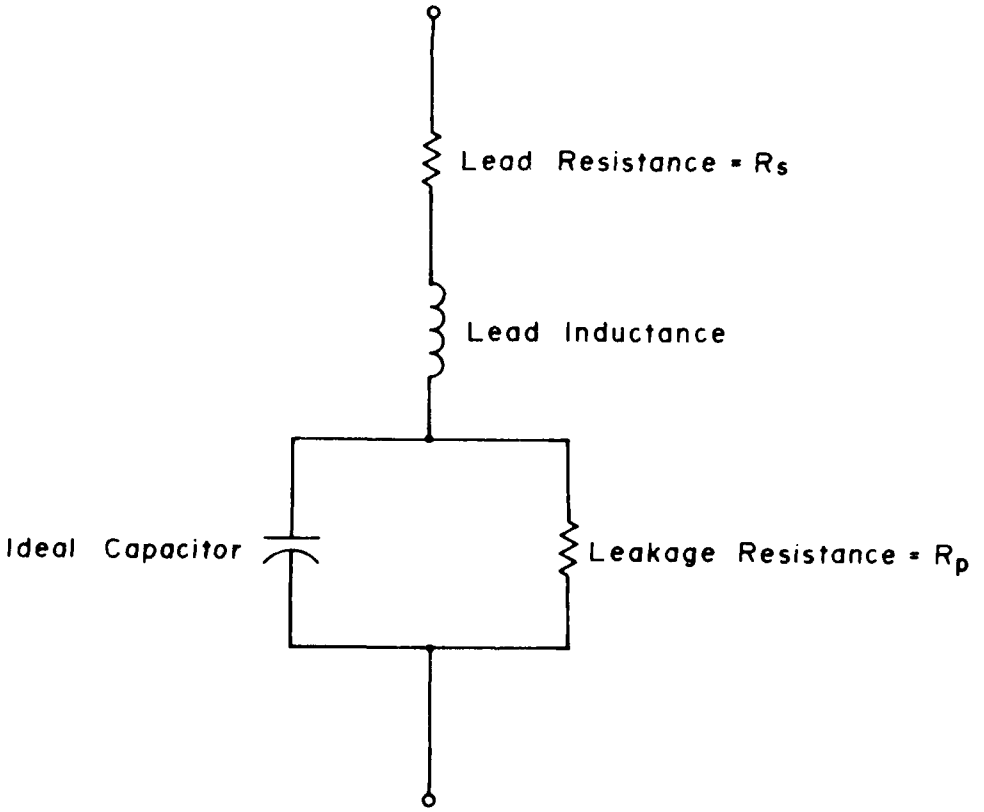

Figure 14-1. Capacitor model.

38

14.2.2 Definitions

Definitions of terms applicable to the capacitor testing procedure are presented below.

EMP Waveform

In the absence of more specific waveforms, a double exponential pulase can be used to simulate the EMP exposure. Rise time, measured from the 10 to 90 percent levels, should be less than 30 nanoseconds and the fall time should be 0.1 to 20 microseconds as determined by the engineer designing the test. Other waveforms pertinent to specific systems should be considered. Wide band pulse waveforms are used because the major portion of the spectral range of an EMP extends from 10 kHz to 100 MHz.

Safe Voltage

The safe voltage is the maximum peak pulse voltage level for a given pulse waveform which does not change the short term capacitor characteristics after a minimum number of pulses. It is anticipated that capacitor failures will occur during the first few pulses. It is suggested therefore, that five EMP pulses be applied to a component.

Failure Criteria

In the recommended test procedures for capacitors, there are two failure criteria. The first performance requirement is concerned with the impedance of the capacitor as a function of frequency and is dependent upon the use or application of the capacitor. For a capacitor used as a decoupling element, the impedance of the capacitor should remain low over the entire frequency range of EMP. This implies that any parallel resonance of the capacitor should occur at some frequency above the upper frequency limit of 100 MHz. For a capacitor used as a coupling element, it would seem advantageous in certain cases for the capacitor to have a high impedance so as not to couple much of the EMP into a circuit. This presents a conflict with the primary purpose of a coupling capacitor. This can be accomplished by choosing a

capacitor that resonates at two to three times the upper operating frequency of the system. Caution must be exercised if phase is important because the capacitor no longer looks like an ideal capacitor in this region since the phase shift approaches zero degrees at resonance.

In the high voltage test procedure, the failure criteria are a change in the parameters or evidence of internal breakdown. The parameter that has been found to change is the dissipation factor (D) due to a change in the leakage resistance. Internal breakdown can be observed in the voltage waveform during application of simulated EMP.

14.2.3 Test Philosophy

These tests are developed to provide an engineer with a procedure which can identify the optimum capacitor for his application. The test procedures are designed for maximum simplicity with minimum implementation expense but provides realistic operating conditions. More elaborate equipment could be considered if large numbers of capacitors are to be tested but the philosophy and equipment may be used as examples for automatic equipment design.

Some EMP capacitor testing has been reported in the literature. These tests have been performed with pulse widths in excess of 100 ns. These reports[1] indicate that tantalum electrolytic capacitors fail at three to six times their dc working voltage. The energy levels for these failures are as low as 60 μjoules, or in the same energy range as semiconductors. Ceramic capacitors, tested with microsecond wide pulses, fail at five to ten times their rated working voltage. The pulse width required for breakdown ranges between two and twenty microseconds.

In developing this procedure, the following factors should be investigated:

1) Effectiveness of the capacitor at EMP frequencies;
2) Failure mode of capacitors and optimum test for this mode;

3) Low impedance voltage EMP source;
4) High impedance current EMP source;
5) Effects of dc bias on voltage level.

A model for a capacitor, Figure 14-1, indicates an inductor in series with the idealized capacitor. The inductance is a lumped inductance which includes lead inductance and internal parasitic inductance due to the physical construction of the capacitor. The lead inductance can be the major contributor of this inductance for some capacitor designs. For instance, a 100 pF ceramic capacitor with 5" leads resonates at 40 MHz, well below the 100 MHz upper frequency in EMP. The same capacitor with 0.1 inch leads resonates at 180 MHz. The effective inductances for these two cases are 150 nH and 8 nH respectively. Therefore, the lead length should be kept to a minimum when capacitors are installed in a system and considered as an important parameter in testing procedures. The internal breakdown in capacitors subjected to simulated EMP appears to require a high voltage pulse lasting in excess of one microsecond. This implies that only the lower frequency components harm the capacitor. If a pulse source with sub-nanosecond rise times is used for testing, this might not be the case.

A common failure mode of capacitors is an internal insulation breakdown causing an increase in the dissipation factor. In general, the peak pulse voltages necessary for capacitor failure are well below the level which would cause arcing around the capacitor case. (An observed exception occurred with 100 pF disc ceramic capacitors tested while developing this test procedure. In that one case, external arcing was noted from one lead to the outside capacitor foil. This resulted in a small chip of the ceramic exterior being blown off.) One example of capacitor damage is demonstrated in Plate 14-I. During the development of this procedure, the dissipation factor, (D), value appeared to exhibit more variation than either the capacitance (C) or leakage resistance (R_p) value. In many instances, however, the value of R_p would change from 10^{10} to 10^6 or less. The failure mode

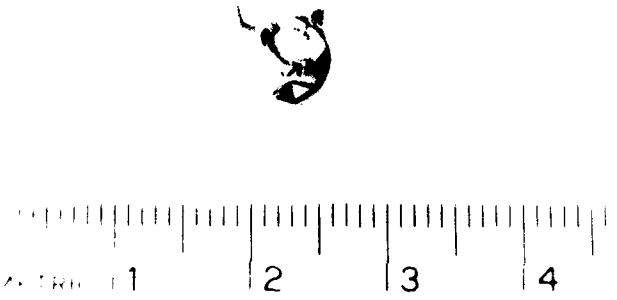

Plate 14-1. Example of capacitor damage.

identified as the easiest to detect is the value of D. A failure can be defined arbitrarily as an increase in the value of D to twice its initial value. Obviously, this is too severe a restriction for many applications but the rate at which capacitors fail is undefined to date. The engineer in charge of the test may find that the circuit is unaffected by a D as high as 0.1 and this may be acceptable for a failure criteria if some high percentage of capacitors dissipation factors do not change from 0.1 to 0.5 with only a few more volts or pulses. Further testing is needed to validate any specific criteria for failure.

The two types of EMP generators that can be considered for capacitor testing are voltage source and current source generators. The voltage source generator (Figure 14-2a) consists of a charged low inductance capacitor which is discharged through a low resistance switch into the capacitor under test (CUT). A resistor in parallel with the capacitor under test determines the discharge time. The applied waveshape has a very fast rise time and a moderate decay.

The current source generator (Figure 14-2b) is similar to the voltage source generator but a current limiting resistor, R_c, is in series with the capacitor. The applied waveshape is considerably different due to the reduced charging current; at the time, to the voltage, V, across a capacitor, C, is given by

$$V = \frac{1}{C} \int_{o}^{t_o} i\,dt \qquad (14\text{-}5)$$

where i is the current flowing into the capacitor as a function of time, t. For example, consider a 10 ampere rectangular current pulse applied to a 1 μF capacitor for 10 microseconds. The peak voltage is only 100 volts.

Obviously, some compromise must be made in determining the size of the current limiting resistor since the voltage supply requirements become proportional to the value of this resistance for a fixed current. When a capacitor discharge source, as

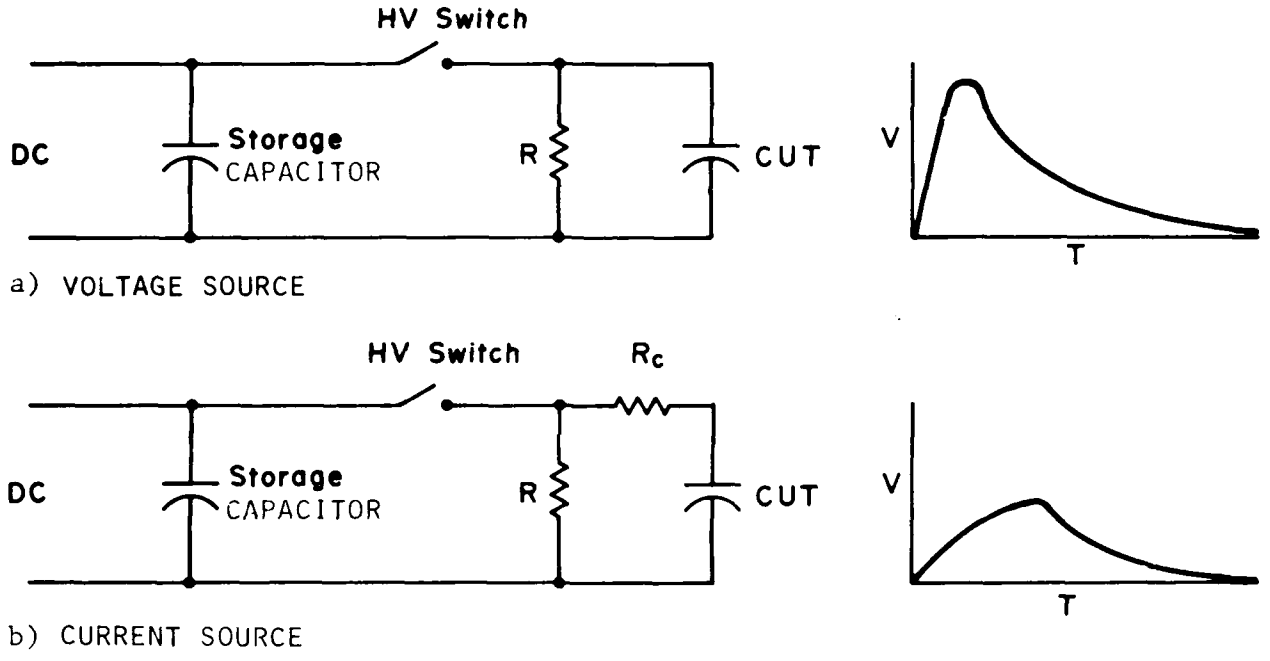

Figure 14-2. Comparison of EMP generators: circuits and waveshapes.

illustrated in Figure 14-2b, is used, a 1 KΩ current limiting resistance is about right for a .01 μF capacitor.

Current-source testing is selected over voltage-source testing because capacitor failure is detected more readily with the former mode of operation. The failure levels established by the two types of test sources are comparable within 10 percent, the experimental error. With voltage source testing, it is necessary to make a measurement of D and record any appreciable change. However, in the case of a current source, the waveshape of the capacitor voltage immediately indicates the presence of breakdown. Therefore, one step in the test procedure is eliminated and a definite proof of voltage breakdown is observed.

A strange phenomena may be observed when testing of paper capacitors with a current-source. If the capacitor is measured on a bridge before and after breakdown, there are no changes of either the capacitance or the dissipation factor. If the same capacitor is tested again, a higher voltage is needed to reach insulation breakdown. As an example, three oscilloscope traces are presented in Figure 14-3 illustrating this phenomena. Note that the capacitor apparently heals itself and improves it characteristics. However, if the initial breakdown had occurred with a voltage source, the D factor would have changed. Therefore, any indication of breakdown with the current source generator indicates an unsafe level to operate the capacitor in an EMP environment.

If the effect of dc bias on the safe level for EMP is to be considered during capacitor testing, then the circuit of Figure 14-4 can be used to bias the capacitor to its maximum rated voltage. This circuit deviates from the normal current-source generator by the addition of negative dc bias voltage to the capacitor through a 100 KΩ resistor and diode. This circuit presents no load to the EMP pulse but provides the desired bias voltage when the EMP is not present. It is nearly identical to the unbiased current-source generator of Figure 14-2b, during the current application of pulses.

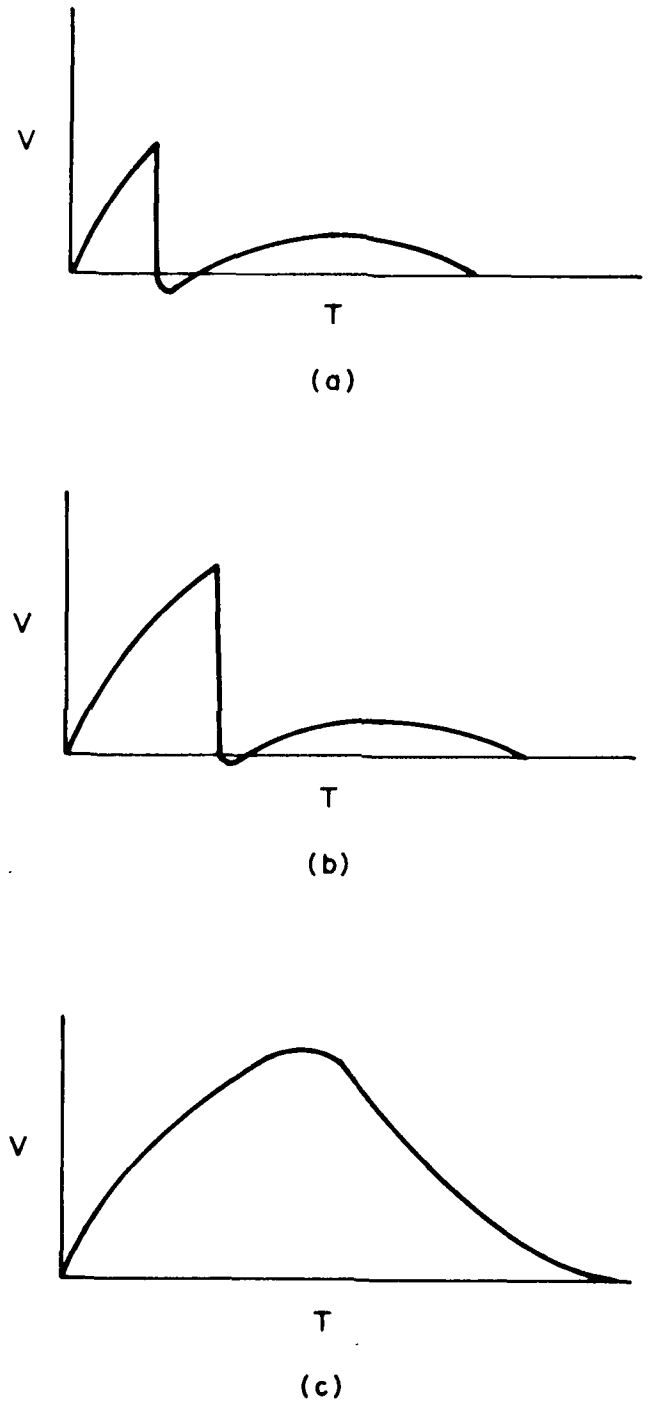

Figure 14-3. Capacitor waveforms for three cases.

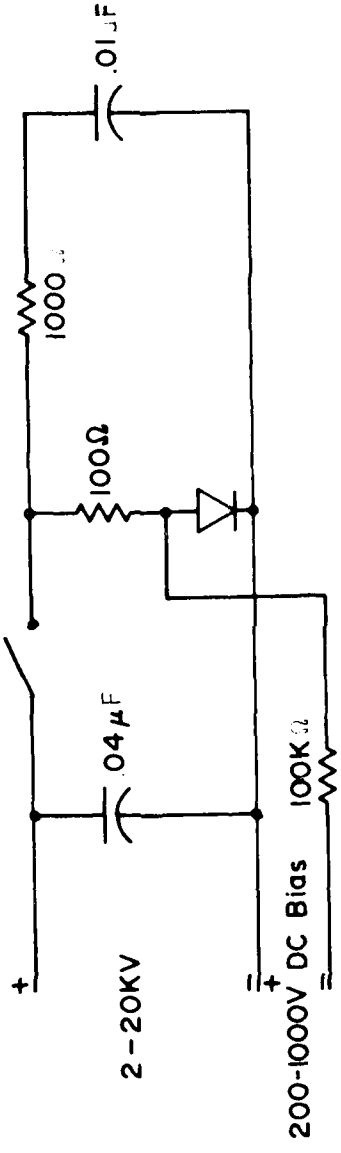

Figure 14-4. Test circuit for measuring safe voltage with a D.C. bias.

14.3 Wide Band Impedance Test Procedure

14.3.1 Scope

This test procedure is developed to guide the engineer in selection of capacitors for use in equipment subjected to high frequency signals. The equipment configuration may be used for all capacitors and voltage ratings. The frequency range covered is 100 kHz to 100 MHz.

14.3.2 Equipment

Several pieces of commercial equipment are required for this test procedure as illustrated in Figure 14-5. The operation is as follows. A swept frequency oscillator (e.g., Hewlett-Packard 8601A) output is connected to the capacitor under test. As the oscillator is electrically swept over the spectral range of interest, the voltage and the current of CUT are monitored by the network analyzer (e.g., Hewlett-Packard 8407A). A swept RF reference, RFR is used by the network analyzer to hetrodyne the current and voltage to a fixed intermediate frequency at which gain is controlled and effective division of V/I and the phase relationships are performed. The complex impedance and/or the phase relationships can be displayed on a dual trace scope. The horizontal drive for the scope is obtained by scaling the electrical sweep drive voltage used in the sweep oscillator. A less automated measurement can be performed using a RF vector impedance meter, such as the Hewlett-Packard 4815A.

14.3.3 Precautions

This procedure can be influenced by parasitic elements in the capacitor mounting fixture and interconnecting leads. Extreme care must be taken to eliminate all parasitic elements. Cables must be terminated in their characteristic impedance to prevent cable reflections from influencing the results.

14.3.4 Procedural Steps

Once the equipment is connected as illustrated in Figure 14-5, the controls must be adjusted to obtain the desired display

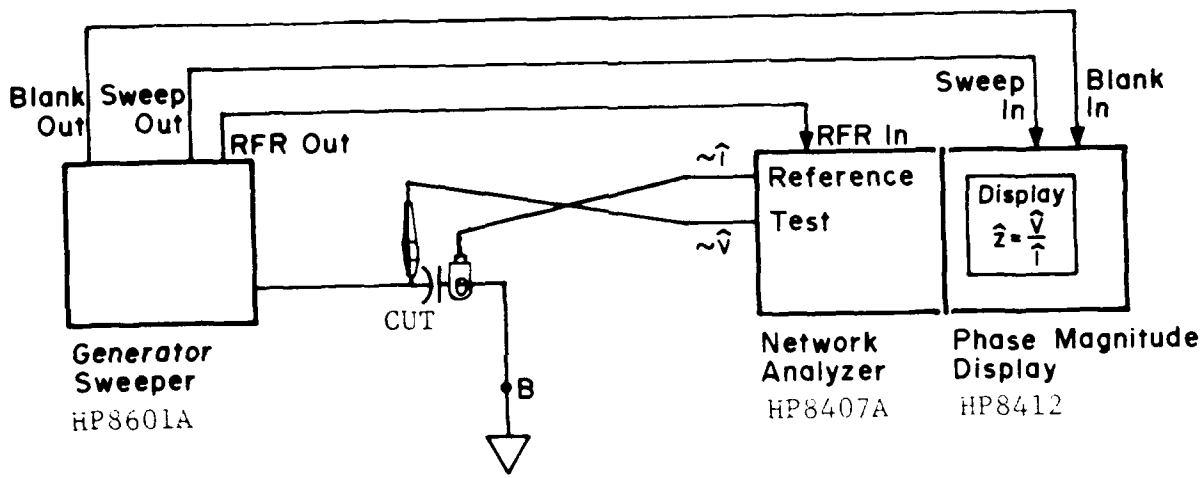

Figure 14-5. Swept impedance measurement setup.

reference levels and scale factors. A calibration is performed by substituting a 50 ohm resistor in place of the CUT and adjusting the system to obtain the desired phase and impedance references. Since many resistors are either slightly inductive or capacitive at high frequencies, these adjustments should be performed at about 1 MHz where the reactances are low. Replace the resistor with the CUT to obtain the spectral response.

14.3.5 Sample Data

Data for a 100 pF disc ceramic capacitor obtained using the described test equipment is presented in Figure 14-6. From both the phase curve and the impedance, the resonant frequency of this capacitor is 58 MHz. Its leads are about 1/4 inch long. Since lead inductance is very important, the lead length should always be given and held fixed for comparative measurements. Data is also shown in Figure 14-7 for a 0.01 μF paper capacitor. The resonance is easily located on the phase trace at about 17 MHz. Lead lengths were about 3/8 inch in this case.

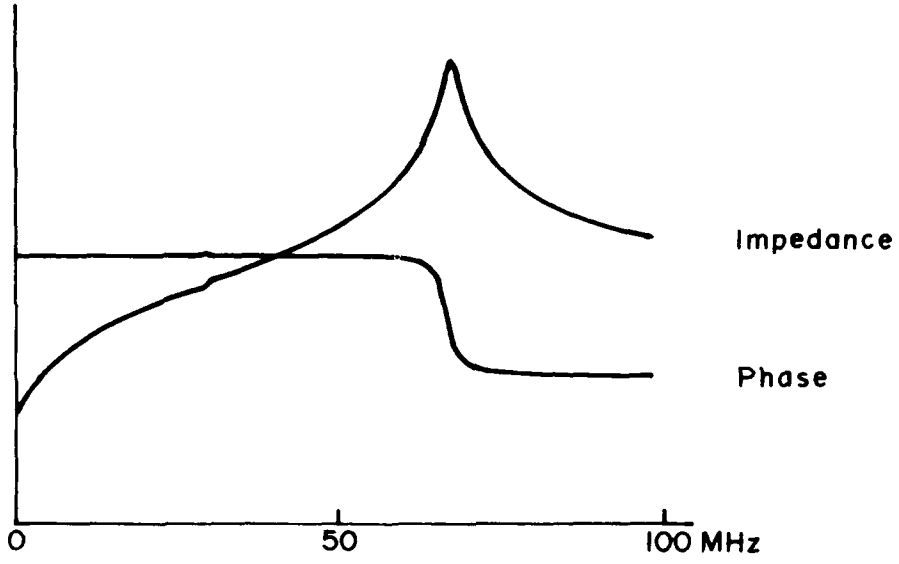

Figure 14-6. Spectral response of 100 pF disc ceramic capacitor.

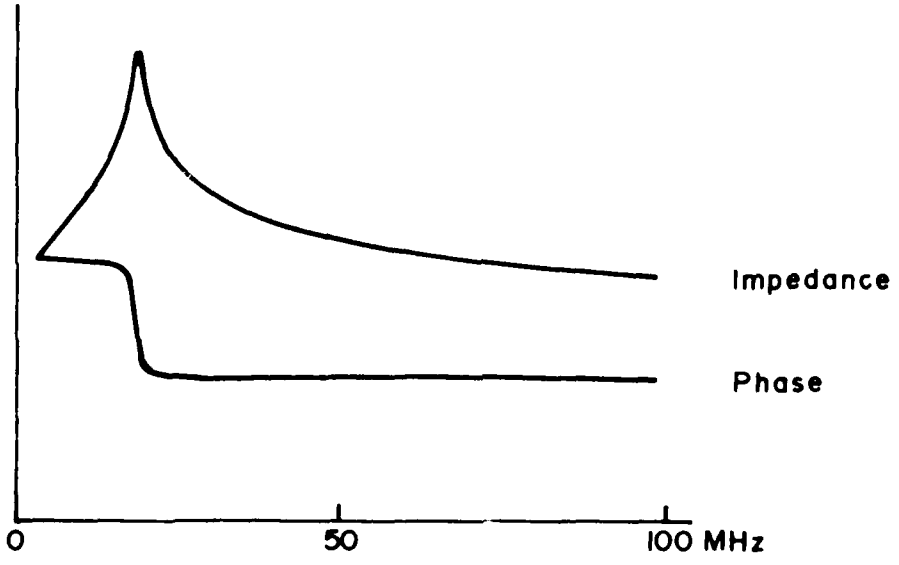

Figure 14-7. Spectral response of .01μF paper capacitor.

14.4 Pulse Test

This test procedure is an alternative to the wide band test described above.

14.4.1 Scope

The objective of this test is to determine the response of a capacitor to the application of a low level fast pulse. By observing the voltage/time response of a capacitor at the leading edge of the pulse, the reactance as a function of frequency, and any nonlinear charging function occurring in some capacitors, can be determined.

The impedance as a function of frequency can be obtained by taking the Fourier transform of the capacitor voltage and of the applied pulse. This transform provides an amplitude vs. frequency for both the input pulse, A_i, and the resultant pulse, A_r. The complex impedance, Z, of the capacitor under test at each frequency can be found by solution of the equation

$$\frac{A_i(j\cdot)}{A_r(j\cdot)} = \frac{50 + Z}{Z} \qquad (14\text{-}6)$$

The advantage of this test over the wide band test is that a network analyzer is not needed. However, in order to rapidly perform the Fourier analysis, the investigator should have access to a computer or programmable calculator.

14.4.2 Equipment

The equipment needed to perform this test is shown in block form in Figure 14-8. The pulse generator must have a fast rise time capability (less than 5 nanoseconds), and should provide at least 10 volts into 50 ohms. Pulse width is not an important parameter in this test procedure. A generator with a trigger pulse output would enhance scope synchronization. The oscilloscope must be capable of measuring pulse rise times faster than the generator pulse and should have a sensitivity of at least 50 millivolts. With this sensitivity the oscilloscope can measure

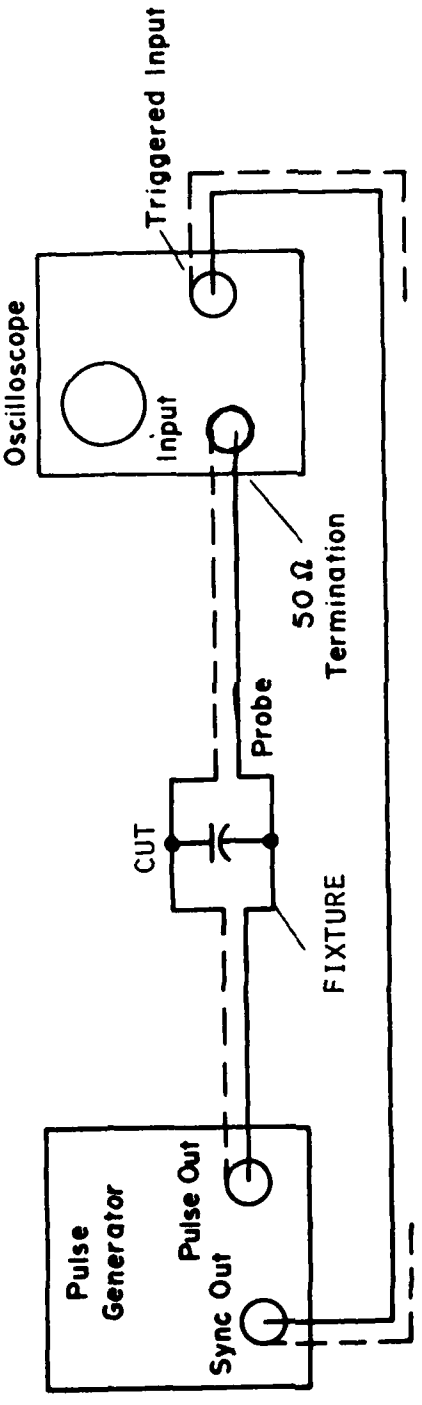

Figure 14-8. Pulse testing of capacitor.

the voltage across a 0.25 ohm impedance down, or the purely capacitive reactance of a 1 μF capacitor at 100 MHz. Higher sensitivities permit measurement of lower impedances, i.e., larger capacitances, but larger capacitances tend to exhibit some inductance resulting in higher impedances at higher frequencies than are normally expected. If the experimenter wants a permanent record of voltage/time response of the capacitor, a photograph can be taken of the trace. The pulse repetition rate should be set to produce scope traces sufficiently bright to be observed or photographed easily.

14.4.3 Measurement Procedure

Connect the equipment as shown in Figure 14-8, keeping the cable between the generator and the capacitor as short as possible. Connect the scope probe as close as possible to the case of the capacitor, investigating the capacitor parameters only. Since most applications of the capacitor require some additional lead length, the probe should be connected at the same distance even though this adds inductance to the circuit. A typical distance is about ½ inch. Observe and/or record the trace obtained for each capacitor type to be investigated.

14.4.4 Data Format

The following data should be recorded:

1) The voltage across the capacitor as a function of time;
2) A description of the test item, including its type, capacitance and working voltage;
3) The amplitude and duration of the applied voltage pulse.

Figure 14-9 illustrates the types of waveforms observed. Sweep speed for these curves are 50 nsec/cm and vertical sensitivity is 5 volts/cm. A 100 volt peak was applied. The pulse response of a 0.01 μF disc ceramic capacitor is presented in Figure 14-9c. No deviation from the behavior of an ideal capacitor is observed. The result for a tabular paper capacitor with short

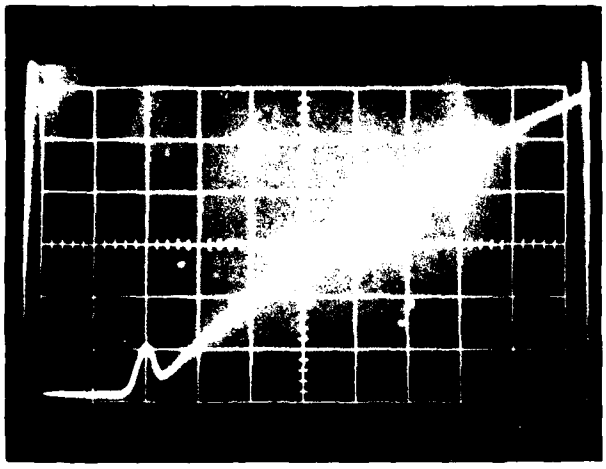

(a) 1.5" lead length
.01 μF paper capacitor
200 W.V
50n sec./div.

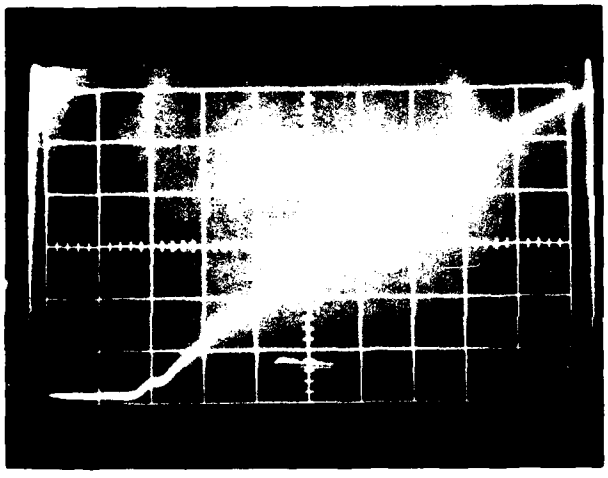

(b) Small lead length
.01 μF paper capacitor
200 W.V
50n sec./div.

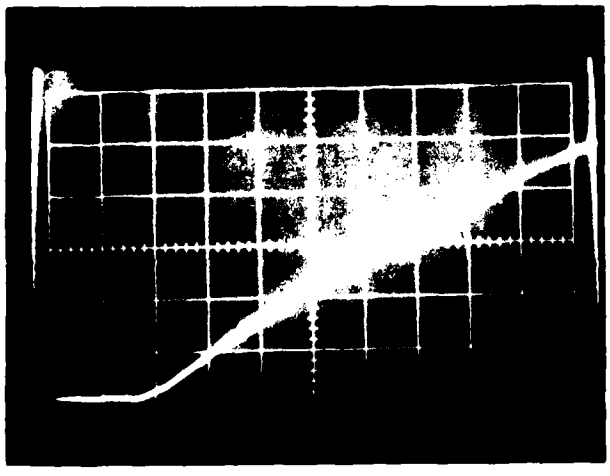

(c) Small lead length
.01 μF Disc Capacitor
1 kV W.V
50 n sec./div.

Figure 14-9. Typical pulse test waveforms (a) high series inductance (b) & (c) low series inductance.

leads is presented in Figure 14-9b. The same capacitor with 1-1/2 inch leads has, in Figure 14-9a, significant deviations due to lead inductance.

14.5 Stand Off Voltage Test Procedure

14.5.1 Scope

This test procedure is presented to guide the engineer in developing a procedure for determining the maximum EMP voltage capacitor can withstand. Various values of capacitors, up to a few microfarads, may be tested with this procedure. The maximum capacitance that can be tested is limited by the ability of the source to develop a significant voltage across a large capacitance in a short time. For instance, 100 amperes for 10 microseconds is required to charge a 10 μF capacitor to 100 volts.

A capacitor with a large series inductance, 10 to 100 nH, may not charge at all, since the inductance in series with the capacitive element, allows only a little charging current to flow. However, the voltage across the physical capacitor is large. Therefore, the internal structure of the capacitor can be subjected to a large voltage gradient. Depending upon the construction, this gradient may be sufficient to cause internal arcing which could severely stress the capacitor during the leading edge of a fast rise time pulse.

14.5.2 Equipment

Figure 14-10 is a block diagram of the equipment required for the test; the interconnections are shown. The high voltage power supply should be capable of providing 0-30 kV at an average current of 100 microamperes. Regulation of 5 percent is adequate. Power supply current limiting is provided by the fifteen series connected resistors (1 watt) of ten megohms each. The energy storage capacitor, C_{ES}, of 0.001 to 0.05 μF, should be selected for its low internal resistance and low inductance. The triggered spark gap should be selected for the voltage ranges expected. They should have at least a 1000 amp rating so that they can be expected to last for many pulses. The trigger transformer should be selected for the largest spark gap selected so that with lower primary voltages it can also be used for the smaller gaps. The low voltage power supply should be adjustable from 200 to 500 volts with

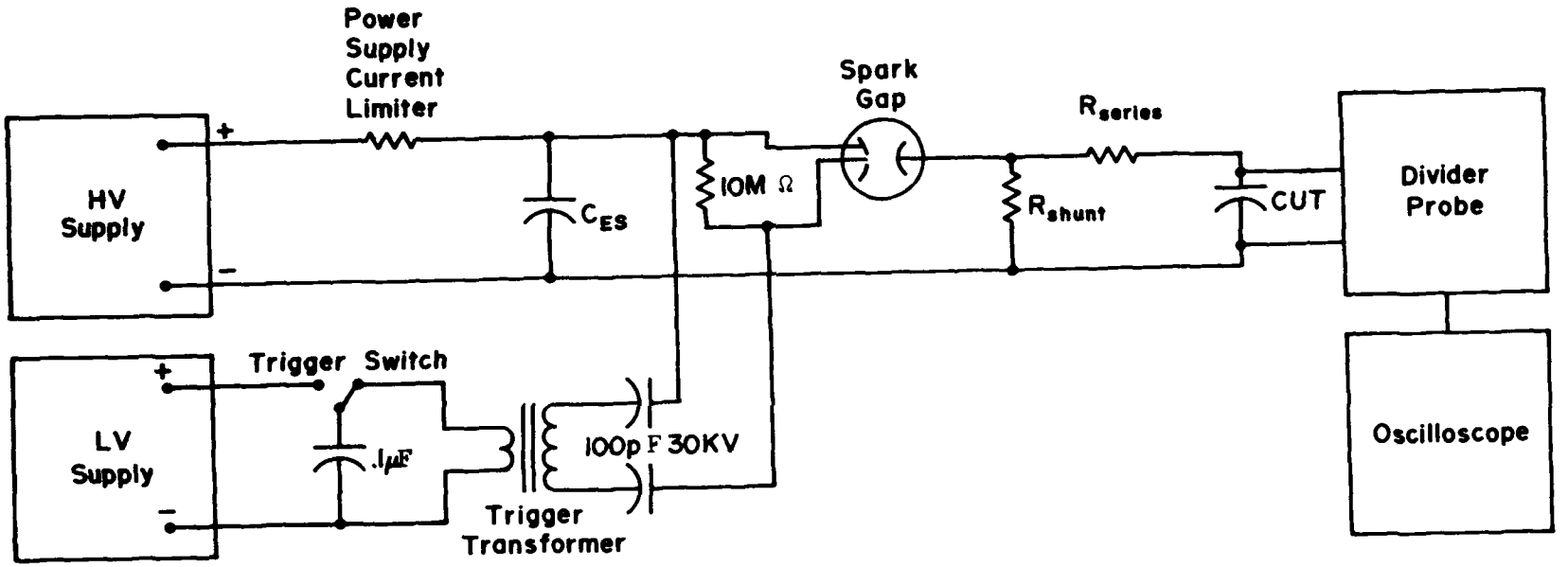

Figure 14-10. Circuit block diagram for high voltage testing.

a few hundred milliamperes average current rating. Regulation is not important for this supply. The shunt resistor, used to adjust the pulse width, should consist of four to eight equal size 1 watt resistors in series. (The pulse width in seconds is defined as the product of the energy storage capacitance in farads and the shunt resistance in ohms.) Each resistor should be stressed to less than 3 kV peak pulse voltage.

The series resistance should also consist of several resistors in series each stressed to no more than 3 kV each. The product of the capacitance under test (CUT) and the series resistance should be equal to or greater than the product of the energy storage capacitance and the shunt resistance. However, the series resistance should not be less than 100 ohms. The oscilloscope probe should be able to withstand up to ten times the capacitor rated working voltage. The scope should have a 100 MHz minimum bandwidth.

14.5.3 Test Fixture

Two special test fixtures should be built for this test procedure. One fixture, Figure 14-11, contains the current-source generator. This fixture operates in the following manner. A high dc voltage is applied through the connector (1), for charging the energy storage capacitors (2). The voltage potential on the capacitors at the time the spark gap is triggered is approximately the peak simulated EMP voltage. When a low voltage (200-500 V) pulse is applied to the trigger transformer (3) through connector (4), a positive high voltage pulse (8-20 kV) is applied to the spark gap (5) triggered through dc blocking capacitors (6). This trigger pulse initiates the discharge of the storage capacitors through the gap to the output connector (7).

The second test fixture, Figure 14-12, is a low inductance fixture for holding the unit under test. This fixture is designed with the requirement of being adaptable to different components. Therefore, the end plate (1) is adjustable. The pulse is applied through connector (2) to the component mounted between bars (3)

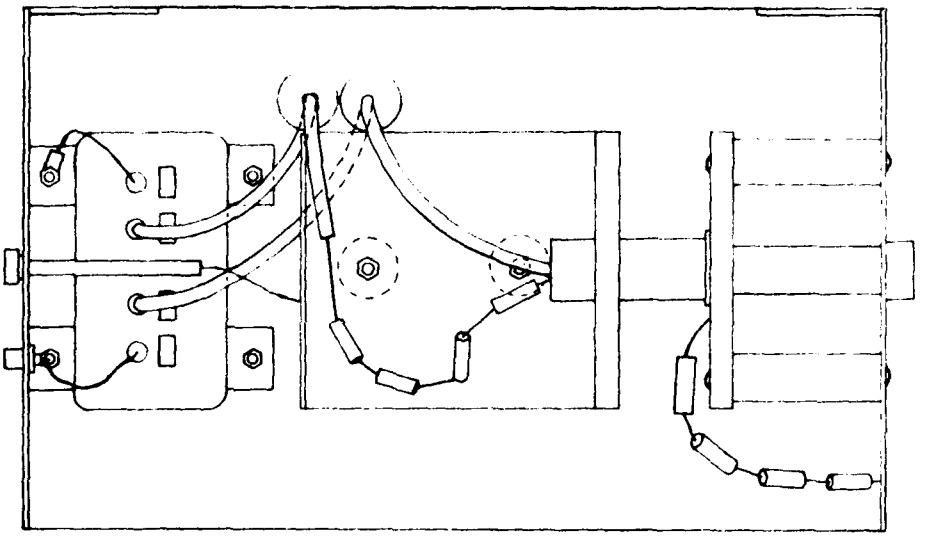

1	DC Input Connector	5	Spark Gap
2	Energy Storage Cap.	6	100pF 30kV Cap.
3	Trigger Trans.	7	Output Connector
4	Trigger Input	8	Shunting Resistor

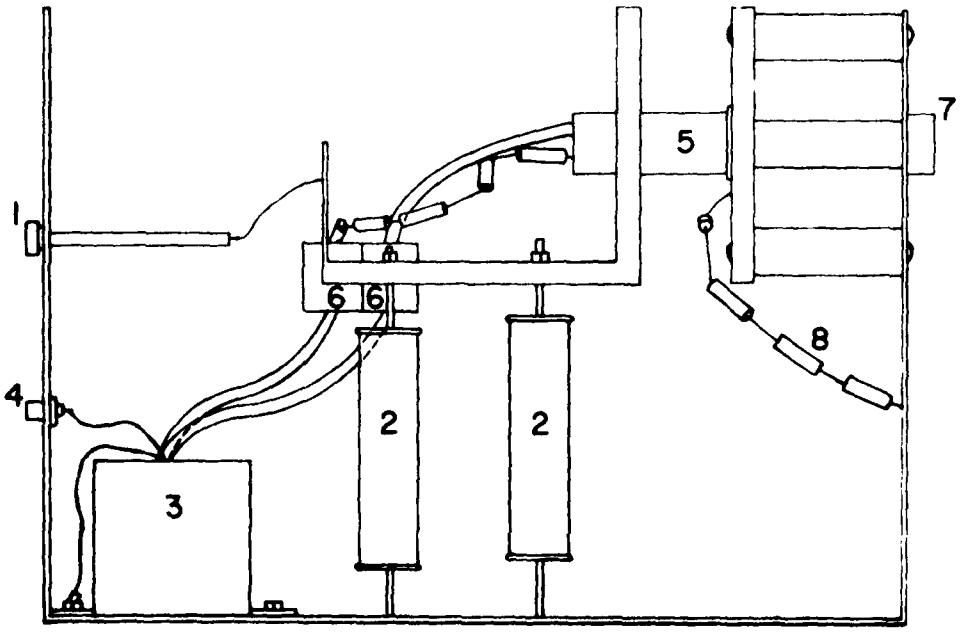

Figure 14-11. Illustration of high voltage switch.

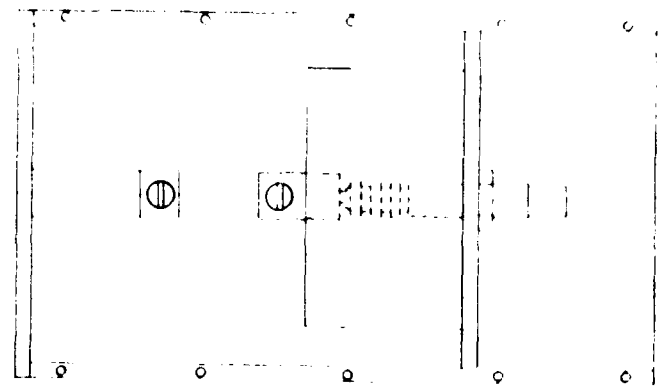

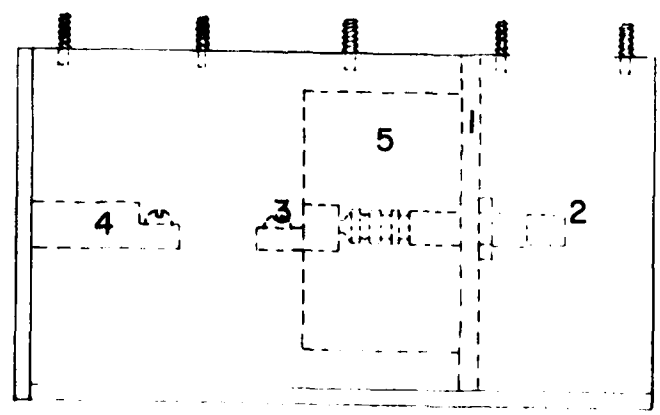

Figure 14-12. Component support fixture.

and (4). An insulator (5) provides mechanical strength necessary for mounting and removing the capacitor.

14.5.4 Precautions

The high voltages used in this procedure are lethal and great care should be exercised when working with the equipment. The fixture housing the storage capacitors and spark gap should be completely enclosed. Provisions should also be made to short circuit the energy storage capacitors to ground when the capacitors are being changed in the component test fixture.

Since currents for large capacitors can exceed 100 amperes, small resistances and parasitic inductors in the ground circuit can degrade the pulse input and the oscilloscope measuring quality.

14.5.5 Measurement Procedure

The step stress method should be used to obtain the safe voltage level for capacitors. Steps less than 10 percent are not used because the unit-to-unit variations cause inaccuracies greater than this magnitude. The stress step method is performed as follows:

1) With the capacitor installed in the test fixture, apply five pulses at an arbitrary initial voltage level. Observe the voltage waveform on an oscilloscope. If all the waveforms are similar to Figure 14-13d, increase the voltage by 25 percent and repeat this step. If any of the five oscilloscope waveforms are similar to Figure 14-13a, b, or c, internal breakdown has occurred due to excessive voltage.

2) Reduce the applied voltage by 10 percent and test a new capacitor with five pulses. If there is any evidence of breakdown for any of these pulses, repeat this step.

3) Test ten additional capacitors at this level with five pulses each. If any pulse indicates breakdown, repeat

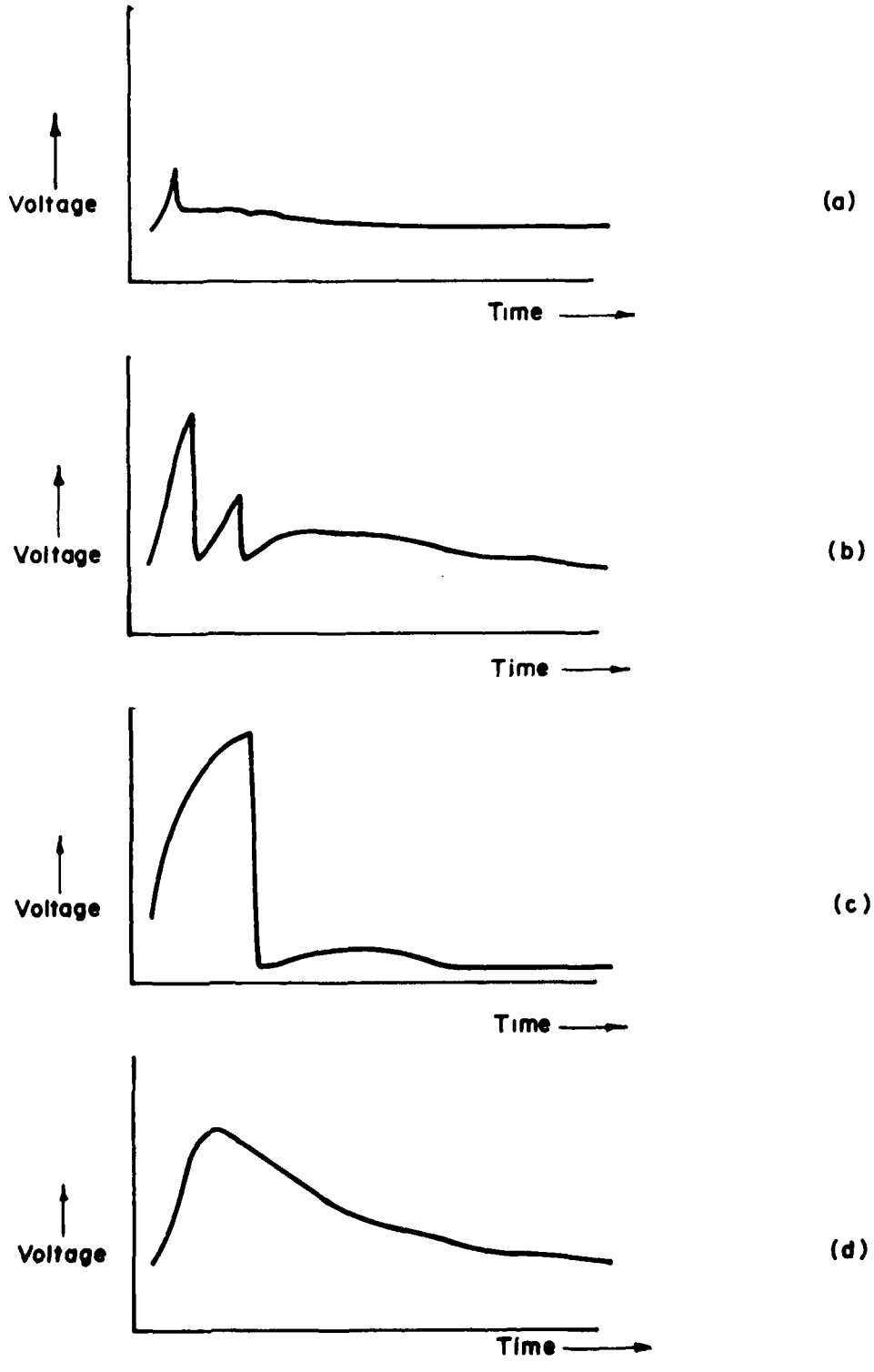

Figure 14-13. Typical pulse waveshape with EMP current simulator for most types of capacitors.

step 2, otherwise record this voltage as the safe pulse voltage.

14.5.6 Sample Data and Data Format

Pictures of oscilloscope traces obtained during testing of a 0.01 μF, 1 kV ceramic capacitor are presented in Figure 14-13. Trace (a) shows breakdown early in the pulse with little rise in voltage. In trace (b) the voltage rises to a level which causes breakdown which is not sustained. The capacitor begins charging again until a second breakdown occurs at a lower voltage. This condition does not always exist. Normally breakdown is sustained to produce a trace as presented in Figure 14-13c. A typical trace with no breakdown is shown in Figure 14-13d.

Typical curves are shown in Figure 14-14 for some 5.6 μF, 6 volt tantalum capacitors. With these larger capacitors the series resistance is reduced to 100 Ω so that more current flows into the capacitor under test during the period of the pulse. The results are somewhat different from those previously described. Figure 14-14c illustrates the decay voltage from a normal low voltage pulse. Figure 14-14a and b deviate from this curve in the early decay time. This rapid decay indicates a lower resistance discharge path which must be due to internal breakdown. If the breakdown causes a leakage resistance of approximately one hundred ohms, then the leakage resistance is comparable to the source resistance and there is a smaller voltage reduction during breakdown than that observed in Figure 14-13. Therefore, when using a low series resistance, the discharge slope needs to be monitored to detect the breakdown phenomena. These tantalum capacitors also appear to exhibit a self-healing quality because there are no measurable parameter changes after breakdown has occurred.

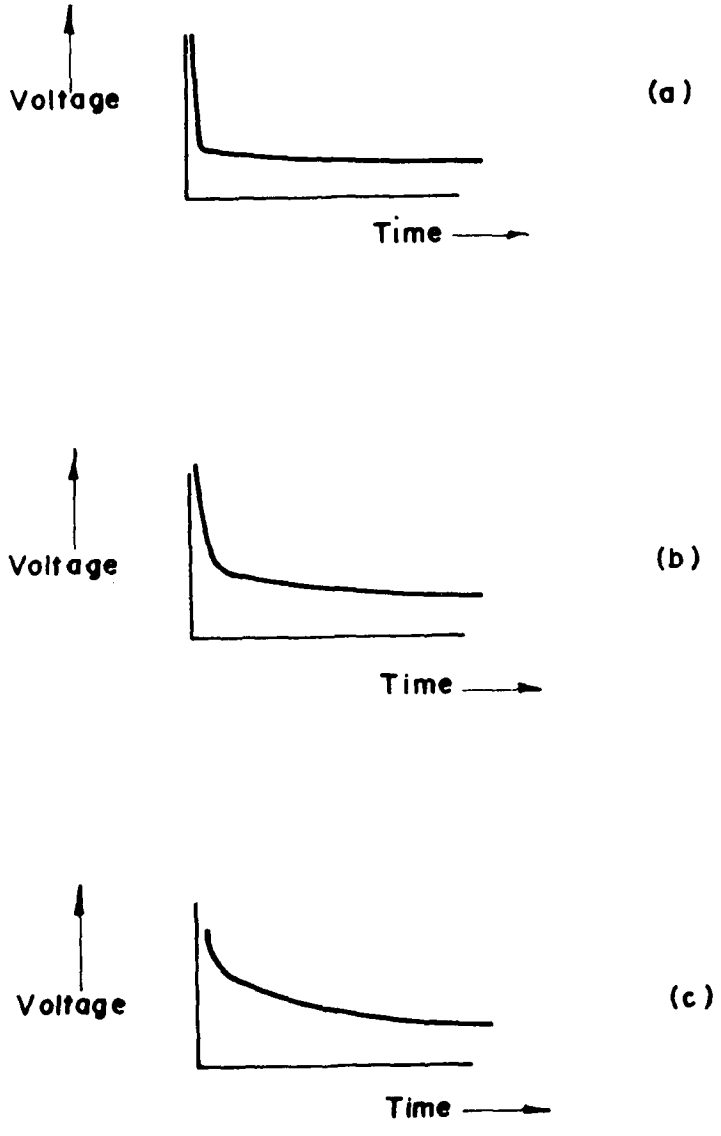

Figure 14-14. Tantalum discharge curves with breakdown (a) and (b) and without breakdown (c).

14.6 References

1. Case, Miletta, "Capacitor Failure Due to High Level Electrical Transients", Internal Memo, Harry Diamond Laboratories.

2. "Standard Test Methods for Electronic Component Parts", Electronic Industries Association (EIA) Standard RS-186-D.

3. For a list of EIA Standards for Capacitors, see the alphabetical index in "Index of EIA and JEDEC Standards and Engineering Publications".

4. "Test Methods for Electronic and Electrical Component Parts", MIL-STD-202E, 16 April 1973.

APPENDIX A

GENERAL COUPLING VIA SURFACE TRANSFER IMPEDANCE AND SURFACE TRANSFER ADMITTANCE

42

The cable being tested is represented in Figure A-1 by a transmission line with characteristic impedance Z_o and propagation constant Γ. The test fixture is also represented by a transmission line with constants Z_o' and Γ'. The two lines have the same length ℓ. The test fixture is excited by a source with amplitude of V_S and a time dependent factor of $\exp(j\omega t)$. The penetration of the cable shield is represented by an induced, series electromotive force per unit length, $E_S(\xi)$, and an induced, shunt current source per unit length, $K_S(\xi)$.

Let $V_e(x,\xi)$ and $I_e(x,\xi)$ be the voltage and current produced at $x = x$ when a unit electromotive force is impressed at $x = \xi$ in series with the line, and let $V_i(x,\xi)$ and $I_i(x,\xi)$ be the voltage and current produced at $x = x$ when a unit current per unit length is impressed at $x = \xi$. Then by superposition

$$V(x) = \int_o^\ell V_e(x,\xi)\, E_S(\xi)\, d\xi + \int_o^\ell V_i(x,\xi)\, K_S(\xi)\, d\xi, \qquad (1)$$

$$I(x) = \int_o^\ell I_e(x,\xi)\, E_S(\xi)\, d\xi + \int_o^\ell I_i(x,\xi)\, K_S(\xi)\, d\xi \qquad (2)$$

Consider the general case of Figure A-2. $V_S(\xi)$ and $I_S(\xi)$ are the series point voltage and shunt point current sources impressed at $x = \xi$, which produce a voltage $V(x,\xi)$ and a current $I(x,\xi)$ at $x = x$. From Schelkunoff we have

$$V_e(x,\xi) = -\frac{1}{d}(\sinh \Gamma x + z_1 \cosh \Gamma x)[\cosh \Gamma(\ell-\xi) + z_2 \sinh \Gamma(\ell-\xi)], \quad x<\xi; \qquad (3)$$

$$= \frac{1}{d}(\cosh \Gamma\xi + z_1 \sinh \Gamma\xi)[\sinh \Gamma(\ell-x) + z_2 \cosh \Gamma(\ell-x)], \quad x>\xi;$$

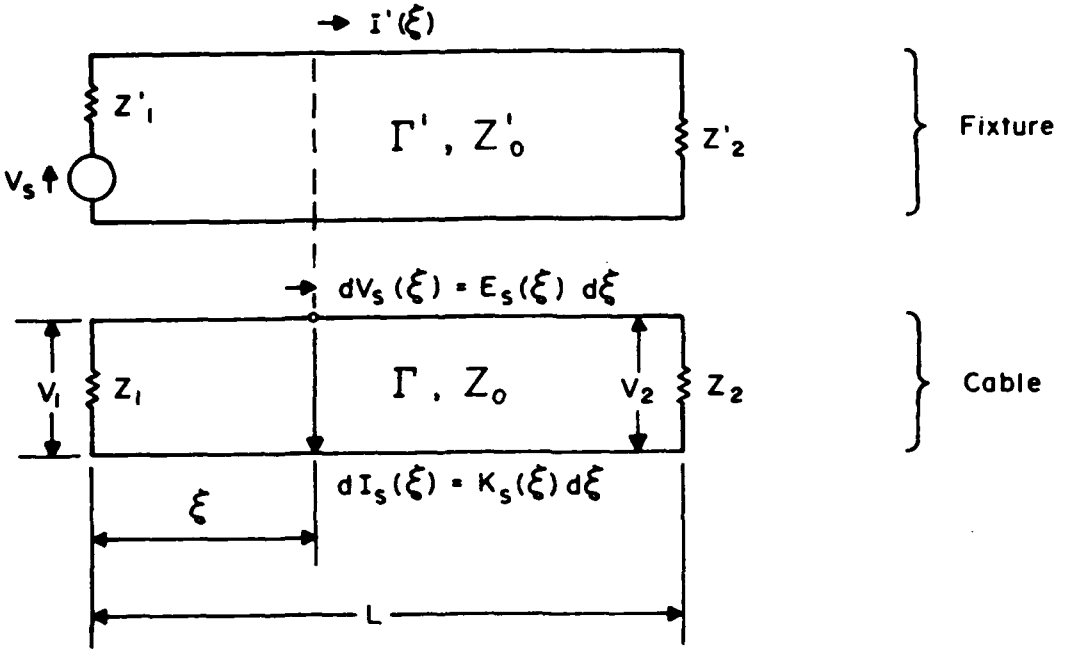

Figure A-1. Transmission line for cable and fixture.

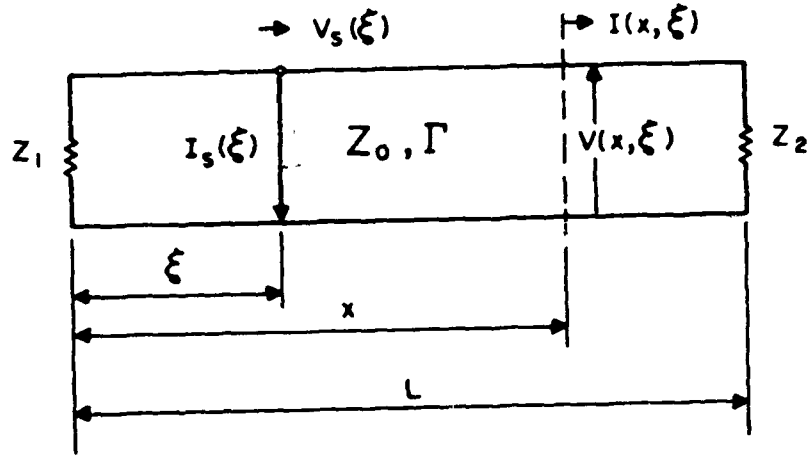

Figure A-2. Voltage and currents on transmission line.

$$I_e(x,\xi) = \frac{1}{Z_o d}(\cosh \Gamma x + z_1 \sinh \Gamma x)[\cosh \Gamma(\ell-\xi) + z_2 \sinh \Gamma(\ell-\xi)],$$
$$x<\xi, \qquad (4)$$
$$= \frac{1}{Z_o d}(\cosh \Gamma\xi + z_1 \sinh \Gamma\xi)[\cosh \Gamma(\ell-x) + z_2 \sinh \Gamma(\ell-x)],$$
$$x>\xi;$$

$$V_i(x,\xi) = -\frac{Z_o}{d}(\sinh \Gamma x + z_1 \cosh \Gamma x)[\sinh \Gamma(\ell-\xi) + z_2 \cosh \Gamma(\ell-\xi)],$$
$$x<\xi, \qquad (5)$$
$$= -\frac{Z_o}{d}(\sinh \Gamma\xi + z_1 \cosh \Gamma\xi)[\sinh \Gamma(\ell-x) + z_2 \cosh \Gamma(\ell-x)],$$
$$x>\xi;$$

$$I_i(x,\xi) = \frac{1}{d}(\cosh \Gamma x + z_1 \sinh \Gamma x)[\sinh \Gamma(\ell-\xi) + z_2 \cosh \Gamma(\ell-\xi)],$$
$$x<\xi, \qquad (6)$$
$$= -\frac{1}{d}(\sinh \Gamma\xi + z_1 \cosh \Gamma\xi)[\cosh \Gamma(\ell-x) + z_2 \sinh \Gamma(\ell-x)],$$
$$x>\xi;$$

where the following definitions have been made:

$$\frac{Z_{1,2}}{Z_o} = z_{1,2}; \quad \frac{Z'_{1,2}}{Z_o} = z'_{1,2} \qquad (7)$$

$$d = (1 + z_1 z_2)\sinh \Gamma\ell + (z_1+z_2)\cosh \Gamma\ell \qquad (8)$$

For the sheath current coupling mode, the $E_S(\xi)$ in Figure A-1 is proportional to $I'(\xi)$, i.e.,

$$E_S(\xi) = Z_T\, I'(\xi) \qquad (9)$$

where Z_T is the surface transfer impedance per unit length of the cable shield. The expression $I'(\xi)$ is obtained by making the following substitutions in Equation (4):

$$x \to \xi,\ \xi \to \xi_o,\ Z_o \to Z'_o,\ \Gamma \to \Gamma',\ z_{1,2} \to z'_{1,2}$$

so

$$\frac{I'_e(\xi,0)}{I'_e(0,0)} = \frac{I'(\xi)}{I'(0)} = \frac{\cosh \Gamma'(\ell-\xi) + z'_2 \sinh \Gamma'(\ell-\xi)}{\cosh \Gamma'\ell + z'_2 \sinh \Gamma'\ell}, \quad (10)$$

and in particular

$$\begin{aligned} I'(0) &= I'(\ell)\ (\cosh \Gamma'\ell + z'_2 \sinh \Gamma'\ell),\ z'_2 \neq \infty \\ I'(\ell) &= 0,\ z'_2 = \infty. \end{aligned} \quad (11)$$

From Equation (9)

$$\begin{aligned} E_S(\xi) &= Z_T\ I'(0)\ \frac{\cosh \Gamma'(\ell-\xi) + z'_2 \sinh \Gamma'(\ell-\xi)}{\cosh \Gamma'\ell + z'_2 \sinh \Gamma'\ell} \\ &= Z_T\ I'(\ell)\ [\cosh \Gamma'(\ell-\xi) + z'_2 \sinh \Gamma'(\ell-\xi)] \end{aligned} \quad (12)$$

and in particular $E_S(\ell) = 0$ if $Z'_2 = \infty$.

For the radial electric field coupling mode, the $K_S(\xi)$ in Figure A-1 is proportional to $V'(\xi)$, i.e.,

$$\begin{aligned} K_S(\xi) &= Y_T\ E_r(\xi) \\ &= \frac{Y_T\ V'(\xi)}{a\ \ell n\ (b/a)} \end{aligned} \quad (13)$$

where Y_T is the surface transfer admittance of the cable shield, a is the radius of the cable shield, and b is the radius of the larger concentric cylinder. The expression $V'(\xi)$ is obtained by making the following substitution in Equation (3):

$$x \to \xi,\ \xi \to \xi_o,\ Z_o \to Z'_o,\ \Gamma \to \Gamma',\ z_{1,2} \to z'_{1,2}$$

so

$$\frac{V'_e(\xi,0)}{V'_e(0,0)} = \frac{V'(\xi)}{V'(0)} = \frac{\sinh \Gamma'(\ell-\xi) + z'_2\cosh \Gamma'(\ell-\xi)}{\sinh \Gamma'\ell + z'_2\cosh \Gamma'\ell} \; ; \qquad (14)$$

and in particular

$$V'(\ell) = \frac{V'(0)}{\frac{1}{z'_2}\sinh \Gamma'\ell + \cosh \Gamma'\ell} \; , \; z'_2 \neq 0,$$
$$= 0, \; z'_2 = 0. \qquad (15)$$

From Equation (13)

$$K_S(\xi) = \frac{Y_T V'(0)}{a \; \ell n(b/a)} \left[\frac{\sinh \Gamma'(\ell-\xi) + z'_2\cosh \Gamma'(\ell-\xi)}{\sinh \Gamma'\ell + z'_2\cosh \Gamma'\ell}\right]$$
$$= \frac{Y_T \; V'(\ell)}{Z'_2 a \; \ell n(b/a)} [\sinh \Gamma'(\ell-\xi) + z'_2\cosh \Gamma'(\ell-\xi)]; \qquad (16)$$

and in particular, $K_S(\xi) = 0$ if $Z'_2 = 0$.

V(x) and I(x) in Equations (1) and (2) can now be calculated using the Equations (3) to (7), (12) and (16). Presented here are the results for V_1 and V_2, the voltages at the ends of the test cable in Figure A-1, which are obtained after straightforward, but rather long calculations.

$$V(0) = V_1 = \frac{z_1 \; I'(0)}{d(\Gamma^2-\Gamma'^2)(\cosh \Gamma'\ell + z'_2\sinh \Gamma'\ell)} \; [Z_T A + Y_T B] \qquad (17)$$

$$V(\ell) = V_2 = \frac{z_2 \; I'(0)}{d(\Gamma^2-\Gamma'^2)(\cosh \Gamma'\ell + z'_2\sinh \Gamma'\ell)} \; [Z_T C + Y_T D] \qquad (18)$$

where

$$A = \Gamma z_2 - \Gamma' z'_2 + [(\Gamma' z_2 - \Gamma z'_2)\sinh \Gamma'\ell + (\Gamma' z_2 z'_2 - \Gamma)\cosh \Gamma'\ell]\sinh \Gamma\ell$$
$$+ [(\Gamma' - \Gamma z_2 z'_2)\sinh \Gamma'\ell + (\Gamma' z'_2 - \Gamma z_2)\cosh \Gamma'\ell]\cosh \Gamma\ell; \qquad (19)$$

$$B = Z_o Z_o' [a\ \ell n(b/a)]^{-1} \cdot \{\Gamma z_2' - \Gamma' z_2$$
$$+ [(\Gamma' z_2' - \Gamma z_2)\sinh \Gamma'\ell + (\Gamma' - \Gamma z_2 z_2')\cosh \Gamma'\ell]\sinh \Gamma\ell$$
$$+ [(\Gamma' z_2 z_2' - \Gamma)\sinh \Gamma'\ell + (\Gamma' z_2 - \Gamma z_2')\cosh \Gamma'\ell]\cosh \Gamma\ell\}; \quad (20)$$

$$C = (\Gamma + \Gamma' z_1 z_2')\sinh \Gamma\ell - (\Gamma z_1 z_2' + \Gamma')\sinh \Gamma'\ell + (\Gamma z_1 + \Gamma' z_2') \cdot$$
$$(\cosh \Gamma\ell - \cosh \Gamma'\ell); \quad (21)$$

$$D = Z_o Z_o' [a\ \ell n(b/a)]^{-1} \cdot [(\Gamma + \Gamma' z_1 z_2')\sinh \Gamma'\ell$$
$$- (\Gamma z_1 z_2' + \Gamma')\sinh \Gamma\ell + (\Gamma z_2' + \Gamma' z_1)(\cosh \Gamma'\ell - \cosh \Gamma\ell)]. \quad (22)$$

Four surface transfer impedances can now be defined:

$$Z_T^{(1)} = \frac{V_1}{I'(0)} = \frac{z_1(Z_T A + Y_T)}{d(\Gamma^2 - \Gamma'^2)(\cosh \Gamma'\ell + z_2' \sinh \Gamma'\ell)}; \quad (23)$$

$$Z_T^{(2)} = \frac{V_2}{I'(0)} = \frac{z_2(Z_T C + Y_T)}{d(\Gamma^2 - \Gamma'^2)(\cosh \Gamma'\ell + z_2' \sinh \Gamma'\ell)}; \quad (24)$$

$$Z_T^{(3)} = \frac{V_1}{I'(\ell)} = Z_T^{(1)} (\cosh \Gamma'\ell + z_2' \sinh \Gamma'\ell); \quad (25)$$

$$Z_T^{(4)} = \frac{V_2}{I'(\ell)} = Z_T^{(2)} (\cosh \Gamma'\ell + z_2' \sinh \Gamma'\ell); \quad (26)$$

By measuring $Z_T^{(1)}$ or $Z_T^{(3)}$ and $Z_T^{(2)}$ or $Z_T^{(4)}$, the two quantities $(Z_T A + Y_T B)$ and $(Z_T B + Y_T D)$ are obtained. Then, Z_T and Y_T can be found by solving the coupled equations if, and only if,

$$\begin{vmatrix} A & B \\ C & D \end{vmatrix} \neq 0. \quad (27)$$

Assuming a non-zero value for the determinant, this system of equations can be solved for Z_T and Y_T, giving

$$Z_T = \frac{(\Gamma^2-\Gamma'^2)d}{AD-BC}\left[\frac{D}{z_1}Z_T^{(3)} - \frac{B}{z_2}Z_T^{(4)}\right]; \tag{28}$$

$$Y_T = \frac{(\Gamma^2-\Gamma'^2)d}{AD-BC}\left[\frac{A}{z_2}Z_T^{(4)} - \frac{C}{z_1}Z_T^{(3)}\right]. \tag{29}$$

These two equations are the fundamental results of this general coupling analysis. Note that $Z_T^{(3)}$ and $Z_T^{(4)}$ are easily determined from measured values of $Z_T^{(1)}$ and $Z_T^{(2)}$, respectively, using Equations (25) and (26). Thus, in the general case, Z_T and Y_T can be determined with two independent measurements and a knowledge of the characteristic impedance, propagation constant, terminating impedances, length, and outer diameter of the sample cable and the test fixture.

If the test fixture is electrically short, i.e., $\Gamma\ell<<1$ and $\Gamma'\ell<<1$, then the coefficients A, B, C, D and d become

$$\begin{aligned} &A\simeq -C\simeq -(\Gamma^2-\Gamma'^2)\ell; \\ &B\simeq \frac{Z_2}{Z_1}D\simeq -Z_2Z_2'\,[a\ \ell n(b/a)]^{-1}\,(\Gamma^2-\Gamma'^2)\ell; \\ &d\simeq z_1+z_2, \end{aligned} \tag{30}$$

assuming that $Z_2' \neq \infty$. Therefore,

$$\begin{aligned} &Z_T\simeq [Z_T^{(4)} - Z_T^{(3)}]\ell; \\ &Y_T\simeq -\frac{a\ \ell n(b/a)}{Z_2'\ \ell}\left[\frac{Z_T^{(3)}}{Z_1} + \frac{Z_T^{(4)}}{Z_2}\right]. \end{aligned} \tag{31}$$

For this case, it is apparent from Equations (25) and (26) that $Z_T^{(1)} = Z_T^{(3)}$ and $Z_T^{(2)} = Z_T^{(4)}$. Thus, it is relatively easy to

compute the values of Z_T and Y_T for the case of an electrically short fixture providing that the condition (27), which is $Z_1+Z_2 \neq 0$, is met.

The fixture which is recommended for the surface transfer impedance test procedure has $Z_1 = Z_2' = 0$, and $Z_2 = 50\Omega$. With these terminations, expression (24) for $Z_T^{(2)}$ (the measured quantity) has the following coefficients:

$$\begin{aligned} d &= e^{\Gamma \ell}; \\ C &= \Gamma \sinh \Gamma \ell - \Gamma' \sinh \Gamma' \ell; \\ D &= Z_o Z_o' \, [a \, \ell n(b/a)]^{-1} \, (\Gamma \sinh \Gamma' \ell - \Gamma' \sinh \Gamma \ell). \end{aligned} \quad (32)$$

This reduces to $Z_T^{(2)} = Z_T \ell$, independent of Z_2 and Y_T when the fixture is electrically short. At higher frequencies, this depends on both Z_T and Y_T and since $Z_T^{(1)}$ and $Z_T^{(3)}$ are zero, it is not possible to obtain the two independent measurements required to determine both coupling parameters.

The recommended test fixture for measuring the surface transfer admittance has $Z_1 = Z_2' = \infty$, and $Z_2 = 50\Omega$. The quantity measured is equivalent to $Y_T^{(2)} = V(\ell)/V'(0)$. $V(\ell)$ is given by Equation (18) and

$$\frac{V'(0)}{I'(0)} = Z_0' \, \frac{\sinh \Gamma' \ell + z_2' \cosh \Gamma' \ell}{\cosh \Gamma' \ell + z_2' \sinh \Gamma' \ell}, \quad (33)$$

which follows from Equations (11), (15) and $V(\ell) = Z_2' I(\ell)$. Substituting (33) into (18) and solving for $Y_T^{(2)}$ gives

$$Y_T^{(2)} = \frac{z_2 \, (Z_T C + Y_T D)}{Z_0' d(\Gamma^2 - \Gamma'^2)(\sinh \Gamma' \ell + z_2' \cosh \Gamma' \ell)}. \quad (34)$$

The coefficients are given by

$$d = z_1(\cosh \Gamma \ell + z_2 \sinh \Gamma \ell);$$

$$C = z_1 z_2' \, (\Gamma' \sinh \Gamma \ell - \Gamma \sinh \Gamma' \ell);$$

$$D = Z_1 Z_2' \, [a \, \ell n(b/a)]^{-1} \, (\Gamma' \sinh \Gamma' \ell - \Gamma \sinh \Gamma \ell) \quad (35)$$

as Z_1 and Z_2' approach infinity.

In general, both coupling modes contribute to $Y_T^{(2)}$. When the test cable is electrically short, (34) reduces to

$$Y_T^{(2)} = -Y_T \, [a \, \ell n(a/b)]^{-1} \, Z_2 \ell, \quad (36)$$

which after some notational changes is the result given in Section 9.4.2.

INDEX

INDEX (Continued)

INDEX (Continued)

INDEX (Continued)

DISTRIBUTION LIST

DEPARTMENT OF DEFENSE

Director
Armed Forces Radiobiology Research Institute
ATTN: Tech. Lib.
ATTN: Robert E. Carter

Commander in Chief
U.S. European Command, JCS
ATTN: Tech. Lib.
ATTN: ECJ6-PF

Commander in Chief, Pacific
JCS
ATTN: J35, Box 13

Director
Defense Advanced Research Projects Agency
ATTN: Tech. Lib.

Director
Defense Civil Preparedness Agency
ATTN: RE (EO)
ATTN: TS AED
ATTN: Admin. Officer

Defense Communication Engineer Center
ATTN: Code R124C, Tech. Lib.
ATTN: Code R720, C. Stansberry

Director
Defense Communications Agency
ATTN: Code 540.5
ATTN: CCTC/C672, Franklin D. Moore
ATTN: Code 930, Monte I. Burgett, Jr.
ATTN: Code 430
ATTN: Tech. Lib.
ATTN: Code 950

Defense Documentation Center
12 cy ATTN: TC

Commander
Defense Electronic Supply Center
ATTN: ECS
ATTN: Tech. Lib.

Assistant to the Secretary of Defense
Atomic Energy
ATTN: Doc. Con

Director
Defense Intelligence Agency
ATTN: DS-4B
ATTN: DI-7D, Edward O'Farrell
ATTN: Tech. Lib.

Director
Defense Nuclear Agency
ATTN: STSI, Archives
ATTN: RATN
ATTN: RAEV
ATTN: DDST
ATTN: STVL
3 cy ATTN: STTL, Tech. Lib.

DEPARTMENT OF DEFENSE (Continued)

Commander
Field Command
Defense Nuclear Agency
ATTN: FCPR

Director
Interservice Nuclear Weapons School
ATTN: Doc. Con
ATTN: Tech. Lib.

Director
Joint Strat. Tgt. Planning Staff, JCS
ATTN: JPST
ATTN: STINFO, Library

Chief
Livermore Division, Field Command, DNA
Lawrence Livermore Laboratory
ATTN: Doc. Con. for L-395
ATTN: FCPRL

National Communications System
Office of the Manager
ATTN: NCS-TS, Charles D. Bodson

Director
National Security Agency
ATTN: Orland O. Van Gunten, R-425
ATTN: TDL
ATTN: Tech. Lib.

OJCS/J-6
ATTN: J-6, ESD-2

DEPARTMENT OF THE ARMY

Asst. Chief of Staff for Intelligence
ATTN: DAMA-TAS, Jack T. Blackwell

Program Manager
BMD Program Office
ATTN: John Shea

Commander
BMD System Command
ATTN: Tech. Lib.
ATTN: BDMSC-TEN, Noah J. Hurst

Deputy Chief of Staff for Research, Development & Acq.
ATTN: DAMA-CSM-N, LTC G. Ogden

Commander
Harry Diamond Laboratories
ATTN: DRXDO-TR, Edward E. Conrad
ATTN: DRXDO-EM, Robert E. McCoskey
ATTN: DRXDO-RCC, John E. Thompkins
ATTN: DRXDO-TI, Tech. Lib.
ATTN: DRXDO-NP, Francis N. Wimenitz
ATTN: DRXDO-EM, John Bombardt
ATTN: DRXDO-RB, Joseph R. Miletta
ATTN: DRXDO-EM, John F. Sweton
ATTN: DRXDO-RCC, John A. Rosado
ATTN: DRXDO-RC, Robert B. Oswald, Jr.

DEPARTMENT OF THE ARMY (Continued)

Commander
U.S. Army Materiel Development & Readiness Cmd.
ATTN: DRCDE-D, Lawrence Flynn
ATTN: Tech. Lib.

Commander
Picatinny Arsenal
ATTN: SMUPA-ND-D-C-2
ATTN: SMUPA-ND-D-B, Edward J. Arber
ATTN: SARPA-ND-C-F, Anna Nordio
ATTN: SMUPA-FR-S-P, Ruth Nicolaides
ATTN: SMUPA-IN, Burton V. Franks
ATTN: SMUPA-QA-N, P. G. Olivieri
ATTN: SMUPA-ND-W
ATTN: Tech. Lib.
ATTN: Hyman Pesternak
ATTN: SMUPA-ND-N-I.
ATTN: SARPA-TS-I-E, Abraham Grinoch

Commander
ERADCOM
ATTN: AIAA-EAC, Francis N. Winans

Commander
Redstone Scientific Information Center
ATTN: DRSMI-RBD, Clara T. Rogers

Director
U.S. Army Ballistic Research Labs.
ATTN: DRXRD-BVL, David L. Rigotti
ATTN: DRXBR-VL, John W. Kinch
ATTN: DRXBR-AM, W. R. VanAntwerp
ATTN: DRXBR-X, Julius J. Meszaros
ATTN: Tech. Lib., Edward Baicy

Commander
U.S. Army Mat. & Mechanics Rsch. Ctr.
ATTN: DRXMR-HH, John F. Dignam
ATTN: Tech. Lib.

Commander
U.S. Army Communications Cmd.
ATTN: ACC-ED-M, Lawrence E. Cork
ATTN: Tech. Lib.

Chief
U.S. Army Communications Sys. Agency
ATTN: SCCM-AD-SV, Library

Commander
U.S. Army Computer Systems Command
ATTN: Tech. Lib.

Commander
U.S. Army Electronics Command
ATTN: DRSEL-CT-HDK, Abraham E. Cohen
ATTN: DRSEL-CE, T. Preiffer
ATTN: DRSEL-TL-IR, Edwin T. Hunter
ATTN: DRSEL-GG-TD, W. R. Werk
ATTN: DRSEL-NL-D
ATTN: DRSEL-TL-EN, Robert Lux
ATTN: DRSEL-WL-D
ATTN: DRSEL-TL-MD, Gerhart K. Gaule
ATTN: DRSEL-TL-ME, M. W. Pomerantz
ATTN: DRSEL-TL-IR, Robert A. Freiberg
ATTN: DRSEL-PL-ENV, Hans A. Bomke

Division Engineer
U.S. Army Engr. Div., Missouri River
ATTN: MRDED-MC, Floyd L. Hazlett

DEPARTMENT OF THE ARMY (Continued)

Commander-in-Chief
U.S. Army Europe & Seventh Army
ATTN: Tech. Lib.

Director
U.S. Army Materiel Sys. Analysis Actv.
ATTN: DRXSY-CC, Donald R. Barthel
ATTN: Tech. Lib.

Commander
U.S. Army Missile Command
ATTN: DRSMI-RGP, Hugh Green
ATTN: DRCPM-LCEX, Howard H. Henriksen
ATTN: DRSI-RGP, Victor W. Rowe
ATTN: DRCPM-PE-EA, Wallace O. Wagner
ATTN: DRCPM-PE-EG, William P. Johnson
ATTN: Tech. Lib.

Commander
U.S. Army Mobility Equip. R & D Ctr.
ATTN: STSFB-HHD, Franklin P. Good
ATTN: STSFB-MW, John W. Bond, Jr.
ATTN: Tech. Lib.
ATTN: STSFB-RN, Donald B. Dinger
ATTN: SMEFB-ES, Robert S. Brantly, Jr.

Commandant
U.S. Army Field Artillery School
ATTN: Tech. Lib.

Commander
U.S. Army Nuclear Agency
ATTN: COL Deverill
ATTN: Tech. Lib.

Commander
U.S. Army Security Agency
ATTN: IACDA-EW
ATTN: Tech. Lib.
ATTN: IARD-T, Robert H. Burkhardt

Commander
U.S. Army Tank Automotive Command
ATTN: DRSTA-RHM, 1LT Peter A. Hasek
ATTN: DRCPM-GCM-SW, Lyle A. Wolcott
ATTN: Tech. Lib.

Commander
U.S. Army Test & Evaluation Comd.
ATTN: DRSTE-EL, Richard I. Kolchin
ATTN: DRSTE-NB, Russell R. Galasso
ATTN: Tech. Lib.

Commander
U.S. Army Training & Doctrine Comd.
ATTN: Tech. Lib.
ATTN: ATORI-OP-SD

Project Officer
U.S. Army Tac. Comm. Systems
ATTN: DRCPM-ATC, COL Dobbins

Commander
White Sands Missile Range
ATTN: STEWS-TE-NT, Marvin P. Squires
ATTN: Tech. Lib.

DEPARTMENT OF THE ARMY (Continued)

Commandant
U. S. Army Signal School
ATTN: ATSO-CTD-CS, CPT G. M. Alexander
ATTN: Tech. Lib.

DEPARTMENT OF THE NAVY

Chief of Naval Operations
ATTN: OP-985
ATTN: Code 604C3, Robert Piacesi

Chief of Naval Research
ATTN: Code 464, R. Gracen Joiner
ATTN: Tech. Lib.
ATTN: Code 464, Thomas P. Quinn
ATTN: Code 427

Officer-in-Charge
Civil Engineering Laboratory
ATTN: Code L-31
ATTN: Tech. Lib.

Commander
Naval Air Systems Command
ATTN: AIR-350F, LCDR Hugo Hart
ATTN: Tech. Lib.

Commander
Naval Electronic Systems Command
Naval Electronic Systems Cmd. Hqs.
ATTN: Tech. Lib.
ATTN: PME 117-215A, Gunter Brunhart
ATTN: Code 5032, Charles W. Neill
ATTN: PME 117-21
ATTN: PME 117-T

Commander
Naval Electronics Laboratory Center
ATTN: Code 2200, Verne E. Hildebrand
ATTN: Tech. Lib.
ATTN: H. F. Wong
ATTN: Code 3100, E. E. McCown
ATTN: Code 2400, S. W. Lichtman

Commanding Officer
Naval Intelligence Support Ctr.
ATTN: NISC-45
ATTN: Tech. Lib.
ATTN: P. Alexander

Superintendent (Code 1424)
Naval Postgraduate School
ATTN: Code 2124, Tech. Rpts. Librarian

Director
Naval Research Laboratory
ATTN: Code 6631, James C. Ritter
ATTN: Code 6603F, Richard L. Statler
ATTN: Code 7770, Leslie S. Levine
ATTN: Code 2027, Tech. Lib.
ATTN: Code 2627, Doris R. Folen
ATTN: Code 7701, Jack D. Brown
ATTN: Code 4004, Emanual L. Brancato

Commander
Naval Sea Systems Command
ATTN: SEA-9931, Riley B. Lane

DEPARTMENT OF THE NAVY (Continued)

Commander
Naval Ship Engineering Center
ATTN: Code 6174D2, Edward F. Duffy
ATTN: Tech. Lib.

Commander
Naval Surface Weapons Center
ATTN: Code E31, Edwin R. Rathburn
ATTN: Code WA-50, John H. Malloy
ATTN: Code WA-501, Navy Nuc. Prgms. Off.
ATTN: Code 223, L. Labello
ATTN: Code WR-43
ATTN: Code 211
ATTN: Code 131, Edwin B. Dean
6 cy ATTN: Code WX-21, Tech. Lib

Commander
Naval Surface Weapons Center
ATTN: Tech. Lib.

Naval Weapons Engr. Support Activity
ATTN: E S A 70

Commanding Officer
Naval Weapons Evaluation Facility
ATTN: Code ATG, Mr. Stanley
ATTN: Lawrence R. Oliver

Commanding Officer
Naval Weapons Support Center
ATTN: Tech. Lib.
ATTN: Code 7024, James Ramsey

Commanding Officer
Naval Weapons Ctr.
ATTN: Code 533, Tech. Lib.

Director
Strategic Systems Project Office
ATTN: NSP-43, Tech. Lib.
ATTN: NSP-2431, Gerald W. Hoskins
ATTN: NSP-2701, John W. Pitsenberger
ATTN: NSP-2342, Richard L. Coleman
ATTN: NSP-27331, Phil Spector
ATTN: NSP-230, David Gold

Commander
U.S. Naval Coastal Systems Laboratory
ATTN: Code 771, Edgar T. Parker

Commander-in-Chief
U.S. Pacific Fleet
ATTN: Doc. Con.

DEPARTMENT OF THE AIR FORCE

Commander
ADC/DE
ATTN: DEEDS, Joseph C. Brannan
ATTN: DDEEN

Commander
ADC/XP
ATTN: XPDQ
ATTN: XPQDQ, Maj G. Kuch

AF Geophysics Laboratory, AFSC
ATTN: J. Emery Cormier

DEPARTMENT OF THE AIR FORCE (Continued)

AF Weapons Laboratory, AFSC
ATTN: ELP, Carl E. Baum
ATTN: ELC
ATTN: DYX, Donald C. Wunsch
ATTN: EL, John Darrah
ATTN: ELA
ATTN: ELA, J. P. Castillo
ATTN: SAT
ATTN: SAB
ATTN: SUL
ATTN: EL
ATTN: EL, Library
ATTN: SA

AFTAC
ATTN: Tech. Lib.

Headquarters
Air Force Systems Command
ATTN: DLCAW
ATTN: Tech. Lib.

Commander
Air University
ATTN: AUL/LSE-70-250

Commander
ASD
ATTN: 4950 Test, W/TZMH, Peter T. Marth
ATTN: Tech. Lib.

Headquarters
Electronic Systems Division, AFSC
ATTN: INDC
ATTN: DCD SATIN IV
ATTN: YWEI
ATTN: YSEV, Lt Col David C. Sparks
ATTN: XRRT
ATTN: Tech. Lib.

Air Force Avionics Laboratory, AFSC
ATTN: Tech. Lib.

Commander
Foreign Technology Division, AFSC
ATTN: TD-BTA, Library
ATTN: ETET, Capt Richard C. Husemann

HQ USAF/IG
ATTN: IGSPB, George Paseur

HQ USAF/RD
ATTN: RDQPN

Commander
Ogden Air Logistics Center
ATTN: Tech. Lib.

Commander
Rome Air Development Center, AFSC
ATTN: EMTLD, Doc. Lib.

SAMSO/DY
ATTN: DYS

SAMSO/IN
ATTN: IND, I. J. Judy

DEPARTMENT OF THE AIR FORCE (Continued)

SAMSO/MN
ATTN: MNNH, Capt B. Stewart
ATTN: MNNH, Maj M. Baran
ATTN: MNNG, Capt David J. Strobel

SAMSO/SK
ATTN: SKF, Peter H. Stadler

Commander
Sacramento Air Logistics Center
ATTN: Tech. Lib.

Commander in Chief
Strategic Air Command
ATTN: XPFS, Maj Brian G. Stephan
ATTN: NRI-STINFO, Library
ATTN: DEF, Frank N. Bousha

ENERGY RESEARCH & DEVELOPMENT ADMINISTRATION

Division of Military Application
U.S. Energy Research & Development Administration
ATTN: Doc. Con. for Class. Tech. Lib.

Los Alamos Scientific Laboratory
ATTN: Doc. Con. for John S. Malik
ATTN: Doc. Con. for Bruce W. Noel
ATTN: Doc. Con. for J. Arthur Freed
ATTN: Doc. Con. for Reports Lib.
ATTN: Doc. Con. for Richard L. Wakefield

Sandia Laboratories
ATTN: Doc. Con. for 3141, Sandia Rpt. Coll.
ATTN: Doc. Con. for Org. 9353, R. L. Parker

Sandia Laboratories
Livermore Laboratory
ATTN: Doc. Con. for Tech. Lib.

Union Carbide Corporation
Holifield National Laboratory
ATTN: Doc. Con. for Tech. Lib.
ATTN: Paul R. Barnes

University of California
Lawrence Livermore Laboratory
ATTN: E. K. Miller, L-156
ATTN: Tech. Info, Dept. L-3
ATTN: Louis F. Wouters, L-48
ATTN: B. Latorre

U.S. Energy Research & Development Administration
Albuquerque Operations Office
ATTN: Doc. Con. for WSSB
ATTN: Doc. Con. for Tech. Lib.

OTHER GOVERNMENT AGENCIES

Administrator
Defense Electric Power Administration
Department of the Interior
ATTN: Doc. Con.

Central Intelligence Agency
ATTN: RD SI, Rm. 5G48, Hq. Bldg. for Tech. Lib.
ATTN: RD/SI, Rm. 5G48, Hq. Bldg. for
William A. Decker

OTHER GOVERNMENT AGENCIES (Continued)

Department of Commerce
National Bureau of Standards
ATTN: Judson C. French
ATTN: Tech. Lib.

NASA
ATTN: Tech. Lib.

DEPARTMENT OF DEFENSE CONTRACTORS

Aerojet Electro-Systems Co. Div.
Aerojet-General Corporation
ATTN: Tech. Lib.
ATTN: Thomas D. Hanscome

Aeronutronic Ford Corporation
Aerospace & Communications Ops.
ATTN: Tech. Info. Section
ATTN: Ken C. Attinger
ATTN: E. R. Poncelet, Jr.

Aeronutronic Ford Corporation
Western Development Laboratories Div.
ATTN: Donald R. McMorrow, M.S. G-30
ATTN: Samuel R. Crawford, M.S. 531
ATTN: Library
ATTN: J. T. Mattingley, M.S. X-22

Aerospace Corporation
ATTN: Bal Krishan
ATTN: Irving M. Garfunkel
ATTN: Julian Reinheimer
ATTN: Melvin J. Bernstein
ATTN: J. Benveniste
ATTN: C. B. Pearlston
ATTN: Norman D. Stockwell
ATTN: Library

Avco Research & Systems Group
ATTN: Research Library, A-830, Rm. 7201

Battelle Memorial Institute
ATTN: Tech. Lib.
ATTN: STOIAC

The BDM Corporation
ATTN: T. H. Neighbors
ATTN: Tech. Lib.

The BDM Corporation
ATTN: Tech. Lib.
ATTN: William Druen

The Bendix Corporation
Navigation & Control Division
ATTN: George Gartner
ATTN: Tech. Lib.

The Bendix Corporation
Communication Division
ATTN: Doc. Con.

The Bendix Corporation
Research Laboratories Division
ATTN: Tech. Lib.
ATTN: Donald J. Niehaus, Mgr., Prgm. Dev.

DEPARTMENT OF DEFENSE CONTRACTORS (Continued)

The Boeing Company
ATTN: Donald W. Egelkrout, M.S. 2R-00
ATTN: David L. Dye, M.S. 87-75
ATTN: D. E. Isbell
ATTN: Howard W. Wicklein, M.S. 17-11
ATTN: Robert S. Caldwell, M.S. 2R-00
ATTN: David Kemle
ATTN: Aerospace Library

Booz-Allen & Hamilton, Inc.
ATTN: Raymond J. Chrisner
ATTN: Tech. Lib.

Brown Engineering Company, Inc.
ATTN: John M. McSwain, M.S. 18
ATTN: P. Shelton, Tech. Lib., M.S. 12

Burroughs Corporation
ATTN: Tech. Lib.
ATTN: Angelo J. Mauriello

Charles Stark Draper Laboratory, Inc.
ATTN: Kenneth Fertig
ATTN: Tech. Lib.

Cincinnati Electronics Corporation
ATTN: C. R. Stump
ATTN: Lois Hammond
ATTN: Tech. Lib.

Computer Sciences Corporation
ATTN: Tech. Lib.

Computer Sciences Corporation
ATTN: Alvin T. Schiff
ATTN: Richard H. Dickhaut

Cutler-Hammer, Inc.
AIL Division
ATTN: Anne Anthony, Central Tech. Files

University of Denver
Colorado Seminary
ATTN: Sec. Officer for Fred P. Venditti
ATTN: Sec. Officer for Tech. Lib.
ATTN: Sec. Officer for Ron W. Buchanon

The Dikewood Corporation
ATTN: Tech. Lib.
ATTN: K. Lee
ATTN: L. Wayne Davis

Effects Technology, Inc.
ATTN: Edward John Steele
ATTN: Tech. Lib.

EG&G, Inc.
Albuquerque Division
ATTN: Hilda H. Hoffman
ATTN: Tech. Lib.

Electronic Communications, Inc.
Subsidiary of NCR
ATTN: John T. Daniel, M.S. 22

E-Systems Incorporated
Greenville Division
ATTN: Library, 8-50100

DEPARTMENT OF DEFENSE CONTRACTORS (Continued)

ESL, Inc.
ATTN: Tech. Lib.
ATTN: William Metzer

Exp. & Math. Physics Consultants
ATTN: Thomas M. Jordan

Fairchild Camera & Instrument Corp.
ATTN: Sec. Dept. for 2-233, David K. Myers
ATTN: Sec. Dept. for Tech. Lib.

Fairchild Industries, Inc.
ATTN: Leonard J. Schreiber
ATTN: Tech. Lib.

The Franklin Institute
ATTN: Tech. Lib.
ATTN: Ramie H. Thompson

Garrett Corporation
ATTN: Tech. Lib.
ATTN: Robert E. Weir, Dept. 93-9

General Dynamics Corporation
Convair Division, San Diego Operation
ATTN: Keith Blair

General Dynamics Corporation
Pomona Operations
ATTN: Tech. Lib.

General Dynamics Corporation
Electronics Division
ATTN: Tech. Lib.

General Electric Company
Re-Entry & Environmental Systems Div.
ATTN: Ray E. Anderson
ATTN: John W. Palchetshy, Jr.
ATTN: Tech. Lib.

General Electric Company
Ordnance Systems
ATTN: Joseph J. Reidl

General Electric Company
Space Division
ATTN: Dante M. Tasca
ATTN: Larry I. Chasen
ATTN: Joseph C. Peden
ATTN: Daniel Edelman
ATTN: James P. Spratt
ATTN: John R. Greenbaum
ATTN: Tech. Info. Ctr.

General Electric Company
TEMPO-Center for Advanced Studies
ATTN: DASIAC
ATTN: Royden R. Rutherford
ATTN: William McNamara

General Electric Company
Aerospace Electronics Systems
ATTN: W. J. Patterson, Drop 233
ATTN: Charles M. Hewison, Drop 624
ATTN: George Francis, Drop 233
ATTN: Tech. Lib.

General Electric Company
ATTN: Doc. Con. for U. Cocca

DEPARTMENT OF DEFENSE CONTRACTORS (Continued)

General Electric Company
ATTN: David W. Pepin, Drop 160
ATTN: Tech. Lib.

General Electric Company-TEMPO
ATTN: DASIAC for William Alfonte

General Research Corporation
ATTN: John Ise, Jr.
ATTN: Robert D. Hill
ATTN: Tech. Info. Office

General Research Corporation
ATTN: David K. Osias

Georgia Institute of Technology
Office of Contract Administration
ATTN: Research Security Coordinator for Res. & Sec. Coord. for Hugh Denny

GTE Sylvania, Inc.
Electronics Systems Grp.-Eastern Div.
ATTN: James A. Waldon
ATTN: Charles A. Thornhill, Librarian
ATTN: Leonard L. Blaisdell

GTE Sylvania, Inc.
ATTN: Mario A. Nurefora, H & V Group
ATTN: Charles H. Ramsbottom
ATTN: Herbert A. Ullman
ATTN: Emil P. Motchok, Comm. Sys. Div.
ATTN: S. E. Perlman, A S M Dept.

Grumman Aerospace Corporation
ATTN: Tech. Lib.
ATTN: Jerry Rogers

Harris Corporation
Harris Semiconductor Division
ATTN: T. L. Clark, M.S. 4040
ATTN: Carl F. Davis, M.S. 17-220
ATTN: Charles Denton, Jr., M.S. 1-500
ATTN: Wayne E. Abare, M.S. 16-111
ATTN: Tech. Lib.

Hazeltine Corporation
ATTN: M. Waite, Tech. Info. Ctr.

Hercules, Incorporated
ATTN: 100K-26, W. R. Woodruff

Honeywell, Incorporated
Government & Aeronautical Products Division
ATTN: R. J. Kell, M.S. S2572
ATTN: Tech. Lib.

Honeywell, Incorporated
Aerospace Division
ATTN: Tech. Lib.
ATTN: Harrison H. Noble, M.S. 725-5A
ATTN: James D. Allen

Honeywell, Incorporated
ATTN: Tech. Lib.

Hughes Aircraft Company
ATTN: John B. Singletary, M.S. 6-D133
ATTN: Dan Binder, M.S. 6-D147
ATTN: Kenneth R. Walker, M.S. D-157
ATTN: Billy W. Campbell
ATTN: Tech. Lib.

DEPARTMENT OF DEFENSE CONTRACTORS (Continued)

Hughes Aircraft Company
Space Systems Division
ATTN: Harold A. Hoyte, M.S. A-1080
ATTN: Tech. Lib.
ATTN: William W. Scott
ATTN: Edward C. Smith

IIT Research Institute
ATTN: ACOAT
ATTN: Lib.

IIT Research Institute
ATTN: Irving N. Mindel
ATTN: Tech. Lib.
ATTN: J. E. Bridges
ATTN: W. C. Emberson
ATTN: V. P. Nanda
ATTN: Dr. W. C. Wells
ATTN: Dr. L. C. Peach
ATTN: L. B. Townsend
ATTN: Dr. P. L. E. Uslenghi

Institute for Defense Analyses
ATTN: IDA, Librarian, Ruth S. Smith

International Telephone & Telegraph Corporation
ATTN: Alexander T. Richardson
ATTN: J. Gulack, Def. Sp. Group
ATTN: Tech. Lib.

Ion Physics Corporation
ATTN: Robert D. Evans
ATTN: H. Milde
ATTN: Tech. Lib.

IRT Corporation
ATTN: Tech. Lib.
ATTN: R. L. Mertz

Jaycor, Incorporated
ATTN: Eric P. Wenaas
ATTN: Ralph H. Stahl

Johns Hopkins University
Applied Physics Laboratory
ATTN: Peter E. Partridge
ATTN: Tech. Lib.

Kaman Sciences Corporation
ATTN: Frank H. Shelton
ATTN: John R. Hoffman
ATTN: Albert P. Bridges
ATTN: Walter L. Ware
ATTN: W. Foster Rich
ATTN: Donald H. Bryce
ATTN: Library

Litton Systems, Inc.
ATTN: Tech. Lib.

Litton Systems, Inc.
Data Systems Division
ATTN: Tech. Lib.

Litton Systems, Inc.
Guidance & Control Systems Division
ATTN: John P. Retzler
ATTN: Val J. Ashby
ATTN: Tech. Lib.

DEPARTMENT OF DEFENSE CONTRACTORS (Continued)

Lockheed Missiles & Space Co., Inc.
ATTN: Lawrence F. Hearne, Dept. 81-14
ATTN: L-365, Dept. 81-20
ATTN: Philip J. Hart, Dept. 81-14
ATTN: Solomon E. Singer, Dept. 81-04
ATTN: Tech. Lib.
ATTN: Edwin A. Smith, Dept. 85-85
ATTN: Benjamin T. Kimura, Dept. 81-14
ATTN: Kevin McCarthy, 0-85-71
ATTN: George F. Heath, Dept. 81-14
ATTN: Samuel I. Taimuty, Dept. 85-85
ATTN: Hans L. Schneemann
ATTN: D. M. Tellep

Lockheed Missiles & Space Company
ATTN: Clarence F. Kooi, Dept. 52-11
ATTN: Tech. Info. Ctr., D/Coll

LTV Aerospace Corporation
Michigan Division
ATTN: James F. Sanson, B-2
ATTN: Tech. Lib.

LTV Aerospace Corporation
Vought Systems Division
ATTN: Tech. Data Ctr.

M.I.T. Lincoln Laboratory
ATTN: Leona Loughlin, Librarian, A-082

Martin Marietta Aerospace
Orlando Division
ATTN: William W. Mras, MP-413
ATTN: Jack M. Ashford
ATTN: Mona C. Griffith

Martin Marietta Corporation
Denver Division
ATTN: Jay R. McKee, Research Library, 6617
ATTN: Ben T. Graham, M.S. PO-454
ATTN: Paul G. Kase

Maxwell Laboratories, Inc.
ATTN: Victor Fargo
ATTN: Tech. Lib.

McDonnell Douglas Corporation
ATTN: Tom Ender
ATTN: Tech. Lib.

McDonnell Douglas Corporation
ATTN: Paul H. Duncan, Jr.
ATTN: Stanley Schneider
ATTN: W. R. Spark
ATTN: A. P. Venditt
ATTN: Tech. Lib. Services

Mission Research Corporation
ATTN: Conrad L. Longmire
ATTN: Daniel F. Higgins
ATTN: Tech. Lib.
ATTN: William C. Hart

Mission Research Corporation
ATTN: David E. Merewether
ATTN: Tech. Lib.

Mission Research Corporation
ATTN: V. A. J. Van Lint

DEPARTMENT OF DEFENSE CONTRACTORS (Continued)

The Mitre Corporation
ATTN: Theodore Jarvis
ATTN: M. E. Fitzgerald
ATTN: Library
ATTN: Louis Brickmore

National Academy of Sciences
ATTN: National Mat. Advisory Board for R. S. Shane

Northrop Corporation
Electronic Division
ATTN: Boyce T. Ahlport
ATTN: John M. Reynolds
ATTN: Vincent R. DeMartino
ATTN: George H. Towner
ATTN: Tech. Lib.

Northrop Corporation
ATTN: David N. Pocock
ATTN: Library
ATTN: Orlie L. Curtis, Jr.
ATTN: James P. Raymond

Northrop Corporation
ATTN: Joseph D. Russo
ATTN: Tech. Lib.

Palisades Inst. for Research Services, Inc.
ATTN: Records Supervisor

Perkin-Elmer Corporation
ATTN: Tech. Lib.
ATTN: Arthur Lee Whitson

Physics International Company
ATTN: Doc. Con. for John H. Huntington
ATTN: Doc. Con. for Bernard H. Bernstein
ATTN: Doc. Con. for Tech. Lib

Procedyne Corporation
ATTN: Peter Horowitz
ATTN: Tech. Lib.

R & D Associates
ATTN: Leonard Schiessinger
ATTN: William R. Graham, Jr.
ATTN: Richard R. Schaefer
ATTN: Tech. Lib.
ATTN: William J. Karzas
ATTN: S. Clay Rogers
ATTN: Gerald K. Schlegel
ATTN: B. Gage

The Rand Corporation
ATTN: Cullen Crain
ATTN: Tech. Lib.

Raytheon Company
ATTN: Harold L. Flescher
ATTN: Tech. Lib.
ATTN: James R. Weckback

Raytheon Company
ATTN: Gajanan H. Joshi
ATTN: Library

RCA Corporation
Government & Commercial Systems
ATTN: Tech. Lib.
ATTN: George J. Brucker

DEPARTMENT OF DEFENSE CONTRACTORS (Continued)

RCA Corporation
Government & Commercial Systems
Missile & Surface Radar Division
ATTN: Eleanor K. Daly
ATTN: Tech. Lib.
ATTN: Andrew L. Warren

RCA Corporation
ATTN: R. W. Rostrom, 13-5-2
ATTN: E. Van Keuren
ATTN: Tech. Lib.

Research Triangle Institute
ATTN: Sec. Officer for Eng. Div.,
Mayrant Simons, Jr.

Rockwell International Corporation
ATTN: J. L. Monroe, Dept. 243-027, Div. 031
ATTN: J. Spetz
ATTN: K. F. Hull
ATTN: George C. Messenger, FB-61
ATTN: L. Apodaca, FA-53
ATTN: N. J. Rudie, FA-53
ATTN: James E. Bell, HA-10
ATTN: Donald J. Stevens, FA-70
ATTN: Tech. Lib.

Rockwell International Corporation
Space Division
ATTN: TIC, D/11-092, AJ01

Rockwell International Corporation
ATTN: T. B. Yates

Sanders Associates, Inc.
ATTN: R. G. Despathy, Sr., PE, 1-6270
ATTN: Moe L. Aitel, NCA, 1-3236
ATTN: Tech. Lib.

Science Applications, Inc.
ATTN: Tech. Lib.
ATTN: R. Parkinson

Science Applications, Inc.
Huntsville Division
ATTN: Noel R. Byrn
ATTN: Tech. Lib.

Science Applications, Inc.
ATTN: J. Roger Hill
ATTN: Richard L. Knight

Science Applications, Inc.
ATTN: William L. Chadsey

Simulation Physics, Inc.
ATTN: John R. Uglum
ATTN: Roger G. Little

The Singer Company
ATTN: Irwin Goldman

The Singer Company, (Data Systems)
ATTN: Tech. Lib.

Sperry Rand Corporation
Univac Division
ATTN: James A. Inda, M.S. 4TT25
ATTN: Tech. Lib.

DEPARTMENT OF DEFENSE CONTRACTORS (Continued)

Sperry Rand Corporation
Sperry Division
ATTN: Tech. Lib.
ATTN: Paul Marraffino
ATTN: Charles L. Craig

Stanford Research Institute
ATTN: Robert A. Armistead
ATTN: Philip J. Dolan

Stanford Research Institute
ATTN: MacPherson Morgan
ATTN: Tech. Lib.

Sunstrand Corporation
ATTN: Curtis B. White

Systems, Science & Software
ATTN: Tech. Lib.

Systems, Science & Software, Inc.
ATTN: Tech. Lib.
ATTN: Andrew R. Wilson

Systron-Donner Corporation
ATTN: Harold D. Morris
ATTN: Gordon B. Dean
ATTN: Tech. Lib.

Texas Instruments, Inc.
ATTN: Tech. Lib.
ATTN: Donald J. Manus, M.S. 72

Texas Tech. University
ATTN: Travis L. Simpson

TRW Systems Group
ATTN: Aaron H. Narevsky, R1-2144
ATTN: Tech. Info. Ctr., S-1930
ATTN: H. H. Holloway, R1-2036
ATTN: O. E. Adams, R1-1144
ATTN: Jerry I. Lubell, R1-1144
2 cy ATTN: Robert M. Webb, R1-1150

DEPARTMENT OF DEFENSE CONTRACTORS (Continued)

TRW Semiconductors
Division of TRW, Inc.
ATTN: Ronald N. Clarke
ATTN: Tech. Lib.

TRW Systems Group
San Bernardino Operations
ATTN: F. B. Fay, 527/710

TRW Systems Group
ATTN: Donald W. Pugsley
8 cy ATTN: Tech. Lib.

United Technologies Corporation
Hamilton Standard Division
ATTN: Raymond G. Giguere
ATTN: Tech. Lib.

United Technologies Corp.
Norden Div.
ATTN: Tech. Lib.

Varian Associates
ATTN: D. C. Lawrence
ATTN: Tech. Lib.

Vector Research Associates
ATTN: W. A. Radasky

Westinghouse Electric Corporation
Astronuclear Laboratory
ATTN: Tech. Lib.

Westinghouse Electric Corporation
Defense & Electronic Systems Ctr.
ATTN: Henry P. Kalapaca
ATTN: Tech. Lib.

Westinghouse Electric Corporation
Research & Development Ctr.
ATTN: Tech. Lib.